Fall 2010

Development of PEGylated polyacridine peptides for in vivo gene delivery of plasmid DNA

Christian Antonio Fernandez
University of Iowa

DEVELOPMENT OF PEGYLATED POLYACRIDINE PEPTIDES FOR IN VIVO GENE DELIVERY OF PLASMID DNA

by

Christian Antonio Fernandez

An Abstract

Of a thesis submitted in partial fulfillment
of the requirements for the Doctor of
Philosophy degree in Pharmacy
in the Graduate College of
The University of Iowa

December 2010

Thesis Supervisor: Professor Kevin G. Rice

ABSTRACT

Gene therapy provides an opportunity to ameliorate several genetic disorders and treat numerous diseases by using nucleic acid-based materials to modulate gene activity. However, the greatest challenge for successful gene therapy applications remains delivery. Two general approaches are currently under investigation to improve gene delivery efficiencies. The first is by encapsulating therapeutic genes into modified viruses that are effective at transfecting cells but that have also caused serious side effects during clinical evaluations in 1999 and 2003. In contrast, non-viral gene therapy provides the safety of conventional pharmaceutical products, but possesses inadequate transfection efficiencies for clinical use. Successful non-viral gene delivery systems require evasion of the reticuloendothelial system (RES) while in circulation, a targeting ligand for efficient cellular uptake, and perhaps several additional components for efficient cellular disposition once the carrier has been internalized.

Engineering sophisticated gene delivery systems requires modular designs that are well characterized and optimized to circumvent each limiting barrier associated with gene delivery. The following thesis is focused on developing stabilized DNA polyplexes for in vivo applications and coupling their administration with current physical methods of non-viral gene delivery. The aim behind this approach is to systematically prepare gene carriers and evaluate their ability to maintain DNA transfection competent in order to determine which bioconjugate is the most successful for ultimately creating gene carriers that do not require physical interventions for gene expression.

The non-viral gene delivery systems presented in the thesis are based on PEGylated polyacridine peptides that bind to DNA predominantly by intercalation rather than by ionic interactions with DNA. The initial experimental chapters deal with the discovery of these novel DNA polyplexes, and the latter chapters focus on the optimization of their design for targeted in vivo gene delivery. The results demonstrate

that PEGylated polyacridine DNA polyplexes possess improved compatibility for in vivo administration and that their flexible design is beneficial for preparing multi-component gene delivery systems.

Abstract Approved: _____
Thesis Supervisor

_____
Title and Department

_____
Date

DEVELOPMENT OF PEGYLATED POLYACRIDINE PEPTIDES FOR IN VIVO GENE DELIVERY OF PLASMID DNA

by

Christian Antonio Fernandez

A thesis submitted in partial fulfillment
of the requirements for the Doctor of
Philosophy degree in Pharmacy
in the Graduate College of
The University of Iowa

December 2010

Thesis Supervisor: Professor Kevin G. Rice

Graduate College
The University of Iowa
Iowa City, Iowa

CERTIFICATE OF APPROVAL

_____

PH.D. THESIS

_____

This is to certify that the Ph.D. thesis of

Christian Antonio Fernandez

has been approved by the Examining Committee
for the thesis requirement for the Doctor of Philosophy
degree in Pharmacy at the December 2010 graduation.

Thesis Committee: _____
Kevin G. Rice, Thesis Supervisor

_____
Maureen D. Donovan

_____
Jennifer Fiegel

_____
Paloma H. Giangrande

_____
Aliasger K. Salem

This thesis is dedicated to the loving memory of my father, Jaime Pérez Fernández.

ABSTRACT

Gene therapy provides an opportunity to ameliorate several genetic disorders and treat numerous diseases by using nucleic acid-based materials to modulate gene activity. However, the greatest challenge for successful gene therapy applications remains delivery. Two general approaches are currently under investigation to improve gene delivery efficiencies. The first is by encapsulating therapeutic genes into modified viruses that are effective at transfecting cells but that have also caused serious side effects during clinical evaluations in 1999 and 2003. In contrast, non-viral gene therapy provides the safety of conventional pharmaceutical products, but possesses inadequate transfection efficiencies for clinical use. Successful non-viral gene delivery systems require evasion of the reticuloendothelial system (RES) while in circulation, a targeting ligand for efficient cellular uptake, and perhaps several additional components for efficient cellular disposition once the carrier has been internalized.

Engineering sophisticated gene delivery systems requires modular designs that are well characterized and optimized to circumvent each limiting barrier associated with gene delivery. The following thesis is focused on developing stabilized DNA polyplexes for in vivo applications and coupling their administration with current physical methods of non-viral gene delivery. The aim behind this approach is to systematically prepare gene carriers and evaluate their ability to maintain DNA transfection competent in order to determine which bioconjugate is the most successful for ultimately creating gene carriers that do not require physical interventions for gene expression.

The non-viral gene delivery systems presented in the thesis are based on PEGylated polyacridine peptides that bind to DNA predominantly by intercalation rather than by ionic interactions with DNA. The initial experimental chapters deal with the discovery of these novel DNA polyplexes, and the latter chapters focus on the optimization of their design for targeted in vivo gene delivery. The results demonstrate

that PEGylated polyacridine DNA polyplexes possess improved compatibility for in vivo administration and that their flexible design is beneficial for preparing multi-component gene delivery systems.

TABLE OF CONTENTS

LIST OF TABLES

LIST OF FIGURES

CHAPTER 1: LITERATURE REVIEW

Abstract

Improving the transfection efficiencies of non-viral gene delivery requires properly engineered nano-scaled delivery carriers that can overcome the multiple barriers associated with the delivery of oligonucleotides from the site of administration to the nucleus or cytoplasm of the target cell. This chapter reviews the current advantages and limitation of polyplex non-viral delivery systems, including the apparent barriers that limit gene expression efficiency compared to physical methods such as hydrodynamic dosing and electroporation. An emphasis is placed on engineered nano-scaled polyplexes of modular design that both self-assemble and systematically disassemble at the desired stage of delivery. It is suggested that polyplexes of increasingly sophisticated designs are necessary to improve the efficiency of the rate limiting steps in gene delivery (reproduced with written permission from (reproduced with written permission from ACS Publications).

Introduction

The central idea behind gene therapy is to introduce therapeutic genes into the body in order to correct a disease through the expression of a protein using plasmid DNA or through the knockdown of a protein using small interfering RNA (siRNA). Viral and non-viral gene therapies are two different strategies under investigation for introducing DNA into cells or tissues. Viral gene therapy consists of using a modified virus to deliver DNA to cells and tissues in animals. This approach has achieved high protein expression, or transfection efficiencies, but has severe limitations due to the strong immunological responses triggered by the viral proteins.[1-3] Conversely, non-viral delivery strategies use synthetic carriers that package DNA into nano-scaled polyplexes or lipoplexes that facilitate transport in vivo. Lipoplexes composed of cationic lipids mixed with DNA were among the first non-viral delivery carriers to be developed and tested for efficacy in several clinical trials. While they have proven to be an efficient in vitro gene transfer

agent, they lack the essential physical properties to direct biodistribution in vivo. Tremendous technical advances have been made by encapsulating DNA in liposomes, which is reviewed in the following references.[4, 5]

Compared to plasmid DNA, which is typically 5000 base pairs in length, siRNA oligonucleotides are shorter with approximately 22-25 base pairs.[6] The science of gene therapy has advanced not only to mediate stable or transient expression of a functional protein using plasmid DNA, but also to block the expression of a protein using a siRNA involved in the RNA interference pathway (RNAi). The RNAi pathway is an endogenous mechanism in most eukaryotic organisms that involves RNAi associated enzymes to prevent mRNA from producing a protein and it is often used as a defense against viral infection.[7] Since siRNA combines with its target RNA-induced silencing complex (RISC) in the cytoplasm, it does not require trafficking into the nucleus. A further advantage of synthetic siRNA is the ability to build in stabilized linkages that resist RNase degradation. Such chemical modifications include the replacement of non-bridging oxygen on the internucleotide phosphate linkage with sulfur (phosphorothioate), boron (boranophosphate), nitrogen (phosphoramidate), or with a methyl group (methyphosphonate).[8, 9] Modification of the 2'- position of the ribose, such as 2'-O-methyl, 2'-fluro, and 2'-O-(2-methoxyethyl) modifications can also improve the nuclease stability of siRNA,[8, 10] but nevertheless the efficacy of both siRNA and DNA can be improved by developing gene delivery systems that can target and protect genes during transit in the blood and facilitate cell entry after reaching the target cell.[11]

Engineered Nano-Scaled Polyplexes

The simplest non-viral vector consists of uncomplexed or "naked" DNA. While naked DNA has shown the ability to mediate gene transfer in muscle[12, 13] and liver[14] via hydrodynamic dosing (discussed on page 25), these approaches are not able to reach all tissue sites and require delivery methods that are potentially harmful. Therefore, the most common approach to creating a pharmaceutically elegant gene delivery system is to

package DNA into nano-scaled polyplexes. These polyplexes are formed through the electrostatic binding between a cationic carrier and an anionic DNA. Common carriers used include cationic lipids, polypeptides, polyethylenimine, and dendrimers. The electrostatic interaction between a carrier and DNA results in compaction of the DNA into nanoparticles similar to the compaction provided by histones in the nucleus.

Uncompacted naked DNA can be as large as 1 μm in diameter of the major axis.[15] In contrast, polyplexes are compacted due to charge neutralization and range in size from 30 to 200 nm in diameter spherical particles. Figure 1-1 illustrates how the cationic peptide Cys-Trp-Lys_{18} (CWK_{18}) neutralizes anionic naked DNA to form compact cationic polyplexes. Numerous studies have illustrated that the length and type of polycation will influence the size of the nanoparticle much more than the size or type of oligonucleotide.[16] In addition, it has been demonstrated that the type of counter ion present on a cationic carrier influences the shape of polyplexes. Farjo et al. demonstrated that an acetate counter ion produces ellipsoid polyplexes, whereas trifluoroacetate counterion results in filamentous structures.[17] Likewise, the size and charge of the polyplex is influenced by the amount of polycation used to compact the DNA. Polyplexes are usually less than 100 nm in diameter and bear an electropositive surface charge due to the excess polycation needed for full compaction. Additionally, the ionic strength and pH of the buffer influences polyplex shape and polydispersity. Generally, dilute buffers, such as 10 mM HEPES at a pH of 7.4, that are devoid of mono and divalent metals, are used for DNA compaction. Sodium chloride or sodium phosphate in buffers are avoided as they result in larger and more polydispersed polyplexes.[18] Consequently, the tonicity can they result in larger and more polydispersed polyplexes.[18] Consequently, the tonicity can be adjusted using mannitol to achieve isotonic formulations that are compatible for iv

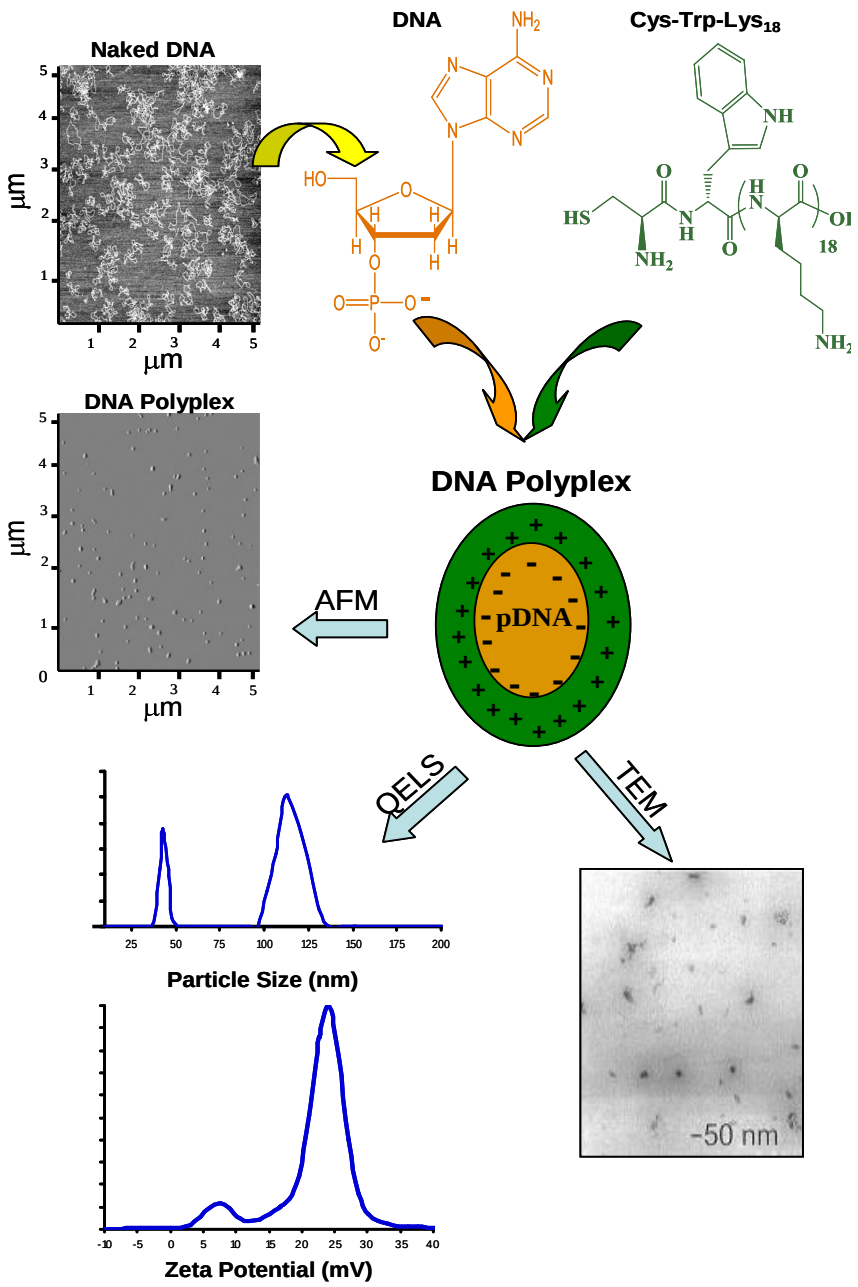

Figure 1-1. *Characterization of Nano-Scaled Polyplexes.* Anionic DNA electrostatically interacts with cationic Cys-Trp-Lys$_{18}$ (CWK$_{18}$) to form positively charged DNA nanoparticles (zeta potential). Atomic force microscopy (AFM) is used to illustrate the shape of plasmid DNA prior to condensation (top). Following compaction into DNA nanoparticles by CWK$_{18}$, AFM, TEM, and QELS analysis all reveal the <100 nm size of DNA polyplexes (bottom).

dosing. Polyplexes are readily prepared at 50 μg/mL for in vitro experiments, whereas higher concentrations of 1-5 mg/mL can only be achieved if the polyplexes contain poly(ethylene) glycol (PEG) to prevent aggregation.[19]

Heterogeneous populations of polyplexes may account for the variability in transfection efficiency.[20] Templeton et al. demonstrated this by extruding lipoplexes to create a more homogenous population of particles.[21] Extruded lipoplexes yielded significantly higher in vitro transfection compared to heterogeneous lipoplexes. In contrast, polyplexes are difficult to extrude due to solubility limitations. However, PEGylated polyplexes are extrudable, and thus improving particle size homogeneity may be important for enhancing the gene transfer efficiency in vivo.

Characterization Methods

Regardless of the cationic carrier used to form polyplexes, there are several general techniques that can be used to monitor their formation. The displacement of a fluorescent intercalator, such as thiazole orange[22] or ethidium bromide,[23] from DNA by a cationic carrier is often used to observe polyplex self-assembly. Typically, the intercalator is added to the DNA and then titrated with different amounts of cationic carrier until the fluorescence intensity of the intercalator has decreased to a minimum.[22] The decrease in fluorescence intensity results from displacement of the fluorophore due to the binding of the cationic carrier to the DNA. An asymptote in the titration curve provides a means to determine the stoichiometry of the fully formed polyplex, where the further addition of cation carrier no longer results in additional binding.[22] Alternatively, the retardation of DNA bands on an agarose gel during electrophoresis can be used to judge polyplex formation,[24] as well as to analyze the relative affinity of the carrier binding to DNA.[25]

Once formed, polyplexes can be characterized using light scattering to determine size and surface charge characteristics. Quasi-elastic light scattering (QELS) uses an

algorithm to calculate the diameter of particles based on the light scattered off of the particles in solution.[26] This method provides information based on the entire sample population, but assumes that all the particles in the sample are spherical. Similarly, light scattering in an electric field (electrophoretic light scattering) is used to determine the electrophoretic mobility, which is used to calculate the surface charge of the polyplexes. Transmission Electron Microscopy (TEM) and Atomic Force Microscopy (AFM) have also been extensively used to characterize polyplexes.[27, 28] While these methods have similar resolutions, TEM requires immobilization and staining protocols with uranyl acetate in ethanol that may distort the size of the polyplex, whereas AFM images can be taken in ambient air as well as in biological liquids. Unlike QELS, both TEM and AFM cannot provide comprehensive population information on the size and distribution of the sample. Consequently, the techniques are used interdependently to describe the physical features of polyplexes (Figure 1-1).

Peptide-Based Formulations

The goal of non-viral gene delivery systems is to achieve site-specific targeting and promote efficient internalization and expression. It is also becoming increasingly clear that it is important to minimize immunogenicity and to extend the duration of transient expression. Peptide-based non-viral delivery systems are advantageous for achieving these goals for several reasons. Compared to other polymers, synthetic peptides are constructed step-wise on solid phase and can be customized to include all natural and unnatural amino acids.[29] Certain residues, such as cysteines, provide a specific chemical conjugation site when preparing bioconjugates, as the thiol on cysteine has been used to attach PEG and targeting ligands to the polyplex.[30] The ability to customize polyplexes and prepare homogeneous peptide-based bioconjugates may provide an advantage in optimizing activity compared to other synthetic polymers.

Acridine Mediated Gene Delivery

High affinity binding to DNA is a prerequisite for any successful gene delivery agent. It is, nevertheless, possible to prepare DNA polyplexes without requiring the condensation of DNA by developing acridine-based gene delivery systems that bind to DNA by intercalation (Figure 1-2A & B). The intercalation of a compound onto DNA is the reversible insertion of the planar aromatic ring system in between consecutive base pairs of DNA (Figure 1-2B).[31] The intercalation of acridine onto DNA has been demonstrated to be reversible, and binds by a combination of hydrophobic, electrostatic, hydrogen-bonding, and dipolar forces.[32] A binding affinity with a K_d below 10^{-9} M has been demonstrated for bis and tris acridine conjugates, and intercalation has also been shown to impede DNA migration during gel electrophoresis presumably due to a reduction of the negative charge of DNA upon binding and neutralization with the amino groups on the compound (pKa ~ 7-9).[33, 34]

Acridine-based gene delivery systems have been previously investigated as a means to attach nuclear localizing sequences (NLS), targeting ligands, and most recently poly(ethylene) glycol. Furthermore, Takehiko et al. developed monoacridine conjugates that attached 9-(aminoacridinyl)-6-aminohexanoic acid to the N-terminus of several peptide nucleic acid (PNA) oligomers by an ethylene glycol linker.[35] Acridinylated PNAs displayed high antisense activity and achieved cellular uptake when polyplexed with lipofectamine without the need of calf thymus DNA, which was required for the polyplex formation, cellular uptake, and antisense activity of non-acridinylated PNAs.

Acridine-based gene delivery systems for targeted DNA delivery have been demonstrated using bisacridine intercalators containing a galactose residue for targeting the asialoglycoprotein receptor in hepatocytes (Figure 1-3).[36] The bioconjugates were synthesized by reacting the secondary amine of bis-(tert-butoxycarbonyl)spermidine hydrochloride with acetyl-protected galactosides terminated by an activated carboxylic acid functional group. The galactose-spermidine conjugates were deprotected and reacted

with 9-phenoxyacridine to yield low molecular weight bisacridine conjugates containing either one or three galactose units. The conjugates were shown to be selective for hepatocyte targeting in vitro, but failed to mediate significant levels of gene expression.[36]

Several acridine bioconjugates have been developed for the non-covalent attachment of NLS sequences to DNA. Boulanger et al. prepared monoacridine-NLS bioconjugates by reacting dichloroacridine with mono-protected α,ω diamino spacers of various lengths.[32] The conjugates were deprotected and reacted with N-succinimidyl-4-(maleimidomethyl)cyclohexane carboxylate (SMCC), where the NLS sequence was attached through the reaction of the maleimide with a cysteine on the NLS sequence. Nevertheless, this method did not improve transfection when incorporated with lipoplexes or polyplexes.[32] In contrast, bis and trisacridines were created by first preparing a boc protected 9-aminoacridine amino acid based on the peptide nucleic acid aminoethyl glycine, and attaching an NLS sequence by an 8-amino-2,6-dioxaoctanoic acid linker.[37, 38] Both conjugates showed similar binding affinities for DNA, and both

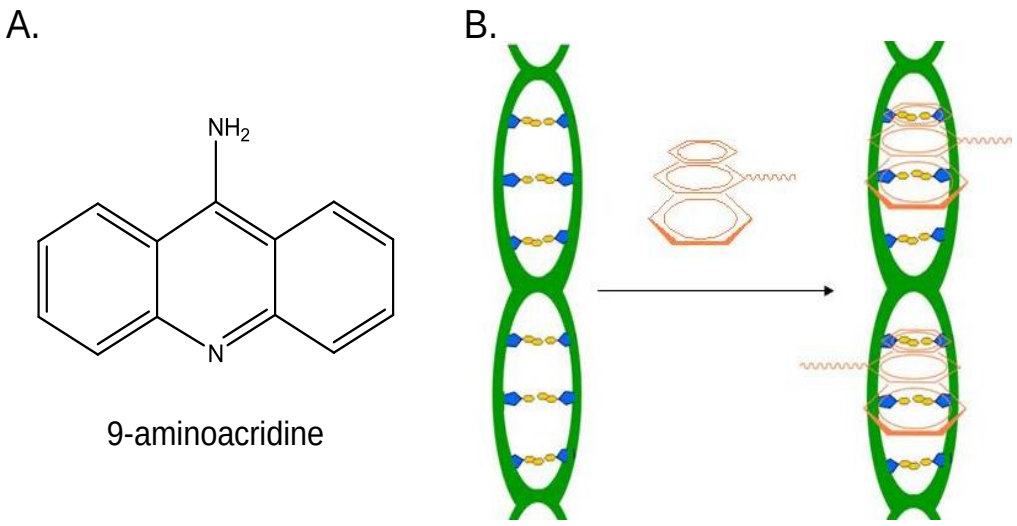

Figure 1-2. *Intercalation of Acridine-Based Gene Delivery Systems*. The structure of 9-aminoacridine is illustrated in Panel A. The intercalation of acridine-based compounds into DNA is illustrated in Panel B as the insertion of the planar aromatic ring system in between consecutive base pairs of DNA.

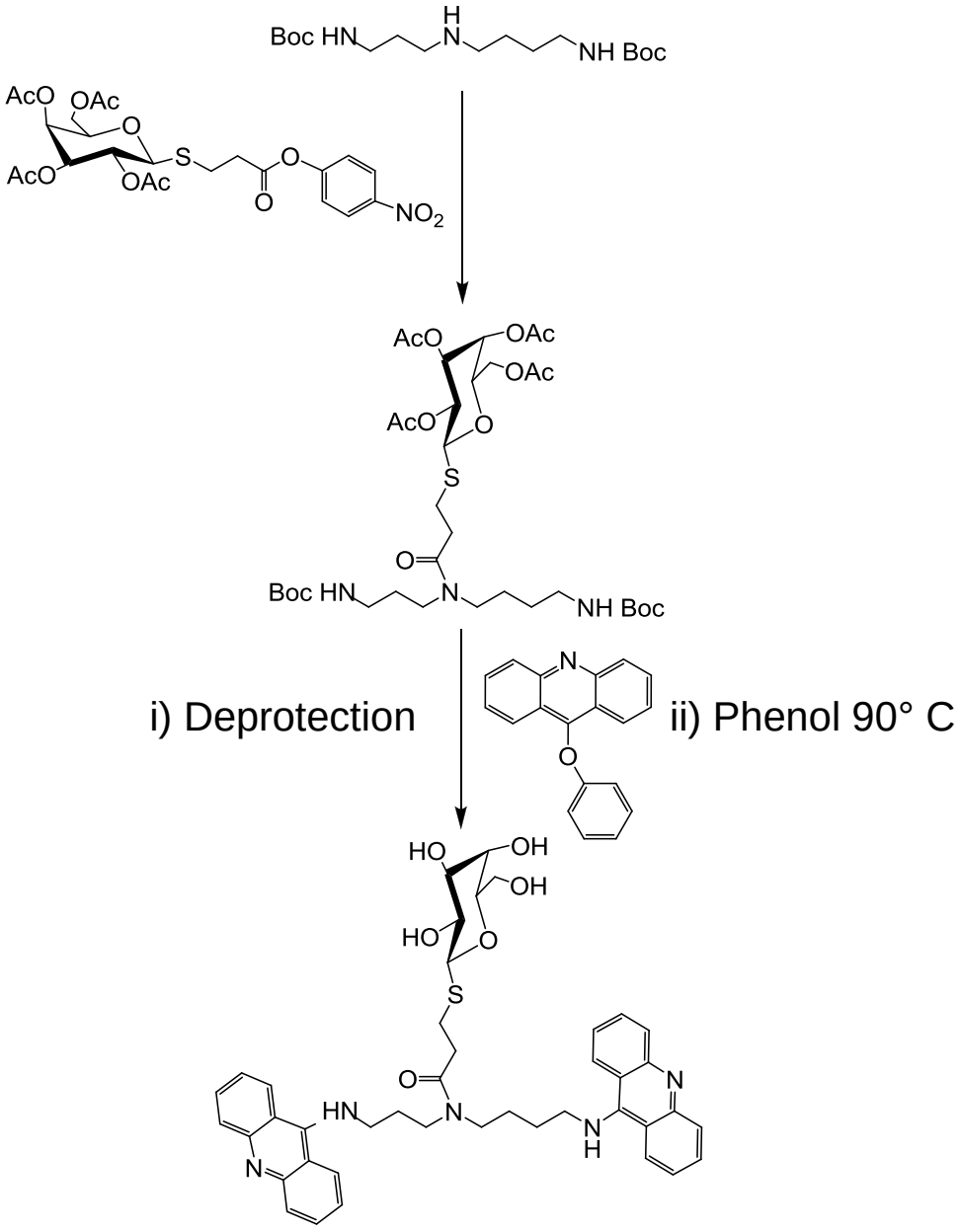

Figure 1-3. *Synthesis of Bisacridine Intercalators for Use as DNA Targeting Ligands*. Galactosyl bisacridine was prepared by conjugation of the free secondary amine of N^1, N^8-bis(tert-butoxycarbonyl)spermidine hydrochloride with a p-nitrophenyl-activated ester protected D-galactose analogue (3-(2,3,4,6-tetra-O-acetyl-1-thio-β-D-galactopyranosyl) propionate), resulting in a protected galactose-spermidine compound. The conjugate was deprotected with TFA and then reacted with 9-phenoxyacridine to yield a galactose-spermidine conjugate that targets the asialoglycoprotein receptor on hepatocytes (adapted from Haensler et al.).[36]

showed improved transfection efficiencies when polyplexed in conjunction with PEI or lipofectamine.[37, 38]

Several acridine bioconjugates have been developed for the non-covalent attachment of NLS sequences to DNA. Boulanger et al. prepared monoacridine-NLS bioconjugates by reacting dichloroacridine with mono-protected α,ω diamino spacers of various lengths.[32] The conjugates were deprotected and reacted with N-succinimidyl-4-(maleimidomethyl)cyclohexane carboxylate (SMCC), where the NLS sequence was attached through the reaction of the maleimide with a cysteine on the NLS sequence. Nevertheless, this method did not improve transfection when incorporated with lipoplexes or polyplexes.[32] In contrast, bis and trisacridines were created by first preparing a boc protected 9-aminoacridine amino acid based on the peptide nucleic acid aminoethyl glycine, and attaching an NLS sequence by an 8-amino-2,6-dioxaoctanoic acid linker.[37, 38] Both conjugates showed similar binding affinities for DNA, and both showed improved transfection efficiencies when polyplexed in conjunction with PEI or lipofectamine.[37, 38]

More recent reports of acridine-based gene delivery systems have included the preparation of trisacridine conjugates containing both an NLS sequence and PEG.[39, 40] A first generation poly(amido amine) dendrimers containing four primary amines were reacted with the heterobifunctional Mal-PEG-NHS. Following purification, the remaining non-reacted amines were acridinylated with 9-acridine isothiocynate, followed by NLS attachment via the maleimide function on PEG. These compounds were the only prior acridine-based systems to demonstrate nuclease protection, and were shown to have a 15-fold improvement on gene transfer when co-complexed with lipofectamine2000, or an 11-fold improvement when co-complexed with exgen500.[39] The results were dependent on the NLS sequence attached to bioconjugate, and similar discoveries were recently described using reducible disulfide polyamines as the delivery vehicle.[39] To date no prior acridine-based bioconjugate has been reported for in vivo applications. Most of the

acridine-based systems previously developed served as a co-complexing agent included on the polyplex to improve cellular or nuclear uptake. Therefore acridine-based gene delivery systems have not been previously tested in vivo due to design limitations, which at least require high affinity binding and nuclease protection for successful in vivo stability of the DNA polyplex in circulation.

PEGylated Polyplexes for Improved Systemic Properties

The circulatory half-life of liposomes were dramatically improved by the addition of a surface layer of poly(ethylene) glycol (PEG).[41] Similarly, the PEGylation of antigens, antibodies, growth factors, cardiovascular agents, blood constituents, immunologically active agents, free radical scavengers, antineoplastic agents, biological receptors, and drugs for hepatitis C has demonstrated improved half-lives.[42] Several PEGylated drugs, such as PEGfilgrastim (PEGylated human granulocyte colony stimulating factor) and PEGASYS (PEGylated interferon alfa-2a), have been approved by the FDA for parenteral administration, reflecting that PEG polymers are safe and non-toxic agents that increase the pharmacokinetic half-life of peptide-based pharmaceutical products.[43] Based on these results, PEGylated polyplexes have been under investigation for over a decade in gene therapy.

PEGylation serves several different key roles for proper polyplex function in addition to blocking protein absorption and improving pharmacokinetic half-life (Figure 1-4).[44, 45] PEG maintains polyplex stability at higher concentrations of DNA (1 mg/mL) which allows for DNA polyplex administration by electroporation without aggregation and for easier storage in reconstitutable freeze-dried formulations.[19, 46] As discussed previously, PEGylated polyplexes may also be extruded, thus providing a method to achieve improved homogeneity.

PEG has been attached to peptides and proteins by conjugation with the side chains of lysine, cysteine, histidine, arginine, aspartic acid, glutamic acid, serine,

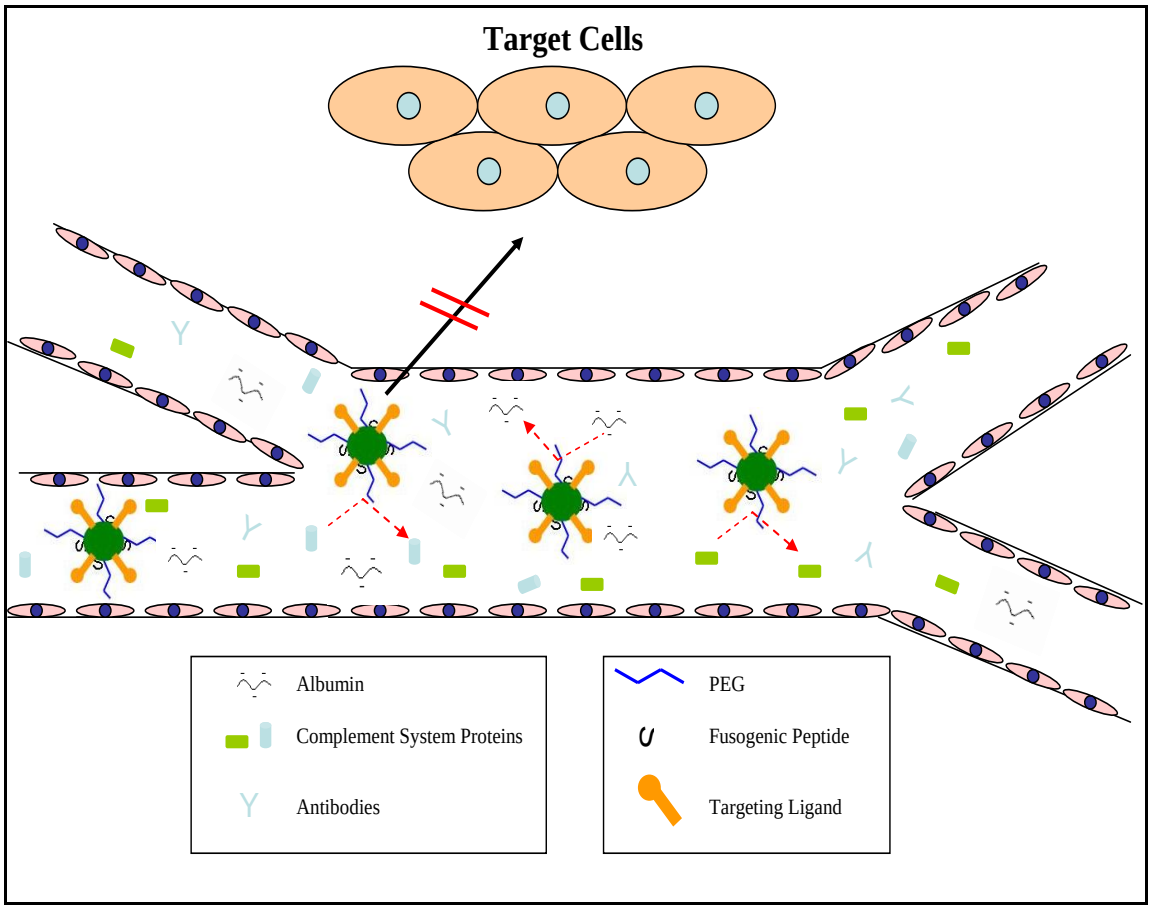

Figure 1-4. *Blood as a Barrier to Polyplex Delivery and the Effect of PEGylation.* The figure illustrates the interaction of polyplex with blood components, as well as the endothelial layer as a barrier to the free diffusion of nanoparticles out of the blood vessels. PEGylation of polyplexes prevents the binding of blood proteins to the surface of polyplex to provide enhanced circulatory half-lives.

threonine, tyrosine, as well as N-terminal amino groups and C-terminal carboxylic acids. Attaching a PEG to a primary amine is the most common modification of polyplexes. PEG N-hydroxysuccinimide (NHS) esters readily react with primary amines on polyplexes to form stable amides.[11] polyplex amines may also be conjugated with PEG-nitrophenyl carbonates and PEG-isocyanates.[47] Additionally, PEGylation of thiols on

cysteines are commonly conjugated using PEG-maleimide, vinyl sulfone, iodoacetamide, and orthopyridyl disulfide depending on the designed stability.[43]

The method chosen to incorporate PEG will depend on the desired properties of the polyplex. While covalent PEGylation improves the pharmacokinetic and biodistribution of polyplexes,[48-51] it has also lead to reduced transfection efficiencies in vitro.[52-54] While a component such as PEG is required for in vivo delivery, a possible strategy to improve the gene transfer of the polyplexes that do internalize into the cell is to release PEG from the polyplex inside the target cell. This controlled reversibility of the PEG can be engineered either through release under the acidic conditions within the endosome, or in the reductive environment of the cytoplasm.[55, 56] Several reversibly-linked, PEGylated polyplexes have been tested that possess an acetal,[57, 58] vinyl ether,[59] ortho ester,[60] or hydrazone linkage.[55] The reductively triggered release of PEG is based upon glutathione reduction of disulfide bonds.

Gene Delivery Barriers

A barrier to DNA delivery encountered in the systemic circulation is presented by the blood components that bind to lipoplexes and polyplexes (Figure 1-4). Unprotected DNA is immediately susceptible to degradation by serum nucleases.[11] Thus, one of the most important functions of the carrier is to protect the DNA from premature metabolism outside of the target cell. Blood proteins such as albumin or immunoglobulin bind to positively charged polyplexes or lipoplexes, resulting in aggregation and non-specific biodistribution. Non-PEGylated cationic polyplexes are cleared immediately from the blood and distribute to the lung where they can cause embolisms. Larger PEGylated polyplexes (> 500 nm) are generally removed from the blood faster than smaller polyplexes (< 100 nm), with a greater percentage of the dose taken up by the spleen relative to the liver. It is therefore desirable to prepare either small, PEGylated anionic or

cationic polyplexes to minimize non-specific biodistribution and to maximize the time in the blood to afford specific targeted biodistribution.

A second major barrier to the successful systemic delivery of polyplexes is the need to cross the endothelial layer of blood vessels. Polyplexes must traverse the blood vessels through the fenestrations of the endothelial capillary (30 nm), the fenestrae of the exocrine glands (50-60 nm), or through the larger fenestra of the liver or spleen (100 nm).[61] For this reason, larger-diameter (100-600 nm) fenestrations formed around tumor blood vessels offers an advantage for liver and tumor targeting of polyplexes.[62] The physiological properties of tumor vascularity allows for selective delivery of polyplexes to solid tumors through a process referred to as the enhanced permeability and retention (EPR) effect.[63] Once polyplexes transverse the endothelium, several intracellular barriers remain that can significantly hinder the delivery of the DNA (Figure 1-5).

Cell Entry

Once a DNA polyplex reaches the targeted cell, it must bind to the surface and cross the cell membrane. The internalization process has been classically characterized into three categories: macropinocytosis, caveolae-mediated endocytosis, or clathrin-mediated endocytosis.[64] Recent studies suggest that not all cell entry pathways lead to productive gene transfer and expression,[65, 66] and while binding to the cell is essential for internalization, DNA polyplexes have been demonstrated to bind through a non-specific association between the cationic DNA polyplex and the anionically charged proteoglycans and glycoproteins on the cell surface.[67] Nevertheless, the endocytosis of cationic polyplexes most likely follows multiple pathways into the cell.[68]

The major route of internalization for targeted DNA polyplexes is through receptor-mediated endocytosis, where the pathway of entry is best defined through the dependency of certain lipids and proteins, such as caveolin and clathrin, on

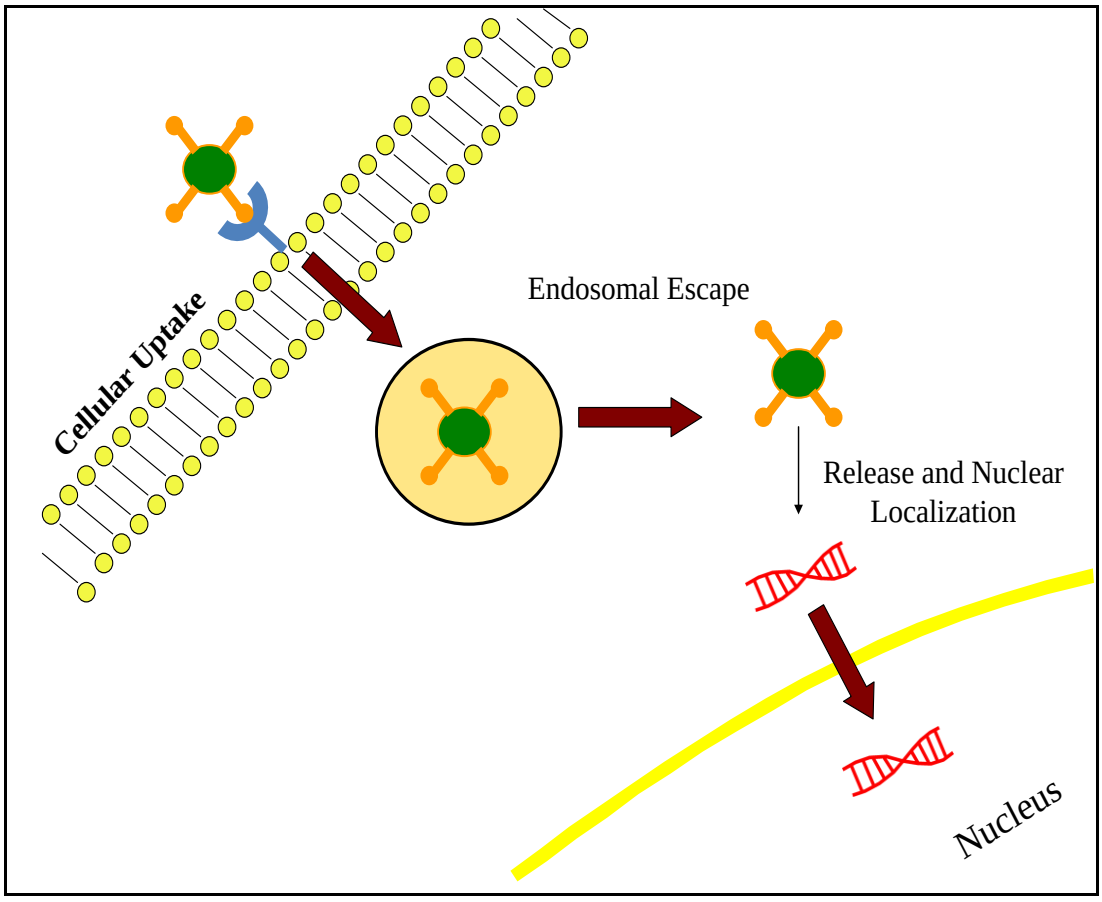

Figure 1-5. *Intracellular Barriers to DNA Delivery*. The schematic represents intracellular barriers associated with DNA delivery. Once the polyplexes reach the target cell, they internalize either by receptor mediated endocytosis or macropinocytosis. Polyplexes must escape from the endosome prior to transport to the lysosome (not depicted in figure). The ultimate target for DNA formulations is the nucleus, which represent the most formidable barrier in gene delivery.

internalization.[69-71] The most evolved polyplexes possess targeting ligands with greatly improved specificity. Several targeting ligands have been used to achieve targeted uptake of DNA polyplexes through receptor-mediated endocytosis (Table 1-1). The incorporation of ligands into polyplexes requires several considerations. The targeting ligand must be presented on the surface of the polyplex in order to properly bind with the

cellular receptor, and it must be efficiently internalized for significant uptake of DNA polyplexes into the cell. The ligand must be oriented to retain high affinity for the receptor, and it must be either on the termini of PEG or sufficient in size to project above the PEG layer on polyplexes. A high cell surface receptor density increases the percent of dose targeted to the cell, and the clustering of ligands on the polyplex may dramatically increase the affinity for cell surface receptor. DNA polyplexes with high selectivity for a particular cellular receptor can be achieved by preparing anionic polyplexes possessing targeting ligands that avoid non-specific binding to proteoglycans.[68]

While a targeting ligand is required to promote specific binding, polyplexes simultaneously require PEG to block non-specific binding. This is illustrated by the EPR effect, which drives PEGylated polyplexes to a tumor and requires high blood perfusion rates to increase the amount of polyplex accumulated (Figure 1-6).[72] PEGylation thereby aids in passive targeting to tumors, resulting in selective accumulation to tumor tissue and an increase in the residence time of the polyplex in the tissue.[73] Once the polyplex has reached the target tissue, targeting ligands enhance the internalization of polyplexes. In one study, PEGylated siRNA polyplexes with and without targeting ligand showed that the highest possible uptake occurs through non-specific macropinocytosis, followed by receptor-mediate endocytosis.[74] In the presence of a receptor agonist, the cellular uptake for the non-targeted polyplexes was not affected, while the targeted polyplexes showed a significant decrease on the cellular uptake. When the same formulations were administered via tail vein injection, PEGylated polyplexes containing the targeting ligand not only showed the highest tumor uptake, but they also showed the greatest luciferase silencing. These findings confirm that while PEG reduces the non-specific uptake of polyplexes, the addition of a targeting ligand on polyplexes improves cellular uptake.

A similar consideration for polyplex targeting design is illustrated through the biodistribution of glycopeptide-targeted polyplexes. A triantennary glycopeptide was used to improve the targeting properties to the hepatocyte asialoglycoprotein receptor.

Table 1-1. Targeting Strategies Used for Receptor-Mediated Endocytosis

Targeting Ligand	Target
RGD	Integrin subunits [75, 76]
Secretin	Pancreas [77]
EGF	Epidermal Growth Factor Receptors [78, 79]
Neurotensin	Neurotensin receptors in the brain [80]
Folate	Folate Receptor [81]
Asialoorosomucoid / Triantennary N-Glycan	Asialoglycoprotein/ Hepatocytes in the Liver [82-85]
High Mannose N-Glycans	Mannose Receptor/Dendritic Cells [86]
Transferrin	Transferrin Receptor [87, 88]
Fibroblast Growth Factors	Fibroblast Growth Factor Receptor [89, 90]
Antibodies	Surface Antigens [91-93]
Anisamide	Sigma Receptors [94]
Antibodies / Aptamers	Prostate Specific Membrane Antigen (PSMA)[95, 96]

Surprisingly, glycopeptide polyplexes were not able to significantly increase specific biodistribution to hepatocytes in the liver. [82] However, PEGylated glycopeptide polyplexes resulted in a significant and specific accumulation of 80% of the dose into

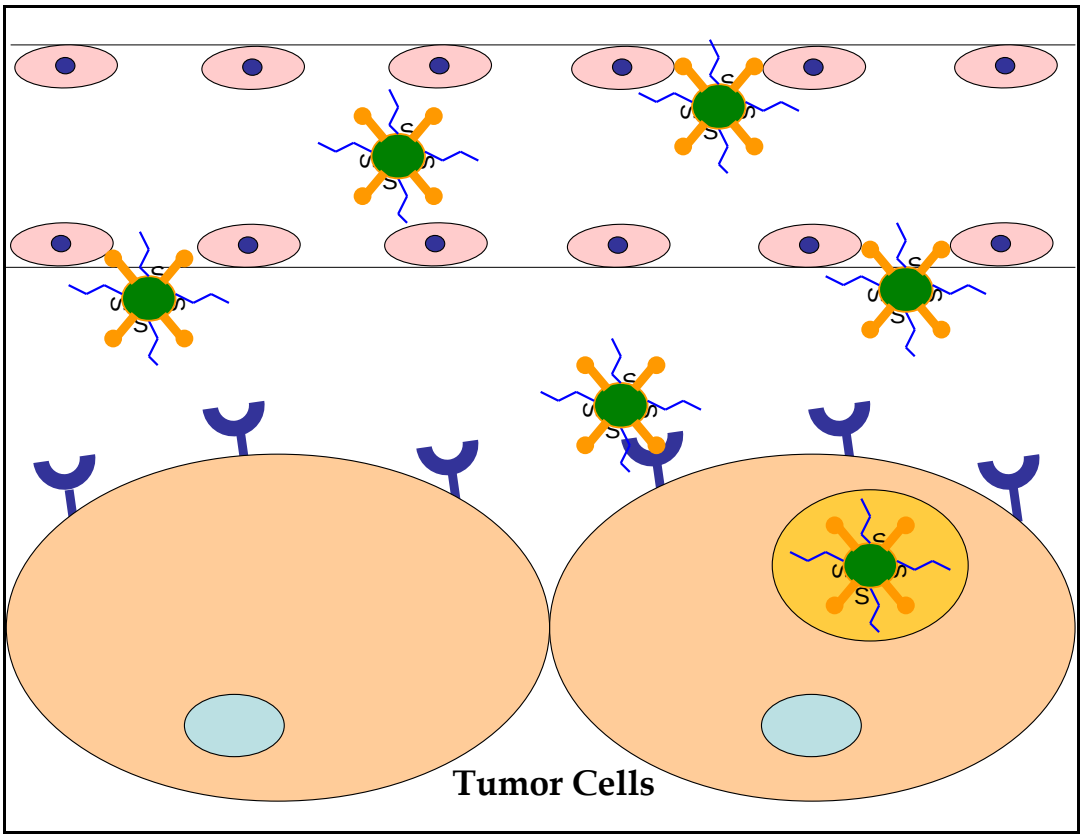

Figure 1-6. *Tumor Targeting Through the EPR Effect and Cellular Internalization.* The leaky blood vessels in solid tumors provides for wide fenestrations allowing the accumulation of PEGylated polyplexes. PEGylation provides for a long half-life and residence time for significant accumulation at the tumor site. Targeting ligands enhance cellular internalization through receptor-mediated endocytosis.

hepatocytes. Thus, a key feature to polyplex design is to maintain the physical properties needed for proper stealthing and ligand binding to achieve primary targeting of DNA in vivo.

Endosomal Escape

Once in the cell, the carrier must be able to escape endosomal trafficking to the lysosome to reach the cytoplasm of the cell and avoid metabolism. The endosome is

initially at a pH of 7, but rapidly acidifies to pH 5 during trafficking.[97] In vitro gene transfer experiments have demonstrated that enhancing endosomal escape through the incorporation of the lysosomotropic agent chloroquine can lead to higher transfection efficiencies.[98] Hence, engineering polyplexes that have built-in endosomal escape will likely improve the transfection properties in vivo.

Endosomal escape has been achieved by two different strategies. Polyethylene-imine (PEI) is the prototypic endosomal buffering agent that functions by buffering against the acidification of the endosome following endocytosis.[99] As the pH of the late endosome decreases, secondary amines on PEI are protonated. This buffering action creates an endosomal osmotic imbalance that results in bursting of the vesicle.[100] PEI has been shown to dramatically enhance gene transfer in vitro where it can be maintained at high concentrations in media, however, this does not translate to enhanced gene expression in vivo due to the dilution of PEI that occurs in the systemic circulation.

A second strategy for releasing DNA into the cytoplasm involves the use of fusogenic peptides. These are a class of 20-30 amino acid peptides that possess an amphiphilic α-helical structure.[101] The α-helical conformation allows insertion of the hydrophobic face into a cell membrane resulting in pore formation and lysis (Figure 1-7).[102] The activity of fusogenic peptides is concentration dependent and may also be pH dependent. Anionic fusogenic peptides are inactive at neutral pH, but become membrane lytic upon forming α-helices at pH 4-5.[103] Melittin and synthetic amphipathic peptides, such as JTS-1 and GALA, are commonly used fusogens to improve the gene transfer of polyplexes.[104-106]

Melittin is a cationic 26 amino acid peptide composed of two α-helices joined by an interrupting proline whose fusogenic activity is pH independent. Chen et al. created analogs of melittin with improved affinity for DNA following sulfhydryl polymerization.[107, 108] Poly-melittin remained inactive while bound to DNA, but rapidly depolymerized in the reducing environment of the cell to release the monomeric melittin

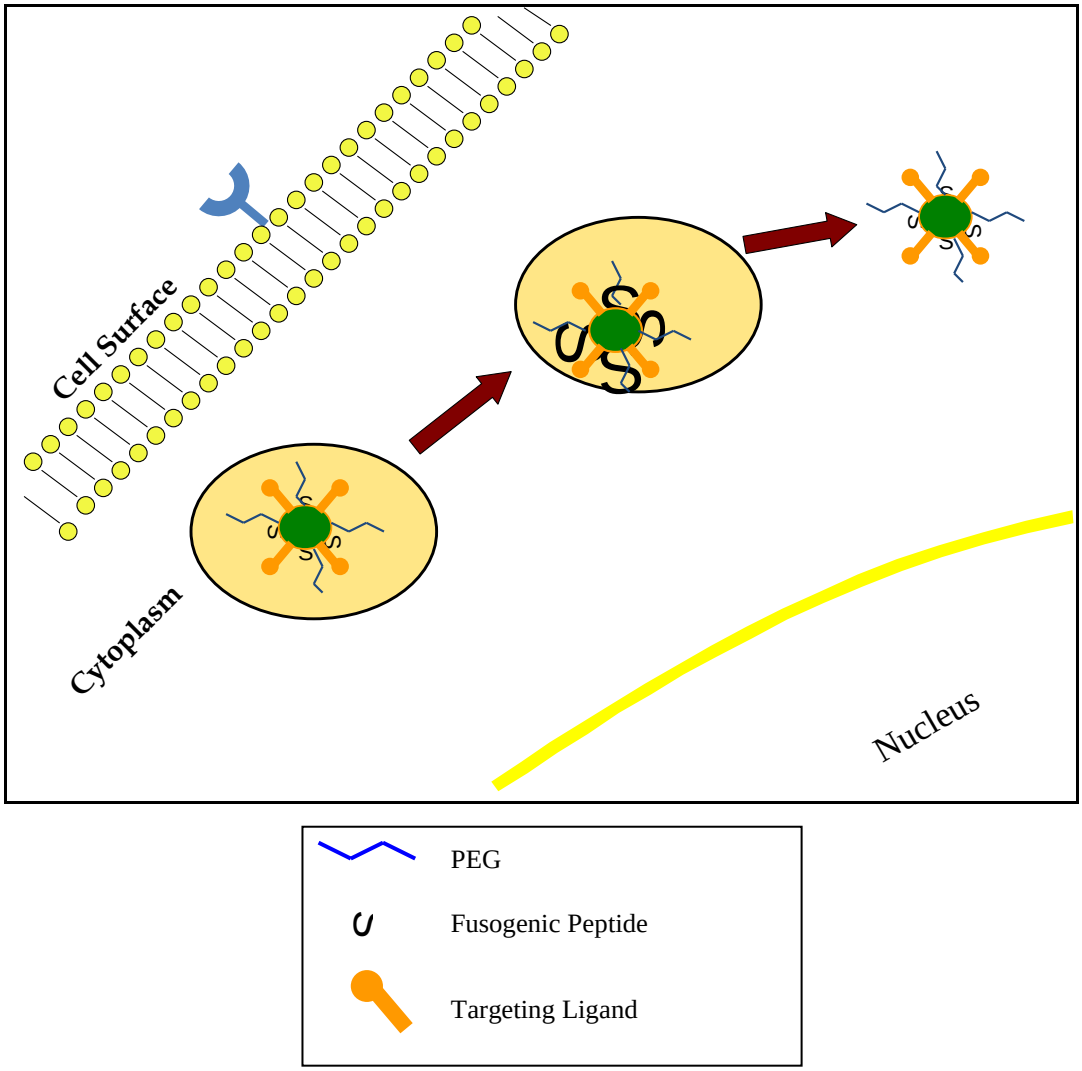

Figure 1-7. *Endosomal Escape and Fusogenic Peptides.* Following cellular internalization, DNA polyplexes can either escape the endosome and be released within the cytoplasm as shown on the figure or be metabolized after fusion with lysosomes by proteases and nucleases (not shown). Optimal DNA polyplex formulations contain pH-triggered fusogenic peptide (see coiled structure) that becomes membrane lytic in the low pH of the late endosome.

that mediated endosomal escape. These results illustrate the importance of releasing fusogenic peptides inside the endosome to increase gene transfer efficiency.

Improving DNA Release from Polyplexes

Once polyplexes escape the endosome and arrive in the cytoplasm, the DNA needs to be released for proper function. The release of DNA will thereby require the polyplex to disassemble with a cytoplasmic specific dissociation (Figure 1-8). Cross-linking strategies has been used to produce a controlled-release of DNA from polyplexes. Cross-linked polyplexes protect DNA from metabolic degradation and can potentially prolong the duration of gene expression.[109] The type of cross-linking strategy used will also influence the particle size, surface charge, biodegradation and release properties of DNA from the polyplex.[110, 111]

Amines on the surface of a polyplex have been cross-linked with dimethyl-3,3'-dithiobispropionimidate (DTBP) or glutaraldehyde. Although DTBP showed increased stability of polyplexes in salt, in vitro analysis indicated poor transfection abilities.[112] Similar results were observed with the glutaraldehyde cross-linked polyplexes. Adami et al. demonstrated that glutaraldehyde cross-linked polyplexes possessed remarkably improved physical and metabolic stability.[113, 114] Nevertheless, the slow reversal of the Schiff base resulted in negligible gene expression in vivo.[82, 113] Therefore, while amine-based cross-linking has shown the ability to improve the stability of polyplexes, this type of surface modification is limited due to the poor release properties of the cross-linked network.

Sulfhydryl cross-linking has also been investigated as a method to improve the stability and in vivo release characteristics of polyplexes. Several groups have shown that a single sulfhydryl group incorporated into cationic lipids dimerizes after binding DNA to enhance transfection properties.[115, 116] Similarly, low molecular weight peptides containing multiple cysteine residues were shown to oxidize after binding DNA.[117] Sulfhydryl cross-linking allows for release of DNA from polyplexes through reduction of disulfide bonds by glutathione in the cytoplasm.[118] McKenzie et al. developed improved DNA condensing peptides by substituting cysteine residues into the Cys-Trp-Lys_{18}

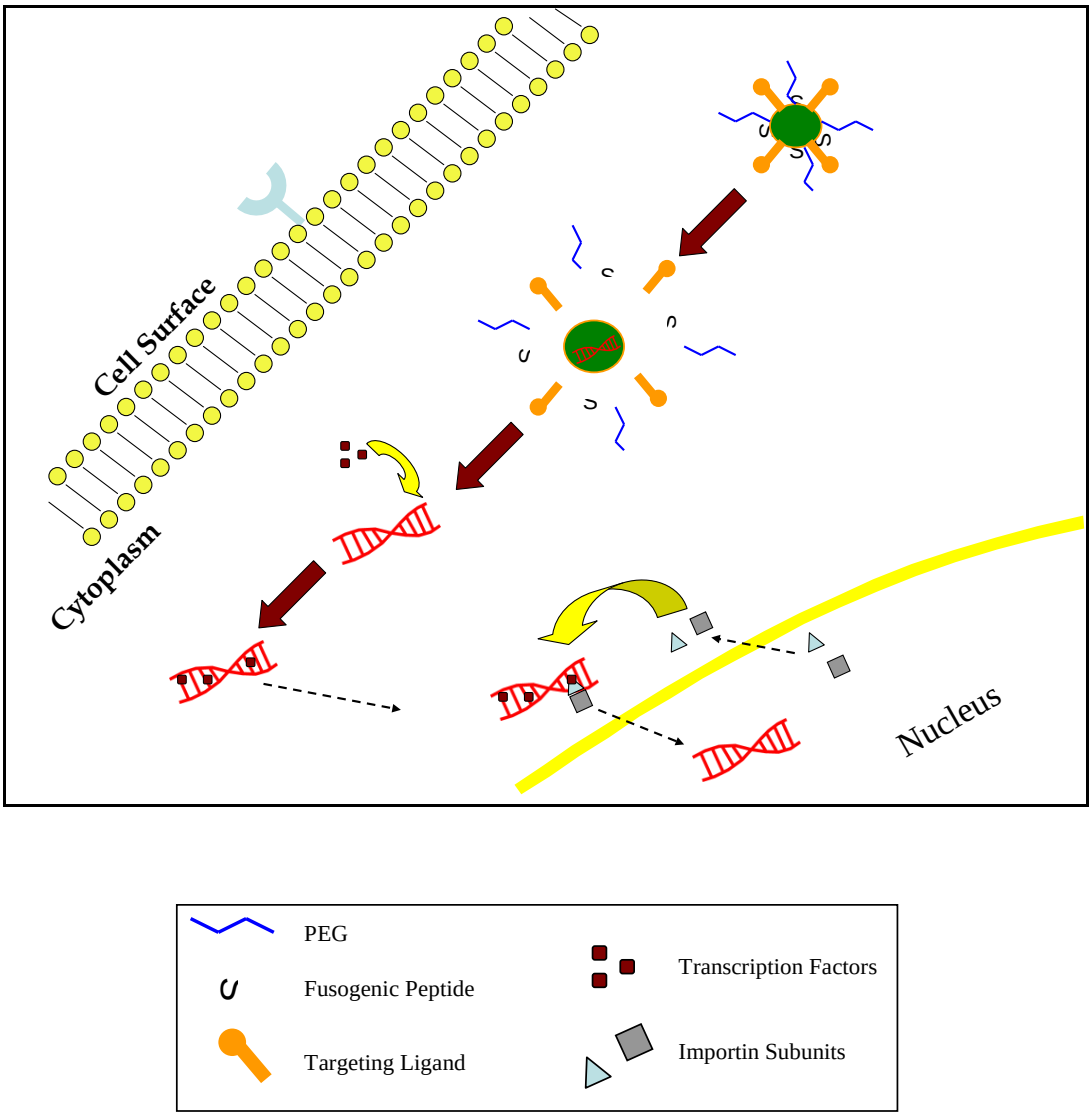

Figure 1-8. *DNA Release from Polyplex and Nuclear Localization of DNA.* Once the polyplex has reached the reducing environment of the cytoplasm, disulfide cross-linked polyplexes rapidly disassemble due to cellular glutathione levels and release DNA into the cytoplasm. Free DNA in the cytoplasm can localize to the nuclear pore complex through the binding of transcription factors that can bind importin α and β for shuttling across the nucleus.

(CWK_{18}).[117] In vitro transfection experiments with CWK_{18}, dimeric-CWK_{18}, and sulfhydryl cross-linked peptides demonstrated that a peptide possessing terminal cysteines ($CWK_{17}C$) mediated the highest gene transfer efficiency. These results have

been extrapolated to prepare sulfhydryl cross-linking glycopeptides and PEG peptides that form polyplexes that maintain stability in circulation, target specific cells, and release DNA in the cytoplasm.[119] Thus, optimal polyplex designs will contain PEG peptides for stealthing, targeting ligands for enhanced cellular uptake, and fusogenic peptides with a cytoplasmic-specific disassembly to maximize the amount of DNA that reaches the cytoplasm (Figure 1-9).

Nuclear Localization

The membrane that surrounds the nucleus contains a multimeric protein nuclear pore complex that regulates transport in and out of the nucleus. Small molecules are capable of passively diffusing across the small (~9 nm) diameter of these pores, whereas molecules larger than 10 nm require nuclear localizing sequences (NLS) for active shuttling into the nuclear envelope.[120] It has been demonstrated that DNA larger than 2000 bp is unable to freely diffuse in the cytoplasm,[121] suggesting that polyplexes require NLS modifications to efficiently transport the DNA that reaches the cytoplasm. NLS sequences provide recognition of the polyplex by members of importin proteins that mediate nuclear transport. Importin α binds to the NLS contained on the polyplex, which allows importin β to bind. The importin heterodimer then docks on the nuclear pore complex and allows for transport of the NLS containing cargo into the nucleus.

There are two approaches that have been attempted to improve polyplex delivery to the nucleus. The first is to incorporate DNA sequences that target plasmids into the nucleus, such as the targeting sequence on the SV40 enhancer (Figure 1-6).[121] These DNA targeting sequences contain binding sites for transcription factors, which shuttle the DNA to the nucleus.[122] The second strategy is by the covalent or non-covalent association of a NLS with DNA. The attachment of a NLS has been attempted by many different groups, [123-126] but none have been able to establish reliable improved in vivo efficiency. Thus it appears that the nuclear localization of polyplexes is one of the greatest hurdles to

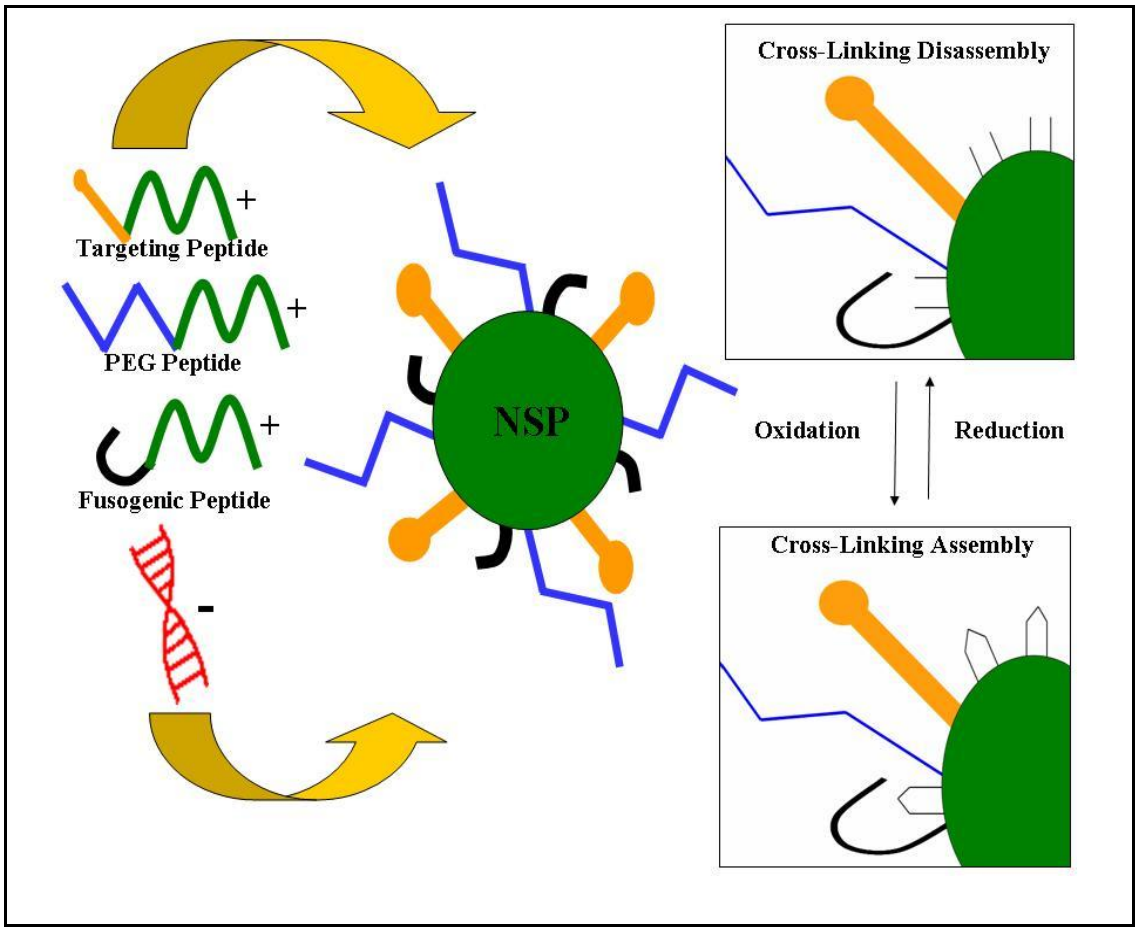

Figure 1-9. *Optimal Polyplex Design for Non-viral Gene Transfer.* Cytoplasmic-specific release can be achieved through the incorporation of thiols on DNA condensing cationic peptides. These peptides bind to DNA and form stabilized polyplexes that have a built-in intracellular triggered release. Optimal polyplex designs contain PEG-peptides for stealthing, targeting ligands for enhanced cellular uptake, and fusogenic peptides to maximize the amount of DNA that reaches the cytoplasm.

overcome. Fortunately, even without a nuclear targeted strategy, polyplexes may be efficient enough to express therapeutic levels of protein to treat certain diseases such as hemophilia.

Physical Methods for Improved DNA Delivery and Gene Expression

Improving cellular uptake, endosomal escape, and nuclear targeting remains a significant challenge in polyplex design. Physical gene transfer methods have been developed to bypass the systemic and cellular barriers associated with gene delivery.[127-131] Hydrodynamic dosing and electroporation are the most efficient non-viral delivery techniques, both of which work by very different delivery mechanisms (Table 1-2). Hydrodynamic delivery requires a rapid tail vein injection of a large volume of plasmid DNA in mice. The procedure results in the accumulation of the bolus in the inferior vena cava and creates high venous pressure that exceeds the pumping capacity of the heart (Figure 1-10).[132] The bolus is therefore directed to the liver due to its large size, expandable structure, and its direct vascular connection to the inferior vena cava.[132] Typically, the liver endothelium serves as a barrier for delivery into hepatocytes as only 6 to 8% of its surface consists of 100 nm diameter fenestrations that are generally too small for macromolecule delivery.[133] However, Zhang et al. demonstrated that the pressure induced during hydrodynamic injection enlarges the liver fenestrae to the micron scale, thus facilitating DNA transport across the capillary endothelial and successfully transfecting 40% of hepatocytes (Figure 1-10). [132]

In contrast, electroporation requires electrical pulses that create a membrane destabilization that allows for transport of macromolecules directly into cells both in vitro and in vivo.[46, 154-157] While tissue damage is typically observed using electrical fields above 100 V/cm,[158, 159] syringe electrodes have been developed that can deliver electric fields directly to the tissue and require field strengths between 50 and 100 V/cm for efficient DNA delivery.[157] Electroporation therefore requires tissue accessibility, and placement of the syringe electrode surrounding the administration site (Figure 1-11). Once in place, electrical pulses are administered that exceed the trans-membrane voltage

Table 1-2. Physical Methods for DNA Delivery

Method	**Driving Force**	**Entry Mechanism**	**Formulation**	**Tissues Transfected**
Electroporation	Electrochemical gradient	Voltage creates pores on the cell membrane that allows for cell entry	Formulation is typically in normal saline and transport favors smaller anionic molecules	Muscle,[134] cornea,[135] tendons,[136] liver,[137] bladder,[138] and brain tissue[139]
Hydrodynamic injection	Hydrostatic Pressure	The large volume administered provides for selective accumulation of macromolecules to highly perfused internal organs (liver)	Formulation is typically in normal saline and requires a rapid iv injection of a large volume (9% body weight)	Liver,[14] kidney,[140]skeletal muscle,[12, 13] myocardium,[141] and tumor tissue[142, 143]
Gene Gun	Particle Acceleration / Kinetic Energy	The DNA coated on the gold particle is released into the cell after the particles are accelerated through the tissue	Requires coating of DNA onto gold particles for delivery	Skin,[144, 145] liver,[146, 147] and tumors[147]
Ultrasound / Sonophoresis	Ultrasonic waves	Ultrasound waves generally enhance membrane permeability of drugs	Typically requires direct tissue injection prior to treatment	Vascular cells[148-151] and muscles[152, 153]

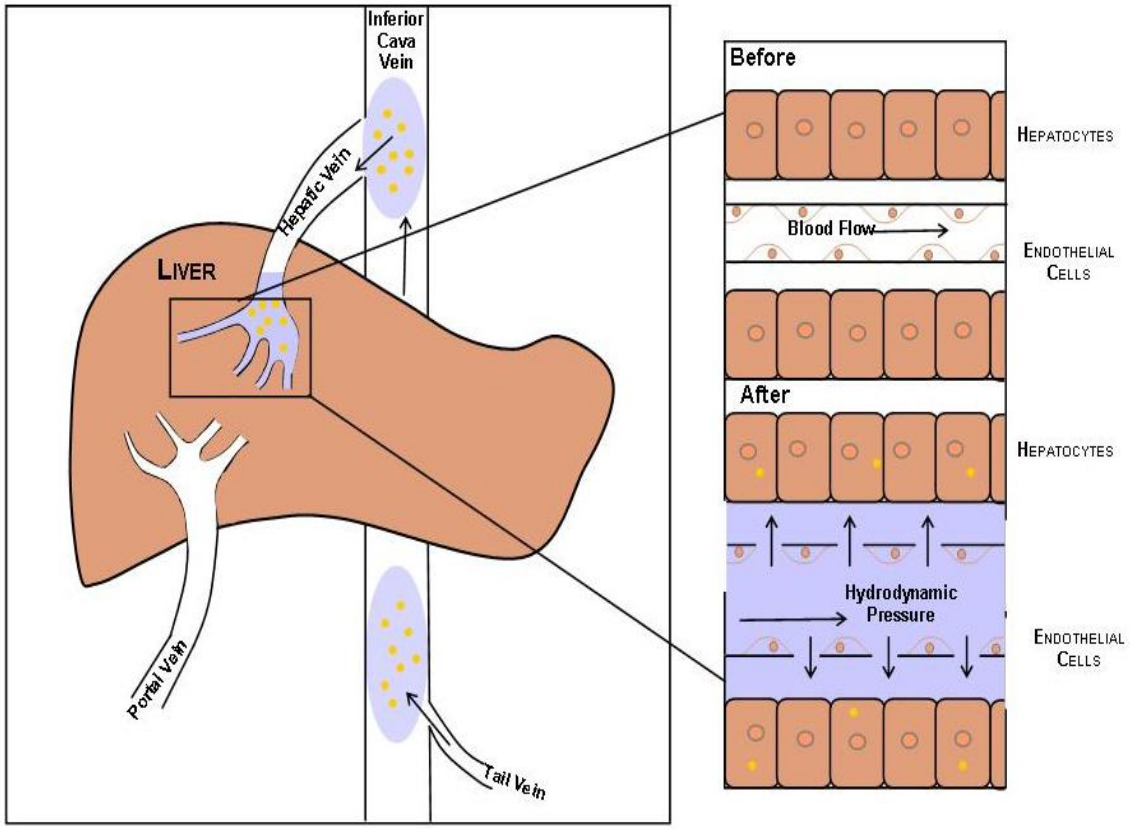

Figure 1-10. *Mechanism of Drug Delivery Using Hydrodynamic Injection*. Hydrodynamic injection requires a large volume bolus equivalent to 9% of the body weight of a mouse administered over 5 seconds. The bolus travels to the inferior cava vein and creates high venous pressure that directs the bolus to the liver through the hepatic vein. The hydrodynamic pressure created during administration enlarges the fenestration of the liver endothelium and allows for delivery of drug directly to the hepatocytes in the liver.

threshold required to create nanometer sized pores (20-120 nm)[156] on the surface of the cell membrane that re-seal within 3 seconds (Figure 1-11).[155, 160] Molecular transport of the drug during electroporation is based on the size, shape, and electric charge of the drug.[160] The mechanism of drug transport can be either through electrophoresis, electroosmosis, or diffusion. Research involving DNA electroporation has suggested that transport into cells during electroporation is mostly due to electrophoresis (Figure 1-12A).[155] Neutral drugs can also be electroporated into cells via the electoosmotic flow

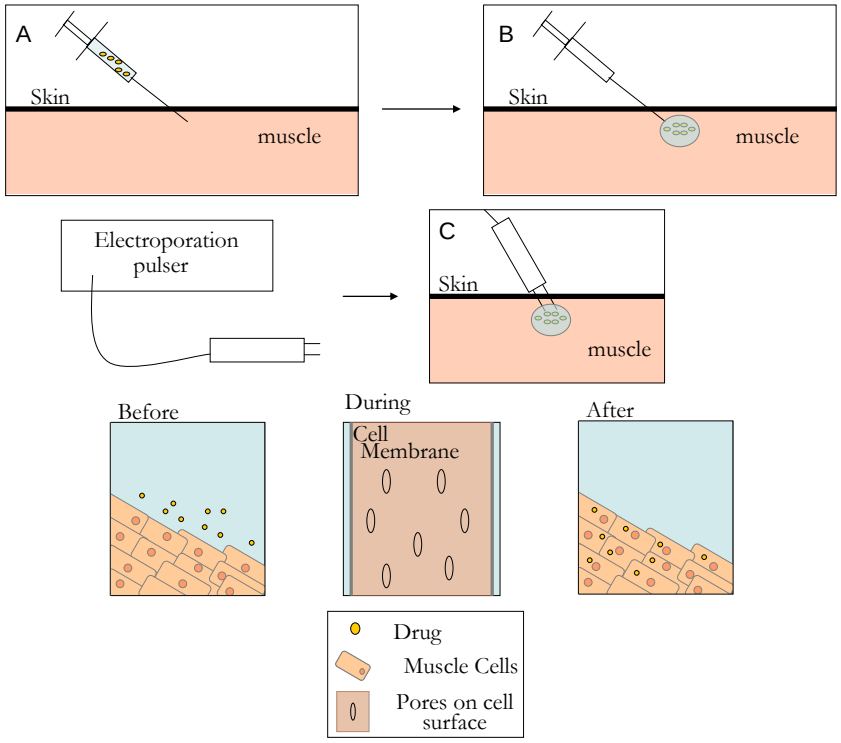

Figure 1-11. *Mechanism of Drug Delivery Using Intramuscular-Electroporation Administration (IM-EP).* Direct tissue injection of drug formulations bypasses biodistribution limitations that can impede drug delivery. IM-EP administration requires a direct intramuscular injection of a formulation prepared in normal saline for optimal drug transport during electroporation (panel A & B). Before the electrical pulses are administered by the electroporation pulser, the drug formulation resides in the fluids surrounding the tissue. The syringe electrode is then introduced into the tissue and is placed into the dosing site (panel C). Consecutive electric pulses are administered to create nanometer sized pores on the cell membrane that allow for transport of the drug into the cell during pulsing.

created by the electric field generated during pulsing, and cationic drugs are transported by a combination of electrophoresis and electroosmosis (Figure 1-12B).

The use of electroporation and hydrodynamic dosing in animals has firmly established that a small quantity of DNA (1 μg) is sufficient to attain therapeutic levels of gene expression in vivo.[161, 162] While these methods depend on different driving forces, they both improve the delivery of naked DNA directly into the cytoplasm relative to

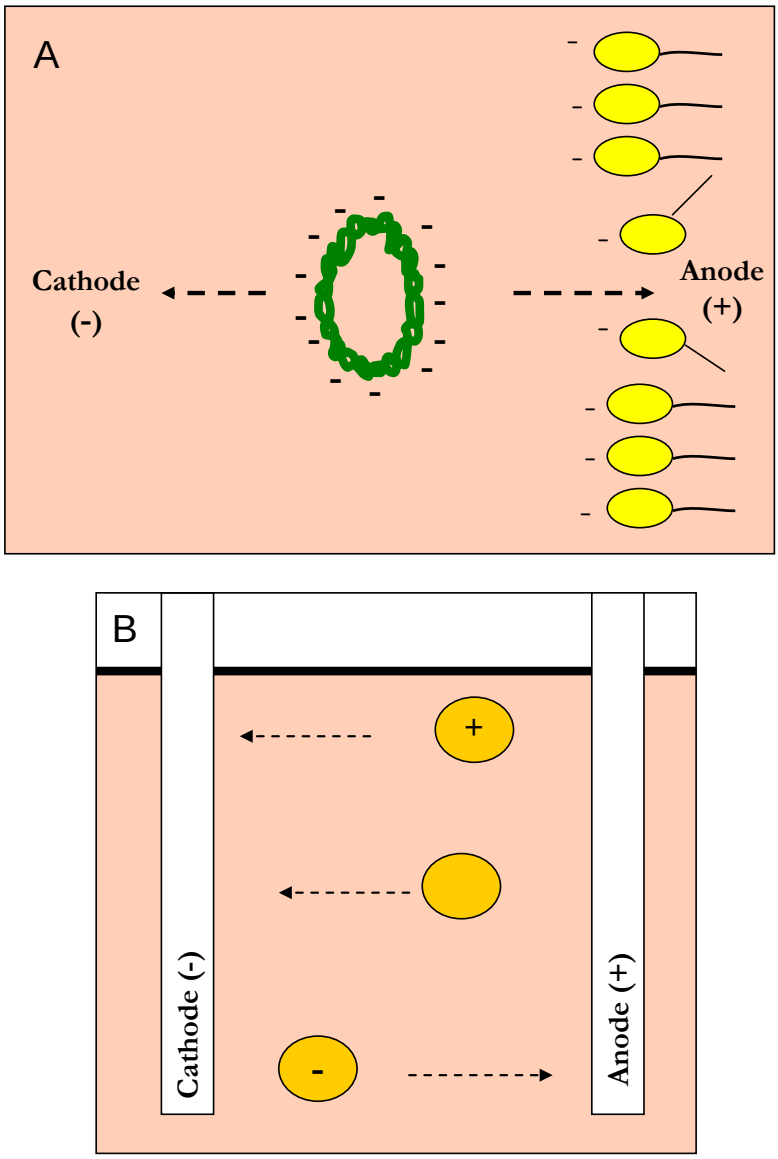

Figure 1-12. *Mechanism of Drug Transport Across the Cell Membrane During Intramuscular-Electroporation Administration (IM-EP).* There are three possible entry mechanisms for drug delivery across the anionic cell membrane during electroporation: electrophoresis, electroosmosis, and diffusion. Anionic molecules such as DNA will migrate towards the anode and uptake into the cell is largely due to electrophoresis (panel A (-) and panel B). Charge neutral drugs or polyplexes can also be transported into cells during electroporation through the electroosmotic flow created during electroporation (panel A), whereas cation polyplexes will be transported into cells by both electroosmosis and electrophoresis (panel A (+)). Diffusion does not play a large role in delivery during electroporation due to the short lifetime of the pores formed during pulsing.

polyplexes. The expression levels achieved by hydrodynamic dosing and electroporation represent the maximum efficiency that can be reached using the current DNA or siRNA constructs, thus serving as a bench mark for expression goals that should be reached by polyplexes. Nevertheless, several drawbacks associated with hydrodynamic dosing and electroporation limit the clinical application of these methods. Hydrodynamically dosed DNA requires large volumes that would be difficult to simulate in humans, while electroporation can possibly lead to tissue damage due to the high voltage applied, in addition to being limited to easily accessible tissues.[163] However, these methods provide an insight into the rate limiting steps that currently hinder polyplex delivery. Since hydrodynamic dosing and electroporation primarily bypass cellular internalization, endosomal escape, and carrier dissociation,[164] these physical methods suggest that current polyplex designs fail to either deliver enough DNA to the cytoplasm, or to release the DNA from the polyplex once in the cytoplasm. Furthermore, microinjection of DNA directly into the cytoplasm has demonstrated that as few as 10 plasmids are needed for gene expression.[122] Based on this and many other observations, it appears that polyplexes are currently limited in their ability to facilitate the delivery of DNA into the cytoplasm and achieve even this minimal delivery into the nucleus of quiescent cells.

Concluding Remarks

Previous non-viral delivery strategies have focused on relatively simple designs to package DNA. These strategies have proven to be insufficient in overcoming the rate limiting delivery barriers that impede transfection. Future non-viral delivery strategies will likely possess multi-component polyplexes to overcome these limitations. The multi-component polyplex will protect the DNA during transport, maximize the amount of DNA that enters the cell, and provide the release characteristics needed for enhanced transfection.

Physical methods of gene delivery suggest that increasing delivery to the cytoplasm may be sufficient to achieve enhanced efficiency. Thus, optimal polyplex designs will likely incorporate multiple delivery molecules, each optimized to overcome an individual barrier until reaching cytoplasm or nucleus. The assembly of such multi-component delivery systems requires careful design to preserve the function of each phase of delivery. Peptide-based carriers appear to provide the greatest synthetic flexibility, thus allowing the design of sophisticated polyplexes that mediate therapeutic levels of gene expression in vivo.

Statement of Problem

The main goals of any gene delivery system is to protect the DNA during transport, biodistribute the polyplex to the tissue of interest, achieve efficient cell entry, and successfully traffic throughout the cellular machinery and reach the destination of drug release. No in vivo non-viral DNA delivery system systemically administered has been capable of successfully achieving targeted DNA delivery and consequently gene expression. Many attempts have focused on improving a single component of the delivery process, and doing so creates polyplexes that are incompatible for in vivo use. While there has been much focus on improving receptor mediated endocytosis by incorporating a targeting ligand onto the DNA polyplex, there has been no thorough demonstration of a successful delivery systems that can extend the pharmacokinetic half-life of DNA by monitoring the metabolic protection of the plasmid in systemic circulation using gel electrophoresis. Improving the pharmacokinetic half-life of DNA is a prerequisite for achieving targeted delivery of DNA polyplexes.

Cationic lipids, peptides and polymers have been used extensively to package DNA by charge neutralization of the phosphate anions on the DNA backbone with the excess amines on the DNA condensing agent. The resulting cationic DNA nanoparticles have shown resistance against nuclease degradation but are nevertheless limited to in

vitro applications due to their surface charges and poor solubility. The multitude of complications that are associated with DNA condensation strategies has lead to the development of physical methods for improved gene delivery, and several are currently under development for clinical use.[165-167]

In order to improve non-viral gene therapy, DNA condensation methods require reform in order to avoid their high cationic surface properties. PEG has been frequently used to improve these limitations, but it falls short of achieving biocompatibility due to the premature dissociation of the nanoparticle while in transit.[82] Cross-linking methods have been used previously to react the excess amines on the surface of DNA nanoparticles, and while cross-linking has shown the ability to extend the metabolic stability of DNA to a liver half-life of 39 hours, no significant gene expression has been reported.[168]

Considering the current status of DNA delivery, the aim of this thesis is to develop anionic non-viral gene delivery systems that are biocompatible for in vivo applications and that can mediate high levels of gene transfer at low doses (1μg or 0.05 mg/kg) and volumes (50 μL) relative to the gene expression that can be obtained using physical interventions. Furthermore, non-viral gene carriers are combined with physical administration methods throughout the thesis in order to provide a positive gene expression read-out assay that can demonstrate gene activity and eventually lead to the development of successful gene carriers. Emphasis in the thesis is placed on preparing DNA polyplexes that are resistant to DNase degradation, and on using the physical properties of the polyplex (binding affinity, size, charge, and morphology) to provide a detailed mechanistic explanation for the results in order to establish reliable predictive tools that can ultimately lead to the goal of successful gene expression.

The main objective of the thesis is to develop anionic DNA polyplexes using peptide-based gene delivery systems. Further objectives are to confirm the high affinity binding of the gene delivery peptides for DNA relative to that Cys-Trp-Lys_{18} which

requires 0.3 nmol per μg of DNA to fully compact the plasmid into nanoparticles.[169] The reversible association of the peptide-based molecular conjugates with DNA is evaluated by measuring the luciferase expression of each formulation when delivered by either electroporation or hydrodynamic injection and measured using bioluminescence imaging (BLI). The ability of anionic DNA polyplexes to extend the pharmacokinetic half-life of plasmid DNA will be evaluated using radiolabeled DNA.

CHAPTER 2: DISCOVERY OF METABOLICALLY STABILIZED ELECTRONEGATIVE POLYACRIDINE-PEG PEPTIDE DNA OPEN POLYPLEXES

Abstract

Cationic condensing peptides and polymers bind electrostatically to DNA to form cationic polyplexes. While many cationic polyplexes are able to achieve in vitro transfection mediated through electrostatic interactions, few have been able to mediate gene transfer in vivo. The present study describes the development and testing of polyacridine PEG-peptides that bind to plasmid DNA by intercalation resulting in electronegative open polyplex DNA. Polyacridine PEG-peptides were prepared by chemically conjugating 6-(9-acridinylamino) hexanoic acid onto side chains of Lys in PEG-Cys-Trp-$(Lys)_{3, 4, or 5}$. The resulting PEG-Cys-Trp-$(Lys\text{-}(Acr))_{3, 4, or 5}$ peptides bound tightly to DNA by polyintercalation, rather than by ionic interactions. Unlike polycationic polyplexes, polyacridine PEG-peptide polyplexes were anionic and open coiled, as revealed by zeta potential and atomic force microscopy. PEG-Cys-Trp-$(Lys\text{-}(Acr))_5$ showed the highest DNA binding affinity and the greatest ability to protect DNA from metabolism by DNase. Polyacridine PEG-peptide DNA open polyplexes were dosed intramuscularly and electroporated in mice to demonstrate their functional activity in gene transfer. These results establish polyacridine PEG-peptide DNA open polyplexes as a novel gene delivery method for in vivo use (reproduced with written permission from ACS Publications).

Introduction

Nonviral gene delivery systems have traditionally relied on reversible binding between cationic carriers and anionic oligonucleotides.[100, 170, 171] The resulting lipoplexes and polyplexes typically possess a positive surface charge as determined by zeta potential measurements. While cationic DNA lipoplexes and polyplexes have shown the ability to

mediate in vitro gene transfer through electrostatic binding to cell surfaces, they exhibit poor gene transfer properties in vivo, in part due to their overall cationic charge.[172, 173] There have been many attempts to mask the positive charge of cationic polyplexes with polyethylene glycol (PEG) to improve blood compatibility.[51, 174-178]

Alternatively, it is difficult to prepare an electronegative DNA polyplex using cationic polymers. This has been attempted by either partially titrating a polycationic polymer with plasmid DNA or by using a layer-by-layer addition of oppositely charged polymers in an attempt to reverse the charge of the polyplexes.[179-181] The resulting electronegative polyplexes are formed in a delicate and unstable equilibrium.[84] Attempting to reverse the charge of a cationic polyplex with the addition of an anionic polymer can lead to dissociation of the DNA. Similarly, if titrated to below the charge equivalency point, the polyplex is not completely protected against DNase, whereas if titrated to charge equivalency, the resulting neutral polyplexes are hydrophobic and aggregate. Titration past the equivalency point, results in collapse of a polyplex into a cationic colloidal particle that is relatively stable but highly cationic and thereby less compatible with blood components.[173] Consequently, we sought to find an alternative approach to ionic binding to DNA that would result in stable electronegative polyplexes.

In principle, the high affinity DNA binding achieved by polyintercalation could result in metabolically stable electronegative polyplexes.[182] Electronegative polyplexes may bind to fewer proteins and thereby be more blood and tissue compatible to allow delivery via intramuscular electroporation (IM-EP).[46, 183-185]

Polyacridine containing polymers have been previously investigated as gene transfer agents by Szoka, Vierling and Neilsen.[32, 36, 38] Their studies utilized polyacridine polymers possessing either one, two or three acridine units conjugated to either a neoglycopeptide or a nuclear localizing sequence. While these polyacridine carriers could bind to DNA, they possessed modest gene transfer activity in vitro.[32, 38] Alternatively, we have recently reported that a polyacridine peptide modified with a melittin fusogenic

peptide is a potent in vitro gene transfer agent.[186] The most potent polyacridine-melittin gene delivery peptide contained four acridines and possessed a sequence of $(Lys\text{-}Acr)_4$-Cys joined to melittin by a disulfide bond. Polyacridine-melittin bioconjugates formed electropositive DNA polyplexes in which their potency was dependent upon the number of acridines, the identity of the spacing amino acid, and the presence of a reducible disulfide bond between polyacridine and melittin.

To date, there are no reports of polyacridine peptides modified with PEG. The present study demonstrates a synthetic strategy to modify the side chains of Lys in PEG-Cys-Trp-$(Lys)_n$ peptides with acridine. The resulting PEG-Cys-Trp-$(Lys(Acr))_n$ peptides bind reversibly to DNA through intercalation and demonstrate the ability to form a unique electronegative open polyplex DNA structure that is protected from DNase and maintains transfection competency in vivo. The unique properties of PEGylated polyacridine DNA electronegative open polyplexes afford desirable characteristics that are more compatible with in vivo non-viral gene delivery compared to cationic polyplexes.

Materials and Methods

N-terminal Fmoc protected amino acids, 9-hydroxybenzotriazole (HOBt), diisopropylcarbodiimide (DIC), and Wang resin were purchased from Advanced ChemTech (Lexington, KY). Sephadex G-25, HEPES buffer, tris(2-carboxyethyl)-phosphine hydrochloride (TCEP), diisopropylethylamine (DIPEA), piperdine, acetic anhydride, triisopropylsilane (TIS), DNase I (EC 3.1.21.1), 9-chloroacridine, and thiazole orange were obtained from Sigma Chemical Co (St. Louis, MO). Acetonitrile, N,N-Dimethylformamide (DMF), and trifluoroacetic acid (TFA) were purchased from Fisher Scientific (Pittsburgh, PA). Agarose was obtained from Gibco-BRL. mPEG-maleimide 5000 Da was purchased from Nektar (Huntsville, AL), mPEG-amine (5,000 Da) was purchased from Creative Biotechnology (Winston-Salem, NC), and bis-amino PEG

(2,000 Da) was purchased from Iris Biotech GmbH (Marktredwitz, Germany). The 5.3 kb luciferase plasmid, pGL3 control vector, containing a SV40 promoter and enhancer was obtained from Promega (Madison, WI). Plasmid DNA was amplified in DH5α strain of *E. coli* and purified according to the manufacturer's instructions.

Synthesis and Characterization of PEGylated Cys-Trp-Lys_n Peptides

Cys-Trp-Lys_n synthesis was carried out using standard Fmoc chemistry on a computer interfaced Advanced Chemtech APEX 396 solid phase peptide synthesizer with 9-hydroxybenzotriazole and diisopropylcarbodiimide double couplings followed by N-capping with acetic anhydride as described previously.[187] Cleavage and deprotection were accomplished by reacting the resin with TFA: TIS: water (95:2.5:2.5) at RT for 3 hrs. The crude peptide was precipitated in cold diethyl ether, centrifuged, and the supernatant was decanted. Crude peptides were reconstituted in 0.1% TFA and purified on a preparatory Isco 2350 RP-HPLC (Lincoln, NE) using a Vydac C18 column (2 x 25 cm) eluted at 10 mL/min with 0.1 v/v% TFA and a gradient of acetonitrile of 5-25% over 30 min while monitoring Abs 280 nm, where the purification parameters used were optimized elsewhere.[169] Purified peptides were reconstituted in 0.1% TFA and quantified by Abs (Trp ε_{280nm} = 5600 M^{-1} cm^{-1})[188] using a Beckman DU 640 spectrophotometer (Fullerton, CA) to determine the isolated yield of 30% (Figure 2-1A-C). The purified peptides were characterized using an Agilent 1100 LC-MS (Waldbronn, Germany) by separation on a Vydac C18 analytical column (0.47 x 25 cm) eluted at 0.7 mL/min with 0.1% TFA and a gradient of acetonitrile of 5-25% over 30 min (Figure 2-2A) while detecting ESI-MS in the positive ion mode (Figure 2-2A, Inset).

PEGylation of the Cys residue on Cys-Trp-$Lys_{3,\ 4\ and\ 5}$ was achieved by reacting 0.9 mol equivalents of peptide with 1 mol equivalent of $PEG_{5000\ Da}$-maleimide in 100mM sodium phosphate buffer pH 7 for 1 hr at RT.[187] PEGylated peptides were purified on a

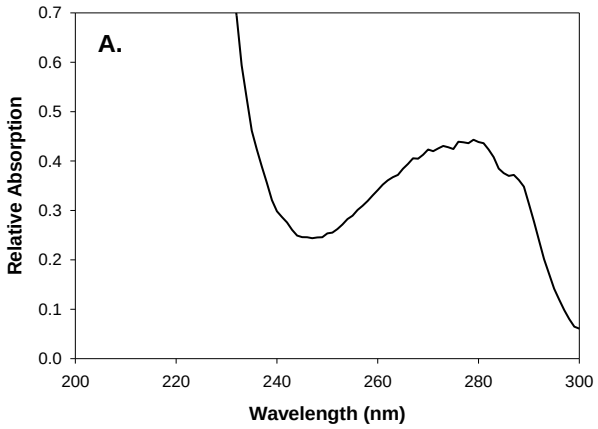

B. Concentration Calculation for Cys-Trp-Lys_3

Abs = Molar Absorptivity *Path Length *Concentration

$$\text{Concentration} = \frac{\text{Abs}}{\text{Path Length x Molar Absorptivity}}$$

$$\text{Concentration} = \frac{0.43851}{1\text{ cm x }5600\ M^{-1} * cm^{-1}} = 78.3\ \mu M$$

C. Reaction Yield

$$\text{Yield} = \left(\frac{\text{Actual Moles of Peptide}}{\text{Predicted Moles of Peptide}}\right) * 100$$

$$\text{Yield} = \left(\frac{300\text{ nmol}}{1{,}000\text{ nmol}}\right) * 100 = 30\%$$

Figure 2-1. *Concentration and Yield Determination of Cys-Trp-Lys3*. The absorption spectra (Panel A) of purified PEG-Cys-Trp-Lys3 reconstituted in 0.1% TFA was quantified (Trp ε_{280nm} = 5600 M^{-1} cm^{-1}) as shown on Panel B to determine an isolated yield of 30% (Panel C).

G-25 column (2.5 x 50 cm, Sigma Chemicals, St. Louis, MO) eluted with 0.1% acetic acid while monitoring Abs 280 nm. The peak corresponding to the PEG-peptide eluted in the void volume (100 mL), was pooled, concentrated by rotary evaporation, and freeze-dried. The PEG-peptide was reconstituted in 0.1% TFA, and quantified by Abs (Trp ε_{280nm} = 5600 M^{-1} cm^{-1}) to determine an isolated yield of 80%. PEG-peptides were characterized by MALDI-TOF MS by combining 1 nmol with α-cyano-4-hydroxycinnamic acid (CHCA) prepared in 50% (v/v) acetonitrile and 0.1% TFA. Samples were spotted onto the target and ionized on a Bruker Biflex III Mass Spectrometer (Billerica, MA) operated in the positive ion mode (Figure 2-3A-B).

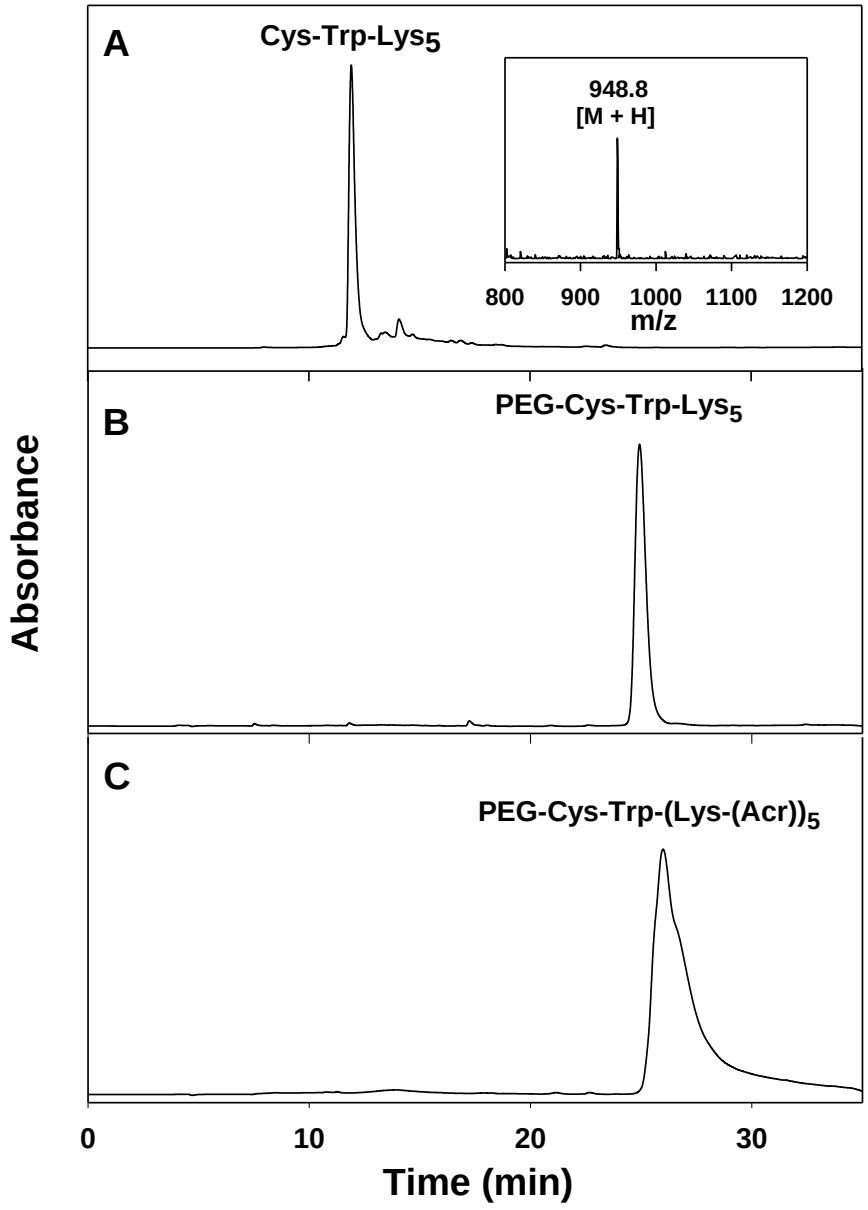

Figure 2-2. *RP-HPLC Analysis of PEG-Cys-Trp-(Lys-(Acr))$_5$*. Cys-Trp-(Lys)$_5$ elutes at 10 min on RP-HPLC eluted with 0.1% TFA and an acetonitrile gradient 5-60% over 30 min while detecting Trp by Abs at 280 nm (panel A). The inset shows the ESI-MS of Cys-Trp-Lys$_5$ with an [M+H] = 982.8 Da. Purified PEG-Cys-Trp-(Lys)$_5$ elutes at 24 min under identical gradient and detection (panel B). Purified PEG-Cys-Trp-(Lys(Acr))$_5$ elutes as a broad peak at 25 min and is detected by Abs 409 nm due to acridine (panel C). Acridine conjugation onto the PEG-peptides was done in collaboration with Kevin Anderson, Medicinal and Natural Product Chemistry, University of Iowa.

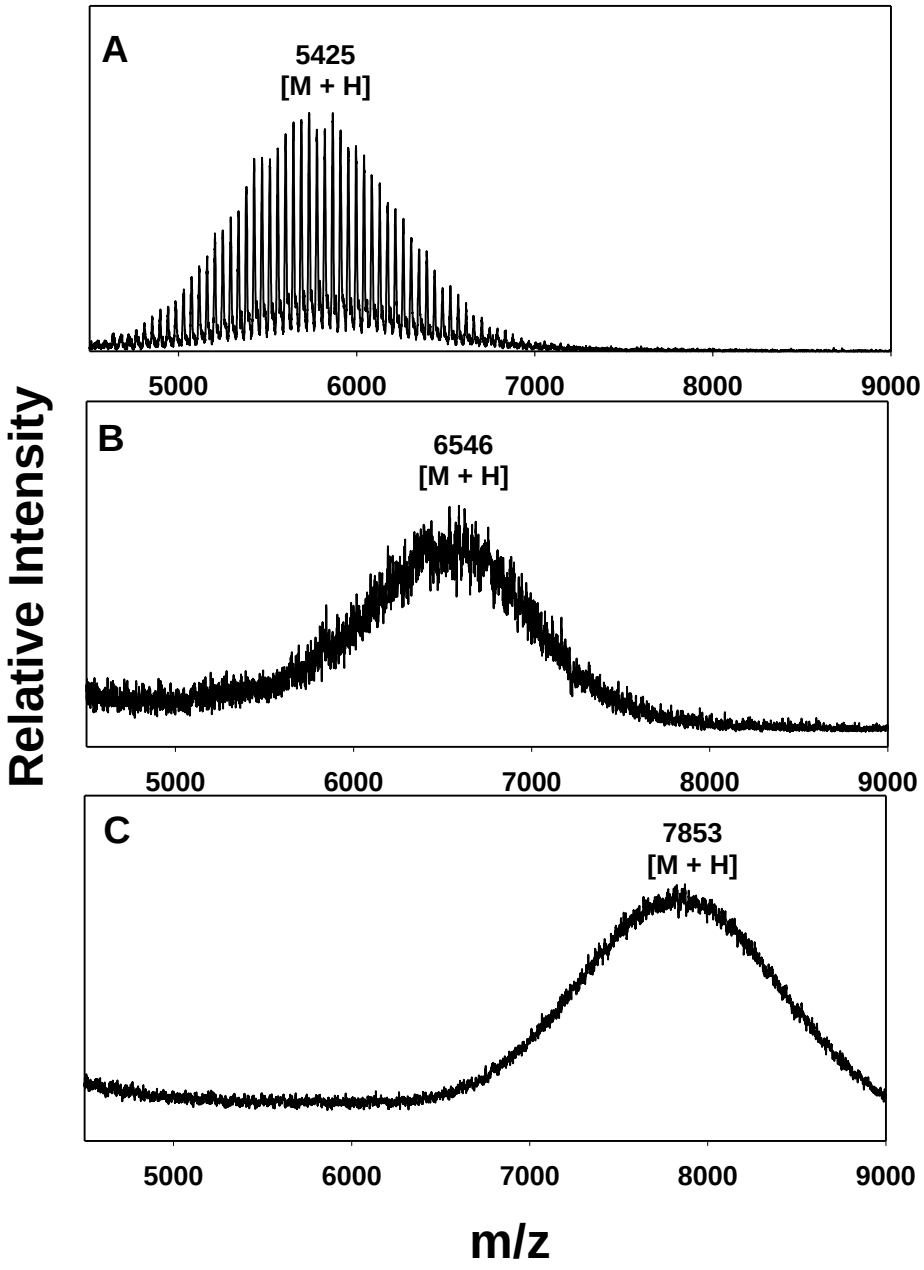

Figure 2-3. *Mass Spectral Analysis of PEG-Cys-Trp-(Lys(Acr))$_5$.* MALDI-TOF MS analysis PEG$_{5000\ Da}$-maleimide resulted in an average mass with m/z of 5425 (panel A). MS analysis of PEG-Cys-Trp-(Lys)$_5$ resulted in a mass shift of 1121 Da, consistent with the formation of the PEG-peptide with m/z of 6546 (panel B). Following conjugation of five 6-(9-acridinylamino) hexanoic acid residues (290 g/mol), the average mass increases by 1307 Da, consistent with the formation of PEG- Cys-Trp-(Lys(Acr))$_5$ with m/z of 7853 (panel C).

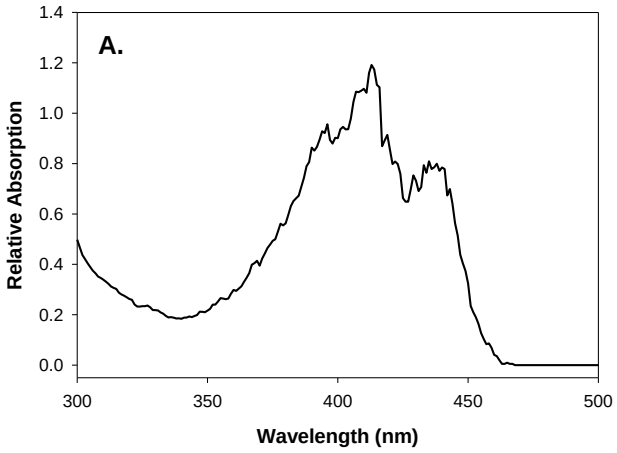

B. Concentration Calculation for PEG-Acridine

Abs = Molar Absorptivity *Path Length *Concentration

$$\text{Concentration} = \frac{\text{Abs}}{\text{Path Length x Molar Absorptivity}}$$

$$\text{Concentration} = \frac{1.08956}{1\text{ cm x }9266\ M^{-1} * cm^{-1}} = 117.6\ \mu M$$

C. Reaction Yield

$$\text{Yield} = \left(\frac{\text{Actual Moles of Peptide}}{\text{Predicted Moles of Peptide}}\right) * 100$$

$$\text{Yield} = \left(\frac{1.26\ \mu mol}{3\ \mu mol}\right) * 100 = 42\%$$

Figure 2-4. *Concentration and Yield Determination of Mono-Acridine PEG*. The absorption spectra (Panel A) of purified PEG-Acridine reconstituted in 0.1% TFA was quantified (Acr ε_{409nm} = 9266 M^{-1} cm^{-1}) as shown on Panel B to determine an isolated yield of 42% (Panel C).

Synthesis of Polyacridine PEG Peptides and Mono and Bis-Acridine PEGs

6-(9-Acridinylamino) hexanoic acid was prepared according to a prior published procedure.[189] The carboxyl group on 6-(9-acridinylamino) hexanoic acid was activated with 1.1 mol equivalents of N,N'-diisopropylcarbodiimide (DIC) and 1-hydroxy-benzotriazole (HOBt) in Dimethylformamide (DMF). Activated 6-(9-acridinylamino) hexanoic acid (12 mol equivalents) was reacted with 2.5 μmol of PEG-Cys-Trp-$Lys_{3,\ 4,\ and\ 5}$ in 3 mL of DMF at RT for 24 hrs. The PEG-Cys-Trp-$(Lys(Acr))_{3,\ 4,\ and\ 5}$ peptides were purified using a G-25 column (2.5 x 50 cm) eluted with 0.1 % acetic acid while monitoring Abs 280 nm. The product peak eluting at 100 mL was pooled, freeze dried on

a Freezone 4.5 (Labconco, Kansas City, MO), and characterized using MALDI-TOF MS as described above (Figure 2-3C). A yield of 42% of PEG-Cys-Trp-(Lys(Acr))$_{3,\ 4,\ \text{and}\ 5}$ peptides was determined by acridine Abs (ε_{409nm} = 9266 M^{-1} cm^{-1})[190] assuming additivity of acridine molar absorptivity and complete conjugation to the ε-amine of Lys (Figure 2-4A-C). Similarly, mono and bis-acridinylated PEGs were prepared by reacting 6 mol equivalents of activated 6-(9-acridinylamino) hexanoic acid with PEG-amine or bis-amino PEG (2 μmol) in 2 mL of DMF. The acridinylated PEGs were purified by G-25 column and characterized by MALDI-TOF MS (Figure 2-5A & B).

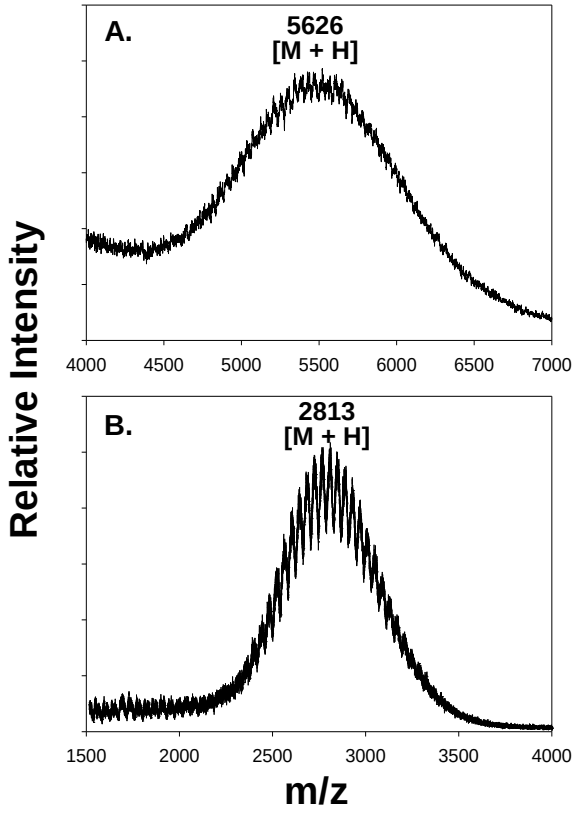

Figure 2-5. *MALDI-TOF MS Characterization of Acridinylated PEGs*. MALDI-TOF MS analysis of purified mono-acridine PEG resulted in an average mass with m/z of 5626 (Panel A). Similarly, MALDI-TOF analysis of Bis-Acridine-PEG resulted in an average mass with m/z of 2813 (Panel B).

Thiazole Orange Displacement Assay

The binding of polyacridine PEG-peptides to DNA was determined using an intercalator dye displacement assay.[117] Plasmid DNA (pGL3, 1 μg) was prepared in 5 mM HEPES pH 7.4 containing 0.1 μM thiazole orange. Polyacridine PEG-peptides were added to pGL3 to prepare samples of 0, 0.25, 0.5, 1, 2, 3, and 4 nmol per μg of DNA in a final volume of 500 μL. The fluorescence intensity of each sample was measured using an LS50B fluorometer (Perkin-Elmer, UK) with an excitation wavelength of 500 nm while monitoring emission at 530 nm. The data were converted to percent by comparison to the fluorescence intensity of thiazole orange in buffer (0%) and pGL3 with fully bound thiazole orange (100%) (Figure 2-6).

Gel Band Shift and DNase Protection Assay

pGL3 (1 μg) or DNA polyplexes (1 μg) prepared in 18 μL of normal saline were combined with 1 nmol of either mono-acridine PEG, bis-acridine PEG, PEG-Cys-(Lys-Acr)$_3$, PEG-Cys-(Lys-Acr)$_4$, or PEG-Cys-(Lys-Acr)$_5$ and 2 μL of loading buffer (40% sucrose, 0.25% bromophenol blue).[113] A 1% agarose gel (50 mL) was prepared in TAE buffer (40 mM Tris-acetate and 1 mM EDTA, pH 8) and microwaved for 30 seconds to dissolve the agarose, and then poured and cooled at room temperature for 30 minutes. The samples were loaded onto gel and electrophoresed in TAE buffer at 80 V for 90 min. The gel was stained in 2 mg/mL ethidium bromide at 5°C overnight, and the transilluminated gels (UVP Dual Intensity UV Transilluminator, Upland, CA) were photographed using Polaroid 667 film. pGL3 (1 μg) or DNA polyplexes (1 μg) prepared with 1 nmol of either mono-acridine PEG, bis-acridine PEG, PEG-Cys-(Lys-Acr)$_3$, PEG-Cys-(Lys-Acr)$_4$, or PEG-Cys-(Lys-Acr)$_5$ in 20 μL of normal saline were incubated with 0.06 U of DNase I at 37°C for 0-20 min.[25] The samples were applied to a 1% agarose gel and electrophoresed as described above.

A. Relative Fluorescence Intensity

Sample	DNA Alone	PEG-Acridine (nmol per μg)					
	0	0.25	0.5	1	2	3	4
1	67.60	70.02	67.58	69.12	58.65	61.99	55.36
2	67.50	68.40	66.68	66.49	67.10	60.59	58.72
3	63.50	68.61	72.68	69.07	68.44	61.07	57.78
Average	66.20	69.01	68.98	68.23	64.73	61.22	57.29
Std	2.34	0.88	3.24	1.50	5.31	0.71	1.73

B. $\text{Percent Fluorescence Intensity (\%)} = \frac{\text{Fluorescence of Polyplex}^{a}}{\text{Fluorescence of DNA}^{a}}$

C. Percent Fluorescence Intensity

	DNA Alone	PEG-Acridine (nmol per μg)					
	0	0.25	0.5	1	2	3	4
%	100.00	104.24	104.19	103.06	97.77	92.47	86.54
Std	3.54	1.33	4.89	2.27	8.02	1.08	2.62

a. Containing 0.1 μm Thiazole Orange

Figure 2-6. *Example Calculation of Thiazole Orange Displacement Assay Results*. DNA samples (1 μg) were prepared in 5 mM HEPES pH 7.4 containing 0.1 μM thiazole orange. Mono-acridine PEG was added to DNA to prepare samples of 0, 0.25, 0.5, 1, 2, 3, and 4 nmol per μg of DNA in a final volume of 500 μL. The fluorescence intensity of each sample was measured (Panel A), and the data was converted to percent (Panel B) by comparison of the fluorescence intensity of pGL3 with fully bound thiazole orange (100%) to that of DNA polyplexes (Panel C).

Particle Size and Zeta Potential of Polyacridine PEG-peptide DNA Open Polyplexes

Polyacridine PEG-peptide DNA polyplexes were formed by combining 10 μg of pGL3 (in 500 μL of 5 mM HEPES pH 7.4) with an equal volume containing either 1, 2, 4, 8, 12, 16, or 20 nmol of polyacridine PEG-peptide while vortexing. The polyplexes were equilibrated at RT for 30 min prior to analysis of particle size (QELS) and zeta potential using a Brookhaven ZetaPlus (Brookhaven Instruments, Holtsville, NY). Clear polystyrene square cuvettes (10 mm, Brookhaven, Holtsville, NY) were used during analysis, and QELS was performed at 25°C with instrumental parameters set with a refractive index of 1.59 and a scatter angle of 90° (Figure 2-7A-C). The apparent particle

size diameters and the zeta potential of the major peak observed (-26.4 mV, Figure 2-7C) are reported as the mean and standard deviation of ten measurements (Figure 2-7A). The polydispersity reported (polydispersity = μ_2 / Γ^2, where Γ and μ_2 are the first two moments of the distribution) has no units and is between 0.000 to 0.020 for monodisperse samples and greater than 0.080 for broad distributions as stated by the operations manual. The data on Figure 2-7A-C supports the formation of polydisperse samples, where the polydispersity is captured by the broad size range observed (Figure 2-7B), and also by the two additional minor peaks detected (-42 and 5 mV) detected during zeta potential analysis (Figure 2-7C) that suggest the formation of DNA polyplexes possessing varying amounts of PEGylated peptide, where less peptide bound to DNA leads to more anionic charges, and more peptide bound leads to the formation of slightly cationic surface charges.

Atomic Force Microscopic Analysis of Polyacridine PEG-Peptide DNA Open Polyplexes

pGL3 was prepared at a concentration of 100 μg per mL in 10 mM Tris containing 1 mM EDTA pH 8. DNA polyplexes were prepared identically with the addition of PEG-Cys-Trp-$(Lys(Acr))_5$ at either 0.2 or 1 nmol per μg of DNA. pGL3 and DNA polyplexes were diluted 10-fold in 40 mM HEPES containing 5 mM nickel chloride pH 6.7, then deposited on the surface of mica that was freshly cleaved using transparent adhesive tape, and the sample was and incubated for 10 min, followed by washing with deionized water.[191] Alternatively, polyacridine-melittin DNA polyplexes were prepared at 0.5 nmol of peptide per μg of DNA at a concentration of 100 μg per mL of DNA and directly deposited on a freshly cleaved mica surface and allowed to bind for 10 min prior to washing with deionized water.[186] Images were captured using an Asylum atomic force microscope (AFM) MFP3D (Santa Barbara, CA) operated in the AC-mode

A. **Sample Data for PEG-Cys-Trp-(Lys(Acr))$_5$**

Run	Diameter	Half-Width	Polydispersity	Zeta Potential	Half-Width
1	290.1	113.2	0.152	-22.3	2.2
2	292.4	121.6	0.173	-30.3	4.7
3	300.1	133.7	0.199	-27.7	3.5
4	304.2	101.4	0.111	-25.6	2.8
5	331.9	150.7	0.206	-27.5	3.2
6	356.7	149.3	0.175	-26.0	5.0
7	324.7	135.4	0.174	-23.6	3.1
8	327.7	118.4	0.130	-26.8	4.4
9	367.7	132.6	0.130	-25.8	6.5
10	359.8	164.4	0.209	-28.5	2.9
Average	325.5	132.1	0.166	-26.4	3.8
Std Err	9.1	6.1	0.011	0.7	0.4

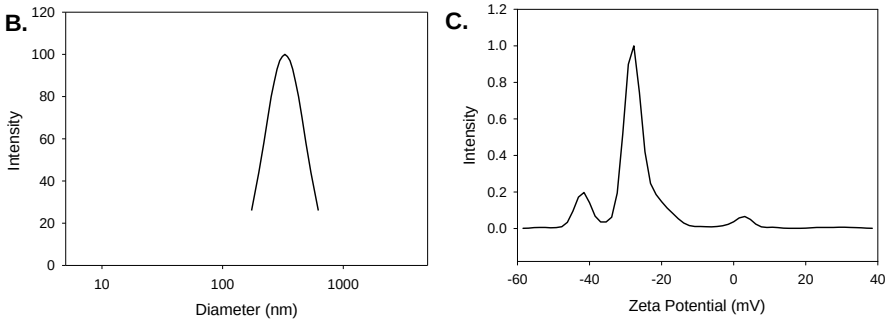

Figure 2-7. *Particle Size and Zeta Potential Sample Data for PEG-Cys-Trp-(Lys(Acr))$_5$ – DNA Polyplexes*. The particle size and zeta potential of DNA polyplexes prepared with PEG-Cys-Trp-(Lys(Acr))$_5$ is illustrated at a peptide stoichiometry of 0.2 nmol per μg of DNA (Panel A). The reported values are means and standard errors of ten repeated measurements. The polydispersity, which describes the size distribution of the samples, is shown on Panel A and the means and sample distributions are illustrated on Panels B and C.

using a silicon cantilever with a 40 N/m spring constant and a probe tip radius of 10 nm (Ultrasharp NSC15/AlBS, MikroMasch).

Intramuscular-Electroporation Administration

Male ICR mice (Harlan), weighing 25-30 g were prepared for IM-EP dosing by anesthetization with an intraperitoneal dose of 200 μL of ketamine/xylazine (20 mg/mL and 2 mg/mL, respectively). The hamstring region was sheared and swabbed with 70%

ethanol prior to administering a 50 μL dose of DNA polyplexes over 10 sec in normal saline to both gastrocnemius muscles in 2 mice by a 1 mL monoject syringe (1cc, 28 G x ½). After dosing, the BTX 2-Needle Array Electrode was inserted through the skin with the electrodes straddling the dosing site. Successive electronic stimulation was generated by the EMC BTX 830, Square-wave Pulse Generator (BTX, Harvard Apparatus) as the power source. At 1 min post-administration of the DNA dose, the pulse generator delivered six successive 100 V pulses over 20 msec with a 100 msec interval between pulses.[157]

Bioluminescence Imaging

Luciferase reporter gene expression was quantified by bioluminescence imaging (BLI) at 2-14 days following IM-EP using an IVIS Imaging System 200 Series (Xenogen).[192] Mice were anesthetized by isofluorane (2% flow with oxygen) and dosed intramuscularly into both gastrocnemius muscles with 40 μL of 30 mg per mL D-Luciferin (GoldBio). Bioluminescent images were acquired 5 min post substrate administration and acquired for 1 min with a 24.6 cm field of view. The resultant grayscale images with a colormap overlay were analyzed using the IgorPro 4.09 software (LivingImage). Luciferase expression is reported as photons/sec/cm^2/steradian within a uniformly defined region of interest (Figure 2-8).

Results

Several polyintercalator constructs that bind to double stranded DNA have been reported in prior studies aimed at delivering plasmid DNA.[32, 36, 38] These studies designed and tested delivery molecules possessing one-three acridine molecules displayed on a branched polymer modified with a neoglycopeptide or a nuclear localizing peptide, the latter of which were shown to mediate in vitro gene expression. [32, 38] These studies established that two to three acridines were required to achieve sufficient DNA binding affinity for in vitro transfection.

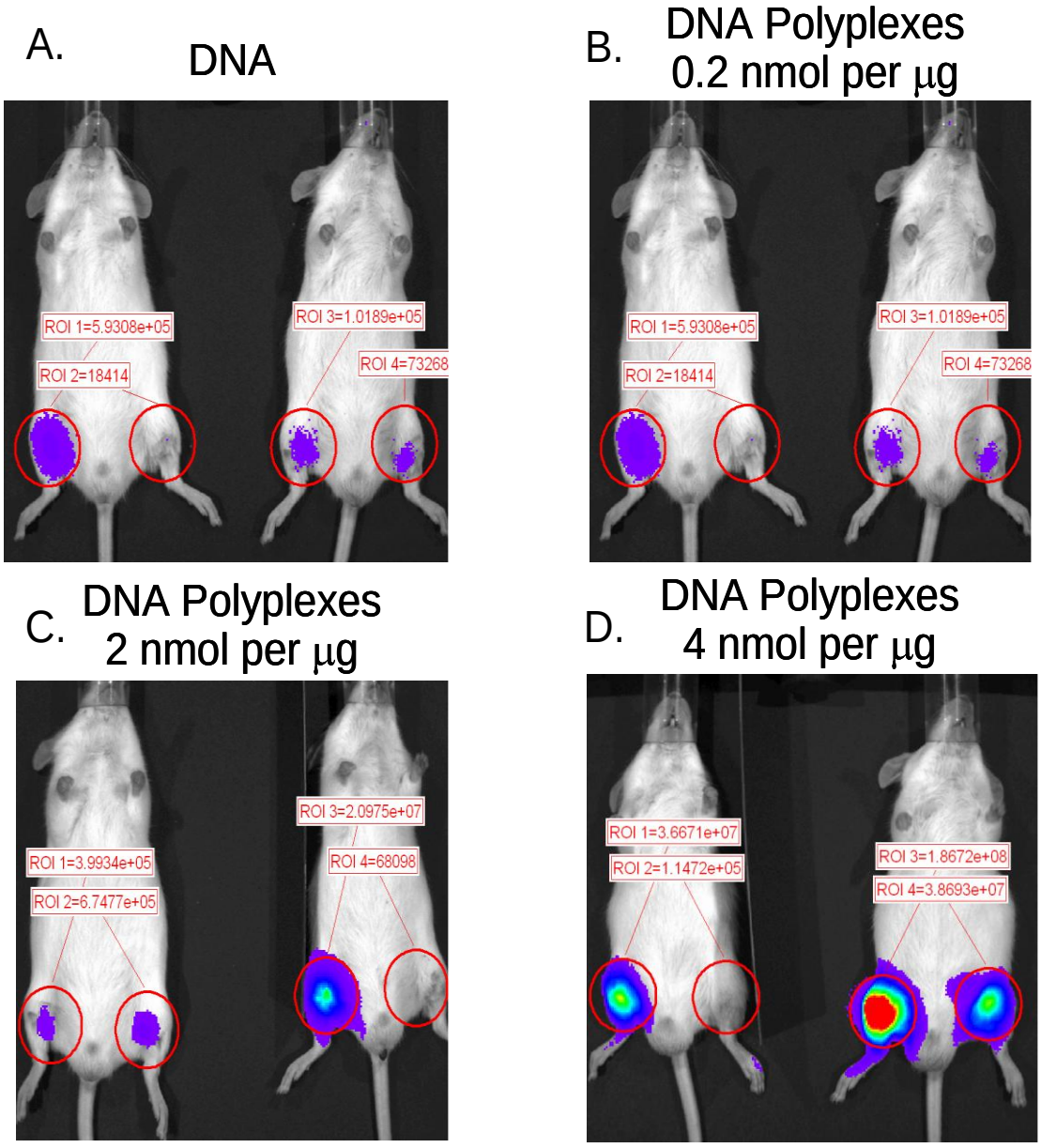

Figure 2-8. *BLI Raw Data of IM-Electroporated PEGylated Polyacridine PEG-Peptide-DNA Polyplexes* The raw BLI data of 1 μg of DNA (Panel A) or of DNA polyplexes prepared with PEG-Cys-Trp-$(Lys(Acr))_5$ at 0.2 nmol (Panel B), 2 nmol (Panel C), or 4 nmol (Panel D) 48 hours after IM-EP is shown on the figures above. The uniformly defined regions of interest (ROI, Panel A-D) indicate the luciferase expression levels for each formulation.

In the present study we sought to use a synthetic strategy that would allow for the incorporation of more than three acridines by covalent modification of the side chain of PEGylated polylysine. This was accomplished by first modifying acridine to possess a 6-amino hexanoic acid and then activating the carboxyl group to allow coupling to the ε-amines of PEG-Cys-Trp-$(Lys)_{3,\ 4,\ and\ 5}$ to afford PEG-Cys-Trp-$(Lys(Acr))_{3,\ 4\ and\ 5}$ (Figure 2-9). In addition, conjugation of acridine 6-amino hexanoic acid directly to PEG-amine and bis amino PEG afforded constructs with either one or two acridines (Figure 2-9). This strategy provided an advantage by allowing the comparison of DNA binding affinity with PEGs modified with 1-5 acridines.

Chromatographic evidence supporting the synthesis of PEG-Cys-Trp-$(Lys(Acr))_5$ is illustrated in Figure 2-2. Modification of Cys-Trp-$(Lys)_5$ with PEG results in a significant delay in elution on RP-HPLC compared to Cys-Trp-$(Lys)_5$. However, upon conjugation of five acridines to PEG-Cys-Trp-$(Lys)_5$, the resulting PEG-Cys-Trp-$(Lys(Acr))_5$ elutes only slightly later, and is detected at $Abs_{409\ nm}$.[190]

The complete conjugation of acridine to each Lys side chain was established using MALDI-TOF MS analysis. Conjugation of Cys-Trp-$(Lys)_5$ (948.8 g/mol) with polydisperse PEG of average mass of 5425 Da results in a PEG-Cys-Trp-$(Lys)_5$ with an apparent average mass of 6546 Da (Figure 2-3A-C). Purified PEG-Cys-Trp-$(Lys(Acr))_5$ produced an average mass of 7853 Da (Figure 2-3D), consistent with the conjugation of an average of 4.4 acridines. Similar mass spectral results were obtained when preparing PEG-Cys-Trp-$(Lys(Acr))_3$ and PEG-Cys-Trp-$(Lys(Acr))_4$ as summarized in Table 2-1.

The relative DNA binding affinity of mono and bis-acridine PEG compared to polyacridine PEG-peptides was established using a thiazole orange displacement assay (Figure 2-10A).[16] Titration of 0.2-4 nmols of mono-acridine PEG with 1 μg of pGL3 resulted in minimal displacement of thiazole orange. By comparison, bis-acridine PEG demonstrated higher affinity, resulting in a decrease in fluorescence intensity by 40% at

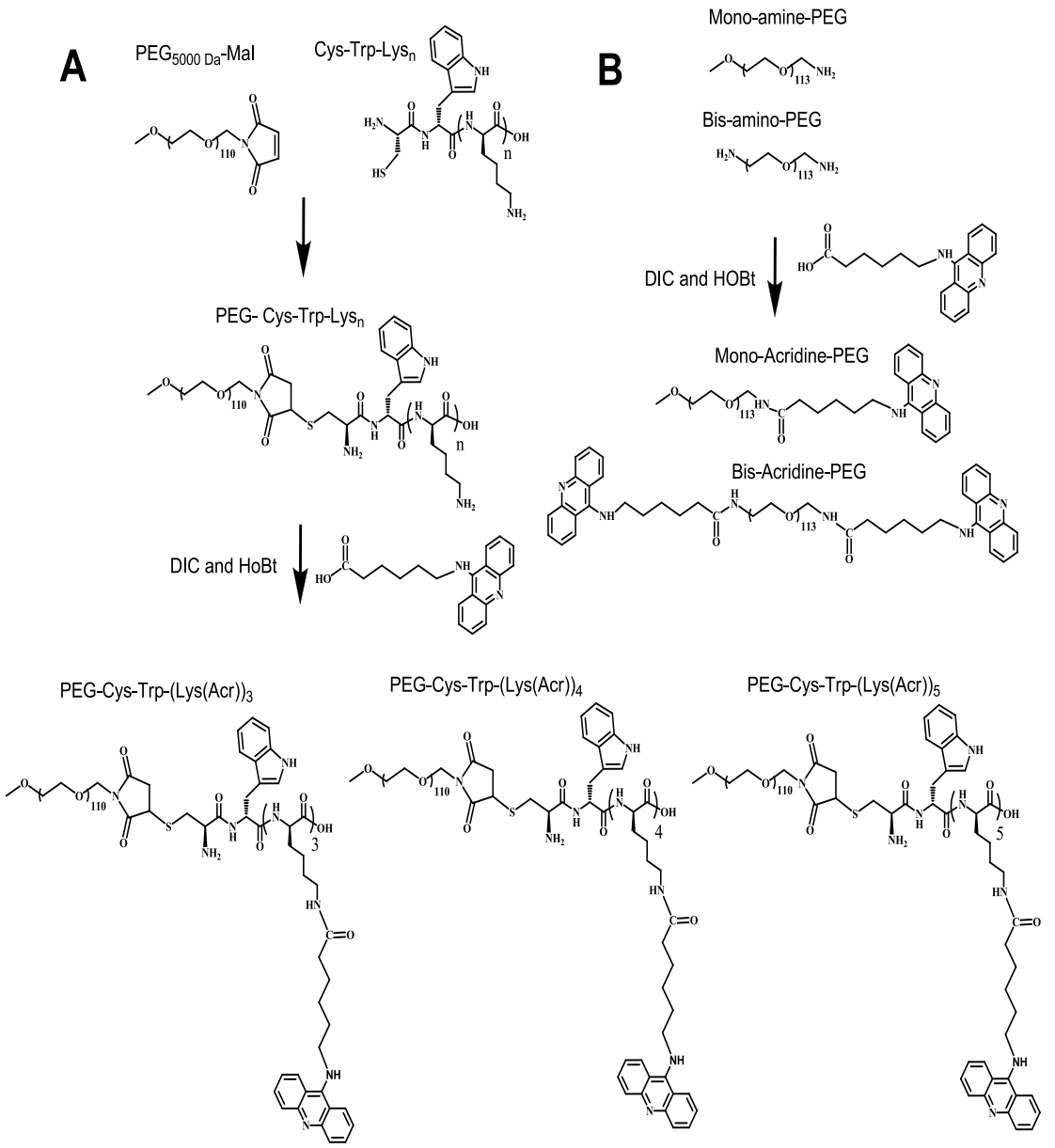

Figure 2-9. *Preparation of PEGylated Polyacridine Bioconjugates.* $PEG_{5000\ Da}$-maleimide was reacted with the Cys residue on Cys-Trp-Lys_3, Cys-Trp-Lys_4, and Cys-Trp-Lys_5 to form PEG-Cys-Trp-$(Lys)_{3,\ 4,\ and\ 5}$. Activated 6-(9-acridinylamino) hexanoic acid was reacted with ε-amines of Lys to form PEG-Cys-Trp-$(Lys(Acr))_{3,\ 4,\ and\ 5}$. Alternatively, mono and bis PEG-amine were reacted with activated 6-(9-acridinylamino) hexanoic acid to prepare mono-Acr-PEG and bis-Acr-PEG.

Table 2-1. MS Analysis of Polyacridine PEG-Peptides and Mono and Bis-Acridine PEG

Sample	Mass (g/mol)	Mass Difference[b]
Mono-amine-PEG	5385	
Mono-acridine-PEG	5626	41 (0.8)[c]
Bis-amine-PEG	2000	
Bis-acridine-PEG	2813	813 (2.8)[c]
Cys-Trp-Lys_3[a]	691.4	
PEG-Cys-Trp-Lys_3	6524	
PEG-Cys-Trp-$(Lys(Acr))_3$	7238	714 (2.5)[c]
Cys-Trp-Lys_4[a]	819.5	
PEG-Cys-Trp-Lys_4	6623	
PEG-Cys-Trp-$(Lys(Acr))_4$	7533	910 (3.1)[c]
Cys-Trp-Lys_5[a]	948.5	
PEG-Cys-Trp-Lys_5	6555	
PEG-Cys-Trp-$(Lys(Acr))_5$	7822	1267 (4.4)[c]

a. Determined by ESI-MS

b. Measured mean difference in MALDI-TOF mass due to the addition of acridine

c. Calculated number of acridine-6-amino-hexanoic acids based on 291 g/mol

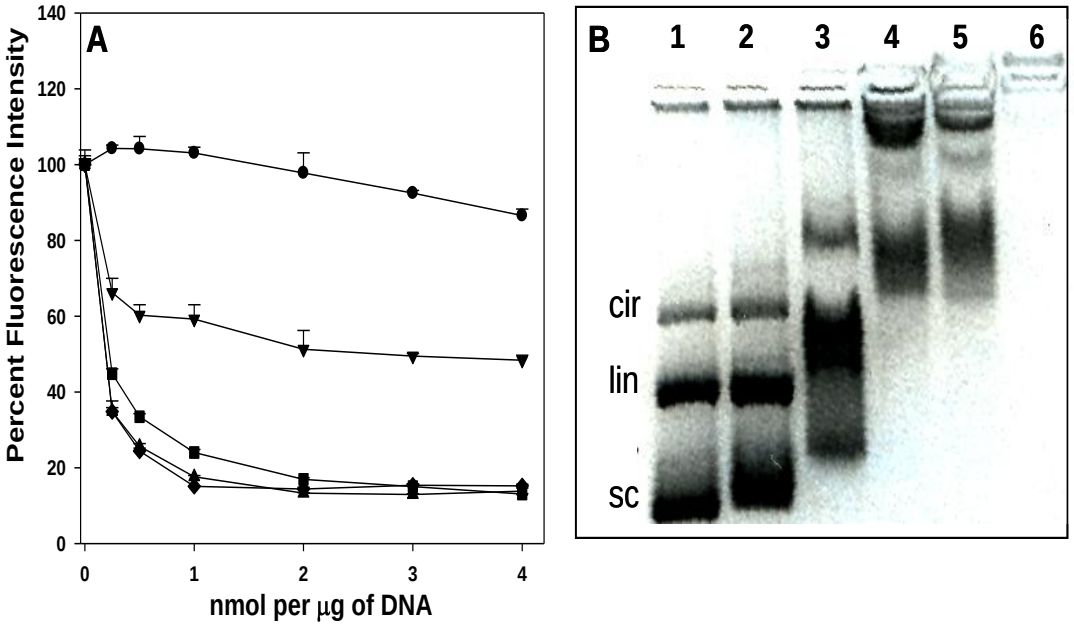

Figure 2-10. *Relative Binding Affinity of Mono-Acridine-PEG, Bis-Acridine-PEG, and Polyacridine Peptides with DNA.* The relative binding affinity of mono and bis-acridine-PEG, and PEG-Cys-Trp-(Lys(Acr))$_{3, 4, \text{ and } 5}$ for DNA was determined using a thiazole orange dye displacement assay and agarose gel band shift assay. Thiazole orange displacement established weak DNA binding for mono (●) and bis-acridine-PEG (▼), with higher and indistinguishable affinity determined for PEG-Cys-Trp-(Lys(Acr))$_3$ (■), 4 (▲), and 5 (♦) (panel A). The relative binding affinities were also confirmed by agarose gel electrophoresis. The circular (Panel B, cir), linear (Panel B, lin) and supercoiled (Panel B, sc) DNA migration bands observed for 1 μg of plasmid DNA (Panel B, lane 1) were compared to the migration of DNA polyplexes prepared with 1 nmol each of mono-acridine PEG (Panel B, lane 2), bis-acridine PEG (Panel B, lane 3), PEG-Cys-(Lys(Acr))$_3$ (Panel B, lane 4), PEG-Cys-(Lys(Acr))$_4$ (Panel B, lane 5), or PEG-Cys-(Lys(Acr))$_5$ (Panel B, lane 6). The results established maximal binding affinity with PEG-Cys-(Lys(Acr))$_5$.

1 nmol per μg of DNA. The apparent DNA binding affinity of PEG-Cys-Trp-(Lys(Acr))$_{3-5}$ was higher than either mono or bis-acridine PEG, resulting in approximately 10% fluorescence intensity at a stoichiometry of 1 nmol per μg of DNA (Figure 2-10A).

The DNA binding affinity was also compared by a band shift assay performed at a constant stoichiometry of 1 nmol per μg of DNA (Figure 2-10B). Mono-acridine PEG failed to produce a band shift relative to plasmid DNA (Figure 2-10B lane 1 and 2),

whereas bis-acridine PEG partially retarded the migration of DNA (Figure 2-10B lane 3). PEG-Cys-Trp-$(Lys(Acr))_{3\ and\ 4}$ both further retarded DNA migration to a similar extent (lanes 4 and 5), whereas PEG-Cys-Trp-$(Lys(Acr))_5$ led to complete retardation of DNA migration and also inhibited intense ethidium staining (Figure 2-10B. Lane 6). Conversely, PEG-Cys-Trp-$(Lys)_5$ was unable to cause a band DNA shift (not shown). Taking the results of the fluorophore displacement assay and the band shift gel assay together suggest the following binding affinity order for each acridinylated compound prepared: PEG-Cys-Trp-$(Lys(Acr))_5$ > PEG-Cys-Trp-$(Lys(Acr))_4$ > PEG-Cys-Trp-$(Lys(Acr))_3$ > Bis-acridine PEG > mono-acridine PEG.

A further demonstration of polyacridine binding to DNA utilized a titration experiment while monitoring both the particle size and zeta potential of DNA polyplexes as a function of increasing concentration of polyacridine (Figure 2-11). The titration of PEG-Cys-Trp-$(Lys(Acr))_3$ with pGL3 results in a decrease in the apparent particle diameter to approximately 200 nm at 0.2 nmols per μg of DNA but then plateaued at higher stoichiometries. These results did not exhibit an apparent decreasing trend in size, indicating that these DNA polyplexes may not be spherical particles. Therefore the morphology of the DNA polyplexes were confirmed by an orthogonal method (AFM, see below) and the apparent size measured using QELS does not accurately depict the size of the DNA polyplexes. In contrast, the zeta potential gradually increased from -15 to -5 mV when titrating with 0.1 to 2 nmol of PEG-Cys-Trp-$(Lys(Acr))_3$ per μg of DNA, indicating that the polyplexes remained electronegative (Figure 2-11A). A nearly identical trend was observed when titrating pGL3 with PEG-Cys-Trp-$(Lys(Acr))_4$ and PEG-Cys-Trp-$(Lys(Acr))_5$ (Figure 2-11B and C), with the exception that the latter reached an asymptote of -5 mV at 1 nmol per μg of DNA due to its greater DNA binding affinity.

The unusual zeta potential properties of the polyacridine DNA polyplexes prompted an investigation into their morphology using atomic force microscopy. Under

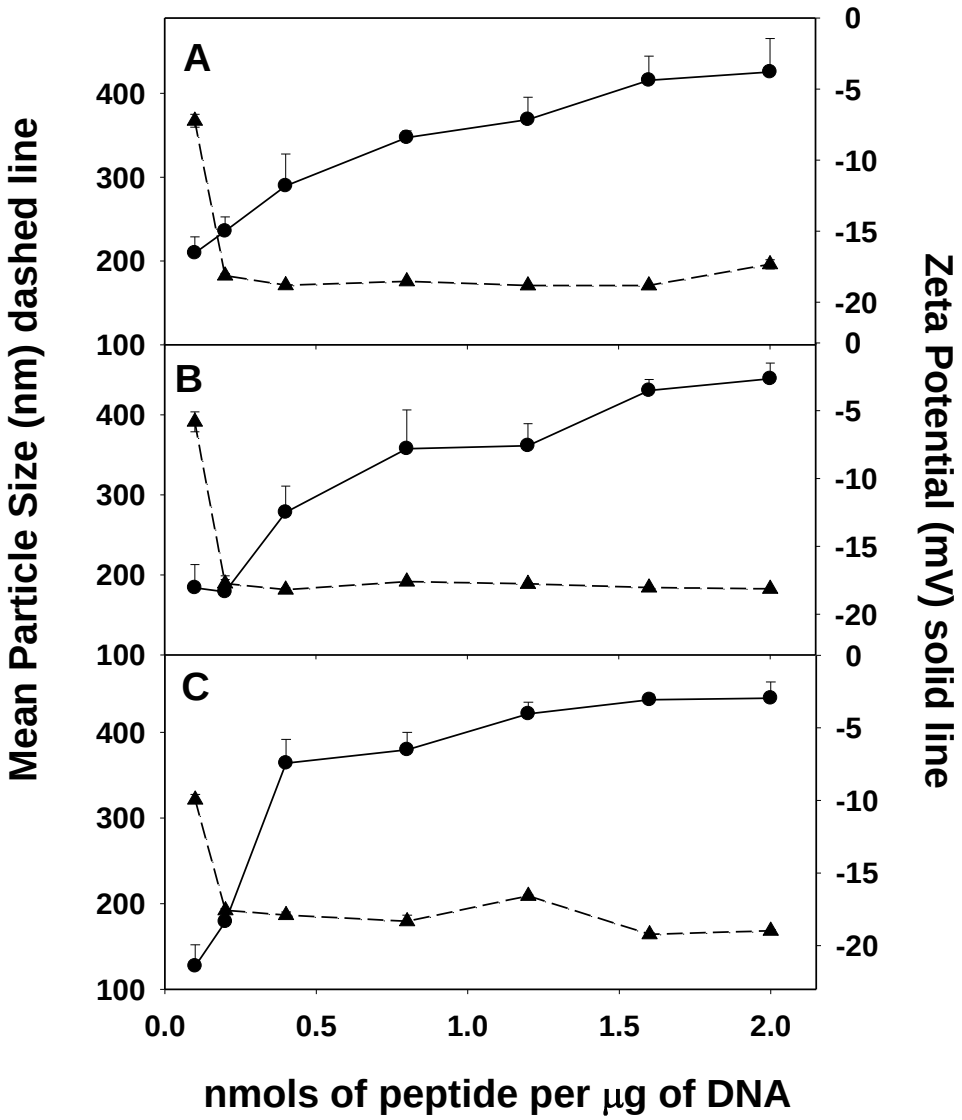

Figure 2-11. *Apparent Particle Size and Zeta Potential of Polyacridine-Peptide DNA Polyplexes.* The mean diameter size and zeta potential of DNA polyplexes prepared with 0.1, 0.2, 0.4, 0.8, 1.2, 1.6, or 2 nmol of PEG-Cys-$(Lys(Acr))_{3,\ 4,\ and\ 5}$ per μg of DNA were compared by light scattering analysis. At 0.2 nmols of polyacridine peptide or higher, PEG-Cys-$(Lys(Acr))_3$ formed polyplexes of apparent mean diameter of 200 nm that remained unchanged throughout the titration (Panel A, dashed line). In contrast, the zeta potential progressively increased from -15mV to approximately -2 mV when titrating from 0.1-2 nmol per μg of DNA (panel A, solid line). Nearly identical results were obtained when titrating with PEG-Cys-$(Lys(Acr))_4$ (panel B) and PEG-Cys-$(Lys(Acr))_5$ (panel C).

analysis by AFM, plasmid DNA is observed as an open circular structure when immobilized onto electropositive mica prepared with immobilized Ni (Figure 2-12A). By comparison, PEG-Cys-Trp-$(Lys(Acr))_5$ DNA polyplexes prepared at either 0.2 or 1 nmol per μg of DNA also resulted in a open circular structure, which we term open polyplexes (Figure 2-12B and C). Comparison of the size and shape of open polyplexes with plasmid DNA reveals a slightly more compact structure that becomes progressively more tightly wound at higher stoichiometry of polyacridine. The appearance of smaller particles in figures 2-12B and C are the result of AFM tip irregularities.[193] Comparing the strand diameter of DNA and DNA polyplexes in figures 2-12B and C by enlarging the images, suggests that the thickness of the open polyplex DNA is reduced by 20% relative to naked DNA. The open polyplex structure observed by AFM is quite unique when compared to an electropositive polyplex prepared with polyacridine melittin (Figure 2-12D).

We conjectured that the DNA in open polyplexes may be protected from metabolic degradation by serum endonucleases. The metabolic stability was evaluated by treating pGL3 with DNase followed by gel electrophoresis. Unprotected pGL3 is significantly degraded by DNase in 5 min and completely degraded by 10 min (Figure 2-13A, lanes 2 and 3). The weak binding affinity afforded by mono or bis-acridine PEG failed to protect DNA from metabolism (Figure 2-13B and C). Comparison of the metabolic stability of PEG-Cys-Trp-$(Lys(Acr))_{3,\ 4\ and\ 5}$ DNA open polyplexes demonstrated that PEG-Cys-Trp-$(Lys(Acr))_3$ and PEG-Cys-Trp-$(Lys(Acr))_4$ provided partial protection (Figure 2-13D and E), whereas PEG-Cys-Trp-$(Lys(Acr))_5$ provided complete protection (Figure 2-13F). Decreasing the stoichiometry from 1 nmol of PEG- Cys-Trp-$(Lys(Acr))_5$ to 0.4 or 0.2 nmol per μg of DNA established that at lower stoichiometries the DNA was more susceptible to metabolism (Figure 2-13G and H).

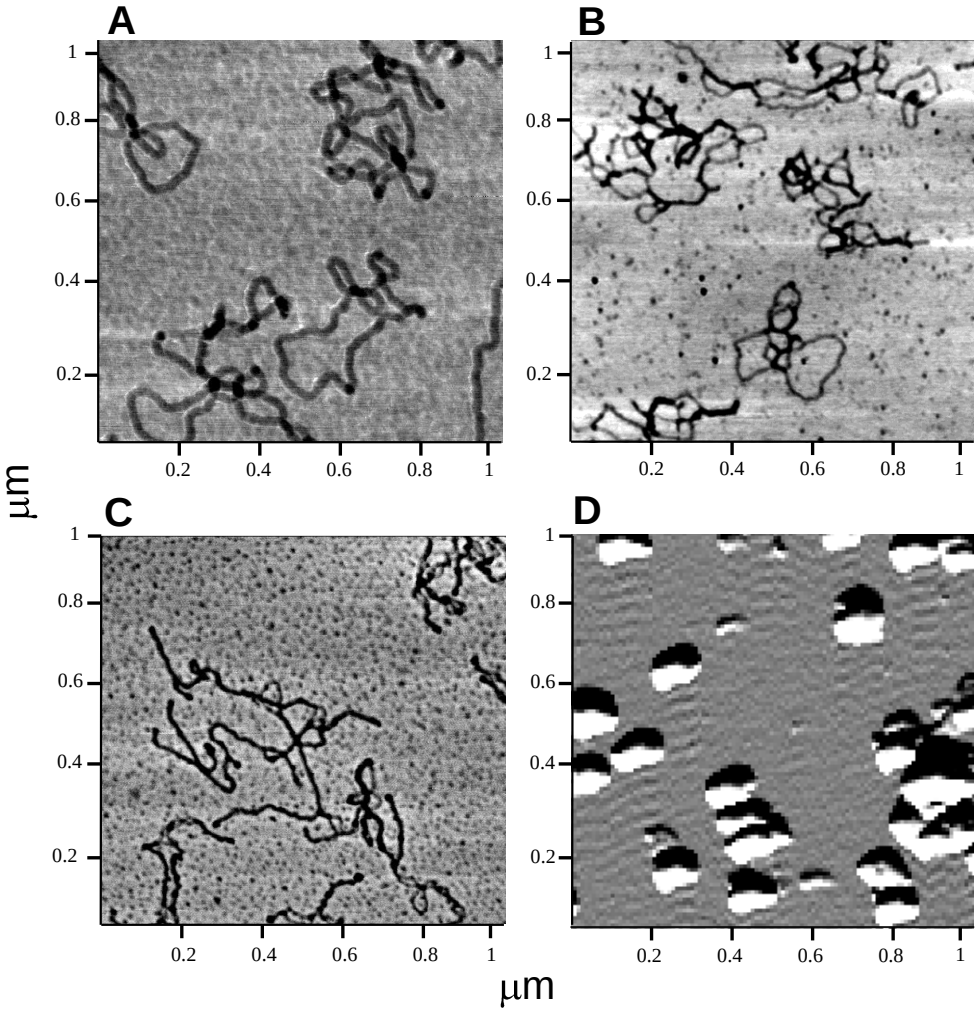

Figure 2-12. *Atomic Force Microscopy Analysis of Plasmid DNA and Polyacridine DNA Polyplexes.* AFM was used to compare the relative morphology of plasmid DNA or PEG-Cys-Trp-(Lys(Acr))$_5$ DNA polyplexes bound to electropositively charged mica in panels A-C. Plasmid DNA appears as an open circular structure (panel A) of comparable dimensions relative to PEG-Cys-Trp-(Lys-Acr)$_5$ DNA polyplexes prepared at either 0.2 nmol per μg of DNA (panel B) or 1 nmol per μg of DNA (panel C). Alternatively, a cationic polyplex prepared with polyacridine melittin binds to electronegative mica and appears as a collapsed structure (panel D). The results establish polyacridine PEG peptides bind to DNA to form electronegative open polyplexes that possess similar morphology as plasmid DNA.

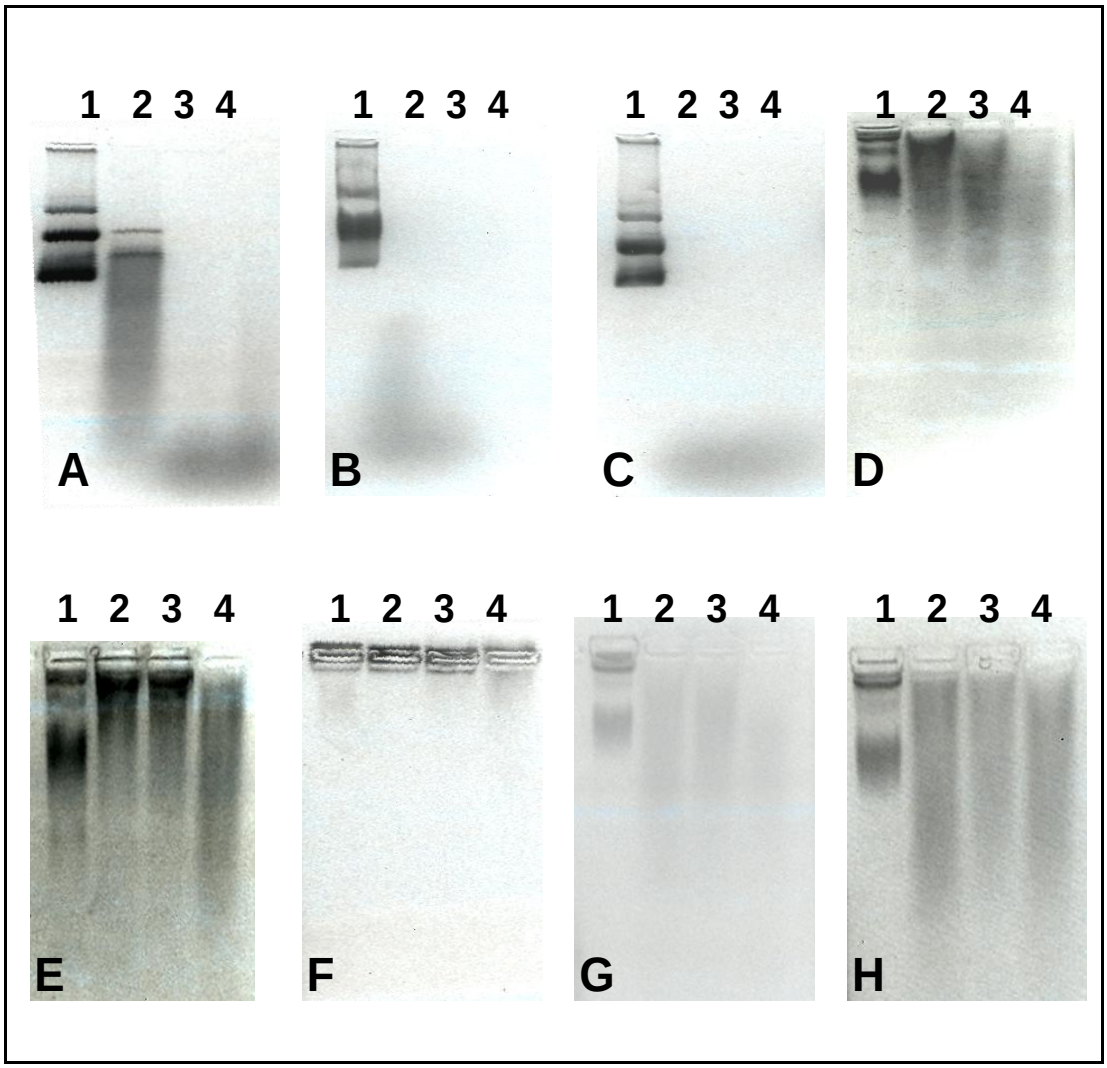

Figure 2-13. *Relative Metabolic Stability of Mono-Acridine-PEG, Bis-Acridine-PEG, and Polyacridine Peptides DNA Polyplexes.* The relative metabolic stability of DNA polyplexes was compared with plasmid DNA by agarose gel electrophoresis. Plasmid DNA (1 μg) (panel A), or DNA polyplexes prepared with 1 nmol each of mono-acridine PEG (panel B), bis-acridine PEG (panel C), PEG-Cys-(Lys(Acr))$_3$ (panel D), PEG-Cys-(Lys(Acr))$_4$ (panel E), or PEG-Cys-(Lys-(Acr))$_5$ (panel F) were incubated with 0.06 U of DNase at 37°C for 0 (lane 1), 5 (lane 2), 10 (lane 3) and 20 (lane 4) min. PEG-Cys-(Lys(Acr))$_5$ DNA polyplexes were also prepared at 0.2 (panel G) and 0.4 (panel H) nmol of polyacridine peptide per μg of DNA and digested with DNase. The results demonstrate that PEG-Cys-(Lys-(Acr))$_5$ provided the greatest protection at 1 nmol per μg of DNA, (panel F) while the lower stoichiometries of 0.2 or 0.4 nmol per μg of DNA (panel G and H) resulted in less stability.

The in vivo gene transfer properties of PEG-Cys-(Lys-(Acr))$_5$-DNA open polyplexes were evaluated in mice following IM-EP. pGL3 and pGL3 PEG-Cys-(Lys-(Acr))$_5$ open polyplexes prepared at 0.2, 2, and 4 nmol per μg of DNA formulations were administered by IM-EP and the expression was monitored for two weeks by bioluminescence imaging (Figure 2-14). At day 2 following dosing, pGL3 and the DNA open polyplexes prepared at 2 nmol per μg of DNA produced identical expression levels. Open polyplexes prepared at 4 nmol per μg of DNA showed approximately 10-fold lower expression, whereas a formulation prepared with 0.2 nmol per μg of DNA resulted in a 100-fold decrease in expression. A similar expression time-course was observed for pGL3 and DNA open polyplexes prepared with 0.2 and 2 nmol of PEG-Cys-(Lys-(Acr))$_5$ per μg of DNA resulting in a 10-fold decrease over 14 days. The expression time-course for open polyplexes prepared at 4 nmol of PEG-Cys-(Lys-(Acr))$_5$ per μg of DNA was extended, resulting in only a 2-3 fold loss in expression across the 14 day sampling period.

Discussion

An important function of a gene delivery carrier is to protect DNA from premature metabolism during transit.[82] The present study demonstrates that polyintercalation provides strong (Figure 2-6) and reversible binding (Figure 2-14) to DNA that delays metabolic degradation. The main advantage of this approach over polycationic polymer binding to DNA is that high affinity can be achieved with a short polyacridine and that the charge of the resulting DNA polyplexes can be controlled to be either positive (by incorporating a fusogenic peptide)[186] or negative, depending on intended applications in vitro or in vivo.

To evaluate the relationship between DNA binding affinity and metabolic stability, five DNA carriers were prepared that varied the number of acridines from 1 to 5. The synthetic strategy conjugated 6-(9-acridinylamino) hexanoic acid with the primary

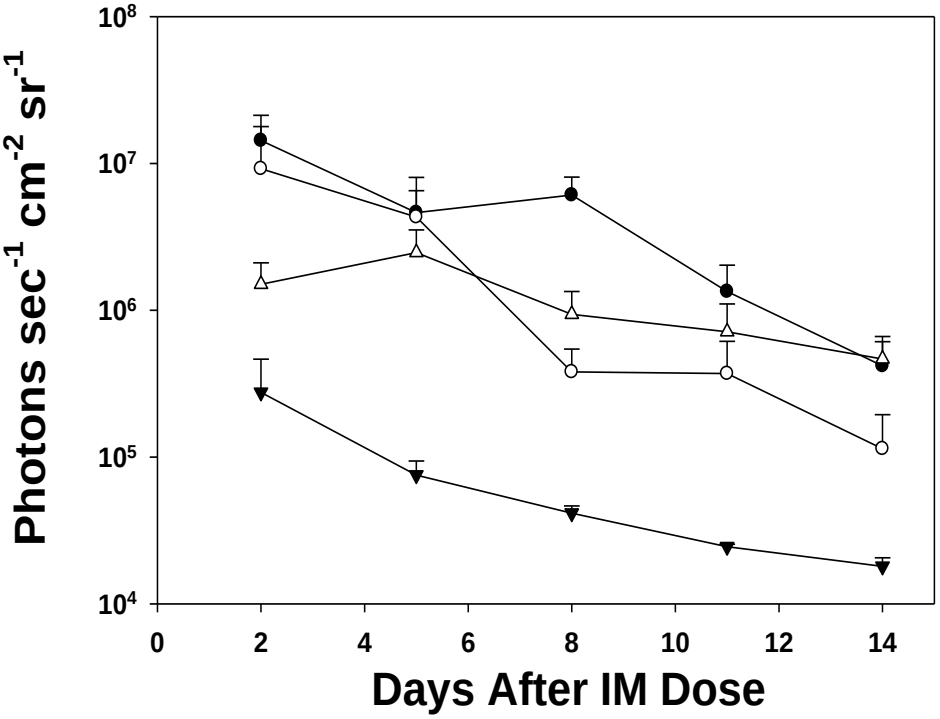

Figure 2-14. *In Vivo Gene Expression Mediated by Polyacridine Peptide DNA Polyplexes.* The gene transfer efficiencies of naked DNA (●) or polyacridine peptide DNA polyplexes prepared with 0.2 (▼), 2 (○), or 4 (Δ) nmol of PEG-Cys-(Lys-(Acr))$_5$ per μg of DNA were determined following i.m. dosing and electroporation of 1 μg of pGL3 in the gastrocnemius muscle of ICR male mice (n=4). The luciferase expression was quantified at times ranging from 2-14 days by bioluminescence imaging (BLI) following an i.m. dose of luciferin. Open polyplexes prepared at 0.2 nmol (▼) of PEG-Cys-(Lys-(Acr))$_5$ per μg of DNA showed the lowest transfection efficiency, while polyplexes prepared at 2 nmol (○) of PEG-Cys-(Lys-(Acr))$_5$ per μg of DNA showed similar expression levels to that of naked DNA. Increasing the stoichiometry to 4 nmol (Δ) PEG-Cys-(Lys-(Acr))$_5$ per μg of DNA resulted in a more sustained expression. The results represent the mean and standard deviation of four doses using two animals.

amine(s) on PEG-amine, bis-amino PEG, and the ε-amines on PEG-Cys-Trp-(Lys)$_{3,\ 4\ or\ 5}$.

This strategy not only simplified the chemical preparation of the delivery molecules, but

also allowed for a long 12 atom tether between each acridine and the peptide backbone to facilitate flexible multivalent binding of acridine with DNA.

The DNA binding affinity significantly increased for PEG-Cys-(Lys-(Acr))$_{3,\ 4,\ \text{and}\ 5}$ compared to mono and bis-acridine PEG as determined by both fluorophore displacement and DNA band shift on agarose gel electrophoresis (Figure 2-10A and 4B). While the QELS particle size suggested the formation of large polyplexes with an apparent diameter of 200 nm, the zeta potential revealed that for PEG-Cys-(Lys-(Acr))$_{3,\ 4,}$ and $_5$ polyplexes were negatively charged. AFM images established that the shape of PEG-Cys-(Lys-(Acr))$_{3,\ 4,\ \text{and}\ 5}$ DNA polyplexes were open coiled structures that closely resemble plasmid DNA (Figure 2-12). The observed electronegative open polyplexes are distinct from electropositive condensed polyplexes that are formed by polycation binding with DNA. The metabolic stability afforded by comparing PEG-Cys-(Lys-(Acr))$_{3,\ 4\ \text{and}\ 5}$ establish a relationship between the apparent DNA binding affinity and the degree of protection from DNase. Additionally, the metabolic protection of DNA afforded by PEG-Cys-(Lys-(Acr))$_5$ was concentration dependent.

IM-EP of cationic DNA polyplexes results in lower gene expression levels compared to naked DNA alone.[46, 194, 195] This may be due to the charge of cationic polyplexes that are unable to electromigrate through the transient pore formed during electroporation due to aggregation of the polyplex at the surface of the cell.[46] In contrast, the IM-EP of DNA versus PEG-Cys-(Lys-(Acr))$_5$ DNA open polyplexes resulted in very similar levels and duration of expression in mice over two weeks. However, at an elevated stoichiometry of PEG-Cys-(Lys-(Acr))$_{5,}$ a lower but more sustained expression was determined, perhaps due to the metabolic protection afforded by the peptide at higher stoichiometries.

The results of this study establish a new family of PEGylated polyacridine gene delivery carriers that bind to DNA and provide protection against DNase. The unique anionic open polyplex structure is compatible with IM-EP. Given the flexibility of

design, polyacridine gene delivery systems could be optimized for a variety of other non-viral gene delivery applications.

CHAPTER 3: ALTERNATIVE ANIONIC DNA POLYPLEXES FOR INTRAMUSCULAR-ELECTROPORATION GENE DELIVERY

Abstract

Optimal DNA formulations for intramuscular-electroporation (IM-EP) require gene delivery systems with controllable surface charges and particle sizes that can prevent aggregation on the surface of the cell during electroporation and protect the oligonucleotide from nuclease degradation before and after administration. The current chapter presents two different methods for preparing anionic DNA polyplexes that maintain metabolic protection properties. The first strategy involves the condensation of DNA with PEGylated Cys-Trp-Lys_{18} and the cross-linking of the primary amines on the surface of the polyplex with glutaraldehyde. The second strategy involves the binding of reducible PEGylated polyacridine peptides to DNA by intercalation rather than solely by electrostatic interactions, as investigated in Chapter 2. The PEG-SS-Cys-Trp-$Lys(Acr)_5$ peptide varies from the previous analogue by incorporating a reducible disulfide bond between the polyacridine peptide and the PEG polymer in order to determine the ability to improve gene transfer upon detachment of PEG within the reductive environment of the cell.

The results in this chapter demonstrate the ability to prepare cross-linked DNA nanoparticles with anionic surface charges and stable particle sizes. Furthermore, AFM images reveal that the structure of cross-linked DNA nanoparticles resembled the shape of open-DNA polyplexes rather than of spherical DNA nanoparticles. In contrast, PEG-SS-Cys-Trp-$Lys(Acr)_5$ yielded cationic DNA polyplexes when prepared above a stoichiometry of 0.4 nmol per μg of DNA that possessed similar DNase stability to the non-reducible polyacridine PEG-peptide presented in Chapter 2, but whose stability was shown to be dependent on PEG, as reduction of the disulfide bond resulted in the immediate degradation of DNA.

In vivo results suggest that neither strategy presented in this chapter was able to sustain gene expression levels similar to that of IM-EP dosed naked DNA. The physical characterization of the polyplexes before and after reduction suggest that the polyplexes failed to achieve gene transfer due to either poor DNA transport during electroporation, poor DNA release from the polyplex, or to poor DNase stability. Furthermore, the data suggest that a reversible linkage between the peptide and the PEG polymer leads to formulations that are incompatible with electroporation.

Introduction

Non-viral gene therapy has the potential to treat various diseases and genetic defects. It provides the safety of conventional pharmaceutical and biological products, and yet, its applications are limited due to the poor in vivo transfection efficiencies reported to date. In order to improve non-viral methods, delivery systems must be engineered to overcome the multitude of barriers that impede delivery. Therefore, as mentioned in the first chapter, several physical methods have been developed that can be coupled with non-viral gene delivery systems to achieve higher gene transfer efficiencies in vivo.

Electroporation is a physical method that can be used to transport DNA into cells in order to improve transfection efficiencies and intersubject variability. The method has been used in several tissues and it can be easily coupled to various administration sites as long as the target tissue is accessible to a direct injection. This technique uses electrical pulses to enhance the uptake of macromolecules by creating a membrane destabilization that forms nanometer sized pores on the cell membrane.[131] The pulses used to create the pores on the membrane also create an electrically driven transport that enhances the cytoplasmic entry of anionic DNA through electrophoresis.[196] This technique allows for the delivery of DNA directly into the cytoplasm, thus eliminating the initial intracellular barriers encountered prior to nuclear transport. [164]

Plasmid DNA administered by IM-EP can be susceptible to DNase degradation inside the cell after electroporation or in peripheral tissue prior to electroporation. Packaging DNA to avoid nuclease degradation may, therefore, provide an advantage over the electroporation of plasmid DNA alone. Nevertheless, Coulberson et al. demonstrated that plasmid DNA packaged with lipofectin, salmon protamine, or with a retroviral vector resulted in lower gene transfer efficiencies than when naked DNA was administered with electroporation alone, or when each lipoplex or polyplex was administered without electroporation.[197] These observations could be due to the particle size of the DNA polyplex or lipoplex relative to the size of the pore formed on the cell membrane during electroporation, or to aggregation of the DNA polyplex or lipoplex on the surface of the cells during electroporation.[46, 198]

The previous chapter investigated the use of non-reducible polyacridine PEG-peptides for intramuscular-electroporation (IM-EP). The results indicated that PEG-Mal-Cys-Trp-Lys(Acr)$_5$ was the peptide that possessed the best binding affinity and physical properties for in vivo compatibility. It was determined that increasing the (Lys(Acr))$_n$ chains resulted in higher binding affinities of the peptide for DNA, and in the ability to protect the DNA from nuclease degradation. IM-EP of DNA polyplexed with PEG-Mal-Cys-Trp-Lys(Acr)$_5$ led to a gene expression profile that was similar to that of electroporated naked DNA. The results demonstrate that electroporation can be coupled with non-viral vectors for improved gene transfer, but nevertheless, the results fall short of improving gene expression relative to IM-EP dosed plasmid DNA.

This chapter investigates two alternative methods of preparing anionic DNA nanoparticles and polyplexes for improved IM-EP gene transfer. The first method requires the formation of cationic DNA nanoparticles that are cross-linked using glutaraldehyde to yield anionic DNA polyplexes that have proven resistance against nuclease degradation.[113] The second strategy involves a reducible polyacridine PEG-peptide that is similar to the non-reducible peptides presented in chapter 2, but that

includes a reducible linkage between the peptide and the PEG polymer in order to determine the ability to improve gene transfer upon detachment of PEG within the reductive environment of the cell.

Materials and Methods

N-terminal Fmoc protected amino acids, 9-hydroxybenzotriazole (HOBt), diisopropylcarbodiimide (DIC), and Wang resin were purchased from Advanced Chemtech (Lexington, KY). Sephadex G-25, HEPES buffer, tris(2-carboxyethyl)-phosphine hydrochloride (TCEP), diisopropylethylamine (DIPEA), piperdine, acetic anhydride, triisopropylsilane (TIS), DNase I (EC 3.1.21.1), 9-chloroacridine, 25% glutaraldehyde grade I, and thiazole orange were obtained from Sigma Chemical Co (St. Louis, MO). Acetonitrile, N,N-Dimethylformamide (DMF), and trifluoroacetic acid (TFA) were purchased from Fisher Scientific (Pittsburgh, PA). Agarose was obtained from Gibco-BRL. mPEG-maleimide and mPEG-OPSS (5,000 Da) were purchased from Laysen Bio (Arab, AL). The 5.3 kb luciferase plasmid, pGL3 control vector, containing a SV40 promoter and enhancer was obtained from Promega (Madison, WI). Plasmid DNA was amplified in DH5α strain of *E. coli* and purified according to the manufacturer's instructions.

Synthesis and Characterization of PEGylated Cys-Trp-Lys_5 and Cys-Trp-Lys_{18} Peptides

The synthesis of Cys-Trp-$Lys_{5 \text{ and } 18}$ was carried out using standard Fmoc chemistry on a computer interfaced Advanced Chemtech APEX 396 solid phase peptide synthesizer with 9-hydroxybenzotriazole and diisopropylcarbodiimide double couplings followed by N-capping with acetic anhydride as described previously.[187] Cleavage and deprotection were accomplished by reacting the resin with TFA: TIS: water (95:2.5:2.5) at RT for 3 hrs. The crude peptide was precipitated in cold diethyl ether, centrifuged, and the supernatant was decanted. Crude peptides were reconstituted in 0.1% TFA and

purified on a preparatory RP-HPLC using a Vydac C18 column (2 x 25 cm) eluted at 10 mL/min with 0.1 v/v% TFA and a gradient of acetonitrile of 5-25% over 30 min while monitoring Abs 280 nm. Purified peptides were reconstituted in 0.1% TFA and quantified by Abs (Trp ε_{280nm} = 5600 M^{-1} cm^{-1}) to determine isolated yields of 34% for Cys-Trp-Lys_{18} and 54% for Cys-Trp-Lys_5. The purified peptides were characterized using LC-MS by separation on a Vydac C18 analytical column (0.47 x 25 cm) eluted at 0.7 mL/min with 0.1% TFA and a gradient of acetonitrile of 5-25% over 30 min while detecting ESI-MS in the positive ion mode.

PEGylation of the Cys residue on Cys-Trp-Lys_{18} or Cys-Trp-Lys_5 was achieved by reacting 0.9 mol equivalents of peptide with 1 mol equivalent of PEG $_{5000\ Da}$-maleimide or PEG $_{5000\ Da}$-orthopyridyldisulfide in 100 mM sodium phosphate buffer pH 7 for 1 hr at RT.[187] PEGylated peptides were purified on a G-25 column (2.5 x 50 cm) eluted with 0.1% acetic acid while monitoring Abs 280 nm. The peak corresponding to the PEG-peptide eluted in the void volume (100 mL), was pooled, concentrated by rotary evaporation, and freeze-dried. The PEG-peptide was reconstituted in 0.1% TFA, and quantified by Abs (Trp ε_{280nm} = 5600 M^{-1} cm^{-1}) to determine isolated yield of 52% for PEG-Mal-Cys-Trp-Lys_{18}, 45% for PEG-SS-Cys-Trp-Lys_{18}, and 58% for PEG-SS-Cys-Trp-Lys_5. PEG-peptides were characterized by MALDI-TOF MS by combining 1 nmol with α-cyano-4-hydroxycinnamic acid (CHCA) prepared in 50% (v/v) acetonitrile and 0.1% TFA. Samples were spotted onto the target and ionized on a Bruker Biflex III Mass Spectrometer operated in the positive ion mode.

Synthesis of Reducible Polyacridine PEG Peptides for IM-EP

6-(9-Acridinylamino) hexanoic acid was prepared according to a prior published procedure.[189] The carboxyl group on 6-(9-acridinylamino) hexanoic acid was activated with 1.1 mol equivalents of DIC and HOBt in DMF. Activated 6-(9-acridinylamino) hexanoic acid (12 mol equivalents) was reacted with 2.5 μmol of PEG-SS-Cys-Trp-Lys_5

in 3 mL of DMF at RT for 24 hrs. The PEG-SS-Cys-Trp-$(Lys(Acr))_5$ peptides were purified using a G-25 column (2.5 x 50 cm) eluted with 0.1 % acetic acid while monitoring Abs 280 nm. The product peak eluting at 100 mL was pooled, freeze dried, and characterized using MALDI-TOF MS as described above. A yield of 38% of PEG-SS-Cys-Trp-$(Lys(Acr))_5$ peptides was determined by acridine Abs (ε_{409nm} = 9266 M^{-1} cm^{-1}) assuming additivity of acridine molar absorptivity and complete conjugation to the ε-amine of Lys.

Preparation and Characterization of Reducible and Non-Reducible Cross-Linked DNA Nanoparticles

Reducible and non-reducible PEGylated DNA nanoparticles were prepared by adding 100 μg of plasmid DNA in 1 mL of 5 mM HEPES buffer to an equal volume containing 30 nmol of either PEG-SS-Cys-Trp-Lys_{18} or PEG-Mal-Cys-Trp-Lys_{18} while vortexing. The DNA nanoparticles were allowed to equilibrate at RT for 30 minutes prior to reaction of the primary amines on the surface of the PEGylated DNA nanoparticles with 1, 3, 5, 10, 20, 30, 40, 50, 60 or 100 mole equivalents of glutaraldehyde per mole of PEGylated Cys-Trp-Lys_{18} for 12 hours at 4 °C. The particle size (QELS) and zeta potential of DNA nanoparticles before and after cross-linking were determined using a Brookhaven ZetaPlus (Brookhaven Instruments, Holtsville, NY). The effect of reduction on cross-linked DNA formulations prepared with PEG-SS-Cys-Trp-Lys_{18} was determined by measuring the size and charge of the polyplex 30 minutes after incubating the reducible DNA nanoparticles with 100 mole equivalents of TCEP. The particle size diameter and zeta potential are reported as the mean and standard deviation of ten measurements.

The shape of PEGylated DNA nanoparticles was determined using atomic force microscopy (AFM). DNA nanoparticles, cross-linked DNA nanoparticles, and reduced DNA formulations were directly deposited on a freshly cleaved mica surface and allowed

to bind for 10 min prior to washing with deionized water.[186] Images were captured using an Asylum AFM MFP3D (Santa Barbara, CA) operated in the AC-mode using a silicon cantilever (Ultrasharp NSC15/AIBS, MikroMasch).

Thiazole Orange Displacement Assay of Reducible Polyacridine PEG-Peptides

The relative binding affinity of reducible PEGylated polyacridine peptides for DNA was determined by a fluorophore exclusion assay before and after reduction.[16] pGL3 (200 μl of 5 μg/ml in 5 mM HEPES pH 7.5 containing 0.1 μM thiazole orange) was combined with 0, 0.2, 0.3, 0.4, 1, 2, or 4 nmol of PEG-SS-Cys-Trp-Lys$(Acr)_5$ peptide in 300 μl of HEPES and allowed to bind at RT for 30 min. Furthermore, the influence of reduction on the binding affinity of the peptides was determined by incubating the sample with 100 mole equivalents of TCEP for 30 minutes. The thiazole orange fluorescence was then measured for all samples using an LS50B fluorometer (Perkin-Elmer, U.K.) by exciting at 498 nm while monitoring emission at 546 nm with the slit widths set at 10 nm. A fluorescence blank of thiazole orange in the absence of DNA was subtracted from all values before data analysis. The data is presented as nmol of PEGylated polyacridine peptide per μg of DNA versus the percent fluorescence intensity ± the standard deviation determined by three independent measurements.

Particle Size and Zeta Potential of Reducible Polyacridine-PEG peptide DNA Polyplexes

The particle size and zeta potential measurements were determined by preparing 2 mL of polyplex in 5 mM HEPES pH 7.5 at a DNA concentration of 30 μg per mL and a PEG-SS-Cys-Trp-Lys$(Acr)_5$ peptide stoichiometry of 0, 0.2, 0.3, 0.4, 0.8, 1.2, 1.6 or 2 nmol per μg of DNA. The effect of reduction on DNA polyplexes prepared with PEG-SS-Cys-Trp-Lys$(Acr)_5$ was determined by measuring the size and charge of the polyplex 30 minutes after incubating the reducible DNA polyplex with 100 mole equivalents of

TCEP. The particle size was measured by quasi-elastic light scattering (QELS) using Brookhaven ZetaPlus particle sizer (Brookhaven Instruments Corporation, NY). The particle size diameter and zeta potential are reported as the mean and standard deviation of ten measurements**.**

Gel Band Shift and DNase Protection Assay of Reducible Polyacridine-PEG peptide DNA Polyplexes

pGL3 (1 μg) or DNA polyplexes (1 μg) prepared in 18 μL of normal saline were combined with 0.1, 0.2, 0.4, 0.8, 1, or 2 nmol of PEG-SS-Cys-Trp-Lys(Acr)$_5$ and 2 μL of loading buffer before and after reduction with 100 mole equivalents of TCEP.[113] The samples were loaded onto a 1% agarose gel (50 mL) and electrophoresed in TAE buffer at 80 V for 90 min. The gel was stained in 2 mg/mL ethidium bromide at 5°C overnight, and the transilluminated gels were photographed using Polaroid 667 film. Similarly, pGL3 (1 μg) or DNA polyplexes (1 μg) prepared with 1 nmol of PEG-SS-Cys-Trp-Lys(Acr)$_5$ in 20 μL of normal saline was incubated with 0.06 U of DNase I at 37°C for 0-20 min before and after reduction with TCEP.[25] The samples were applied to a 1% agarose gel and electrophoresed as described above.

Intramuscular-Electroporation Dosing

Male ICR mice (Harlan), weighing 25-30 g were prepared for IM or IM-EP dosing by anesthetization with an intraperitoneal dose of 200 μL of ketamine/xylazine (20 mg/mL and 2 mg/mL, respectively). The hamstring muscles were sheared and swabbed with 70% ethanol prior to administering a 50 μL dose over 10 sec in normal saline to both gastrocnemius muscles in 2 mice by a 1 mL monoject syringe (1cc, 28 G x ½). For samples requiring electroporation, the BTX 2-Needle Array Electrode was inserted into the skin with the electrodes straddling the dosing site. Successive electronic stimulation was generated by the EMC BTX 830, Square-wave Pulse Generator (BTX, Harvard Apparatus) as the power source. At 1 min post-administration of the DNA dose,

the pulse generator delivered six successive 100 V pulses over 20 msec with a 100 msec interval between pulses.[157]

Bioluminescence Imaging

Luciferase reporter gene expression was quantified by bioluminescence imaging (BLI) following IM-EP using an IVIS Imaging System 200 Series (Xenogen).[192] Mice were anesthetized by isofluorane (2% flow with oxygen) and dosed intramuscularly with 40 μL of 30 mg per mL D-Luciferin (GoldBio). Bioluminescent images were acquired 5 min post substrate administration and acquired for 1 min with a 24.6 cm field of view. The resultant grayscale images with a colormap overlay were analyzed using the IgorPro 4.09 software (LivingImage). Luciferase expression is reported as photons/sec/cm^2/steradian within a uniformly defined region of interest.

Results

Improving DNA formulations for intramuscular-electroporation (IM-EP) requires molecular conjugates that reversibly bind to plasmid DNA and form anionic polyplexes that allow for favorable transport during electroporation, while providing nuclease protection to the DNA in the tissue after administration. The current chapter presents two strategies for the preparation of anionic DNA polyplexes for IM-EP administration. Both methods require the covalent attachment of polyethylene glycol (PEG) onto the Cys residue of a Cys-Trp-Lys_n peptide to form PEGylated polylysine peptides with either 18 or 5 lysine residues (Figure 3-1A & B). A PEG-maleimide (PEG-Mal) or PEG-orthopyridyldisulfide (PEG-OPSS) of 5,000 Da was used to form PEG peptides with a non-reducible or reducible covalent linkage between the polymer and the peptide. PEGylated Cys-Trp-Lys_{18} peptides were designed to electrostatically condense plasmid DNA and form PEGylated DNA nanoparticles, whereas PEG-SS-Cys-Trp-Lys_5 was designed for further conjugation to form reducible polyacridine PEG-peptides that bind to DNA through intercalation rather than solely through electrostatic condensation.

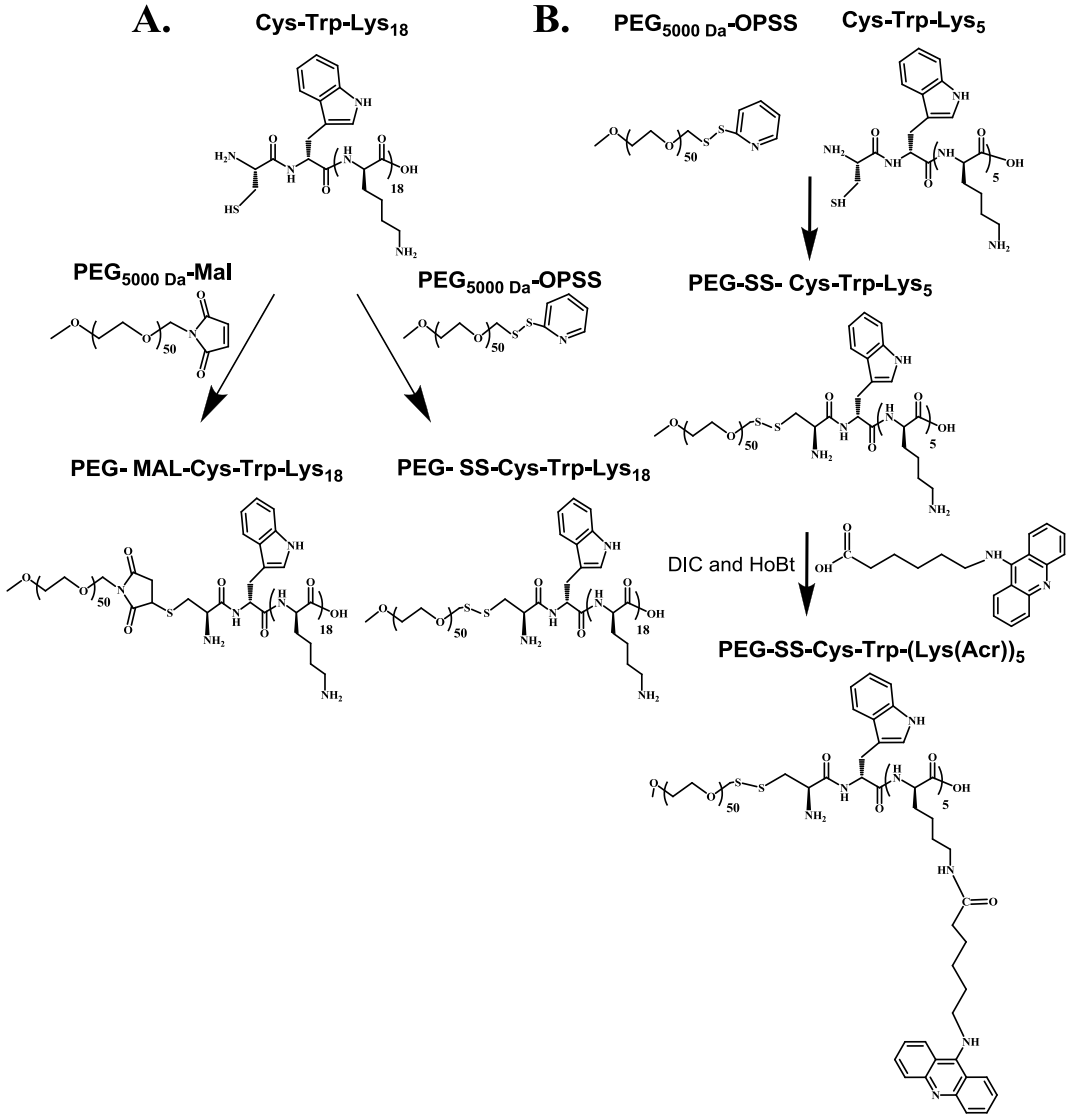

Figure 3-1. *Preparation of PEGylated Peptides and Reducible PEGylated Polyacridine Peptides for Gene Transfer.* Cys-Trp-Lys_n peptides were prepared using solid phase peptide synthesis. The Cys residue on Cys-Trp-Lys_n was reacted with $PEG_{5000\ Da}$-OPSS or $PEG_{5000\ Da}$- Mal to form PEG-Cys-Trp-Lys peptides with either a reducible (SS) or a non-reducible (Mal) linkage between the PEG polymer and the peptide (panel A). Reducible PEGylated polyacridine peptides were prepared by reacting activated 6-(9-acridinylamino) hexanoic acid with the ε amines of Lys on PEG-SS-Cys-Trp-Lys_5 to form PEGylated polyacridine peptides with the general structure of PEG-SS-Cys-Trp-$(Lys(Acr))_5$ (panel B).

Therefore, reducible PEGylated polyacridine peptides were prepared by reacting the ε-amines on the side chain of PEG-SS-Cys-Trp-Lys_5 with activated 6-(9-acridinylamino) hexanoic acid to afford PEG-SS-Cys-Trp-$(Lys(Acr))_5$ (Figure 3-1B). The ability to release PEG for both PEG-SS-Cys-Trp-Lys_{18} and PEG-SS-Cys-Trp-$(Lys(Acr))_5$ in the reductive environment of the cell may provide the DNA nanoparticle or polyplex with improved transfection efficiencies due to improved surface interactions on the cell surface prior to cell entry, or inside the cellular components after entry.[55]

Previous results have demonstrated that 0.3 nmol of PEG-Cys-Trp-Lys_{18} is required to fully condense 1 μg of plasmid DNA into DNA particles of approximately 100 nm in size.[169] The primary amines on the surface of PEGylated peptide DNA nanoparticles can be cross-linked using a homobifunctional agent such as glutaraldehyde (Figure 3-2). The resulting cross-linked polyplex has been demonstrated to enhance metabolic stability against nucleases and prevents premature polyplex dissociation during transit.[113, 168] Cross-linked DNA nanoparticles may, therefore, improve the in vivo transfection efficiencies of PEGylated DNA nanoparticles by enhancing DNA stability and decreasing the surface charge of the polyplexes, thus making it more compatible for in vivo applications.

To determine the influence of cross-linking on the size and charge of DNA nanoparticles, plasmid DNA was condensed with PEG- Mal -Cys-Trp-Lys_{18} (Figure 3-3) or PEG-SS-Cys-Trp-Lys_{18} (Figure 3-4A) at 0.3 nmol per μg of DNA prior to cross-linking. The PEGylated DNA nanoparticles (reducible and non-reducible) were below 200 nm in size as determined QELS, and possessed slight cationic surface properties (4 mV and 10 mV respectively). The extent of interparticle cross-linking was determined by monitoring the particle size as function of mole equivalents of glutaraldehyde added relative to the moles of PEG-Cys-Trp-Lys_{18} (Figure 3-3, --▲--). Cross-linking DNA polyplexes prepared with non-reducible or reducible PEG-peptides and cross-linked with 1 to 100 mole equivalents of glutaraldehyde resulted in no evidence of interparticle cross-

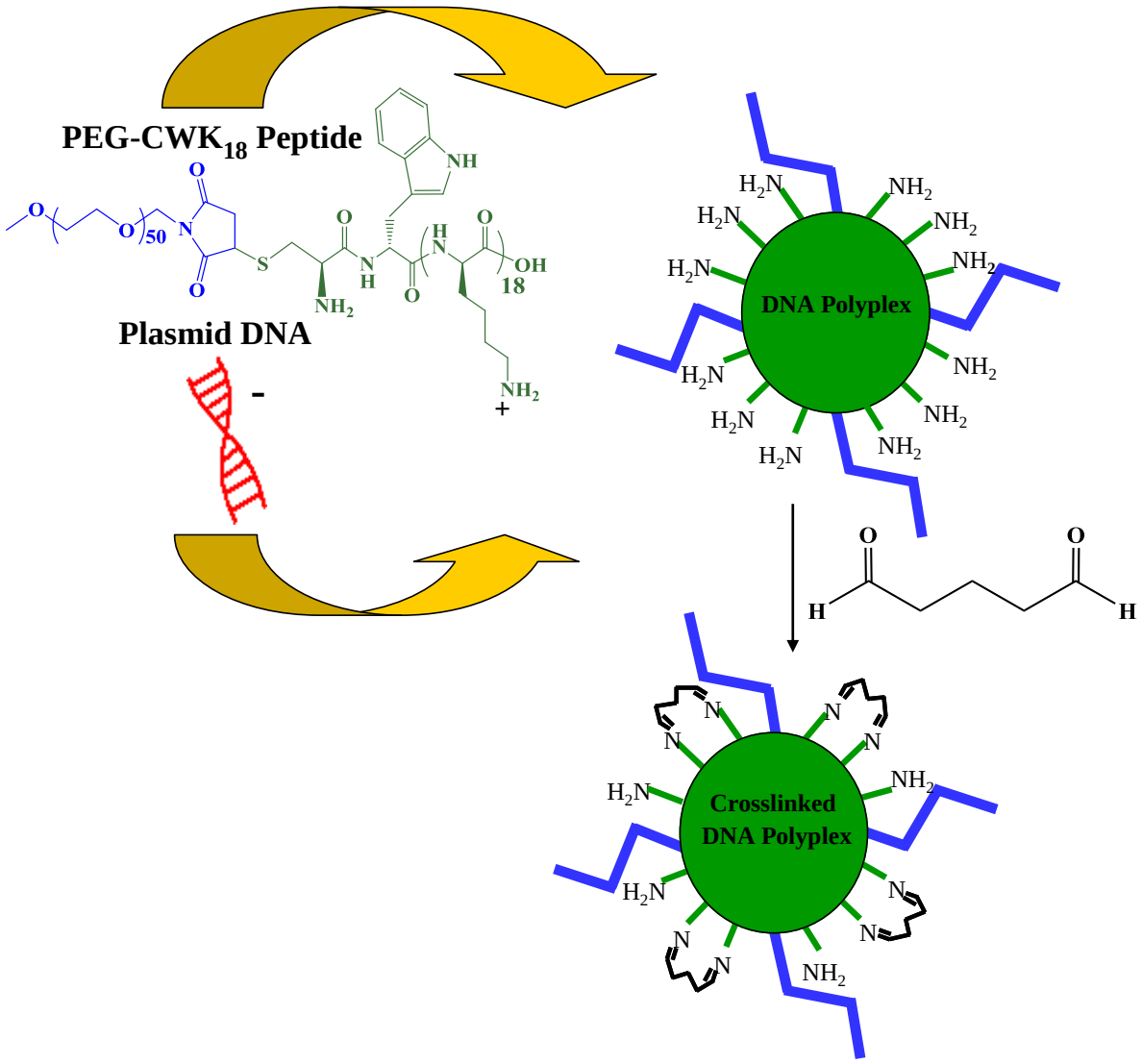

Figure 3-2. *Glutaraldehyde Cross-Linking of DNA Polyplexes*. PEG-Mal-Cys-Trp-Lys_{18} binds to plasmid DNA through electrostatic interactions to form condensed DNA polyplexes with an average size of below 200 nm. The resulting polyplexes are cationic in charge due to the residual amines on the surface of the DNA nanoparticles. Glutaraldehyde reacts with adjacent amines on the surface of the polyplex forming two Schiff-bases that result in cross-linked DNA polyplexes. The extent of cross-linking is dependent on the mole equivalents of glutaraldehyde used relative to the PEGylated peptide.

linking, as no change in particle size was observed in any case (Figure 3-3 & 5-4A). Zeta potential measurements confirmed reaction of the amines on the DNA nanoparticles with glutaraldehyde, as a decrease in the surface charge is observed for both non-reducible and reducible PEG-peptide DNA nanoparticle up to an asymptotic value of – 2mV peptides that is reached at 100 mole equivalents of glutaraldehyde (Figure 3-3 & 5-4B). Non-reducible, cross-linked DNA nanoparticles prepared with PEG-Mal-Cys-Trp-Lys_{18} became anionic at a degree of cross-linking of 40 mole equivalents of glutaraldehyde (Figure 3-3, 40X). In contrast, reducible formulations prepared with PEG-SS-Cys-Trp-Lys_{18} required 60 mole equivalents of glutaraldehyde to achieve anionic surface charges (Figure 3-4B, 60X). Perhaps the additional glutaraldehyde needed to reach negative surface charges is due to the higher initial zeta potential observed for PEG-SS-Cys-Trp-Lys_{18} DNA polyplex prior to cross-linking (Figure 3-4, 0X compared to Figure 3-3, 0X).

Detachment of PEG from the DNA nanoparticle via the reducible disulfide linkage on PEG-SS-Cys-Trp-Lys_{18} results in the exposure of the native charge of the polyplex. Therefore, PEGylated anionic polyplexes become more anionic upon PEG detachment after reduction, while cationic polyplexes should become more cationic. This trend is observed in the data, as an increase in the zeta potential is seen for polyplexes cross-linked from 0 to 1 mole equivalents of glutaraldehyde after reduction with TCEP (Figure 3-4B). Similarly, a decrease in the zeta potential is observed for polyplexes prepared from 3 to 60 mole equivalents of glutaraldehyde, whereas polyplexes cross-linked with 100 mole equivalents of glutaraldehyde showed no change in the charge of the polyplex after reduction (Figure 3-4B). Cross-linked polyplexes prepared at higher mole equivalents of glutaraldehyde presumably showed very little change in size and charge due to the extensive cross-linked network created, and due to the reaction of a high percentage of the free amines on the surface of the particle with glutaraldehyde.

The atomic force microscope (AFM) was used to determine the influence of cross-linking on the shape of the DNA nanoparticle (Figure 3-5A-D). DNA nanoparticles

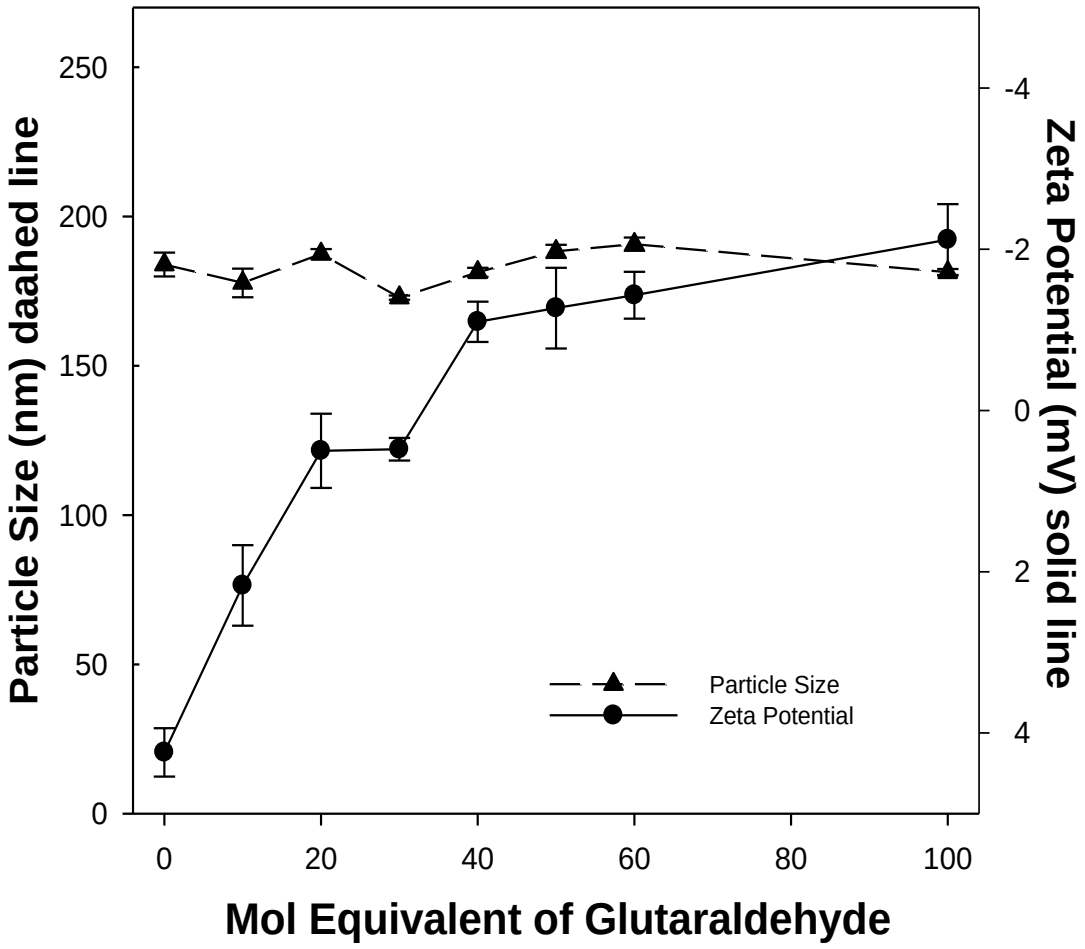

Figure 3-3. *The Effect of Glutaraldehyde Cross-Linking on the Particle Size and Zeta Potential of PEGylated DNA nanoparticles*. PEGylated DNA nanoparticles were prepared using PEG-Mal-Cys-Trp-Lys_{18} at a stoichiometry of 0.3 nmol of peptide per μg of DNA. The polyplexes were cross-linked with 0 to 100 mole equivalents of glutaraldehyde and the reaction resulted in no obvious effect on the particle size of the polyplex producing DNA nanoparticles below 200 nm in size (--▲--). In contrast, the zeta potential decreased significantly from 4 mV at 0 mole equivalent to -2 mV at 100 mole equivalents of glutaraldehyde (-●-), providing evidence of the reaction of free amines with glutaraldehyde on the surface of the polyplex.

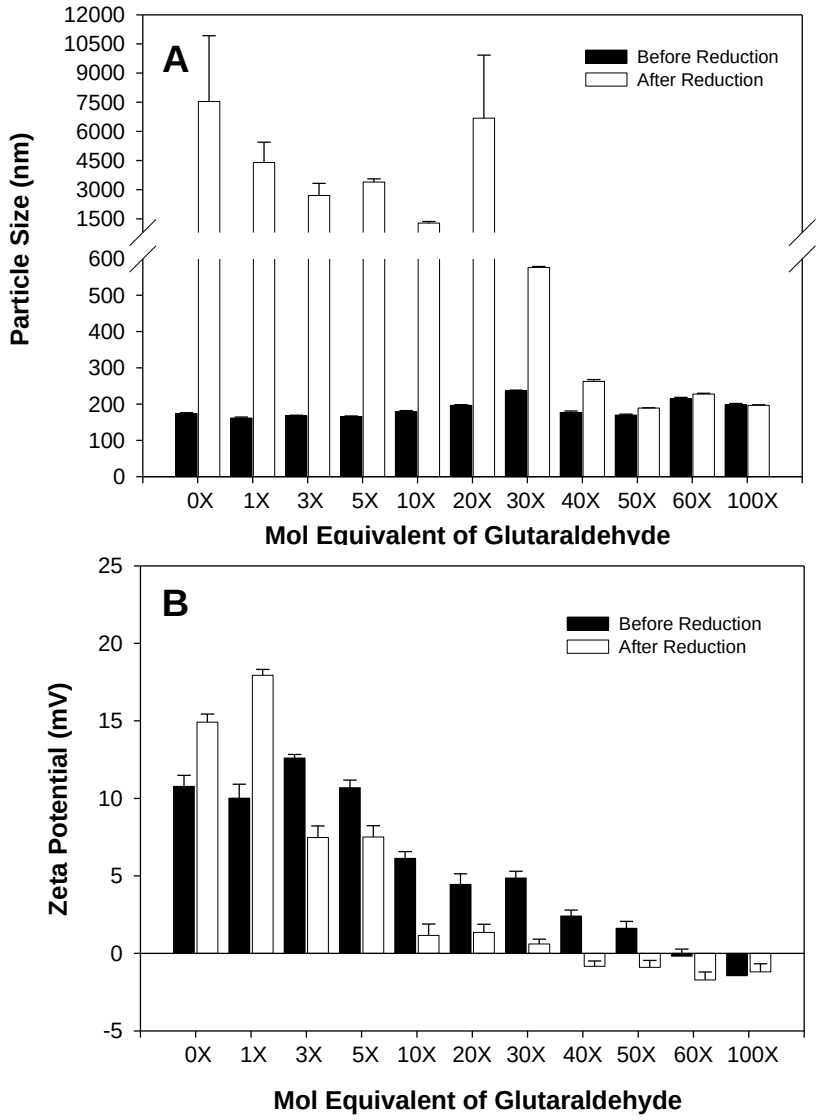

Figure 3-4. *The Effect of Glutaraldehyde Cross-Linking on the Particle Size and Zeta Potential of Reducible PEGylated DNA Nanoparticles*. PEGylated DNA nanoparticles prepared with PEG-SS-Cys-Trp-Lys_{18} were cross-linked with 0 to 100 mole equivalents of glutaraldehyde (white bars) and then reduced with 100 X TCEP (filled bars). Cross-linking resulted in no apparent change in the size of the polyplex (panel A, white bars), but yet reduced the surface charge of the polyplexes from 10 mV at 0 mole equivalents to – 2 mV at 100 mole equivalents (panel B, white bars). Upon reduction, a large increase in the particle size was observed for polyplexes cross-linked with 0 to 30 mole equivalents of glutaraldehyde (panel A, filled bars). The zeta potential increased upon reduction for polyplexes cross linked with 0 to 1 mole equivalent of glutaraldehyde, and decreased from 3 to 60 mole equivalents (panel B, filled bars).

prepared with PEG-Mal-Cys-Trp-Lys_{18} at 0.3 nmol per μg of DNA resulted in spherical particles with a diameter ranging between 100 and 300 nm (Figure 3-3A). Cross-linking these DNA nanoparticles with 10 mole equivalents of glutaraldehyde decreased the binding affinity of the nanoparticles for anionic mica due to the diminished surface charge resulting from cross-linking (Figure 3-5B). The 5 x 5 μm AFM scan reveals that upon cross-linking with 40 mole equivalents, a second population of DNA polyplexes exists rather than a single population of spherical nanoparticles. This second population appears as dissembled DNA nanoparticles that more so resemble the shape of DNA open-polyplexes (Figure 3-5B). Additionally, reducible cross-linked formulations possess very similar properties, where polyplexes prepared with 3 mole equivalents of glutaraldehyde demonstrate a clear mixture of DNA nanoparticles and DNA open-polyplexes. Upon reduction of these polyplexes with TCEP, the size of the polyplexes increase from approximately 100 nm in size (Figure 3-5C) to over 1 μm (Figure 3-5D), which correlates with the QELS particle size analysis (Figure 3-4A).

The second approach to preparing anionic DNA polyplexes involved the polyintercalation of PEG-SS-Cys-Trp-$(Lys(Acr))_5$, which is a similar analogue to the peptide introduced in chapter 2, but includes a disulfide bond linkage between the peptide and the polymer. The binding affinity of this reducible PEGylated polyacridine PEG-peptide was determined using the thiazole orange displacement assay and the band shift gel assay. Both methods coincide and suggest complete polyplex formation at a stoichiometry of 1 nmol per μg of DNA for PEG-SS-Cys-Trp-$(Lys(Acr))_5$ (Figure 3-6A, -●-, and Figure 3-6B, lane 7). This data confirm that both PEG-SS-Cys-Trp-$(Lys(Acr))_5$ and PEG-Mal-Cys-Trp-$(Lys(Acr))_5$ have similar binding affinities for DNA.

The effect of reduction on the relative binding affinity of PEG-SS-Cys-Trp-$(Lys(Acr))_5$ peptides to DNA was also investigated using the thiazole orange displacement assay and the band shift gel assay. The fluorophore displacement assay demonstrated no difference in the binding affinity after reduction (Figure 3-6A, -○-),

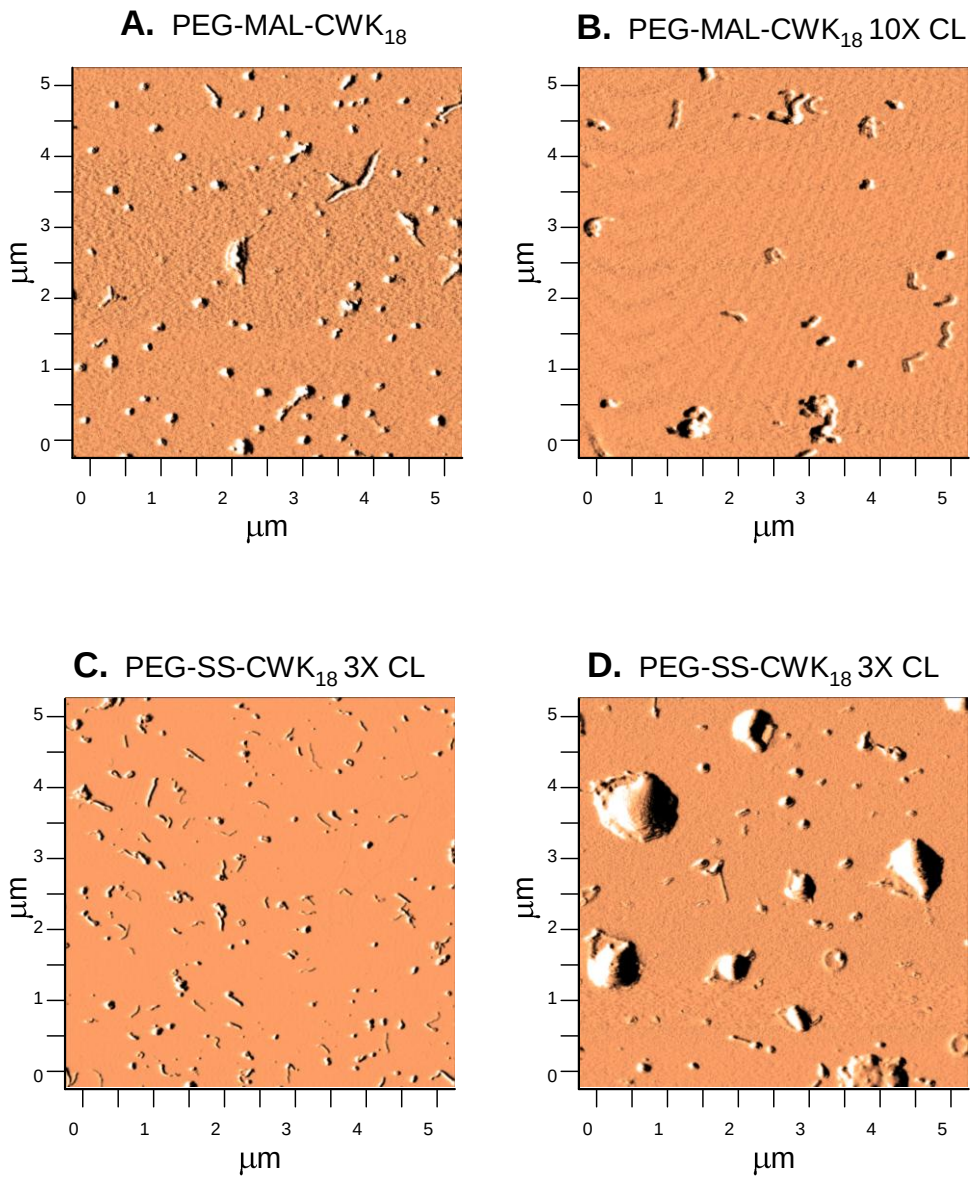

Figure 3-5. *Influence of Glutaraldehyde Cross-Linking on the Shape of DNA Polyplexes Prepared with Reducible and Non-reducible PEGylated Cys-Trp-Lys$_{18}$.* The atomic force microscope (AFM) was used to determine the shape of DNA polyplexes prepared with either PEG-Mal-Cys-Trp-Lys$_{18}$ (panel A & B, non-reducible) or PEG-SS-Cys-Trp-Lys$_{18}$ (panel B & C, reducible) cross-linked with 10 or 3 mole equivalents of glutaraldehyde. The 5 X 5 µm scans demonstrate that upon cross-linking the shape of the polyplex changes to resemble the appearance of an open DNA polyplex (panel A compared to panel B & C). Upon reduction a large increase in polyplex size is observed for reducible DNA polyplexes (panel D).

whereas the band shift gel assay suggests complete polyplex formation upon reduction at a stoichiometry of 0.4 nmol per μg of DNA (Figure 3-6C, lane 5), rather than at 1 nmol per μg prior to reduction (Figure 3-6B, lane 7). An increase in the binding affinity after reduction may indicate an interference of PEG with the binding of acridine to DNA. This change in affinity may also lead to a change in the release properties of DNA from the peptide, and perhaps influence gene transfer efficiencies.

The particle size and zeta potential of PEG-SS-Cys-Trp-$(Lys(Acr))_5$ DNA polyplexes was determined as a function of peptide stoichiometry (Figure 3-7A &B, -●-). Previous results generated with non-reducible PEG-Mal-Cys-Trp-$(Lys(Acr))_5$ peptide determined that anionic DNA open-polyplexes were formed with apparent sizes of 200 nm, regardless of the stoichiometry of peptide. Additionally, the PEG-Mal-Cys-Trp-$(Lys(Acr))_5$ peptide formed DNA polyplexes with maximum surface charges of -2 mV when prepared at a stoichiometry of 2 nmol per μg of DNA (Figure 2-4A). In comparison, the result for reducible polyacridine PEG peptides illustrates a dependency of size and charge on the stoichiometry of peptide (Figure 3-7A & B, -●-). The titration reveals a decrease in the size of the polyplex from 200 nm at a stoichiometry of 0.1 nmol per μg of DNA to a size of 120 nm at 0.8 nmol per μg and above. Furthermore, the data demonstrate that increasing the stoichiometry of peptide results in an increase in the zeta potential, and that polyplexes can be prepared at various surfaces charges ranging from -20 mV at 0.2 nmol per μg of DNA to 16 mV at 2 nmol per μg. The data indicate that when prepared at 0.8 nmol per μg of DNA or above, the DNA polyplexes possess cationic surface charges (Figure 3-7B, -●-). These observations are rather different from those observed with the non-reducible PEG-Mal-Cys-Trp-$(Lys(Acr))_5$, where anionic DNA polyplexes formed at all ratios were evaluated. Combining the particle size and zeta potential data, the results suggest that anionic open DNA polyplexes are formed at or below a stoichiometry of 0.4 nmol per μg of DNA, and that cationic DNA nanoparticles form at and above a stoichiometry of 0.8 nmol per μg. These conclusions are based on

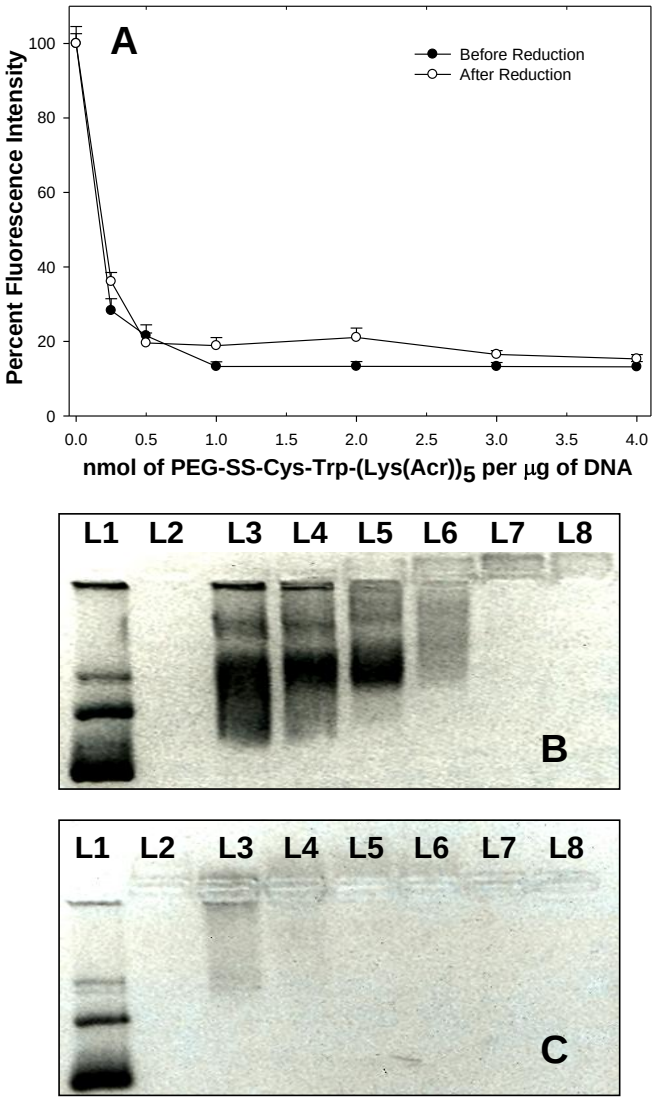

Figure 3-6. *Binding Affinity of Reducible PEGylated Polyacridine Peptides with DNA Before and After Reduction*. The binding affinity of PEG-SS-Cys-Trp-$(Lys(Acr))_5$ for DNA was determined using the thiazole orange displacement assay and the band shift gel analysis. The thiazole orange analysis demonstrates complete polyplex formation at stoichiometry of 1 nmol of peptide per μg of DNA and indicates no change in binding affinity of the peptide to DNA upon reduction with TCEP (panel A). Furthermore, 1 μg of DNA (lane 1), 1 nmol of polyacridine PEG-peptide alone (lane 2), and 1 μg of DNA polyplexes prepared at 0.1 (lane 3), 0.2 (lane 4), 0.4 (lane 5), 0.8 (lane 6), 1 (lane 7), and 2 nmol per μg of DNA (lane 8) were run on a 1% agarose gel and confirmed complete polyplex formation at a stoichiometry of 1 nmol per μg of DNA (panel B, lane 7). Upon reduction with TCEP DNA migration was inhibited at a stoichiometry of 0.4 nmol per μg of DNA (panel C, lane 5).

the observed charge neutralization of DNA, where at a stoichiometry of 0.8 nmol per μg of DNA the excess amines on the peptide convert the over all charge of the polyplex from electronegative at 0.4 nmol per μg to cationic at 0.8 nmol per μg (Figure 3-7B). Furthermore, this stoichiometry coincides with asymptotic particle size reached during the titration, thus indicating the collapse of the DNA structure from an open polyplex with an apparent size of 200 nm when prepared below 0.8 nmol per μg, to a DNA nanoparticle with an apparent size of 100 nm when prepared at or above 0.8 nmol per μg (Figure 3-7A).

Reduction of PEG-SS-Cys-Trp-$(Lys(Acr))_5$ DNA polyplexes with TCEP resulted in no significant change in the size of the polyplex compared to the polyplexes prior to reduction (Figure 3-7A, -○- compared to-●-). Furthermore, anionic DNA polyplexes (0.1 to 0.4 nmol per μg) become more anionic upon detachment of PEG, whereas cationic DNA polyplexes (0.8 to 2 nmol per μg) become more cationic after reduction (Figure 3-7B, comparing closed and open circles). These results share similarities with reducible cross-linked formulations (Figure 3-4), where a change in surface charge is observed after reduction, yet PEG-SS-Cys-Trp-$(Lys(Acr))_5$ DNA polyplexes are unique due to their stability in particle size upon reduction (Figure 3-7A, comparing closed and open circles).

An essential feature discovered using non-reducible polyacridine PEG-peptides is their ability to protect plasmid DNA against DNase degradation (Figure 2-13F). The protection capabilities of PEG-SS-Cys-Trp-$(Lys(Acr))_5$ DNA polyplexes was therefore determined at the same stoichiometry of 1 nmol per μg of DNA before and after reduction (Figure 3-8). The results confirm similar DNA protection properties as previously observed with PEG-Mal-Cys-Trp-$(Lys(Acr))_5$, as no evidence of DNase degradation is observed up to DNase incubation periods of 20 minutes (Figure 3-8A, lane 4). Additionally, the upward migration observed toward the cathode (Figure 3-8A, lane1-lane 4) verifies the cationic properties of these polyplexes, which was not observed

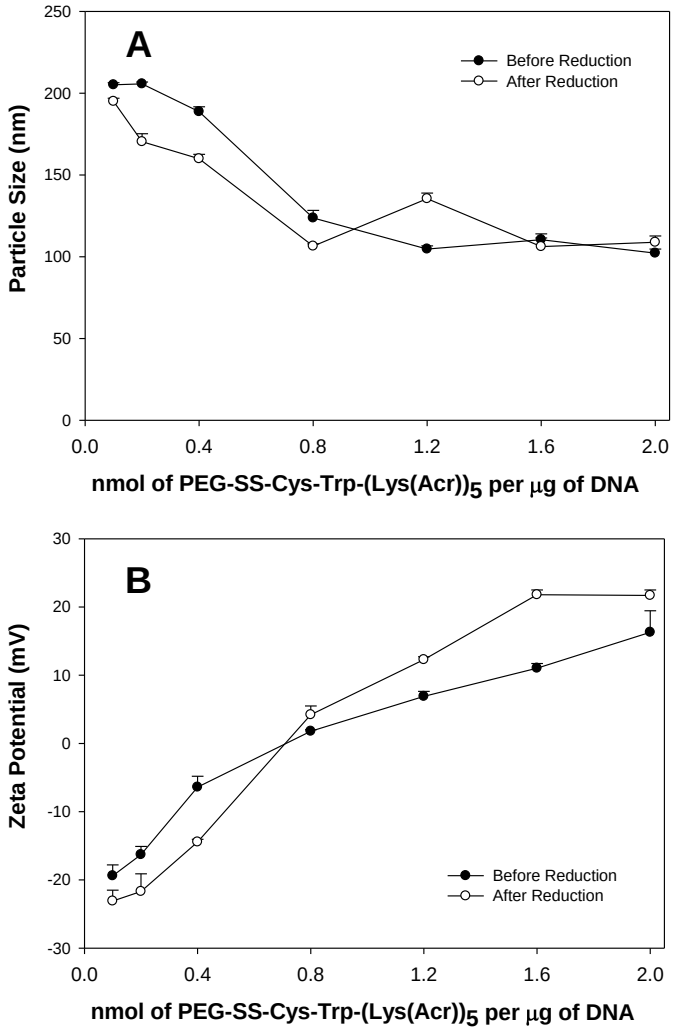

Figure 3-7. *Particle Size and Surface Charge of Reducible Polyacridine PEG Peptide DNA Polyplexes*. The particle size and zeta potential was determined for DNA polyplexes prepared with PEG-SS-Cys-Trp-$(Lys(Acr))_5$ at various stoichiometries of peptide before (-●-) and after reduction (-○-) with TCEP. The results demonstrate a decline in particle size for DNA polyplexes from 200 nm at 0.2 nmol per μg of DNA to approximately 100 nm between stoichiometries of 0.8 to 2 nmol per μg of DNA (panel A, -●-). Similarly, the surface charge of the polyplexes increase during the titration from -20 mV at 0.2 nmol per μg of DNA to 16 mV at 2 nmol per μg of DNA (panel B). The titration indicates that cationic DNA polyplexes form at a stoichiometry of 0.8 nmol per μg of DNA and above (panel B). Reduction of the polyplexes reveals no obvious change in the particle size of the polyplexes, while the surface charges either increase for cationic polyplexes (panel B (-○-), 0.8 to 2 nmol/μg), or decrease for anionic polyplexes (panel B (-○-), 0.2 to 0.4 nmol/μg) as PEG is shed.

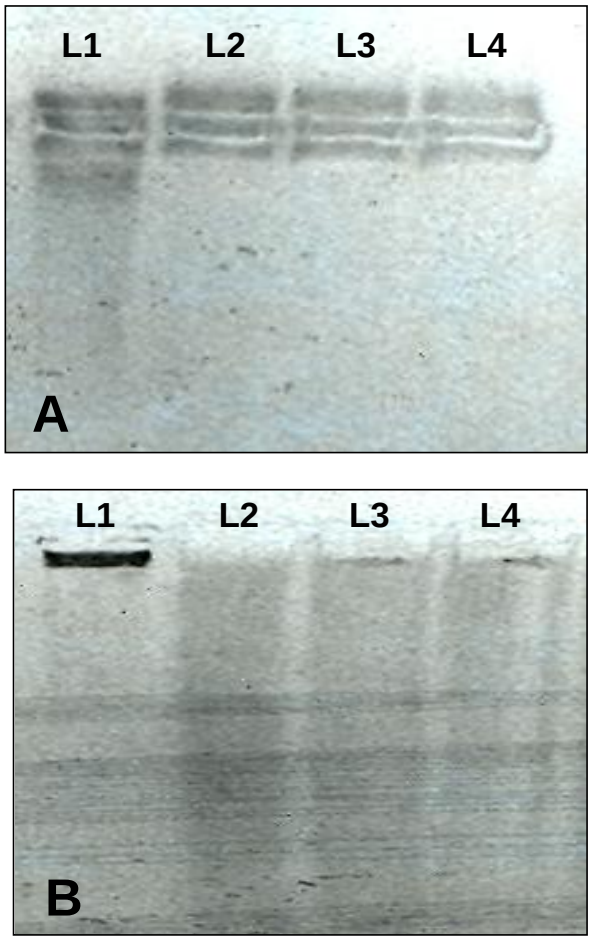

Figure 3-8. *Metabolic Stability of Reducible Polyacridine PEG Peptide DNA Polyplexes*. DNA polyplexes were prepared at 1 nmol per μg of DNA with PEG-SS-Cys-Trp-$(Lys(Acr))_5$ and incubated with 0.06 U of DNase for 0 (lane 1), 5 (lane 2), 10 (lane 3), and 20 minutes (lane 4) before (panel A) and after (panel B) reduction with TCEP and run on a 1% agarose gel. The results demonstrate protection of the DNA from metabolic degradation throughout the 20 minute analysis (panel A, lanes 1-4) using PEG-SS-Cys-Trp-$(Lys(Acr))_5$. Polyplexes reduced with TCEP prior to DNase challenge resulted in the immediate degradation of DNA (panel B, lanes 1-4). These results suggest that PEG is essential on the bioconjugate in order to provide metabolic protection against DNase.

for the non-reducible PEGylated polyacridine-DNA polyplexes (Figure 2-10, Panel B and Figure 2-11C) In contrast, reduction of DNA polyplexes with TCEP results in immediate DNase susceptibility, as degradation is observed within 5 minutes of incubation (Figure 3-8B, lane 2). This observation suggests that the PEG incorporated onto the peptide is

necessary for nuclease protection, whereas binding by polyacridine peptide alone is insufficient for protection.

In order to determine the necessity of physical intervention for IM dosed DNA formulations, a dose dependent gene expression response was investigated for DNA or DNA nanoparticles administered IM (Figure 3-9). Plasmid DNA and DNA nanoparticles prepared with PEG-Mal-Cys-Trp-Lys_{18} or PEG-SS-Cys-Trp-Lys_{18} at 0.3 nmol per μg of DNA were IM administered in each gastrocnemius muscle in mice at a dose of 20 or 100 μg of DNA in 50 μL of normal saline. The gene expression of each formulation was determined by bioluminescence imaging (BLI) 24 hours after administration, and by first IM dosing 1.2 mg in 40 μL of luciferin to each leg. The gene expression was monitored for over three weeks, and the results indicate that naked DNA achieves slightly higher expression levels compared to polyplexed DNA. Additionally, there seems to be no effect of dose escalation on gene expression for any formulation evaluated, and the low levels of expression achieved were only slightly above the lower limit of detection of the instrument.

The benefits of electroporation on the gene expression of IM dosed formulations was determined by IM administration of 1 μg of DNA or 1 μg of DNA polyplexes prepared with PEG-Mal-Cys-Trp-Lys_{18} at 0.3 nmol per μg of DNA in mice and electroporated 1 minute after dosing (Figure 3-10). Gene expression was determined by BLI 24 hours after administration, and the results indicate a 74-fold improvement for naked DNA with electroporation compared to IM alone. Likewise, a 33-fold improvement is observed for DNA polyplexes prepared with PEG-Mal-Cys-Trp-Lys_{18} when coupled with electroporation. Luciferase expression was monitored out to 30 days and throughout the time course of the study, a 98-fold loss in luciferase expression is observed for naked DNA, while a 72 fold loss in expression is observed for polyplexed DNA throughout the same time course. These results suggest that polyplexed DNA

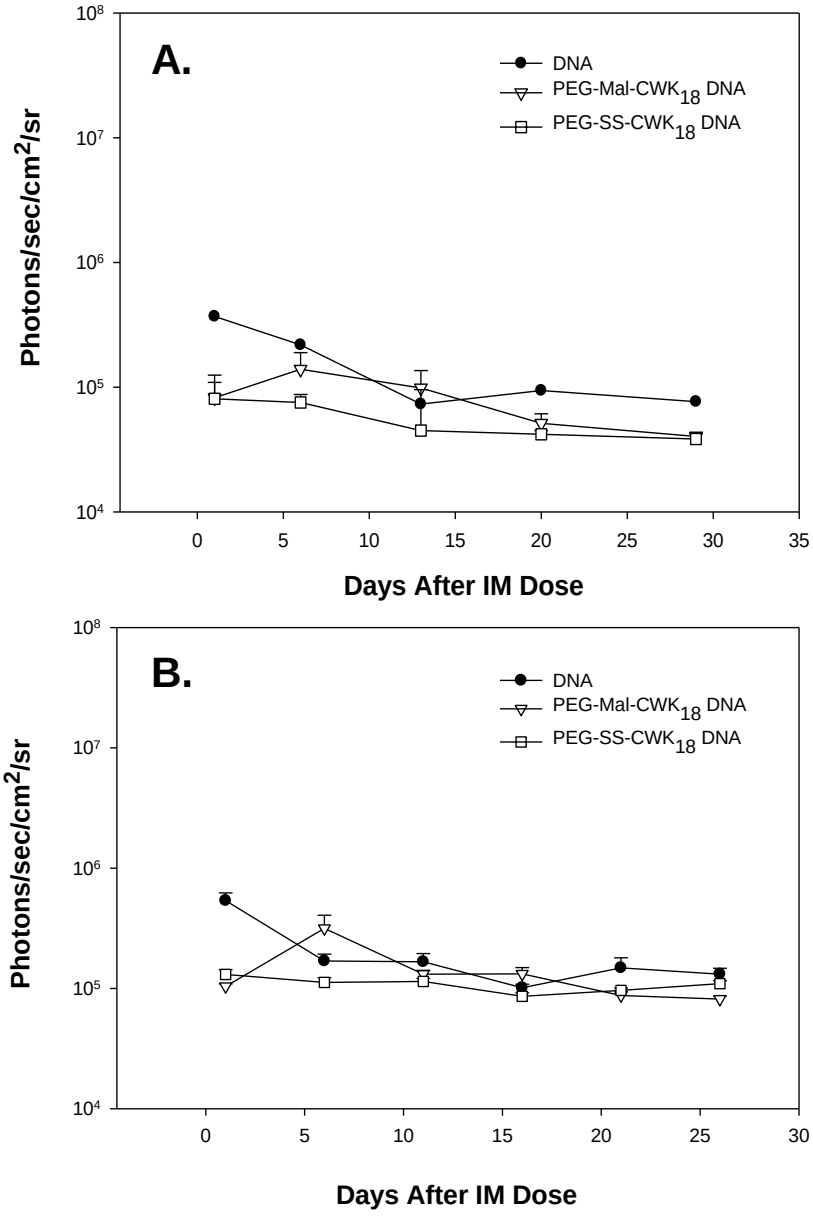

Figure 3-9. *Intramuscular Administration of PEGylated DNA Nanoparticles*. DNA or DNA polyplexes prepared with either PEG-Mal-Cys-Trp-Lys_{18} or PEG-SS-Cys-Trp-Lys_{18} at 0.3 nmol of peptide per μg of DNA were IM administered in each gastrocnemius muscle of mice at a dose of either 20 μg (panel A) or 100 μg (panel B) in 50 μl (n = 4). The results reveal low gene transfer efficiencies for all formulations evaluated using this administration route, and furthermore the lack of dose dependency observed suggest that the DNA formulations fail to deliver a substantial amount of DNA to the nucleus of the cells.

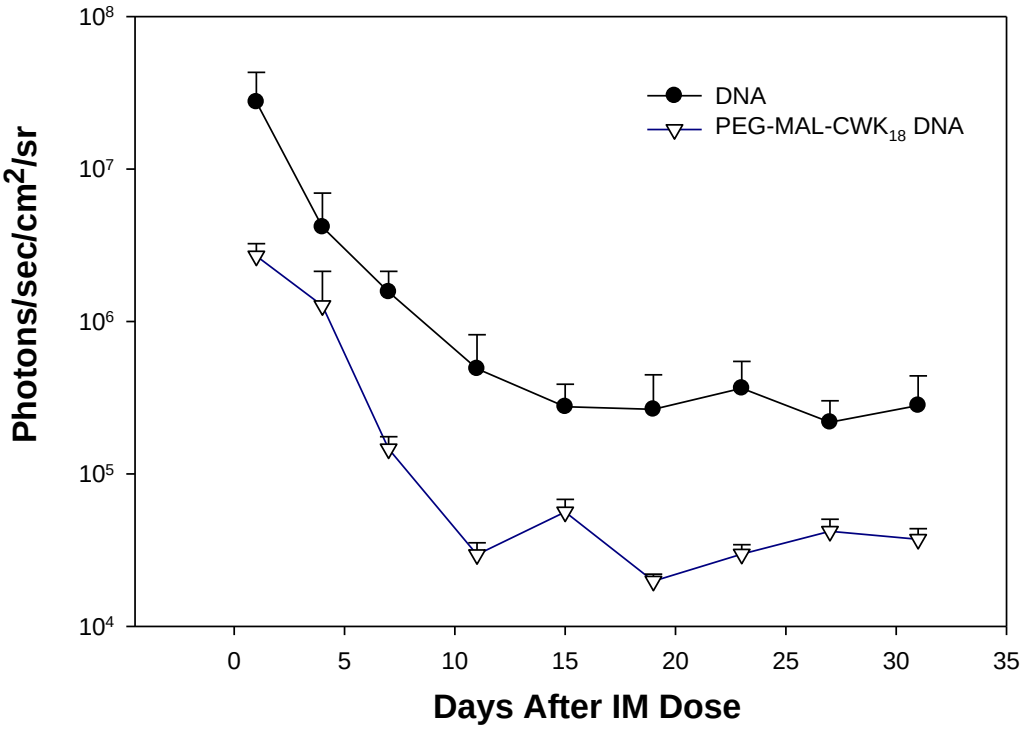

Figure 3-10. *Intramuscular Electroporation (IM-EP) of PEGylated DNA Nanoparticles*. DNA (1μg in 50 μL) or DNA polyplexes prepared with PEG-Mal-Cys-Trp-Lys_{18} at 0.3 nmol of peptide per μg of DNA (1μg in 50 μL) were administered IM to each gastrocnemius muscle of mice and electroporated using an electrode syringe (n = 4). The results demonstrate a sharp improvement in gene transfer efficiency for DNA and DNA polyplexes using IM-EP even at a low dose of DNA (1 μg), and detectable levels of gene expression (above 10^5 Photons/sec/cm^2/sr) persist for up to 30 days after administration.

provides greater nuclease stability throughout the study compared to the IM-EP of naked DNA.

In an attempt to improve the gene expression of IM-EP dosed DNA formulations, two main parameters where investigated. The first was to test the influence of a reducible linkage between the polymer and the peptide for all DNA formulations prepared, and the second was to determine the influence of cross-linking on gene expression, both of which maintain anionic surface charges. Non-reducible or reducible DNA nanoparticles were prepared with PEG-Mal-Cys-Trp-Lys_{18} or PEG-SS-Cys-Trp-Lys_{18} at 0.3 nmol per μg.

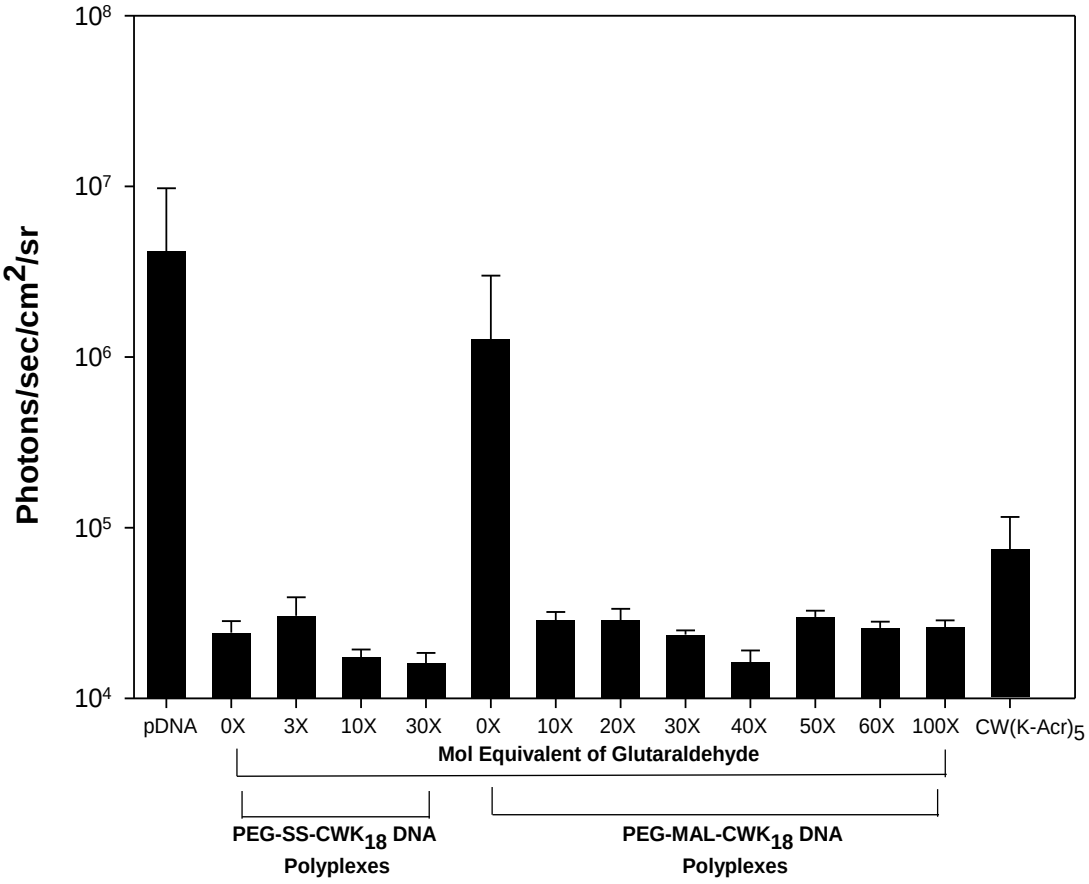

Figure 3-11. *Gene Transfer Efficiency of Cross-Linked DNA Polyplexes and Reducible Polyacridine PEG Peptide DNA Polyplexes*. Plasmid DNA or DNA polyplexes (1 μg / 50 μL) were IM dosed and electroporated in each gastrocnemius muscle in mice and gene expression was measured 48 hours after administration. The effect of cross-linking DNA nanoparticles was evaluated by preparing polyplexes with PEG-SS-Cys-Trp-Lys_{18} or PEG-Mal-Cys-Trp-Lys_{18} at 0.3 nmol per μg of DNA and glutaraldehyde cross-linking the amines with 0 to 100 mole equivalents of glutaraldehyde. Reducible polyacridine PEG peptide DNA polyplexes were prepared using PEG-SS-Cys-Trp-$(Lys(Acr))_5$ of a stoichiometry of 2 nmol per μg of DNA and administered as described above. The results indicate that cross-linking DNA polyplexes results in low levels of gene expression. Reducible DNA polyplexes prepared with PEG-SS-Cys-Trp-Lys_{18} (0X) resulted in nearly a two order magnitude loss in gene expression compared to the non-reducible polyplexes prepared with PEG-Mal-Cys-Trp-Lys_{18} (0X). Furthermore, reducible polyacridine PEG peptides resulted in comparatively low levels of gene expression compared to DNA alone.

Non-reducible DNA nanoparticles were cross-linked with 0 to 100 mole equivalents of glutaraldehyde, while reducible DNA nanoparticles were cross-linked with 0 to 30 mole equivalents of glutaraldehyde. Additionally, reducible polyacridine PEG-peptide DNA polyplexes were prepared with PEG-SS-Cys-Trp-$(Lys(Acr))_5$ at 2 nmol per μg of DNA, which was the optimal ratio for gene expression using PEG-Mal-Cys-Trp-$(Lys(Acr))_5$ observed previously (Figure 2-8, -○-). All formulations contained 1 μg of DNA in 50 μL and were IM dosed in the gastrocnemius muscle of mice and electroporated 1 minute after administration. Gene expression was determined 48 hours after administration, and the results indicate that cross-linking DNA nanoparticles, regardless of the degree of cross-linking, or whether the polyplex possessed a reversible or non-reversible linkage between the peptide and polymer, yielded negligible levels of gene expression (Figure 3-11). Furthermore, the data illustrate that reversible linkage between the peptide and PEG for DNA nanoparticles resulted in over a 50-fold loss in gene expression (Figure 3-11, 0X, PEG-SS-CWK_{18} and 0X, PEG-Mal-CWK_{18}). This observation further extends to polyacridine PEG-peptide-DNA polyplexes where over a 100-fold loss is expression is observed for PEG-SS-Cys-Trp-$(Lys(Acr))_5$ compared to non-reducible PEG-Mal-Cys-Trp-$(Lys(Acr))_5$ polyplexes prepared at the same stoichiometry (Figure 3-11, $CW(K-Acr)_5$ compared to Figure 2-8, open circle, Day 2). The results suggest that a reversible disulfide bond between the peptides and PEG results in gene delivery peptides that are incompatible with IM-EP.

Discussion

Several delivery barriers impede efficient in vivo gene transfection. Direct tissue injections of DNA formulations bypass any complications that may arise from poor pharmacokinetic properties or biodistribution limitations. Additionally, plasmid DNA has been shown to transfect skeletal muscle, and expression levels have been shown to persist

for up to 6 months.[199] Nevertheless, packaging DNA in cationic delivery vehicles has been shown to be incompatible with IM-EP.[200]

This chapter introduces two different strategies for the preparation of anionic DNA polyplexes for improved biocompatibility with electroporation. The first strategy involves the condensation of DNA with PEGylated Cys-Trp-Lys_{18}, where the lysine residues on the peptide electrostatically bind to DNA and form DNA nanoparticles, and the PEG on the bioconjugate serves to reduce the cationic surface charge that results from the primary amines of the excess peptide required for DNA condensation. The resulting PEGylated DNA nanoparticles possess sizes of approximately 200 nm in diameter with surface charges below 15 mV (Figure 3-3 and Figure 3-4A & B). In order to prepare anionic DNA nanoparticles using PEGylated Cys-Trp-Lys_{18}, the primary amines on the surface of the nanoparticles were cross-linked using glutaraldehyde (Figure 3-2). The degree of cross-linking determined the extent of decrease in the surface charge observed for the DNA nanoparticles. The results show that anionic particles are formed when 40 mole equivalents of glutaraldehyde is reacted with PEG-Mal-Cys-Trp-Lys_{18} DNA polyplexes, and that 60 mole equivalents of glutaraldehyde is required to form anionic DNA nanoparticles with PEG-SS Cys-Trp-Lys_{18} (Figure 3-3 & Figure 3-4B).

The second strategy for the preparation on anionic DNA polyplexes involves the binding of PEGylated polyacridine peptide to DNA by intercalation rather than solely by electrostatic interactions, as previously investigated in Chapter 2. The PEG-SS-Cys-Trp-$Lys(Acr)_5$ peptide varies from the previous analogue by incorporating a reducible disulfide bond between the polyacridine peptide and the PEG polymer. Previous in vitro studies using PEG-SS-Cys-Trp-Lys_{18}, which contains a reducible disulfide linkage, demonstrated a significant improvement on transfection efficiencies compared to a similar non-reducible peptide.[169] Furthermore, a 34-fold increase in cell binding was determined for DNA nanoparticles with a reducible linkage between the peptide and PEG, suggesting that PEG is released on the cell surface and its loss facilitates cellular

update. Therefore this chapter evaluates both reducible polyacridine PEG-peptide DNA polyplexes, and reducible PEGylated DNA nanoparticles with and without glutaraldehyde cross-linking for similar attributes.

The influence of reduction on the size, charge, and shape of reducible polyacridine PEG-peptide DNA polyplexes and reducible PEGylated DNA nanoparticles was also investigated to determine the important parameters required for optimal DNA delivery. While PEG was responsible for diminishing the surface charge of all polyplexes (Figure 3-4B and Figure 3-7B), reduction with TCEP only affected those DNA nanoparticles cross-linked with 0 to 30 mole equivalents of glutaraldehyde (Figure 3-4A, white bars). In contrast, no change in size was observed after the reduction for polyplexes prepared with PEG-SS-Cys-Trp-Lys(Acr)$_5$ (Figure 3-7B). The results suggest that the aggregation observed after reduction was largely due to a disruption of the electrostatic interaction between the peptide and DNA. This conclusion is based on two observations. The first is the stability in size observed after reduction for polyplexes prepared with PEG-SS-Cys-Trp-Lys(Acr)$_5$, which bind to DNA through a combination of electrostatic interactions and intercalation (Figure 3-7A). The second is due to the particle size stability observed at 40 mole equivalents of glutaraldehyde, which coincides with the first degree of cross-linking that yields anionic DNA nanoparticles after reduction (Figure 3-4B, 40X, white bars).

Preliminary in vivo intramuscular (IM) experiments illustrate the necessity of physical administration methods for overcoming drug delivery barriers. IM injections of DNA or DNA nanoparticles prepared with PEG-Mal-Cys-Trp-Lys$_{18}$ or PEG-SS-Cys-Trp-Lys$_{18}$ at 0.3 nmol per μg at a dose of 20 or 100 μg of DNA resulted in background levels of expression, regardless of the dose administered or whether the plasmid was naked or polyplexed with PEG-peptide (Figure 3-9A&B). The lack of a dose-dependent response for IM dosed DNA suggests that actual amount of plasmid that reaches the nucleus is similar in both circumstances, regardless of the five fold increase in dose. Therefore,

these results indicate that IM dosed DNA is significantly limited in activity due to the cellular barriers that severely impede gene delivery. In order to improve these limitations, intramuscular administrations have been coupled with electroporation devices to bypass limitations due to inefficient drug delivery into the cytosol of cells.[7,8] The intramuscular-electroporation (IM-EP) of 1 μg of DNA or 1 μg of DNA polyplexes prepared with PEG-Mal-Cys-Trp-Lys_{18} at 0.3 nmol per μg resulted in gene expression levels nearly two orders of magnitude greater than that observed by the IM dosing alone of DNA or DNA polyplexes (Figure 3-10 compared to Figure 3-9B). While recent investigations have concluded that the gene transfer efficiencies of cationic DNA polyplexes are diminished when coupled with electroporation,[9,10] the data presented indicates that IM-EP can be used to improve the gene delivery of DNA polyplexes in addition to that of naked plasmid DNA.

In order to further improve the transfection efficiencies observed with electroporation, DNA polyplexes that improve the transport of DNA inside the cell during electroporation must be prepared without compromising the solubility of the polyplex in order to avoid aggregation during electroporation.[46] Given the incompatibility of cationic DNA polyplexes with IM-EP delivery, polyplexes that possess anionic surface charges may improve transport during electroporation and lead to higher gene transfer. Nevertheless, the results in this chapter show that cross-linked DNA nanoparticle formulations led to poor gene transfer (Figure 3-11) regardless of their surface charges. These observations could be due to the morphological changes that occur upon cross-linking (Figure 3-5), or perhaps it is due to poor DNA release properties from the cross-linked polyplex.

Including a reducible disulfide linkage between the peptide and PEG resulted in diminished in vivo activity in all cases (Figure 3-11). PEGylated DNA nanoparticles prepared with PEG-Mal-Cys-Trp-Lys_{18} or PEG-SS-Cys-Trp-Lys_{18} possessed similar sizes and surface charges, indicating that the cellular transport of DNA polyplexes during

electroporation should have also been similar. Given the large change in size of the polyplex upon reduction, the results suggest that the reduction of the polyplex is responsible for the poor gene transfer efficiencies observed. Nevertheless, the same explanation cannot be true for DNA polyplexes prepared with PEG-SS-Cys-Trp-Lys$(Acr)_5$ since there is no apparent change in the size of the polyplex upon reduction. Rather the reason for their inefficient gene transfer may be due to its poor DNase stability after reduction, or perhaps it is due to poor DNA release properties that may result from the increased binding affinity of the peptide for DNA after reduction (Figure 3-6C).

Controlling the size and surface charge of DNA polyplexes is an essential component of a gene delivery system for improved in vivo transfection efficiencies. The apparent methods of improving the gene transfer using IM-EP is to either achieve higher initial gene expression surpassing that of plasmid DNA, or to create a sustained released formulation that can mediate high levels of expression for longer periods. This chapter introduces two distinct methods of creating anionic DNA formulations for IM-EP that both create stable DNA formulations with controllable surface charges. Nevertheless, neither strategy was able to sustain gene expression levels similar to that of naked DNA either due to poor transport during electroporation, poor DNA release from the polyplex, or to poor DNase stability. In order to determine which factor is responsible for the poor transfection levels observed, radiolabeled DNA can be used to elucidate the delivery mechanism. After IM-EP administration of each formulation, the muscle tissue can be harvested, washed, and gamma counted to verify the amount of DNA that internalized during electroporation. The DNA can then extracted and run on gel to verify the integrity of the DNA in the tissue. If lower transfection levels are observed compared to naked DNA, and the formulations possess similar transport and metabolic protection properties, then it would be concluded that the DNA is irreversibly associated with the polyplex.

The findings presented in this chapter suggest that a reversible linkage between the peptide and the PEG polymer leads to formulations that are incompatible with

electroporation. Therefore, incorporating the results from both electroporation chapters, the data suggest that future molecular conjugates for IM-EP should be designed with non-reducible PEG linkage between the peptide and the polymer, and should include an anionic moiety, in addition to DNA binding sequence, to improve the amount of DNA that enters the cell without compromising the DNase stability or the solubility of the polyplex.

CHAPTER 4: ELECTRONEGATIVE POLYACRIDINE-PEG PEPTIDE DNA OPEN POLYPLEXES STIMULATE HIGH LEVELS OF GENE EXPRESSION IN THE LIVER

Abstract

Engineering polyacridine PEG-peptide DNA polyplexes that are blood compatible requires high affinity binding peptides that create anionic or neutral polyplexes with DNA in order to avoid recognition by the reticuloendothelial system (RES). The previous chapters have demonstrated that polyacridine PEG-peptides protect DNA from nuclease metabolism, bind reversibly to DNA, and maintain suitable solubility properties that are required for high expression with IM-EP administration. Nevertheless, improving the synthetic strategy used to prepare the polyacridine PEG-peptides will lead to homogenous products that are easier to prepare, characterize, and purify, while also improving inter-batch reproducibility.

The present chapter introduces a new class of gene delivery peptides that also bind to plasmid DNA through polyintercalation and produce unique, anionic open-polyplexes. These peptides share the general structure $(Acr\text{-}X)_4$-Cys-PEG, where each (Acr-X) unit consists of two amino acids. The first is a lysine that has been modified on the ε-amine with an acridine (Acr), and the second is a spacing amino acid X that was varied to be either a Lys, Arg, Leu or Glu residue. The peptides were designed to establish a clear structure-activity relationship by comparing the binding affinity, surface charge, and shape of the different polyplexes to their ability to stimulate in vivo gene expression in mice. The results demonstrate that polyacridine-PEG peptide polyplexes are stable in the systemic circulation for up to 30 minutes, and that a high binding affinity of polyacridine-PEG peptides to DNA is essential in order to mediate high levels of stimulated gene expression in mice (reproduced with written permission from ACS Publications).

Introduction

Despite the inception of non-viral gene therapy in the 1990's, the field has yet to produce a vector that can efficiently target a polyplex formulation from the site of administration to the cytoplasm of diseased cells. A major reason for the limited success of non-viral vectors resides in the inherent incompatibility of cationic DNA nanoparticles in the systemic circulation. Most non-viral gene delivery systems rely on electrostatic interactions between the negatively charged phosphates on oligonucleotides and the positively charged amines on a polymer, peptide, or lipid. The resulting cationic nanoparticles that form have been shown to mediate high levels of gene expression in vitro, but fail to achieve similar levels of gene expression in vivo, presumably due to their rapid clearance from the blood.[130, 201-207]

Strategies to enhance the biocompatibility of non-viral vectors with the blood have typically involved PEGylation methods that limit phagocytosis by the reticulo-endothelial system (RES) cells in order to improve the circulatory half-life of the DNA polyplexes. While including polyethylene glycol (PEG) onto the surface of polyplexes has resulted in improved pharmacokinetic properties, it has also led to decreased transfection efficiencies and premature dissociation of the polyplex during transit in systemic circulation.[48-54]

In order to develop nonviral gene delivery agents that function with greater efficiency in vivo following iv dosing, it is necessary to control the size, charge and metabolic stability of polyplexes.[208] Previous chapters have demonstrated that the biding affinity of polyacridine PEG-peptides can be controlled by varying the units of acridine incorporated onto the PEG-peptide. The results determined that five lysine-acridine chains were needed for high affinity binding to plasmid DNA and that polyacridine PEG-peptides produced anionic DNA open-polyplexes with apparent sizes below 200 nm in diameter, regardless of the stoichiometry of peptide used for polyplex preparation. The PEG on the polyacridine PEG-peptide was determined to be essential for nuclease

protection, and the PEG-Mal-Cys-Trp-(Lys-(Acr))$_5$ peptide proved capable of mediating gene transfer in vivo when delivered by im-electroporation. [209]

The present chapter introduces a novel series of polyacridine-PEG peptides each possessing the general structure (Acr-X)$_4$-Cys-PEG, where the rational behind their design was to elucidate the physical properties required to create DNA polyplexes that are stable against metabolism in the blood. The results demonstrate that polyacridine-PEG peptides form anionic open structures that are capable of mediating high levels of stimulated gene expression when the iv administration of DNA formulations are followed by a hydrodynamic dose of normal saline in mice. The findings suggest that a high binding affinity between the polyacridine-PEG peptide and DNA is essential in order to maintain metabolically stabilized DNA that can stimulate high levels of gene expression in vivo.

Materials and Methods

Unsubstituted Wang resin, 9-hydroxybenzotriazole, Fmoc-protected amino acids, O-(7-Azabenzo-triazol-1-yl)-N,N,N',N'-tetramethylurionium hexafluorophosphate (HATU), Fmoc-Lysine-OH, and N-Methyl-2-pyrrolidinone (NMP) were obtained from Advanced Chemtech (Lexington, KY). N,N-Dimethylformamide (DMF), trifluoroacetic acid (TFA), and acetonitrile were purchased from Fisher Scientific (Pittsburgh, PA). Diisopropylethylamine, piperidine, acetic anhydride, Tris(2-carboxyethyl)-phosphine hydrochloride (TCEP), 9-chloroacridine and thiazole orange were obtained from Sigma Chemical Co. (St. Louis, MO). Agarose was obtained from Gibco-BRL. mPEG-maleimide and mPEG-OPSS (5,000 Da) were purchased from Laysen Bio (Arab, AL). D-Luciferin and luciferase from *Photinus pyralis* were obtained from Roche Applied Science (Indianapolis, IN). pGL3 control vector, a 5.3 kb luciferase plasmid containing a SV40 promoter and enhancer, was obtained from Promega (Madison, WI). pGL3 was

amplified in a DH5α strain of *Escherichia coli* and purified according to manufacturer's instructions.

Synthesis and Characterization of $(Acr\text{-}X)_4$-Cys Peptides

9-Phenoxyacridine and Fmoc-Lysine(Acridine)-OH were prepared as recently reported.[210, 211] The polyacridine peptides reported in Table 4-1 were prepared by solid phase peptide synthesis on a 30 µmol scale on an APEX 396 Synthesizer using standard Fmoc procedures including 9-hydroxybenzotriazole and HATU activation while employing double coupling of Fmoc-Lys(Acr)-OH and triple coupling for the spacing amino acid while using a 5-fold excess of amino acid over resin and omitting N-capping of truncated peptide species. Peptides were removed from resin and side chain deprotected using a cleavage cocktail of TFA/ethanedithiol/water (93:4:3 v/v/v) for 3 hrs followed by precipitation in cold ether. Precipitates were centrifuged for 10 min at 5000 x g at 4ºC and the supernatant decanted. Peptides were then reconstituted with 0.1 v/v % TFA and purified to homogeneity on RP-HPLC by injecting 0.5-2 µmol onto a Vydac C18 semi-preparative column (2 x 25 cm) eluted at 5 mL per min with 0.1 v/v % TFA with an acetonitrile gradient of 20-30 v/v % over 30 min while monitoring acridine at 409 nm. The major peak was collected and pooled from multiple runs, concentrated by rotary evaporation, lyophilized, and stored at -20ºC. Purified peptides were reconstituted in 0.1 v/v % TFA and quantified by absorbance (acridine $\varepsilon_{409\ nm} = 9266\ M^{-1}\ cm^{-1}$ assuming additivity of ε for multiple acridines) to determine isolated yield (Table 4-1). Purified peptides were characterized by LC-MS by injecting 2 nmol onto a Vydac C18 analytical column (0.47 x 25 cm) eluted at 0.7 mL per min with 0.1 v/v % TFA and an acetonitrile gradient of 10-55 v/v % over 30 min while acquiring ESI-MS in the positive mode. Synthesis of peptides was done in collaboration with Nicholas J. Baumhover, Medicinal and Natural Products Chemistry, University of Iowa.

Synthesis and Characterization of PEGylated $(Acr\text{-}X)_4$-Cys Peptides

PEGylation of the Cys residue on $(Acr\text{-}X)_4$-Cys was achieved by reacting 1 μmol of peptide with 1.1 μmol of $PEG_{5000\ Da}$–maleimide or $PEG_{5000\ Da}$-OPSS in 4 mL of 10 mM ammonium acetate buffer pH 7 for 12 hrs at RT. PEGylated peptides were purified by semipreparative HPLC as previously described and eluted with 0.1 v/v % TFA with an acetonitrile gradient of 25-65 v/v %, while monitoring acridine at 409 nm.[169] The major peak was collected and pooled from multiple runs, concentrated by rotary evaporation, lyophilized, and stored at -20ºC. Reconstitution of the PEGylated polyacridine peptide in water after this step resulted in peptides possessing a TFA counterion. The necessity to exchange the counterion of the PEGylated peptides was indirectly determined, and counterion exchange was accomplished by chromatography on a G-25 column (2.5 x 50 cm) equilibrated with 0.1 v/v % acetic acid to obtain the peptide in an acetate salt form. The major peak corresponding to the PEG-peptide eluted in the void volume (100 mL) was pooled, concentrated by rotary evaporation, and freeze-dried. PEG-peptides were reconstituted in water and quantified by Abs_{409nm} to determine isolated yield (Table 4-1). PEG-peptides were characterized by MALDI-TOF MS by combining 1 nmol with 10 μL of 2 mg per mL α-cyano-4-hydroxycinnamic acid (CHCA) in 50 v/v % acetonitrile and 0.1 v/v % TFA. Samples were spotted onto the target and ionized on a Bruker Biflex III Mass Spectrometer operated in the positive ion mode. Synthesis of peptides was done in collaboration with Nicholas J. Baumhover, Medicinal and Natural Products Chemistry, University of Iowa.

Characterization of PEGylated Polyacridine Peptide DNA Polyplexes

The relative binding affinity of PEGylated polyacridine peptides for DNA was determined by a fluorophore exclusion assay.[16] pGL3 (200 μL of 5 μg/mL in 5 mM

HEPES pH 7.5 containing 0.1 μM thiazole orange) was combined with 0, 0.2, 0.3, 0.4, 0.5, or 1 nmol of PEGylated polyacridine peptide in 300 μL of HEPES and allowed to bind at RT for 30 min. Thiazole orange fluorescence was measured using an LS50B fluorometer (Perkin-Elmer, U.K.) by exciting at 498 nm while monitoring emission at 546 nm with the slit widths set at 10 nm. A fluorescence blank of thiazole orange in the absence of DNA was subtracted from all values before data analysis. The data is presented as nmol of PEGylated polyacridine peptide per μg of DNA versus the percent fluorescence intensity ± the standard deviation determined by three independent measurements.

The particle size and zeta potential were determined by preparing 2 mL of polyplex in 5 mM HEPES pH 7.5 at a DNA concentration of 30 μg per mL and a PEGylated polyacridine peptide stoichiometry of 0, 0.2, 0.3, 0.4, 0.5, 0.6, 0.8 or 1 nmol per μg of DNA. The particle size was measured by quasi-elastic light scattering (QELS) at a scatter angle of 90º on a Brookhaven ZetaPlus particle sizer (Brookhaven Instruments Corporation, NY). The zeta potential was determined as the mean of ten measurements immediately following acquisition of the particle size.

The shape of PEGylated polyacridine polyplexes was determined using atomic force microscopy (AFM). pGL3 alone, or anionic PEGylated polyacridine polyplexes at 0.2 and 0.8 nmol of peptide per μg of DNA, were prepared at a concentration of 100 μg per mL of DNA in 10 mM Tris, 1 mM EDTA pH 8. Polyplexes were diluted to 1 μg per mL in 40 mM HEPES 5 mM nickel chloride pH 6.7 and deposited on a fresh cleaved mica surface for 10 min followed by washing with deionized water. Images were captured using an Asylum AFM MFP3D (Santa Barbara, CA) operated in the AC-mode using a silicon cantilever (Ultrasharp NSC15/AlBS, MikroMasch).

Gel Band Shift Assay

pGL3 (1 μg), or pGL3 polyplexes (1 μg) prepared at 0.5 nmol with either (Acr-Arg)$_4$-Cys-PEG, (Acr-Lys)$_4$-Cys-PEG, (Acr-Leu)$_4$-Cys-PEG, or (Acr-Glu)$_4$-Cys-PEG in 20 μL of 5 mM HEPES buffer pH 7.4 and 2 μL of loading buffer.[113] The samples were loaded onto a 1% agarose gel (50 mL) and electrophoresed in TAE buffer at 80 V for 90 min. The gel was post-stained with 0.1 μg per mL of ethidium bromide at 4°C overnight and then imaged on a UVP Biospectrum Imaging System (Upland, California).

Hydrodynamic Stimulation and Bioluminescence Imaging

pGL3 (1 μg) was prepared in a volume of normal saline corresponding to 9% wt/vol of the mouse's body weight (1.6 – 2.3 mL based on 15-23 g mice). The DNA dose was administered by tail vein to 4-5 mice in 5 sec according to a published procedure.[14, 212] Mice (4-5) were also dosed via the tail vein with 1 μg of PEGylated polyacridine polyplex in 50 μL of HBM (5 mM HEPES, 0.27 M mannitol, pH 7.4). At times ranging from 5-120 min, a stimulatory hydrodynamic dose of normal saline (9% wt/vol of the body weight) was administered over 5 sec. At 24 hrs post-DNA dose, mice were anesthetized by 3% isofluorane, then administered an i.p. dose of 80 μL (2.4 mg) of D-luciferin (30 μg/μL in phosphate-buffered saline). At 5 min following the D-luciferin dose, mice were imaged for bioluminescence (BLI) on an IVIS Imaging 200 Series (Xenogen). Images were acquired at a 'medium' binning level and a 20 cm field of view. Acquisition times were varied (1 sec - 1 min) depending on the intensity of the luminescence. The Xenogen system reported bioluminescence as photons/sec/cm^2/seradian in a 2.86 cm diameter region of interest covering the liver. The integration area was transformed to pmols of luciferase in the liver using a previously reported standard curve.[213] The results were determined to be statistically significant ($p \leq 0.05$) based on a two-tailed unpaired t-test. Administration was performed in

collaboration with Jason Duskey, Medicinal and Natural Products Chemistry, University of Iowa.

Results

A panel of PEGylated polyacridine peptides were prepared and tested for their ability to bind and transport DNA in vivo. The peptides were designed to evaluate the influence of DNA binding affinity on gene transfer efficiency. In order to examine the influence of spacing amino acid on the binding affinity, four peptides of the general structure $(Acr\text{-}X)_4$ were prepared, where X is either Lys, Arg, Leu or Glu (Table 4-1). Each polyacridine-PEG peptide also possessed a C-terminal Cys residue that was modified with a poly(ethylene) glycol polymer. Conjugation of each polyacridine peptide with PEG was accomplished by reaction of the Cys residues with either PEG-maleimide or PEG-OPSS, resulting in PEGylated polyacridine peptides with a reducible disulfide or a non-reducible maleimide linkage (Figure 4-1). The reaction was monitored by RP-HPLC in which the polyacridine peptide (Figure 4-2A) was mostly consumed, resulting in formation of a later eluting PEG-peptide (Figure 4-2B). Preparative RP-HPLC purification produced PEG peptides free of non-reacted polyacridine peptide and PEG as established by analytical RP-HPLC and MALDI-TOF analysis (Figure 4-2C). Each PEGylated polyacridine peptide produced a MALDI-TOF MS with multiple peaks due to the polydispersity of $PEG_{5000\ Da}$, with average mass closely correlated to the calculated mass for the PEGylated peptide (Table 4-1).

The relative binding affinity of PEGylated polyacridine peptides for pGL3 was compared by determining the concentration of peptide that completely displaces a thiazole orange intercalator dye, resulting in decreased fluorescence. Comparison of PEGylated $(Acr\text{-}X)_4$ (X is either Arg, Lys, Leu or Glu) established the importance of cationic amino acids to increase binding affinity. Both the Lys and Arg analogue demonstrated high affinity by completely displacing thiazole orange at 0.4 nmol of

peptide per μg of DNA. Conversely, the Leu analogue demonstrated weaker binding resulting in full displacement at 1 nmol, and the Glu analogue was the overall weakest binder, only achieving 40% displacement at 1 nmol (Figure 4-3A). The relative binding affinity of PEGylated polyacridine peptides for pGL3 was compared by determining the concentration of peptide that completely displaces a thiazole orange intercalator dye, resulting in decreased fluorescence. Comparison of PEGylated $(Acr\text{-}X)_4$ (X is either Arg, Lys, Leu or Glu) established the importance of cationic amino acids to increase binding affinity. Both the Lys and Arg analogue demonstrated high affinity by completely displacing thiazole orange at 0.4 nmol of peptide per μg of DNA. Conversely, the Leu

Table 4-1. PEGylated Polyacridine Peptides Prepared for In Vivo Analysis

Polyacridine Peptides	**Mass (calc / obs)[a]**	**% Yield**
$(Acr\text{-}Arg)_4$-Cys	1967.4 / 1967.2	30 %
$(Acr\text{-}Lys)_4$-Cys	1855.3 / 1855.1	26 %
$(Acr\text{-}Leu)_4$-Cys	1795.3 / 1795.1	31 %
$(Acr\text{-}Glu)_4$-Cys	1859.1 / 1859.0	22 %
PEGylated Polyacridine Peptides	**Mass (calc / obs)[b]**	**% Yield**
$(Acr\text{-}Arg)_4$-Cys-Mal-PEG	7467 / 7218	53 %
$(Acr\text{-}Arg)_4$-Cys-SS-PEG	7467 / 7450	44 %
$(Acr\text{-}Lys)_4$-Cys-Mal-PEG	7355 / 7218	55 %
$(Acr\text{-}Leu)_4$-Cys-Mal-PEG	7295 / 7110	46 %
$(Acr\text{-}Glu)_4$-Cys-Mal-PEG	7359 / 7262	35%

a. Determined by ESI-MS

b. Determined by MALDI-TOF MS

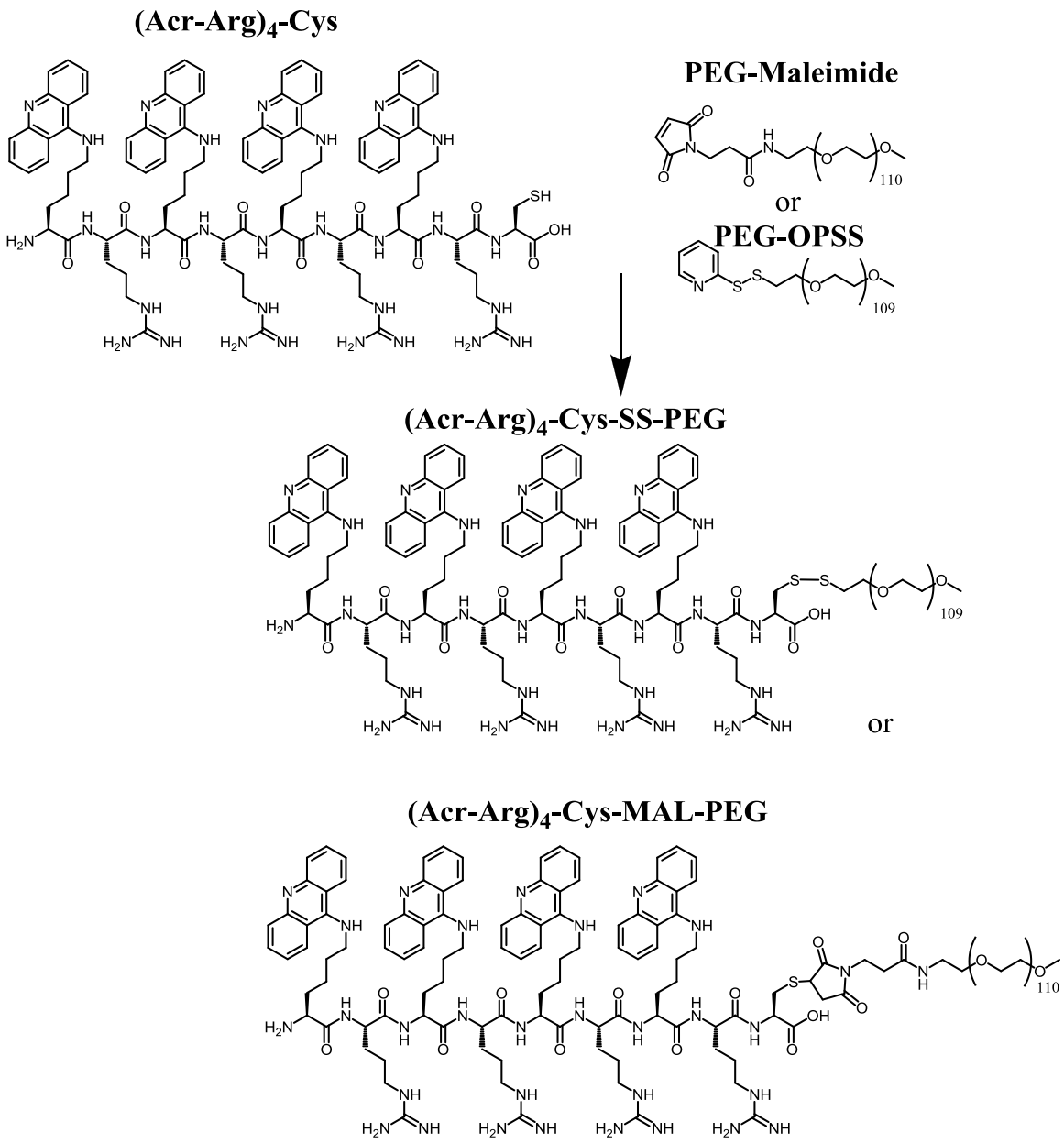

Figure 4-1. *Synthetic Strategy for PEGylated Polyacridine Peptides.* The approach used to prepare $(Acr\text{-}Arg)_4$-Cys-Mal-PEG and $(Acr\text{-}Arg)_4$-Cys-SS-PEG is demonstrated as an example of how all other polyacridine PEG-peptides described in Table 4-1 were prepared. $(Acr\text{-}Arg)_4$-Cys (where Acr is Lys modified on the ε-amine with an acridine) was prepared by solid phase peptide synthesis. The Cys thiol was then reacted with either 5 kDa PEG-maleimide or PEG-OPSS, resulting in $(Acr\text{-}Arg)_4$-Cys-Mal-PEG or $(Acr\text{-}Arg)_4$-Cys-SS-PEG.

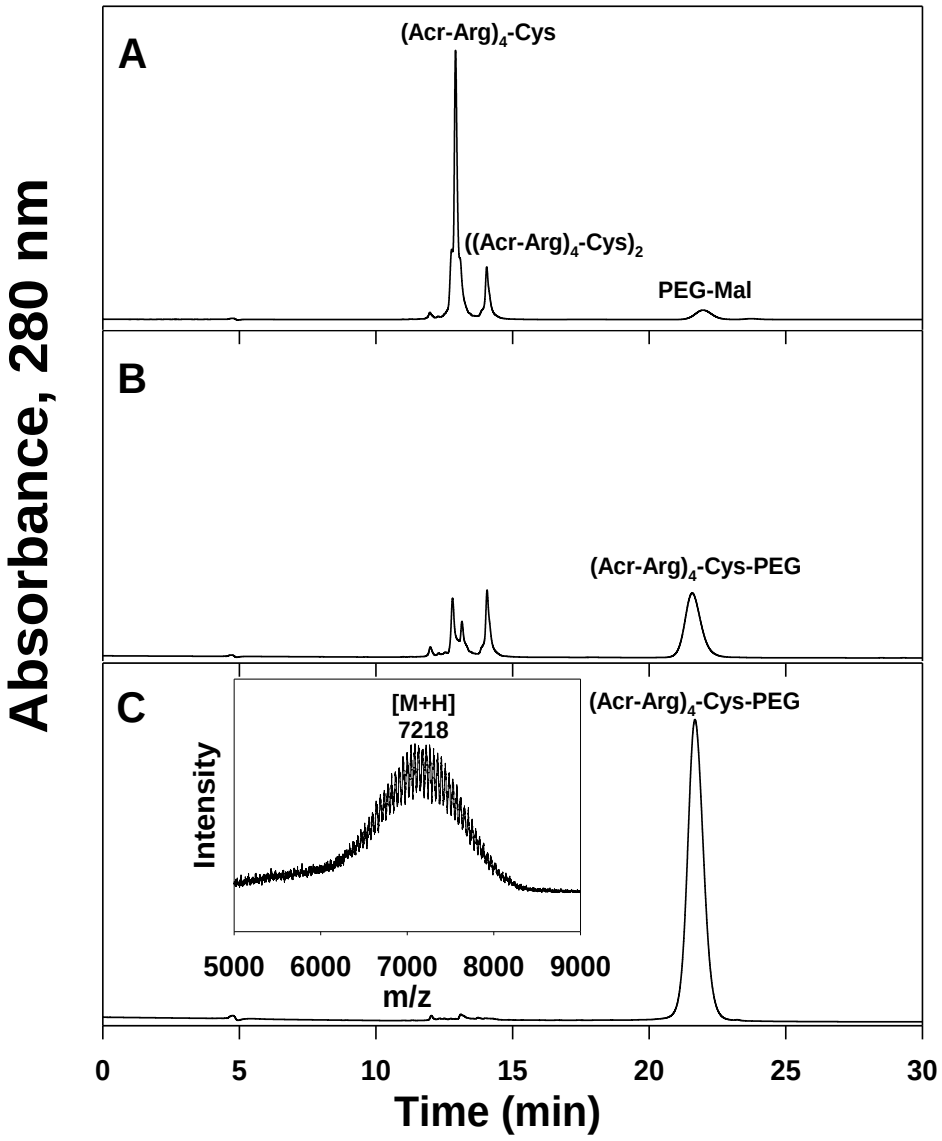

Figure 4-2. *RP-HPLC Analysis of Polyacridine PEG-Peptide Synthesis.* Reaction of (Acr-Arg)$_4$-Cys with 1.1 mol equivalents of PEG-Mal (panel A), results in the formation of (Acr-Arg)$_4$–Cys-PEG detected at 280 nm with simultaneous consumption of (Acr-Arg)$_4$ and formation of dimeric peptide ((Acr-Arg)$_4$-Cys)$_2$ (panel B). The HPLC purified product (Acr-Arg)$_4$–Cys-PEG rechromatographed on RP-HPLC as a single peak (panel C) and is characterized by MALDI-TOF MS (panel C, inset), resulting in an observed m/z corresponding to the calculated mass (Table 4-1). The preparation of (Acr-X)$_4$–Cys-PEG and (Acr-X)$_4$–Cys-SS-PEG peptides described in Table 4-1 produced equivalent chromatographic evidence. HPLC analysis was performed in collaboration with Nicholas J. Baumhover, Medicinal and Natural Products Chemistry, University of Iowa.

analogue demonstrated weaker binding resulting in full displacement at 1 nmol, and the Glu analogue was the overall weakest binder, only achieving 40% displacement at 1 nmol (Figure 4-3A).

The relative binding affinity of PEGylated polyacridine peptides for pGL3 was compared by determining the concentration of peptide that completely displaces a thiazole orange intercalator dye, resulting in decreased fluorescence. Comparison of PEGylated $(Acr\text{-}X)_4$ (X is either Arg, Lys, Leu or Glu) established the importance of cationic amino acids to increase binding affinity. Both the Lys and Arg analogue demonstrated high affinity by completely displacing thiazole orange at 0.4 nmol of peptide per μg of DNA. Conversely, the Leu analogue demonstrated weaker binding resulting in full displacement at 1 nmol, and the Glu analogue was the overall weakest binder, only achieving 40% displacement at 1 nmol (Figure 4-3A).

The relative binding affinity of PEGylated polyacridine peptides was also compared by a band shift gel assay performed at a constant stoichiometry of 0.5 nmol per μg of DNA (Figure 4-3B). The data suggest that the $(Acr\text{-}Lys)_4$ and $(Acr\text{-}Arg)_4$ peptides (Figure 4-3B, lane 2 and 3) possess a relatively higher binding affinity than the other analogues tested, as not only did binding result in a complete retardation of DNA relative to the migration of plasmid DNA (Figure 4-3B, lane 1), but furthermore, only these two polyacridine-PEG peptides prevented DNA staining by ethidium bromide. In contrast, the $(Acr\text{-}Glu)_4$ polyacridine-PEG peptide (Figure 4-3B, lane 5) showed the weakest binding affinity compared to all other analogues tested, while the PEGylated $(Acr\text{-}Leu)_4$ peptide (Figure 4-3B, lane 4) demonstrated an intermediate binding affinity, nearly inhibiting DNA migration from the well.

The size and charge of DNA polyplexes are often a function of the stoichiometry of peptide bound to DNA. To examine this relationship for PEGylated polyacridine polyplexes, QELS particle size and zeta potential were measured as a function of peptide to DNA ratio. One unusual property of PEGylated polyacridine polyplexes was their

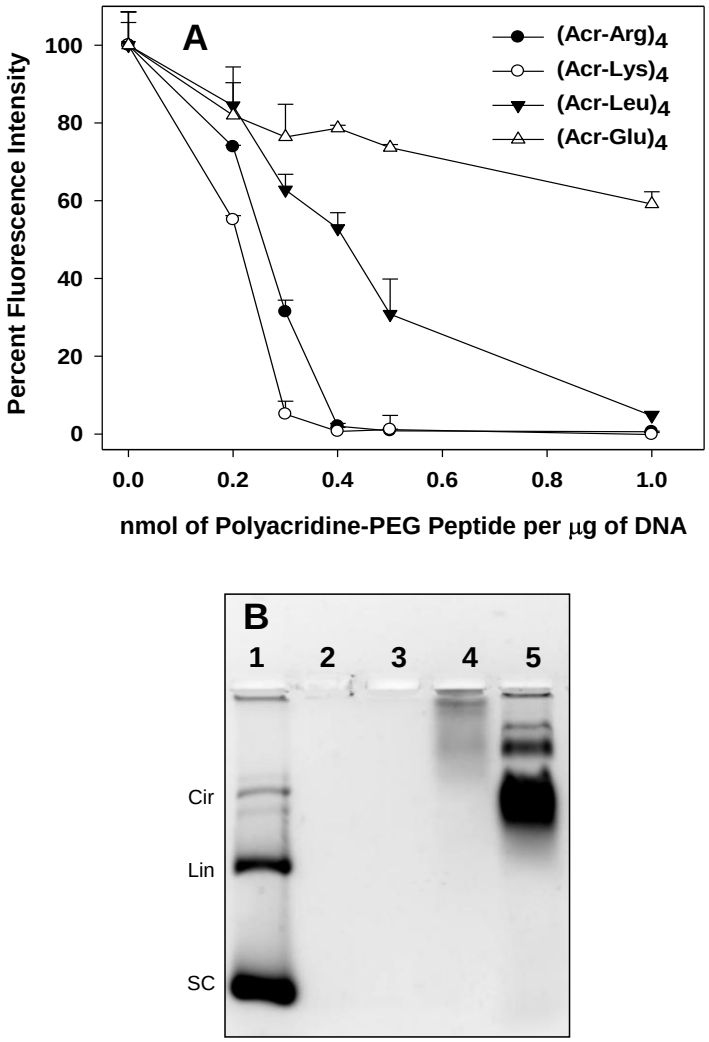

Figure 4-3. *DNA Binding Affinity of PEGylated Polyacridine Peptides*. A thiazole orange displacement assay was used to determine the relative binding affinity of polyacridine PEG peptides for DNA. 1 μg of pGL3 in 5 mM HEPES pH 7.0 and 0.1 μM thiazole orange was combined with 0.2 to 1 nmol of $(Acr\text{-}Arg)_4$-Cys-PEG (●), $(Acr\text{-}Lys)_4$-Cys-PEG (○), $(Acr\text{-}Leu)_4$-Cys-PEG (▼), or $(Acr\text{-}Glu)_4$-Cys-PEG (Δ). The results in panel A established that PEGylated $(Acr\text{-}Arg)_4$ and $(Acr\text{-}Lys)_4$ possessed a higher affinity for DNA compared to PEGylated $(Acr\text{-}Glu)_4$ and $(Acr\text{-}Leu)_4$. In panel B, the relative binding affinity was determined by comparing the relative migration of DNA (lane 1) to the band shifts observed with DNA polyplexes by agarose gel electrophoresis. The band shifts observed for pGL3 (1 μg) polyplexed with 0.5 nmol of either $(Acr\text{-}Arg)_4$-Cys-PEG (lane 2), $(Acr\text{-}Lys)_4$-Cys-PEG (lane 3), $(Acr\text{-}Leu)_4$-Cys-PEG (lane 4), or $(Acr\text{-}Glu)_4$-Cys-PEG (lane 5) confirmed the results observed in panel A.

QELS mean diameter remained constant throughout the titration (Figure 4-4A-F). Each of the polyplexes had an apparent mean diameter of approximately 100-200 nm, with the exception of PEGylated $(Acr\text{-}Leu)_4$ and PEGylated $(Acr\text{-}Glu)_4$ which produced polyplexes of an 200-400 nm mean diameter (Figure 4-4B and C).

A second unusual property of PEGylated polyacridine polyplexes was the observed zeta potential charges at each peptide stoichiometry evaluated (Figure 4-4). Titration with PEGylated $(Acr\text{-}Arg)_4$ resulted in an increase (more cationic) in zeta potential from -15 mV to a maximum of -0.44 mV at 0.5 nmols of peptide per μg of DNA or higher (Figure 4-4A). Similar zeta potential titration curves were determined for PEGylated $(Acr\text{-}Leu)_4$, and $(Acr\text{-}Lys)_4$, each of which resulted in polyplexes with a negative zeta potential when fully titrated (Figure 4-4B, D and E). The stoichiometry of peptide at the maximal asymptotic charge observed reflects the complete formation of DNA polyplexes. Therefore stoichiometries above this point on the titration result in no further binding of the PEGylated polyacridine peptides to DNA. The complete polyplex formation stoichiometries observed for the various analogues were 0.5 nmols per μg of DNA for PEGylated $(Acr\text{-}Arg)_4$, 0.6 nmols per μg for $(Acr\text{-}Lys)_4$, and 1.0 nmols per μg for $(Acr\text{-}Leu)_4$. In contrast, PEGylated $(Acr\text{-}Glu)_4$ produced no change in zeta potential during the titration (Figure 4-4C), indicating that this polyacridine-PEG peptide possesses a poor binding affinity for DNA. These data suggested that, unlike polylysine or PEI polyplexes that condense DNA into smaller polyplexes of 50-100 nm with charge of +25 mV,[214, 215] PEGylated polyacridine peptides bind without dramatically changing DNA size and can maintaining a negative zeta potential as a fully formed DNA polyplexes.

The shape and relative charge of PEGylated polyacridine polyplexes was further examined by atomic force microscopy (AFM) (Figure 4-5). Polyplexes prepared either at 0.2 or 0.8 nmol per μg of DNA using PEGylated $(Acr\text{-}Arg)_4$, $(Acr\text{-}Lys)_4$, $(Acr\text{-}Leu)_4$ and $(Acr\text{-}Glu)_4$, resulted in open-DNA polyplexes that bound to the surface of cationically charged mica that was prepared with immobilized nickel (Figure 4-5A-H). The relative

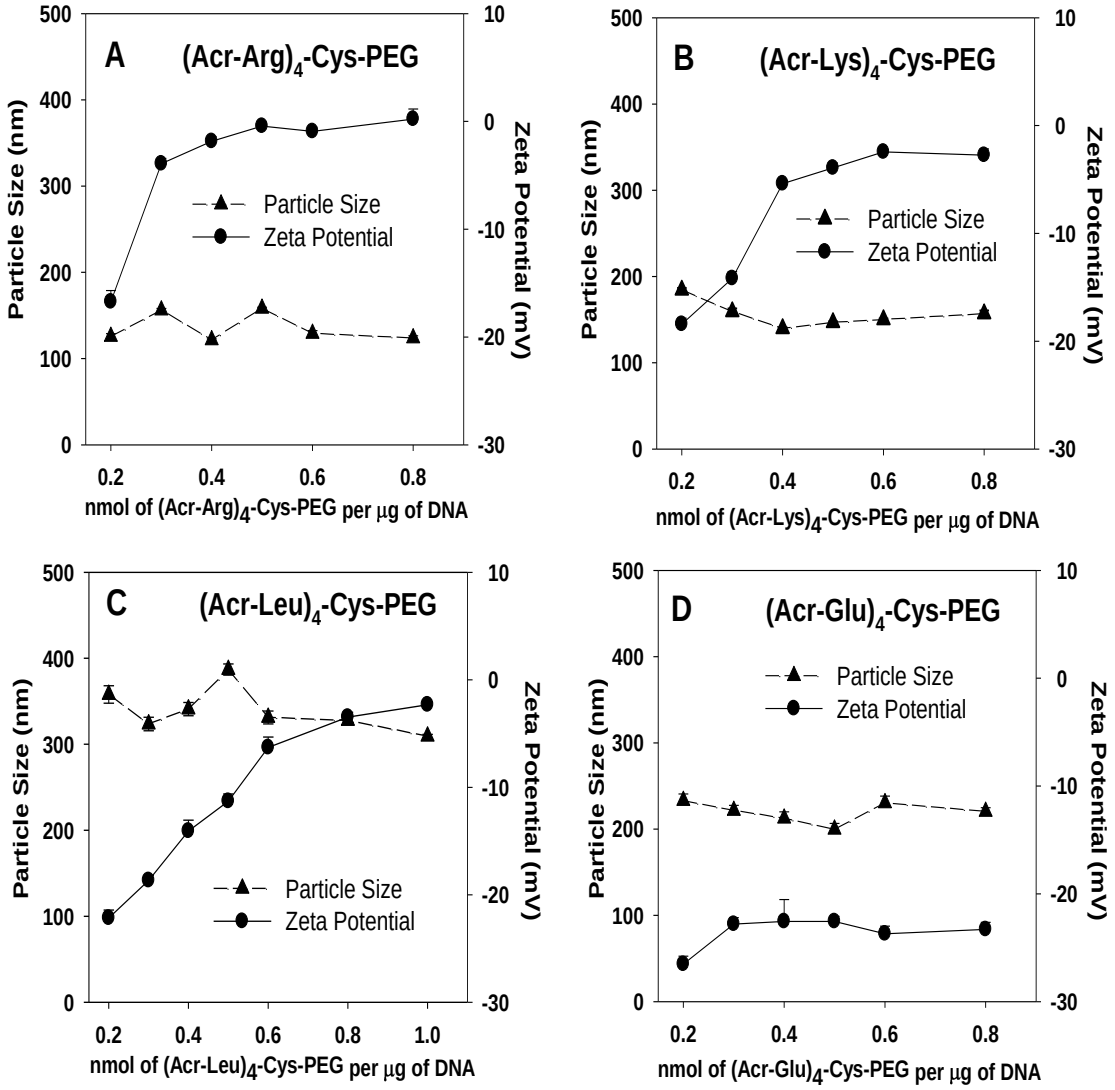

Figure 4-4. *Size and Charge of PEGylated Polyacridine Polyplexes.* The QELS particle size (--▲--) and zeta potential (-●-) of polyplexes, prepared at concentrations ranging from 0.2-1 nmol of peptide per μg of DNA, are illustrated for (Acr-Arg)$_4$-Cys-PEG (A), (Acr-Lys)$_4$-Cys-PEG (B), (Acr-Leu)$_4$-Cys-PEG (C), or (Acr-Glu)$_4$-Cys-PEG (D). The results establish no significant change in particle size throughout the titration, whereas the zeta potential charges increases from -20 to 0 mV when titrating with peptides containing spacing amino acids Arg, Lys, or Leu (panels A, B, C).

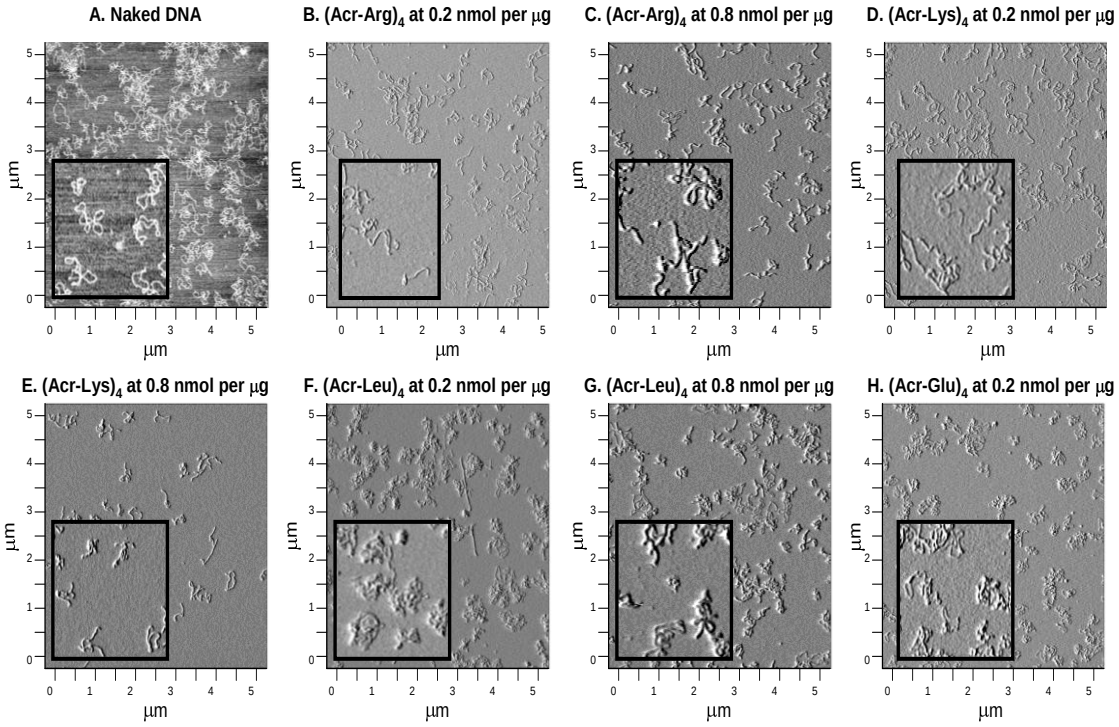

Figure 4-5. *Shape of PEGylated Polyacridine DNA Polyplexes*. Atomic force microscopy (AFM) was used to analyze the shape of DNA (pGL3) (Panel A) or DNA polyplexes prepared either at 0.2 or 0.8 nmol per μg of DNA respectively with $(Acr\text{-}Arg)_4$-Cys-PEG (panel B-C), $(Acr\text{-}Lys)_4$-Cys-PEG (panel D-E), $(Acr\text{-}Leu)_4$-Cys-PEG (panel F-G), and $(Acr\text{-}Glu)_4$-Cys-PEG (panel H). Anionic PEGylated polyacridine polyplexes produced open polyplex structures (panel B-H) that appeared slightly more rigid and dense than plasmid DNA (panel A). Each inset represents a 1 x 1 μm enlargement.

shape of these DNA polyplexes (Figure 4-5B-H) is similar in morphology to plasmid DNA (Figure 4-5A), but more rigid and dense with no apparent circular conformation. Furthermore, when increasing the stoichiometry of PEGylated $(Acr\text{-}Arg)_4$, or $(Acr\text{-}Lys)_4$, from 0.2 to 0.8 nmol per μg of DNA, the AFM confirms their anionic charge and suggests no apparent formation of DNA nanoparticles. The unique shape and charge of anionic PEGylated open-polyplexes should minimize binding to serum proteins and extend the pharmacokinetic half-life of plasmid DNA, provided that the DNA remains protected from premature metabolism.

To determine if polyacridine peptides would also mediate gene transfer, we chose to examine the ability of PEGylated DNA polyplexes to produce luciferase expression in the liver of mice, 24 hrs following a 1 μg dose of pGL3. This dosing route was chosen over IM-EP administration based on the results from Chapter 2 demonstrating anionic surface properties (Figure 2-11) and nuclease stability (Figure 2-14) for PEGylated polyacridine-DNA polyplexes, which we now hypothesize would result in more blood compatible DNA polyplexes compared to cationic DNA nanoparticles formed with cationic peptides, lipids, or polymers. Hydrodynamic dosing of 1 μg of pGL3 produced 10^8 photon/sec/cm^2/sr determined using a calibrated bioluminescence assay (Figure 4-6, HD DNA). When pGL3 (1 μg in 50 μL) was dosed via the tail vein without hydrodynamic delivery, there was no detectable luciferase expression (not shown). In an attempt to stimulate gene expression, PEGylated polyacridine peptide polyplexes were administered via the tail vein (1 μg of pGL3 in 50 μL) and after 30 min a hydrodynamic dose (2 mL) of saline was used to stimulate liver uptake and gene expression (Figure 4-6). In the subsequent studies described below, stimulated expression produced 10^7-10^9 photon/sec/cm^2/sr, the magnitude being dependent on the time delay between primary and stimulation dose, the volume of the hydrodynamic bolus, the structure of the PEGylated polyacridine peptide, and the charge ratio at which the polyplex was prepared. At a fixed dose of 1 μg of pGL3 and time delay of 30 min between primary and stimulatory dose, polyplexes prepared at 0.5 nmol of PEGylated (Acr-Arg)$_4$, in which the PEG was attached by a maleimide (Mal) or a reducible disulfide (SS) linkage, were administered to mice and analyzed by BLI after 24 hrs. Approximately 5-fold higher luciferase expression was observed for Mal versus SS, indicating that a reducible linkage offered no advantage for stimulated expression (Figure 4-6). Comparison of the Mal peptide prepared as either an acetate or TFA salt form (ion paired with Arg) resulted in an approximately 10-fold loss of gene transfer for the TFA form that was determined to be statistically significant using a two-tailed unpaired t-test (*$p \leq 0.05$). These results

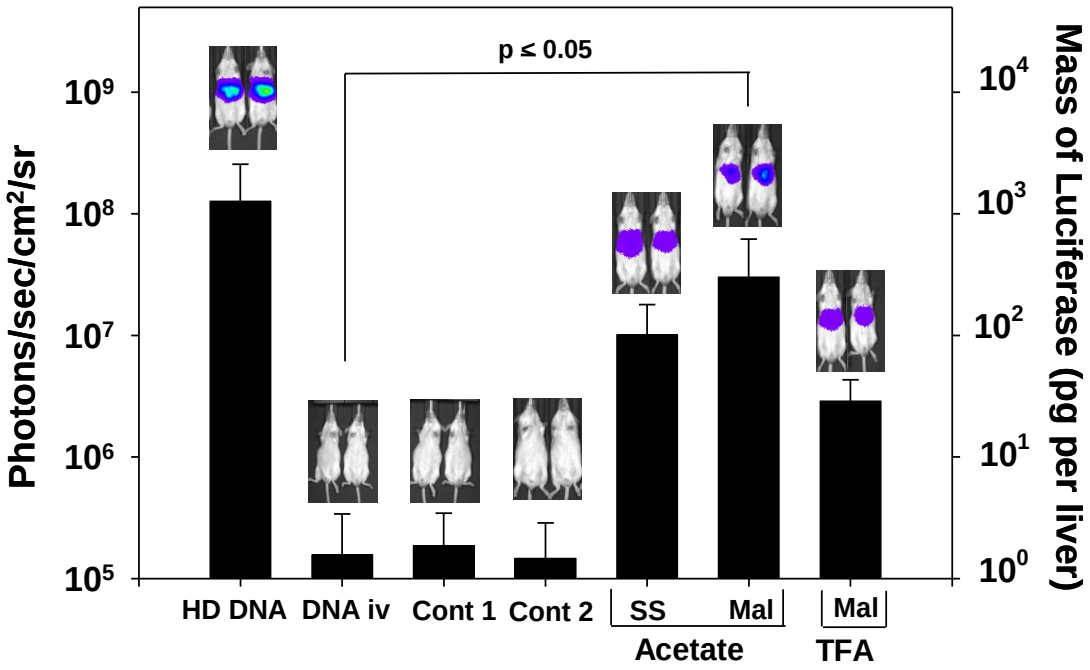

Figure 4-6. *Stimulated In Vivo Gene Expression Mediated by PEGylated DNA Polyplexes.* Direct Hydrodynamic (HD) administration of 1 μg of pGL3 in multiple mice results in a mean BLI response of 10^8 photons/sec/cm^2/sr (HD DNA). Alternatively, mice tail vein dosed with pGL3 (1 μg in 50 μL) in complex with 0.5 nmol of (Acr-Arg)$_4$–Cys-Mal-PEG (Mal, maleimide linkage) or (Acr-Arg)$_4$–Cys-SS-PEG (SS, disulfide linkage) followed by HD stimulation 30 min after DNA delivery, results in approximately 10^7 photons/sec/cm^2/sr. Omission of HD stimulation (not shown) or PEGylated polyacridine peptide (DNA iv) results in no gene expression. Likewise, 1 μg of DNA complexed with PEG-Mal-Cys-Trp-Lys$_{18}$ (Cont 1) or a PEGylated glycoprotein described previously (Cont 2)[216] failed to produce HD stimulated gene expression. The effect of an acetic acid (Mal, Acetate) or TFA (Mal, TFA) counterion on the stimulated gene expression was determined only for (Acr-Arg)$_4$–Cys-Mal-PEG DNA polyplexes. The data indicate that an acetic acid counterion (Mal, Acetate) on (Acr-Arg)$_4$–Cys-Mal-PEG DNA polyplexes results in nearly a 10-fold increase in expression relative to a TFA counter ion (Mal, TFA). Statistical analysis was performed using a two-tailed unpaired t-test (*p ≤0.05). In collaboration with Jason Duskey, Medicinal and Natural Products Chemistry, University of Iowa.

justified the use of Mal peptides in the acetate salt form for further comparisons.

Several controls were applied to further establish that PEGylated polyacridine peptides were necessary to achieve stimulated expression. The administration of a 1 μg dose of pGL3 followed by a stimulatory dose of saline after 30 min resulted in no detectable luciferase expression at 24 hrs (Figure 4-6, iv DNA). Likewise, there was no detectable luciferase expression with a 1 μg dose of pGL3 prepared as a PEGylated-Cys-Trp-Lys_{18} polyplex (Figure 4-6, Cont 1),[169] or PEGylated glycoprotein polyplex (Figure 4-6, Cont 2).[216] These controls confirmed that naked DNA was not responsible for the observed expression and also established that not all gene formulations were capable of mediating stimulated expression.

The stimulated expression mediated by PEGylated $(Acr\text{-}Arg)_4$ polyplexes (1 μg) was examined to determine the influence of the delay time between primary and stimulatory dose. Varying the delay from 5-120 min established a 10-fold loss in luciferase expression between 5 and 30 min, followed by a two orders of magnitude loss in stimulated expression at 60 min and longer (Figure 4-7A). Interestingly, the magnitude of stimulated gene expression at a delay time of 5 min was approximately 5-fold greater than direct hydrodynamic dosing of 1 μg of pGL3 (Figure 4-6 and Figure 4-7A).

In order to establish the minimum volume of hydrodynamic bolus required to maintain the elevated levels of stimulated gene expression observed, the volume of the hydrodynamic bolus was varied to be either 9, 5 or 2.5 wt/vol % (Figure 4-7B). DNA polyplexes (1 μg of pGL3 in 50 μL) prepared with 0.5 nmols of PEGylated $(Acr\text{-}Arg)_4$ were administered via the tail vein in mice and stimulated after a 30 min dwell time by the various hydrodynamic boluses of normal saline. The results determined that only the 9 % wt/vol (approximately 2 mL for a 20 g mouse) hydrodynamic doses are capable of achieving high stimulated gene expression.

To determine how the spacing amino acids influence stimulated gene expression, PEGylated peptides of general structure $(Acr\text{-}X)_4$, possessing X as either Lys, Arg, Leu

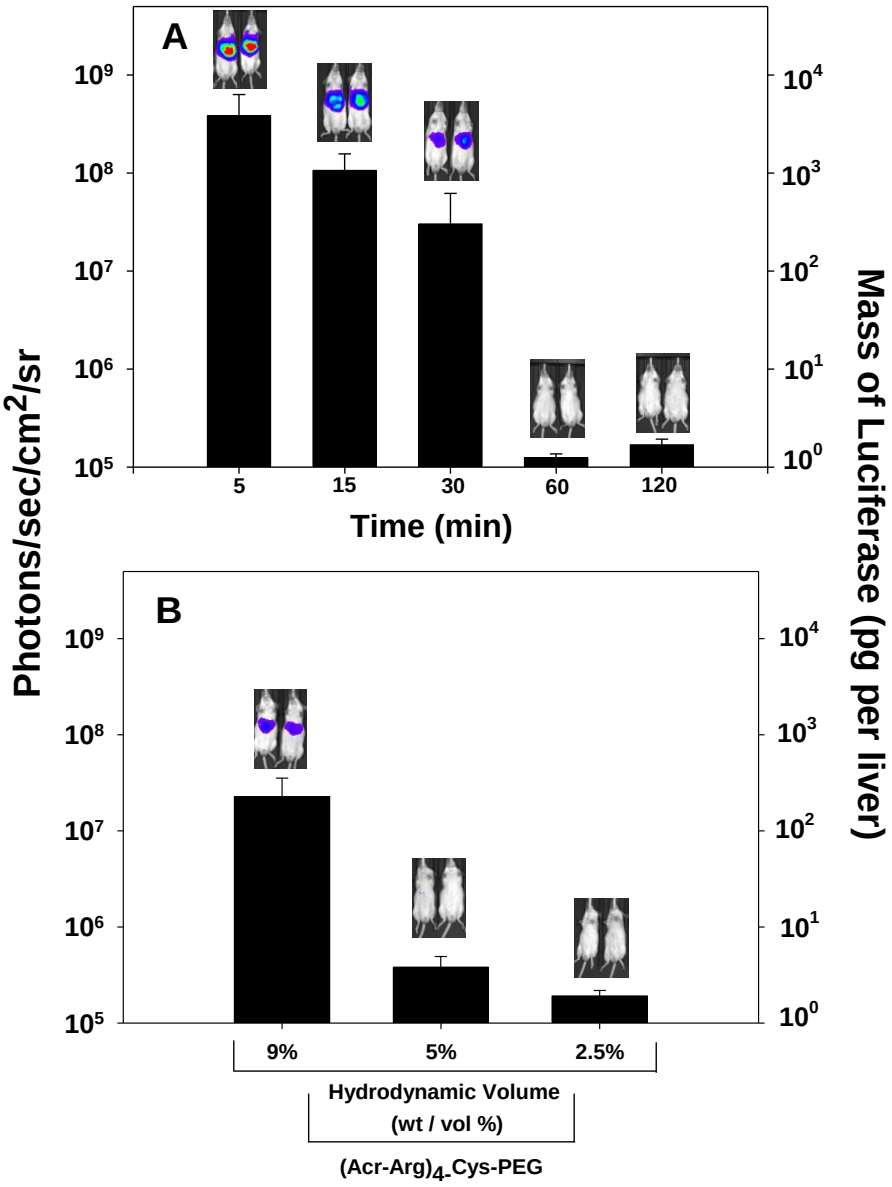

Figure 4-7. *Stimulated In Vivo Gene Expression Using PEGylated (Acr-Arg)$_4$ DNA Polyplexes.* Varying the dwell time of the HD stimulation from 5-120 min established a maximum of 30 min between administration and stimulation for the DNA polyplexes prepared with PEGylated (Acr-Arg)$_4$ at 0.5 nmol per μg (panel A). Similarly, varying the volume of HD stimulation at a 30 min dwell time (panel B) for 1 μg of DNA polyplexed with 0.5 nmol (Acr-Arg)$_4$–Cys-Mal-PEG revealed that high levels of gene expression are only achievable at the standard HD volume of 9% wt/vol. In collaboration with Jason Duskey, Medicinal and Natural Products Chemistry, University of Iowa.

or Glu were used to prepare polyplexes that were dosed in mice and stimulated to express luciferase. While the DNA dose was fixed at 1 μg, and the delay time was 30 min, the stoichiometry of PEGylated peptide to DNA was adjusted, based on the results of zeta potential titration (Figure 4-4), to favor complete polyplex formation. The results established that only PEGylated peptides possessing an Arg or Lys spacing amino acid produced appreciable levels of luciferase expression (Figure 4-8A), whereas peptides with Glu and Leu spacers were essentially inactive.

The stoichiometry of both Lys and Arg spaced PEGylated polyacridine peptide was varied from 0.2-1 nmol of peptide per μg of DNA, then dosed via tail vein and stimulated after 30 min. A 1 μg open DNA polyplex prepared with 0.6 nmol of PEGylated $(Acr\text{-}Arg)_4$ or 0.8 nmol of PEGylated $(Acr\text{-}Lys)_4$ mediated maximal luciferase expression when assayed by BLI at 24 hrs (Figure 4-8B). Both the Lys and Arg spaced PEGylated peptide mediated approximately 100-fold lower gene expression at 0.2 nmols of peptide compared to the stoichiometry of maximal expression (Figure 4-8B). Likewise, at stoichiometries greater than maximal expression, a decline in luciferase expression was observed, thus producing a parabolic expression profile in stimulated gene expression for these DNA polyplexes as a function of peptide stoichiometry. While no statistical significance was observed between the PEGylated $(Acr\text{-}Arg)_4$ and $(Acr\text{-}Lys)_4$ DNA polyplexes, the results suggested that a Lys spacer may have a slight advantage over Arg.

Discussion

Successful gene delivery systems will contain multiple components that each serve to improve a barrier of delivery. The PEGylated polyacridine peptides designed were created to form polyplexes with comparable binding affinities to that of cationic DNA condensing agents, but that formed complexes with anionic surfaces charges in an attempt to make DNA polyplexes that are more biocompatible with the blood, which is

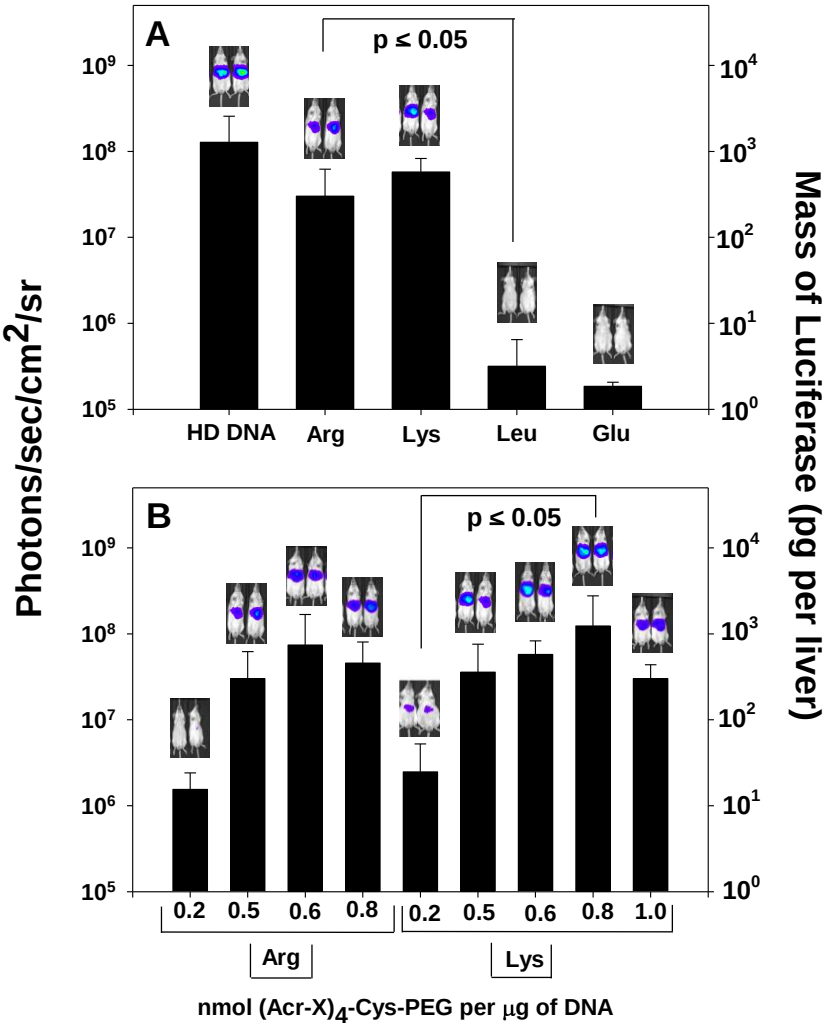

Figure 4-8. *Structure-Activity Relationships for Stimulated Gene Expression.* The BLI analysis at 24 hrs following tail vein dosed and HD stimulated (30 min post-DNA administration) pGL3 (1 μg in 50 μL) in complex with 0.5 nmol of either $(Acr\text{-}Arg)_4$-Cys-PEG (panel A, Arg), 0.6 nmol of $(Acr\text{-}Lys)_4$-Cys-PEG (panel A, Lys), 1 nmol of $(Acr\text{-}Leu)_4$-Cys-PEG (panel A, Leu), or 0.8 nmol of $(Acr\text{-}Glu)_4$-Cys-PEG (panel A, Glu) are compared with direct HD delivery of 1 μg of pGL3. The results establish polyacridine PEG-peptides with Arg and Lys spacing amino acids mediate 10^7-10^8 photons/sec/cm^2/sr whereas substitution with Leu and Glu results in negligible expression. Varying only the stoichiometry of PEGylated polyacridine peptide to DNA for $(Acr\text{-}Arg)_4$-Cys-Mal-PEG (panel B, Arg) and $(Acr\text{-}Lys)_4$-Cys-Mal-PEG (panel B, Lys), established a maximal expression at 0.6 for Arg and 0.8 for Lys (panel B). Statistical analysis was performed using a two-tailed unpaired t-test (*p ≤0.05). Formulation administration was performed in collaboration with Jason Duskey, Medicinal Chemistry and Natural Products, University of Iowa.

the first delivery barrier associated with gene delivery.

A prerequisite for any gene delivery agent is a reversible association with the oligonucleotide in order to maintain proper function in the cell yet provides high affinity binding with the gene to avoid premature dissociation while in transit. Prior published results from our lab demonstrated the high affinity binding polyacridine-PEG peptide could be synthesized containing 3, 4, or 5 (Lys-Acr) chains.[209] Nevertheless, the amine chemistry used to create these delivery peptides resulted in heterogeneous mixtures that were difficult to characterize due to the incorporation of the intercalator, acridine, during the final stage of synthesis. Therefore, the current synthetic strategy required the preparation of Fmoc-Lysine(Acridine)-OH in order to incorporate the intercalator during peptide synthesis using this amino acid, which yielded homogenous polyacridine peptides that were easily characterized by RP-HPLC and ESI-LC-MS.

It was determined that a spacing amino acid was needed in between each Lys(Acr) amino acid in order to synthesize these polyacridine peptides at acceptable yields. The spacing amino acid was varied to be either a Lys, Arg, Leu, or Glu (Table 4-1). These amino acids were selected to either improve the binding affinity of the peptides to DNA (Lys and Arg) or to form anionic polyplexes when bound to DNA (Leu and Glu). The polyacridine peptides created were then PEGylated with either a PEG-maleimide or a PEG-orthopyridyl disulfide (OPSS) of 5,000 Da to create polyacridine PEG peptides with the general structure $(Acr\text{-}X)_4$-Cys-PEG, where each polyacridine PEG peptides was characterized using RP-HPLC and MALDI-TOF MS.

PEGylated polyacridine peptides possessing four Acr residues spaced by either Glu or Leu demonstrated weak binding to DNA (Figure 4-3A and B), resulting in no stimulated gene expression (Figure 4-8A) due to the inability to protect DNA from metabolism in vivo. Conversely, PEGylated $(Acr\text{-}Lys)_4$ or $(Acr\text{-}Arg)_4$ possessed higher affinity for binding with DNA (Figure 4-3A and B), which correlated with their ability to produce stimulated expression (Figure 4-8A) presumably due to their ability to stabilize

DNA from premature metabolism in vivo. We previously reported that PEGylated Cys-Trp-Lys_{18} formed polyplexes that readily dissociate in the blood, resulting in rapid DNA metabolism.[82] It was therefore anticipated that stimulation of iv dosed PEGylated Cys-Trp-Lys_{18} polyplexes would not produce gene expression (Figure 4-6, Cont 1). Thus, a combination of polyintercalation and ionic binding to plasmid DNA results in improved affinity and stable polyplexes, where either functionality alone is insufficient.

One of the more unique aspects of PEGylated polyacridine polyplexes is their open polyplex structures that resemble naked DNA (Figure 4-5A-H) and that appear to form at all stoichiometries of peptide to DNA evaluated. PEGylated $(Acr\text{-}Lys)_4$ and $(Acr\text{-}Arg)_4$ produced anionic or nearly neutral polyplexes across the titration range tested with charges of -2.75 and 0.21 mV respectively at the stoichiometry of 0.8 nmol per μg of DNA (Figure 4-4A and B). When DNA polyplexes were iv dosed and allowed to circulate for 30 min, the level of stimulated expression was dependent upon the stoichiometry of peptide to DNA, thus resulting in a parabolic peptide dose-response curve (Figure 4-8B). These results suggest that higher stoichiometries lead to more binding of polyacridine-PEG peptide to the DNA and afforded the polyplex improved metabolic stability, which in turn lead to higher luciferase expression levels. However, above 0.8 or 1.0 nmol per μg of DNA for PEGylated $(Acr\text{-}Lys)_4$ and $(Acr\text{-}Arg)_4$ respectively, the gene expression decreased unexpectedly. It is not apparent what led to the diminished gene expression observed, but perhaps it was due to the formation of unstable polyplexes at higher stoichiometries which were also associated with higher surface charges.

The mechanism of stimulated gene expression remains unknown. In contrast, a direct hydrodynamic dose requires a rapid large volume administration in order to bypass nucleases degradation in the blood and to selectively target hepatocytes in the liver.[132] In order to elucidate the mechanism behind stimulated gene expression, detailed pharmacokinetics and biodistribution analysis is required to determine if the polyplexed

DNA resides in or on the surface of the liver and is transported into hepatocytes upon stimulation, or if the DNA resides predominantly in the blood and share a similar mechanism to a direct hydrodynamic administration.

In conclusion, this is the first report of high-level stimulated gene expression from a nonviral delivery system that mirrors the expression levels produced by the same dose administered by direct hydrodynamic dosing. PEGylated polyacridine peptides were demonstrated to have high affinity binding for DNA and to form anionic open polyplexes that are more compatible with blood, but that require a hydrodynamic bolus to achieve gene transfer. Future PEGylated polyacridine peptides should be designed to improve the binding affinity of the peptides for DNA while maintaining anionic surface charges in order to retain the blood compatibility demonstrated by this gene delivery system. Furthermore, given the size and shape of the DNA polyplexes formed, we anticipate that iv dosed formulations will likely biodistribute to organs with larger blood vessel fenestrations, which would include the liver, spleen, and solid tumors.

CHAPTER 5: LONG-CIRCULATING PEGYLATED POLYACRIDINE PEPTIDE DNA POLYPLEXES STABILIZED AGAINST METABOLISM MEDIATE HYDRODYNAMICALLY STIMULATED GENE EXPRESSION IN THE LIVER

Abstract

A novel class of PEGylated polyacridine peptides was developed to mediate potent stimulated gene transfer in the liver of mice. Previously, $(Acr\text{-}X)_4$-Cys-PEG peptides, spaced by either Lys, Arg, Leu or Glu were evaluated and revealed that a Lys or Arg spacing amino acid was required for high affinity binding to DNA and for high levels of stimulated gene expression in vivo. The present chapter identifies $(Acr\text{-}Lys)_6$-Cys-PEG as an optimal PEGylated polyacridine peptide for DNA delivery possessing high affinity binding by polyintercalation that stabilizes DNA from metabolism by DNase. AFM images reveal that the shape of DNA polyplexes prepared by $(Acr\text{-}Lys)_6$-Cys-PEG is dependent on the stoichiometry of peptide, forming anionic open DNA polyplexes at 0.2 nmol per μg of DNA, while forming cationic DNA nanoparticles at 0.8 nmol per μg of DNA. A tail vein dose of PEGylated polyacridine peptide DNA polyplexes (1 μg in 50 μL), followed by a stimulatory hydrodynamic dose of normal saline at times ranging from 5-60 min post-DNA administration, led to a high level of luciferase expression in the liver, equivalent to levels mediated by direct hydrodynamic dosing of 1 μg of pGL3. Comparing the in vivo properties of PEGylated polyacridine DNA polyplexes suggests that $(Acr\text{-}Lys)_6$-Cys-PEG peptides yield polyplexes possessing high levels of stimulated gene expression while best extending the pharmacokinetic half-life of DNA over all other polyplexes prepared with $(Acr\text{-}Lys)_n$-Cys-PEG peptides. The biodistribution of DNA polyplexes demonstrates a predominant accumulation of the dose in the liver and in the blood. These results establish the unique properties of PEGylated polyacridine peptides as a new and promising class of gene delivery agents that facilitate

reversible binding to plasmid DNA, protecting it from DNase in vivo, extending the circulatory half-life, and releasing transfection-competent DNA into the liver to mediate a high-level of gene expression after a hydrodynamic bolus (data and figures reproduced with written permission from ACS Publications).

Introduction

In order to improve the targeting of non-viral gene delivery systems, polyplexes with enhanced pharmacokinetic properties must be developed. The blood and its components remain a significant obstacle for non-viral gene therapy, as oligonucleotides are immediately susceptible to degradation by serum nucleases, and furthermore, blood proteins such as albumin or immunoglobulin can bind to positively charged polyplexes and result in either aggregation or rapid clearance of the oligonucleotide from the blood.[11]

New gene delivery agents are therefore needed that function by efficiently mediating targeted non-viral gene delivery in vivo. Some of the most successful delivery agents developed to date, such as PEI and cationic lipids, produce robust gene transfer in vitro, but fail to mediate significant gene expression in vivo.[130, 201-207] In contrast, hydrodynamic (HD) dosing and electroporation are proven physical methods that are highly efficient in delivering plasmid DNA to animals and may find utility in humans.[14, 157, 184, 217-220] However, due to the invasiveness of HD dosing, there is a need for new gene delivery agents that produce gene expression at levels comparable to HD dosing, but without the requirement of high-volume administration.

Polyacridine PEG-peptides have demonstrated a high binding affinity for DNA, improved physical properties for in vivo application, and the peptides possess the flexibility required for improved gene delivery systems. Chapters 2 and 3 of the thesis introduced polyacridine PEG-peptides as gene delivery carrier and verified their compatibility with IM-EP. The high gene transfer observed following IM-EP correlated anionic surface charges, open-DNA polyplex structures, and high affinity binding with

improved DNA delivery properties. Chapter 4 presented a series of peptides with the general structure $(Acr\text{-}X)_4$-Cys-PEG, where the identity of the spacing amino acid (X) was varied to identify a structure activity relationship. In order to evaluate the utility of $(Acr\text{-}X)_4$-Cys-PEG peptides, DNA polyplex were iv dosed and followed by a hydrodynamic injection of normal saline 30 minutes after iv administration in order to determine if the polyplexed DNA remained transfection competent compared to a direct hydrodynamic does of naked DNA. The results in chapter 4 demonstrated that only lysine and arginine spaced peptides possessing a high binding affinity for DNA were capable of stimulating high levels of gene expression. These data suggest that a combination of intercalation and ionic forces are required to maintain a stable DNA polyplex in the blood.

In the present chapter, a new panel of $(Acr\text{-}Lys)_n$-Cys-PEG peptides was prepared to establish their utility in mediating gene expression following iv dosing. These peptides were prepared to improve the intercalation of the polyacridine PEG-peptide in order to further the discoveries presented in chapter 4. The data in this chapter determines an apparent structure-activity relationship by which protection of the DNA in blood and liver by a PEGylated polyacridine peptide results in the ability to stimulate high level gene expression in liver with a delayed hydrodynamic dose of saline. The results further demonstrate the ability to extend the circulatory half-life of iv dosed DNA, which is an important prerequisite for achieving targeted gene delivery to organs and tissues. The synthetic adaptability of polyacridine peptides, along with the ability to prepare either anionic-open or cationic-closed-polyplexes that mediate gene transfer in vivo, demonstrate the unique importance of poly-intercalative binding to achieve gene delivery.

Materials and Methods

Unsubstituted Wang resin, 9-hydroxybenzotriazole, Fmoc-protected amino acids, O-(7-Azabenzo-triazol-1-yl)-N,N,N',N'-tetramethylurionium hexafluorophosphate (HATU), Fmoc-Lysine-OH, and N-Methyl-2-pyrrolidinone (NMP) were obtained from Advanced Chemtech (Lexington, KY). N,N-Dimethylformamide (DMF), trifluoroacetic acid (TFA), and acetonitrile were purchased from Fisher Scientific (Pittsburgh, PA). Diisopropylethylamine, piperidine, acetic anhydride, Tris(2-carboxyethyl)-phosphine hydrochloride (TCEP), 9-chloroacridine and thiazole orange were obtained from Sigma Chemical Co. (St. Louis, MO). Agarose was obtained from Gibco-BRL. mPEG-maleimide was purchased from Laysen Bio (Arab, AL). D-Luciferin and luciferase from *Photinus pyralis* were obtained from Roche Applied Science (Indianapolis, IN). pGL3 control vector, a 5.3 kb luciferase plasmid containing a SV40 promoter and enhancer, was obtained from Promega (Madison, WI). pGL3 was amplified in a DH5α strain of *Escherichia coli* and purified according to manufacturer's instructions.

Synthesis and Characterization of $(Acr\text{-}Lys)_n$-Cys-Peptides

9-Phenoxyacridine and Fmoc-Lysine(Acridine)-OH were prepared as recently reported.[210, 211] The $(Acr\text{-}Lys)_n$-Cys peptides were prepared by solid phase peptide synthesis on a 30 µmol scale on an APEX 396 Synthesizer using standard Fmoc procedures including 9-hydroxybenzotriazole and HATU (O-(7-Azabenzo-triazol-1-yl)-N,N,N',N'-tetramethylurionium hexafluorophosphate) activation while employing double coupling of Fmoc-Lys(Acr)-OH and triple coupling for the spacing amino acid while using a 5-fold excess of amino acid over resin and omitting N-capping of truncated peptide species. Peptides were removed from resin and side chain deprotected using a cleavage cocktail of TFA/ethanedithiol/water (93:4:3 v/v/v) for 3 hrs followed by precipitation in cold ether. Precipitates were centrifuged for 10 min at 5000 x g at 4ºC and the supernatant decanted. Peptides were then reconstituted with 0.1 v/v % TFA and

purified to homogeneity on RP-HPLC by injecting 0.5-2 μmol onto a Vydac C18 semi-preparative column (2 x 25 cm) eluted at 5 mL per min with 0.1 v/v % TFA with an acetonitrile gradient of 20-30 v/v % over 30 min while monitoring acridine at 409 nm. The major peak was collected and pooled from multiple runs, concentrated by rotary evaporation, lyophilized, and stored at -20ºC. Purified peptides were reconstituted in 0.1 v/v % TFA and quantified by absorbance (acridine $\varepsilon_{409\ nm}$ = 9266 M^{-1} cm^{-1} assuming additivity of ε for multiple acridines) to determine isolated yield (Table 5-1). Purified $(Acr\text{-}Lys)_n$-Cys peptides were characterized by LC-MS by injecting 2 nmol onto a Vydac C18 analytical column (0.47 x 25 cm) eluted at 0.7 mL per min with 0.1 v/v % TFA and an acetonitrile gradient of 10-55 v/v % over 30 min while acquiring ESI-MS in the positive mode. Synthesis performed in collaboration with Nicholas J. Baumhover, Medicinal Chemistry and Natural Products, University of Iowa.

Synthesis and Characterization of PEGylated $(Acr\text{-}Lys)_n$ Peptides

PEGylation of the Cys residue on $(Acr\text{-}Lys)_n$-Cys was achieved by reacting 1 μmol of peptide with 1.2 μmol of $PEG_{5000\ Da}$–maleimide in 4 mL of 10 mM ammonium acetate buffer pH 7 for 12 hrs at RT. PEGylated peptides were purified by semipreparative HPLC as previously described and eluted with 0.1 v/v % TFA with an acetonitrile gradient of 25-65 v/v % acetonitrile while monitoring acridine at 409 nm.[169] The major peak was collected and pooled from multiple runs, concentrated by rotary evaporation, lyophilized, and stored at -20ºC. Counterion exchange was accomplished by chromatography on a G-25 column (2.5 x 50 cm) equilibrated with 0.1 v/v % acetic acid to obtain the peptide in an acetate salt form. The major peak corresponding to the PEG-peptide eluted in the void volume (100 mL) was pooled, concentrated by rotary evaporation, lyophilized, and stored at -20ºC. PEG-peptides were reconstituted in water and quantified by Abs_{409nm} to determine isolated yield (Table 5-1). $(Acr\text{-}Lys)_n$-Cys-PEG

were characterized by MALDI-TOF MS by combining 1 nmol with 10 μL of 2 mg per mL α-cyano-4-hydroxycinnamic acid (CHCA) in 50 v/v % acetonitrile and 0.1 v/v % TFA. Samples were spotted onto the target and ionized on a Bruker Biflex III Mass Spectrometer operated in the positive ion mode. Synthesis performed in collaboration with Nicholas J. Baumhover, Medicinal Chemistry and Natural Products, University of Iowa.

Characterization of PEGylated Polyacridine Peptide DNA Polyplexes

The relative binding affinity of PEGylated polyacridine peptides for DNA was determined by a fluorophore exclusion assay.[16] pGL3 (200 μL of 5 μg/mL in 5 mM HEPES pH 7.5 containing 0.1 μM thiazole orange) was combined with 0, 0.2, 0.3, 0.4, 0.5, or 1 nmol of PEGylated polyacridine peptide in 300 μL of HEPES and allowed to bind at RT for 30 min. Thiazole orange fluorescence was measured using an LS50B

Table 5-1. PEGylated $(Acr\text{-}Lys)_n$ Peptides for In Vivo Analysis

Polyacridine Peptide	**Mass (calc/obs)[a]**	**% Yield**
$(Acr\text{-}Lys)_2$-Cys	988.5 / 988.3	37%
$(Acr\text{-}Lys)_4$-Cys	1855.3 / 1855.1	26%
$(Acr\text{-}Lys)_6$-Cys	2722.4 / 2722.0	20%
PEGylated Polyacridine Peptide	**Mass (calc/obs)[b]**	**% Yield**
$(Acr\text{-}Lys)_2$-Cys-Mal-PEG	6488 / 6531	64%
$(Acr\text{-}Lys)_4$-Cys-Mal-PEG	7355 / 7218	55%
$(Acr\text{-}Lys)_6$ -Cys-Mal-PEG	822 /8116	66%

a. Determined by ESI-MS

b. Determined by MALDI-TOF-MS

fluorometer (Perkin-Elmer, U.K.) by exciting at 498 nm while monitoring emission at 546 nm with the slit widths set at 10 nm. A fluorescence blank of thiazole orange in the absence of DNA was subtracted from all values before data analysis. The data is presented as nmol of PEGylated polyacridine peptide per μg of DNA versus the percent fluorescence intensity ± the standard deviation determined by three independent measurements.

The particle size and zeta potential were determined by preparing 2 mL of polyplex in 5 mM HEPES pH 7.5 at a DNA concentration of 30 μg per mL and a PEGylated polyacridine peptide stoichiometry of 0, 0.2, 0.3, 0.4, 0.5, 0.6, 0.8 or 1 nmol per μg of DNA. The particle size was measured by quasi-elastic light scattering (QELS) at a scatter angle of 90º on a Brookhaven ZetaPlus particle sizer (Brookhaven Instruments Corporation, NY). The zeta potential was determined as the mean of ten measurements immediately following acquisition of the particle size.

The shape of PEGylated polyacridine polyplexes were determined using atomic force microscopy (AFM). pGL3 alone, or anionic PEGylated polyacridine polyplexes at 0.2 nmol of peptide per μg of DNA, were prepared at a concentration of 100 μg per mL of DNA in 10 mM Tris, 1 mM EDTA pH 8. Polyplexes were diluted to 1 μg per mL in 40 mM HEPES 5 mM nickel chloride pH 6.7 and deposited on a fresh cleaved mica surface (cationic mica) for 10 min followed by washing with deionized water. Cationic PEGylated polyacridine polyplexes prepared at 0.8 nmol of PEGylated $(Acr\text{-}Lys)_6$ per μg of DNA, at 100 μg per mL of DNA in 10 mM Tris, 1 mM EDTA pH 8 were deposited directly on a freshly cleaved mica surface (anionic mica) and allowed to bind for 10 min prior to washing with deionized water. Images were captured using an Asylum AFM MFP3D (Santa Barbara, CA) operated in the AC-mode using a silicon cantilever (Ultrasharp NSC15/AlBS, MikroMasch).

Gel Band Shift and DNase Protection Assay

pGL3 (1 μg), or pGL3 polyplexes (1 μg) were prepared at either 0.2 or 0.8 nmol of PEGylated $(Acr\text{-}Lys)_{2,\ 4,\ or\ 6}$, in 20 μL of 5 mM HEPES buffer pH 7.4. The ability of polyplexes to resist digestion with DNase was determined by incubation with 0.06 U of DNase I for 10 min. DNase was inactivated by the addition of 500 μL of 0.5 mg per mL proteinase K (in 100 mM sodium chloride, 1% SDS and 50 mM Tris pH 8.0) followed by incubation at 37°C for 30 min. The polyplexes were extracted with 500 μL of phenol/chloroform/isoamyl alcohol (24:25:1) to remove PEGylated peptides, followed by precipitation of DNA with the addition of 1 mL of ethanol. The precipitate was collected by centrifugation at 13,000 g for 10 min, and the DNA pellet was dried and dissolved in 5 mM HEPES buffer pH 7.4. DNA samples were combined with 2 μL of loading buffer and applied to a 1% agarose gel (50 mL) and electrophoresed in TBE buffer at 70 V for 60 min.[113] The gel was post-stained with 0.1 μg per mL ethidium bromide at 4°C overnight then imaged on a UVP Biospectrum Imaging System (Upland, California).

Pharmacokinetic Analysis of PEGylated Polyacridine Polyplexes.

Radioiodinated pGL3 was prepared as previously described.[221] Triplicate mice were anesthetized by ip injection of ketamine hydrochloride (100 mg per kg) and xylazine hydrochloride (10 mg per kg) then underwent a dual cannulation of the right and left jugular veins. An iv dose of ^{125}I-DNA (3 μg in 50 μL of HBM, 1.2 μCi) or ^{125}I-DNA polyplex (3 μg) was administered via the left catheter, and blood samples (10 μL) were drawn from the right catheter at 1, 3, 6, 10, 20, 30, 60, 90 and 120 min and immediately frozen, then replaced with 10 μL of normal saline. The amount of radioactivity in each blood time point was quantified by direct γ-counting. Radiolabeled DNA was extracted from the blood and the PEGylated polyacridine peptide by first adding 500 μL of 0.5 mg per mL proteinase K (in 100 mM sodium chloride, 1% SDS and 50 mM Tris pH 8.0) to

inactivate DNase. Blood samples were then incubation at 37°C for 30 min, followed by extraction of DNA with 500 μL of phenol/chloroform/isoamyl alcohol (24:25:1). DNA was then precipitated with the addition of 1 mL of ethanol and collected by centrifugation at 13,000 g for 10 min. The DNA pellet was dried and dissolved in 5 mM HEPES buffer pH 7.4. The separation of the circular, linear, and supercoiled DNA bands were determined by gel electrophoresis as described above. The gel was dried on a zeta probe membrane and autoradiographed on a Phosphor Imager (Molecular Devices, Sunnyvale CA) following a 15 hr exposure. Pharmacokinetic analysis of radioiodinated DNA was calculated with PCNON-LIN (SCI Software, Lexington, KY) using a two-compartment model. In collaboration with Sanjib Khargharia, Medicinal Chemistry and Natural Products, University of Iowa.

Biodistribution Analysis of PEGylated $(Acr\text{-}Lys)_n$ Peptides

Triplicate mice were anesthetized and a single catheter was placed in the left jugular vein. ^{125}I-DNA (1.5 μg in 50 μL of HBM, 0.6 μCi) or ^{125}I-DNA polyplexes (1.5 μg) were dosed iv and the jugular vein isolated was tied off following administration. After 5, 15, 30, 60, or 120 min, mice were sacrificed by cervical dislocation and the major organs (liver, lung, spleen, stomach, kidney, heart, large intestine, and small intestine) were harvested, and rinsed with saline. No further sample preparation was required, as the radioactivity in each organ was directly determined by γ-counting. The results are expressed as the percent of the dose in each organ. In collaboration with Sanjib Khargharia, Medicinal Chemistry and Natural Products, University of Iowa.

Hydrodynamic Stimulation and Bioluminescence Imaging

pGL3 (1 μg) was prepared in a volume of normal saline corresponding to 9% wt/vol of the mouse's body weight (1.6 – 2.3 mL based on 15-23 g mice). The DNA dose was administered by tail vein to 4-5 mice in 5 sec according to a published procedure.[14, 212] Mice (4-5) were also dosed tail vein with 1 μg of PEGylated polyacridine polyplex in

50 μL of HBM (5 mM HEPES, 0.27 M mannitol, pH 7.4). At times ranging from 5-120 min, a stimulatory hydrodynamic dose of normal saline (9% wt/vol of the body weight) was administered over 5 sec. At 24 hrs post-DNA dose, mice were anesthetized by 3% isofluorane, then administered an ip dose of 80 μL (2.4 mg) of D-luciferin (30 μg/μL in phosphate-buffered saline). At 5 min following the D-luciferin dose, mice were imaged for bioluminescence (BLI) on an IVIS Imaging 200 Series (Xenogen). Images were acquired at a 'medium' binning level and a 20 cm field of view. Acquisition times were varied (1 sec - 1 min) depending on the intensity of the luminescence. The Xenogen system reported bioluminescence as photons/sec/cm^2/seradian in a 2.86 cm diameter region of interest covering the liver. The integration area was transformed to pmols of luciferase in the liver using a previously reported standard curve.[213] The results were determined to be statistically significant ($p \leq 0.05$) based on a two-tailed unpaired t-test. In collaboration with Jason Duskey, Medicinal Chemistry and Natural Products, University of Iowa.

Results

The results from chapter 4 supported the preparation of PEGylated polyacridine peptides possessing an acetate counterion and maleimide link between the PEG polymer and the peptide (Figure 4-6A). Additionally, a Lys spacing amino acid on PEGylated $(Acr\text{-}X)_4$ peptides proved most efficient in gene transfer, which warranted an expansion of $(Acr\text{-}Lys)_n$ peptides to include repeats of 2 and 6. During the course of synthesis, the synthetic yields of polyacridine peptides were improved by Nicholas Bauhmhover (Medicinal Chemistry and Natural Products, University of Iowa) using HATU to activate amino acids during coupling. Improved yields were also the result of applying triple coupling of the spacing amino acids, omitting N-capping to avoid a side reaction with acridine, and using ethanedithiol as a scavenger during workup. Under these conditions, $(Acr\text{-}Lys)_n$ peptides with repeats ranging from 2 to 6 were prepared in 20-37% isolated

yields, and each polyacridine peptide produced an ESI-MS consistent with their theoretically calculated mass (Table 5-1). PEGylation of $(Acr\text{-}Lys)_n$ peptides were achieved via reaction of the C-terminal Cys with a 5 kDa PEG maleimide resulting in the formation of PEGylated $(Acr\text{-}Lys)_{2,\ 4,\ and\ 6}$ (Figure 5-1). The reaction was monitored by RP-HPLC, and purified products were rechromatographed as a single peak by analytical HPLC (Figure 5-2). MALDI-TOF-MS verified an average mass for each product closely matching the calculated mass for each PEGylated polyacridine peptide (Table 5-1).

The relative binding affinity of PEGylated $(Acr\text{-}Lys)_n$ peptides was determined as function of peptide stoichiometry using the thiazole orange displacement assay.[117] Comparing the binding affinities of PEGylated $(Acr\text{-}Lys)_{2,\ 4\ and\ 6}$ for DNA suggest that addition of (Acr-Lys) units onto the peptides results in an increases their affinity for DNA, such that PEGylated $(Acr\text{-}Lys)_6$ completely displaced thiazole orange at 0.2 nmols of peptide per μg of DNA, whereas PEGylated $(Acr\text{-}Lys)_{4\ and\ 2}$ completely displace thiazole at 0.4 and 0.5 nmol of peptide per μg of DNA respectively (Figure 5-3A). The band shift gel assay showed that when 1 μg of DNA is polyplexed with 0.2 nmol of either PEGylated $(Acr\text{-}Lys)_{2,\ 4\ ,\ or\ 6}$ that both PEGylated $(Acr\text{-}Lys)_{4\ and\ 6}$ possess high affinity binding for DNA at this stoichiometry sufficient to limit the migration of DNA relative to control (Figure 5-3B, lane 1).

Zeta potential titrations at each peptide stoichiometry evaluated revealed that increasing the number of (Acr-Lys) on PEGylated polyacridine peptides resulted in a shift in the observed zeta potential to more cationic charges (Figure 5-4A). Similarly, the titrations demonstrated that PEGylated $(Acr\text{-}Lys)_{2\ and\ 4}$ resulted in anionic polyplex when fully bound to DNA, while PEGylated $(Acr\text{-}Lys)_6$ resulted in cationic polyplexes above stoichiometries of 0.3 nmol per μg of DNA and yielding charges as high as 9 mV at a stoichiometry of 0.8 nmol per μg (Figure 5-4A). Therefore, PEGylated $(Acr\text{-}Lys)_6$ was the only peptide that could form either anionic or cationic polyplexes depending on the stoichiometry peptide. QELS particle size analysis showed that there was no apparent

change in the size of the DNA polyplexes prepared with PEGylated $(Acr\text{-}Lys)_{2,\ 4\ ,\ or\ 6}$ at any stoichiometry of peptide evaluated (Figure 5-4B), thus indicating that these DNA polyplexes are not forming spherical nanoparticles.

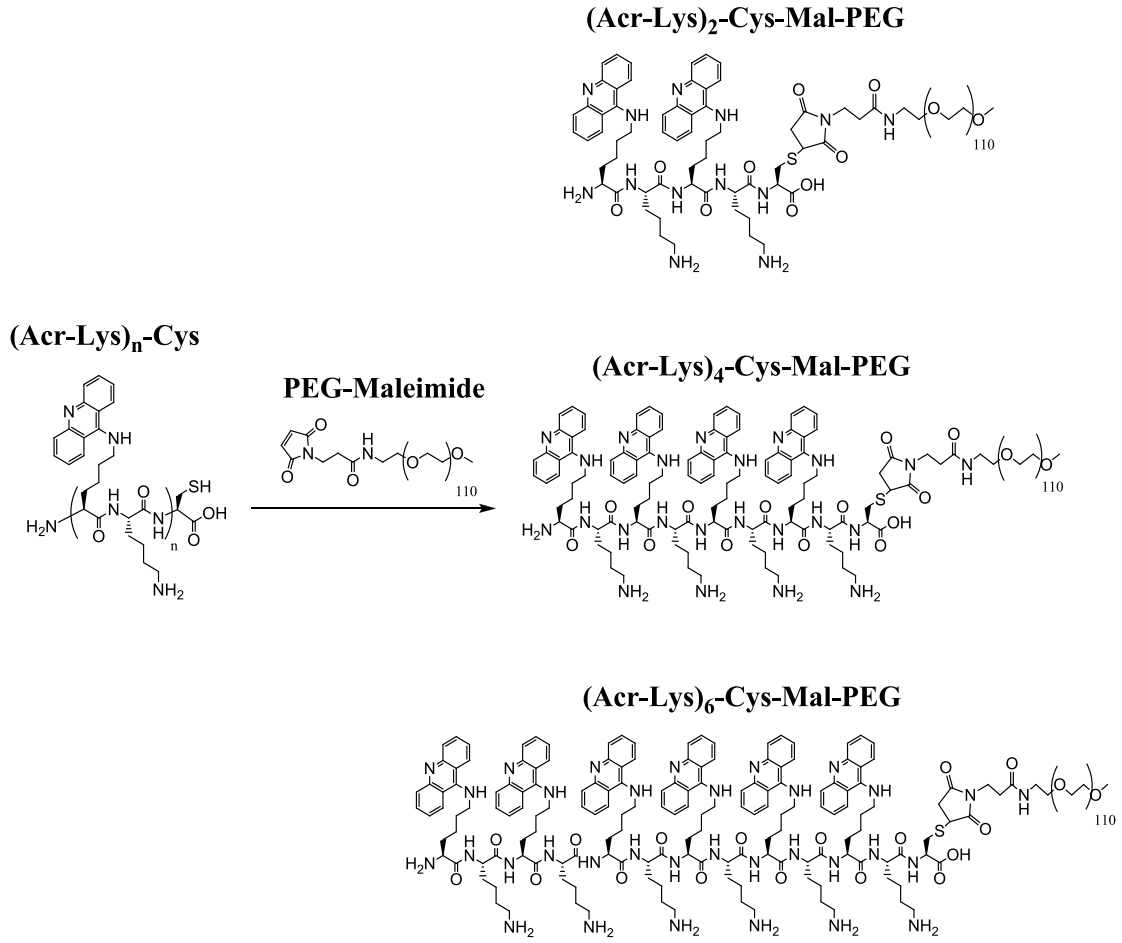

Figure 5-1. *Synthetic Strategy for PEGylated (Acr-Lys)$_n$ Peptides*. Polyacridine peptides with the general structure $(Acr\text{-}Lys)_n$-Cys possessing a Lys modified on the ε-amine with an acridine (Acr) and spaced by a Lys amino acid were prepared by solid phase peptide synthesis. The Cys thiol on the polyacridine peptides was then reacted with a 5 kDa PEG maleimide resulting in the formation of PEGylated $(Acr\text{-}Lys)_n$ peptides containing two, four, or six (Acr-Lys) units.

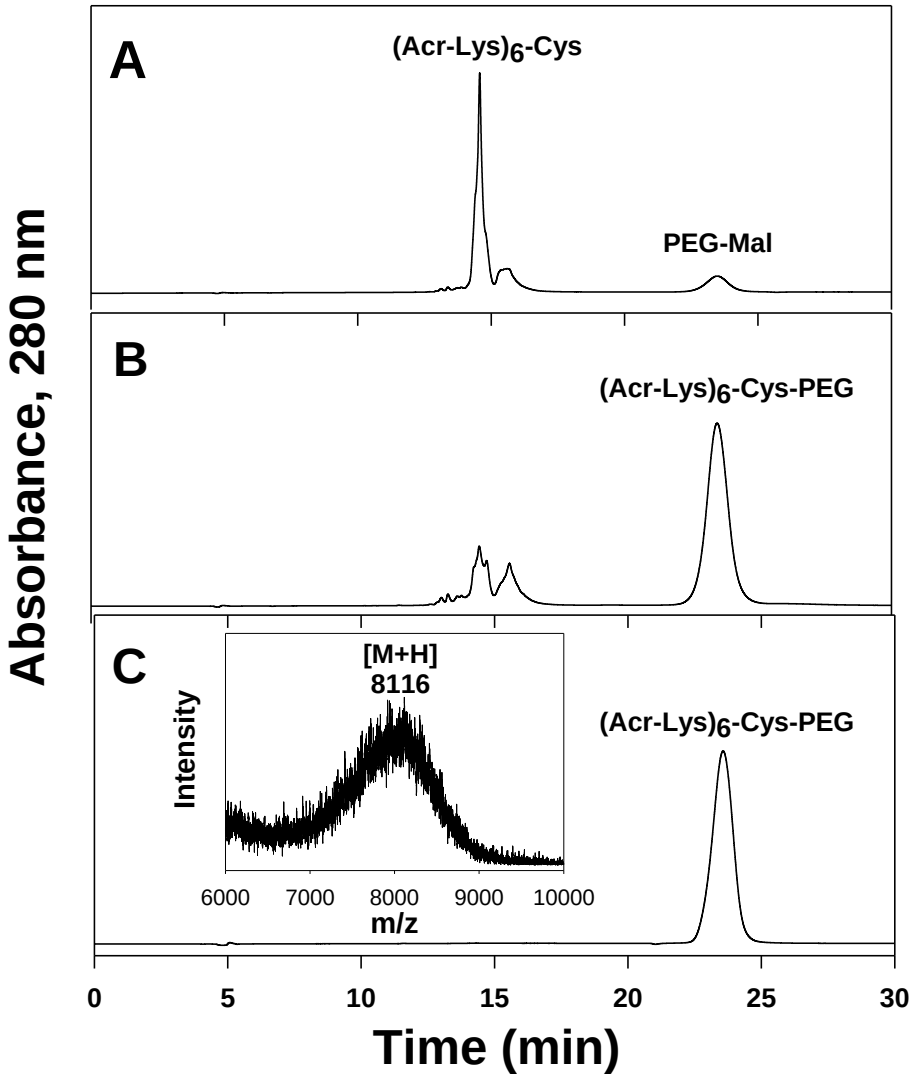

Figure 5-2. *RP-HPLC Analysis of (Acr-Lys)$_6$-Cys-Mal-PEG Synthesis.* Reaction of (Acr-Lys)$_6$-Cys with 1.2 mol equivalents of a PEG maleimide of 5 kDa (panel A) results in the formation of (Acr-Lys)$_6$-Cys-PEG and consumption of the (Acr-Lys)$_6$-Cys peptide (panel B), as shown under elution with 0.1% TFA and an acetonitrile gradient of 25-65% over 30 minutes while monitoring absorption at 280 nm. The PEGylated polyacridine peptide was purified by preparatory HPLC and rechromatographed on RP-HPLC as single peak (panel C) and further characterized by MALDI-TOF-MS (panel C, inset). All other PEGylated (Acr-Lys)$_n$ peptides produced equivalent chromatographic and MS evidence. HPLC analysis was performed in collaboration with Nicholas J. Baumhover, Medicinal Chemistry and Natural Products, University of Iowa.

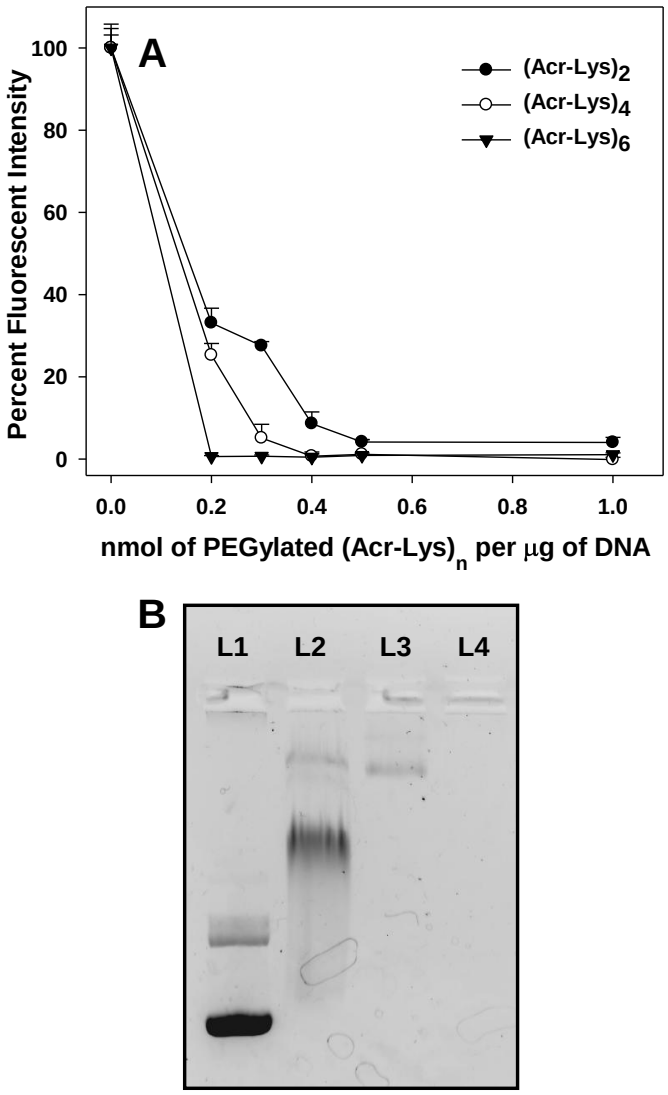

Figure 5-3. *Relative DNA Binding Affinity of PEGylated (Acr-Lys)$_n$ Peptides.* The thiazole orange displacement assay was used to compare the relative binding affinity of PEGylated (Acr-Lys)$_n$ peptides for DNA. PEGylated (Acr-Lys)$_2$ (●), (Acr-Lys)$_4$ (○), and (Acr-Lys)$_6$ (▼) were titrated from 0.2 to 1 nmol with 1 μg of DNA and 0.1 μM thiazole orange (panel A). The results establish that that increasing the units of (Acr-Lys) incorporated onto the peptide results in an increase in the binding affinity of the peptide for DNA. A band shift gel assay was used to confirm the relative binding affinity of the PEGylated (Acr-Lys)$_n$ peptides (panel B) where 1 ug of DNA was polyplexed with 0.2 nmol of either PEGylated (Acr-Lys)$_2$ (panel B, lane 2), (Acr-Lys)$_4$ (panel B, lane 3), or (Acr-Lys)$_6$ (panel B, lane 4). The results confirm a band shift relative to the DNA control lane (lane 1) and verify high affinity binding for both PEGylated (Acr-Lys)$_4$ and (Acr-Lys)$_6$.

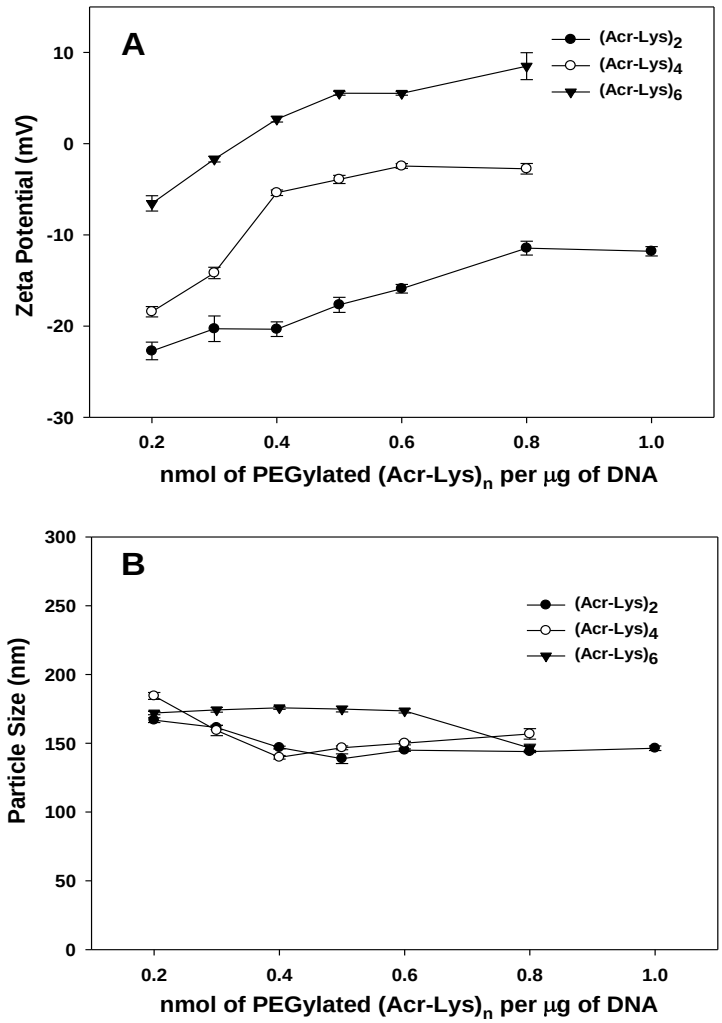

Figure 5-4. *Surface Charge and Particle Size of PEGylated (Acr-Lys)$_n$ Peptide DNA Polyplexes*. The zeta potential and QELS particle size of DNA polyplexes were determined at various stoichiometries of PEGylated polyacridine peptide. Polyplexes were prepared with either PEGylated (Acr-Lys)$_2$ (●), (Acr-Lys)$_4$ (○), and (Acr-Lys)$_6$ (▼) at stoichiometries ranging from 0.2 to 1 nmol of peptide per μg of DNA. The zeta potential titration curve (panel A) reveals that increasing the units of (Acr-Lys) incorporated onto the peptide results in a shift in the zeta potential to more cationic charges. Furthermore, the curve illustrates that both PEGylated (Acr-Lys)$_2$ and (Acr-Lys)$_4$ form anionic DNA polyplexes when fully bound to DNA, while PEGylated (Acr-Lys)$_6$ forms cationic DNA polyplexes at a stoichiometry of 0.4 nmol per μg of DNA and above. The particle size analysis (panel B) demonstrates that there is no change in the apparent size of DNA polyplexes during the titration.

The shape of DNA polyplexes prepared with PEGylated $(Acr\text{-}Lys)_6$ was evaluated using the atomic force microscope (AFM). 5 x 5 μm scans of DNA or DNA polyplexes bound to the surface of cationic mica prepared with immobilized nickel or anionic mica (no nickel) is shown on Figure 5-5A-D. The results demonstrate that open DNA polyplexes form at a stoichiometry of 0.2 nmol per μg of DNA and bind to cationic mica (Figure 5-5B). In contrast, polyplexes prepared at 0.8 nmol per μg no longer bind to the surface or cationic mica (Figure 5-5C), but rather bind to native anionic mica (no nickel) to reveal the compaction of DNA into nanoparticles (Figure 5-5D). The results determine that only polyplexes prepared with PEGylated $(Acr\text{-}Lys)_6$ can be controlled to be either open-DNA polyplex or DNA nanoparticles depending on the stoichiometry of peptide.

In order to investigate the metabolic stability of DNA polyplexes, PEGylated $(Acr\text{-}Lys)_{2,\ 4,\ and\ 6}$ polyplexes were digested with DNase, followed by phenol-chloroform extraction to remove peptide and gel electrophoresis to determine the status of the plasmid DNA (Figure 5-6). Unique band shifts occurred for PEGylated $(Acr\text{-}Lys)_{2,\ 4,\ and\ 6}$ polyplexes prepared at either 0.2 or 0.8 nmols of peptide per μg of plasmid DNA (Figure 5-6, lane 2 and 3 of panels A, B, C). However, phenol-chloroform extraction removed the PEG-peptide allowing recovery of the DNA which migrated coincident with control (Figure 5-6, lane 4 of panels A, B and C). When challenged with a DNase digestion, PEGylated $(Acr\text{-}Lys)_{2\ or\ 4}$ polyplexes prepared at 0.2 nmol per μg of DNA failed to protect DNA from metabolism (Figure 5-6, panel A and B, lane 5 and 6). In contrast, polyplexes formed at 0.2 nmols of PEGylated $(Acr\text{-}Lys)_6$ protected the DNA from DNase resulting in the recovery of bands following extraction (Figure 5-6, panel C, lanes 5 and 6). At a higher stoichiometry of 0.8 nmols, PEGylated $(Acr\text{-}Lys)_{2,\ 4\ and\ 6}$ each protected DNA from metabolism (Figure 5-6, panel A-C, lanes 7 and 8). These results establish a

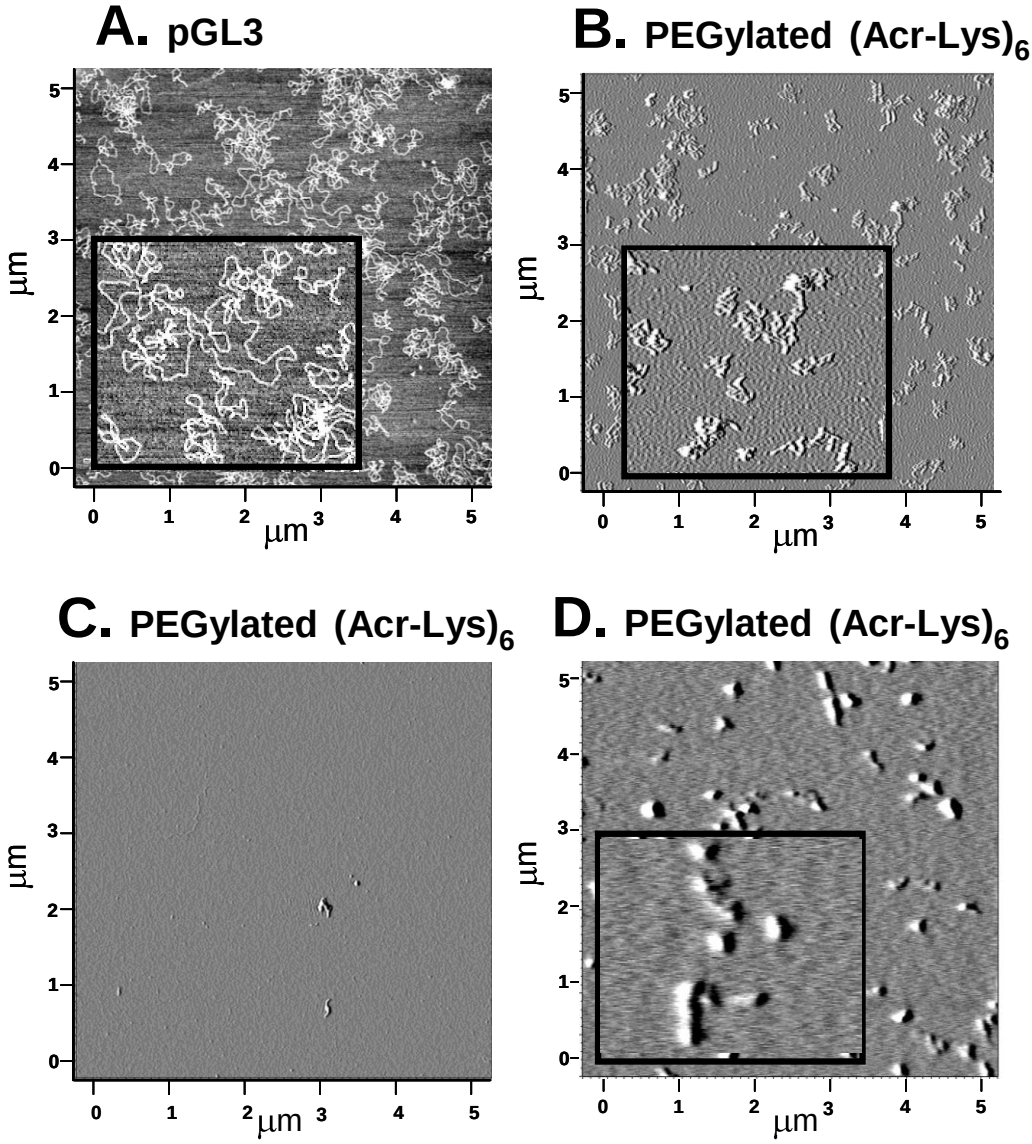

Figure 5-5. *Morphology of PEGylated (Acr-Lys)$_6$-DNA Polyplexes by Atomic Force Microscope*. The atomic force microscope (AFM) was used to determine the shape of DNA polyplexes prepared with PEGylated (Acr-Lys)$_6$ at either 0.2 or 0.8 nmol per μg of peptide. The AFM image of DNA polyplexes prepared at 0.2 nmol per μg (panel B) reveals the formation of anionic open DNA polyplexes that resemble the shape of naked DNA (panel A). In contrast, DNA polyplexes prepared at 0.8 nmol per μg collapse the open structure of plasmid DNA into cationic DNA nanoparticles (panel D) that no longer bind to the surface of cationic mica (panel C).

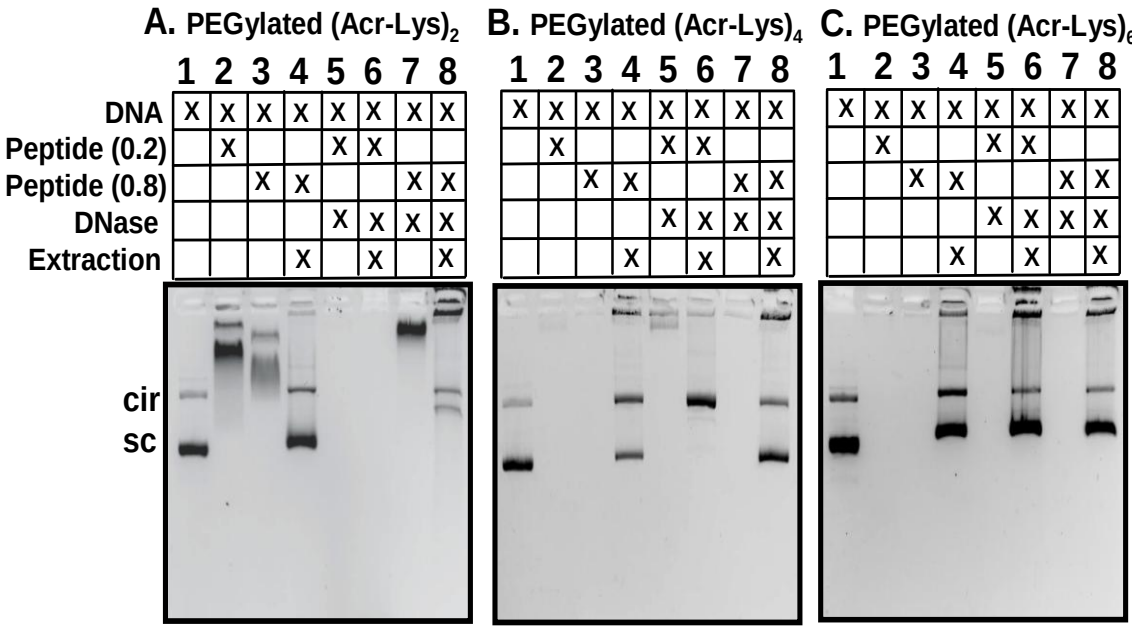

Figure 5-6. *Metabolic Stability of PEGylated Polyacridine DNA Polyplexes.* Protection of DNA from nuclease digestion by PEGylated polyacridine peptides was determined by agarose gel electrophoresis. The lanes of each gel (1-8) are labeled above the table placed over the gels. The "x's" in each column of the table represent the components combined in each lane of the gel, where the first lane (1) of each gel only contains plasmid DNA. Agarose gel electrophoresis of (1) plasmid DNA, (2) PEGylated $(Acr\text{-}Lys)_n$ polyplex (n is 2, 4 or 6) at 0.2 nmol of peptide per μg of DNA, (3) PEGylated $(Acr\text{-}Lys)_n$ polyplex at 0.8 nmol of peptide per μg of DNA, (4) release of DNA from PEGylated $(Acr\text{-}Lys)_n$ polyplex at 0.8 nmol per μg of DNA, (5) PEGylated $(Acr\text{-}Lys)_n$ polyplex at 0.2 nmol per μg of DNA following DNase digest, (6) released PEGylated $(Acr\text{-}Lys)_n$ polyplex at 0.2 nmol per μg of DNA following DNase digest, (7) PEGylated $(Acr\text{-}Lys)_n$ polyplex at 0.8 nmol per μg of DNA following DNase digest, (8) released PEGylated $(Acr\text{-}Lys)_n$ polyplex at 0.8 nmol per μg of DNA following DNase digest. The results establish the partial or complete protection of DNA from DNase at 0.8 nmol of PEGylated $(Acr\text{-}Lys)_2$ (panel A lane 8) and $(Acr\text{-}Lys)_4$ (panel B lane 8), and the complete protection of DNA from DNase at 0.2 and 0.8 nmol of $(Acr\text{-}Lys)_6$-PEG (panel C lane 6 and 8).

clear correlation between polyacridine DNA binding affinity (Figure 5-3A) and metabolic stability of polyplexes. Most importantly, PEGylated $(Acr\text{-}Lys)_6$ is resistant against DNase metabolism as an anionic open-polyplexes when prepared at 0.2 nmol per μg of DNA, as well as cationic closed-polyplexes prepared at 0.8 nmol per μg of DNA.

PEGylated polyacridine peptides were also subjected to trypsin digestion to determine if they could be digested by a common serine protease, suggesting that perhaps they could also be more easily cleared from cells. The data (not shown) indicates that even as little as 100 mU of trypsin catalyzed the formation of a dipeptide of Lys-Lys(Acr) with mass of 451 g/mol, to a reaction completion within 1 hr. Thereby, the high-affinity DNA binding of PEGylated polyacridine peptides is greatly reduced upon proteolytic digestion.

Comparison of the stimulated gene expression (30 min) mediated by PEGylated $(Acr\text{-}Lys)_{2,\ 4\ and\ 6}$ polyplexes (1 μg pGL3) prepared at 0.8 and 0.2 nmols of peptide established that PEGylated $(Acr\text{-}Lys)_2$ was completely inactive (Figure 5-7 and Figure 5-8). In contrast, PEGylated $(Acr\text{-}Lys)_6$ at 0.2 nmols matched the luciferase expression of PEGylated $(Acr\text{-}Lys)_4$ at 0.8 nmols (Figure 5-7 & Figure 5-8). Nevertheless, when the stoichiometry is lowered to 0.2 nmols for PEGylated $(Acr\text{-}Lys)_4$, a 50-fold loss in expression is observed (Figure 5-7 and Figure 5-8). These results correlate a higher binding affinity by PEGylated $(Acr\text{-}Lys)_6$ (Figure 5-3) and a greater capability to protect DNA from metabolism (Figure 5-6), with the ability to mediate stimulated gene expression even at a low stoichiometry of 0.2 nmols per μg of DNA (Figure 5-7).

PEGylated $(Acr\text{-}Lys)_6$ polyplexes were administered in mice to determine the effect of peptide stoichiometry on stimulated gene expression (Figure 5-9 and Figure 5-10). The results established that a 1 μg dose of pGL3 polyplex, stimulated at 30 min, produced equivalent gene expression across the range of 0.2-0.8 nmols of peptide (Figure 5-9A). These results are in sharp contrast to those determined for PEGylated $(Acr\text{-}Lys)_4$ and $(Acr\text{-}Arg)_4$ (Figure 4-7B), in which the gene expression was highly dependent on the stoichiometry of peptide to DNA. Furthermore, since PEGylated $(Acr\text{-}Lys)_6$ was the only peptide to produce a zeta potential titration that started anionic (-5 mV) at 0.2 nmol and titrated to cationic charge (+9 mV) at 0.8 nmols (Figure 5-4A), it appears that the stimulated gene expression mediated by PEGylated $(Acr\text{-}Lys)_6$ is fully functional as both

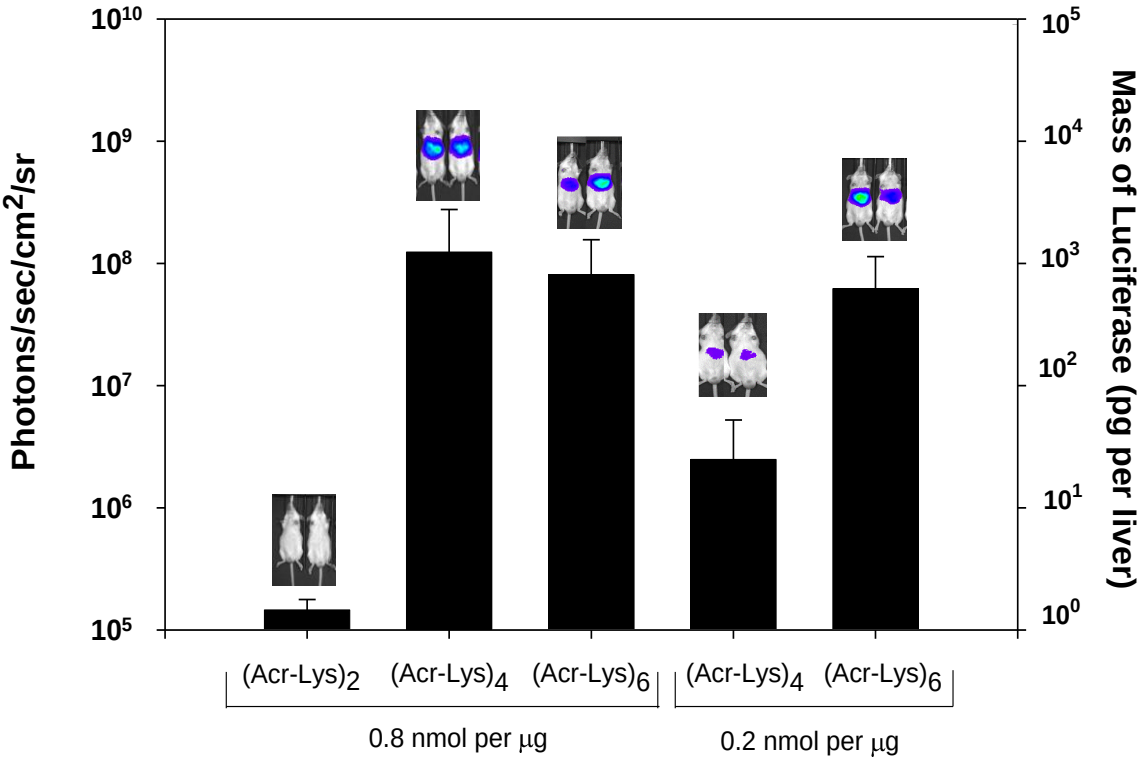

Figure 5-7. *Stimulated Gene Expression of PEGylated (Acr-Lys)$_n$ DNA Polyplexes*. Luciferase expression was determined for DNA polyplexes prepared with PEGylated (Acr-Lys)$_2$, (Acr-Lys)$_4$, and (Acr-Lys)$_6$ at 0.8 or 0.2 nmol per μg of DNA and HD stimulated 30 min after iv administration and reported as photons/sec/cm^2/seradian (left y-axis) and transformed to pmols of luciferase in the liver (right y-axis) using a previously reported standard curve.[213] The results indicate that PEGylated (Acr-Lys)$_4$ and (Acr-Lys)$_6$ DNA polyplexes achieve high gene expression when prepared at 0.8 nmol per μg of DNA. Only PEGylated (Acr-Lys)$_6$ DNA polyplexes maintained high gene expression at a stoichiometry of 0.2 nmol per μg of DNA. In contrast, PEGylated (Acr-Lys)$_2$ DNA polyplexes failed to stimulate similar levels of gene expression at the stoichiometry evaluated. See figure 5-9 for larger scale images of the representative mice above each bar. Formulation administration was performed in collaboration with Jason Duskey, Medicinal and Natural Product Chemistry, University of Iowa.

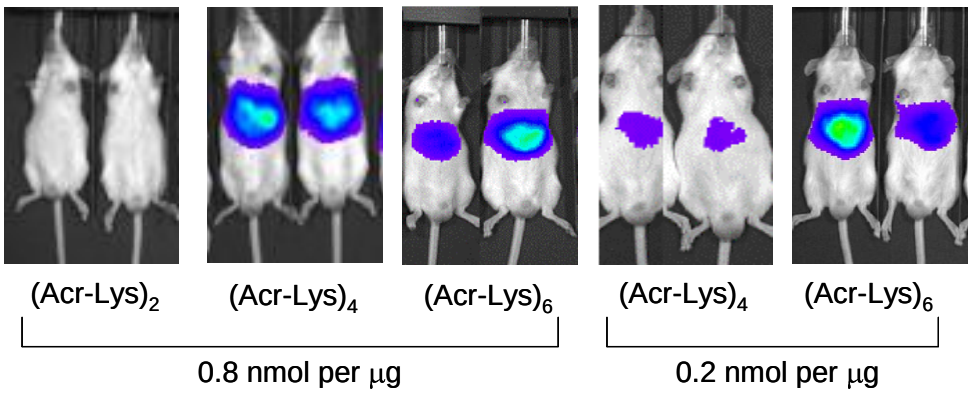

Figure 5-8. *Bioluminescence Images of the Stimulated Gene Expression Mediated by PEGylated (Acr-Lys)$_n$ DNA Polyplexes.* The luciferase expression of representative mice is shown in the figure for PEGylated (Acr-Lys)$_n$ DNA polyplexes 24 hours after administration by bioluminescence imaging (BLI). The average expression mediated by each formulation was calculated and reported photons/sec/cm^2/seradian and pmols of luciferase in the liver on figure 5-7.

an anionic open polyplex (Figure 5-5B), and as an cationic closed polyplex (Figure 5-5D).

To determine if the unique DNA binding properties of PEGylated (Acr-Lys)$_6$ would also extend the delay time allowed between primary and stimulatory dose, polyplexes (1 μg) were prepared with 0.2 nmols of peptide and administered with a time delay varying from 0 to 120 min. Delaying the stimulation from 5 to 60 min resulted in only a slight 2-3 fold decrease in expression, whereas with a 120 min delay the expression decreased 100-fold (Figure 5-9B). Using a zero delay time resulted in a nearly 5-fold increase in gene expression relative to dose equivalent direct HD administration of pGL3 (Figure 5-9B). These results demonstrate that PEGylated (Acr-Lys)$_6$ mediates significant high-level gene expression, even with a 60 min delay time, compared to PEGylated (Acr-Arg)$_4$ which failed to mediate detectable expression following a 60 min delay in stimulation (Figure 4-7A).

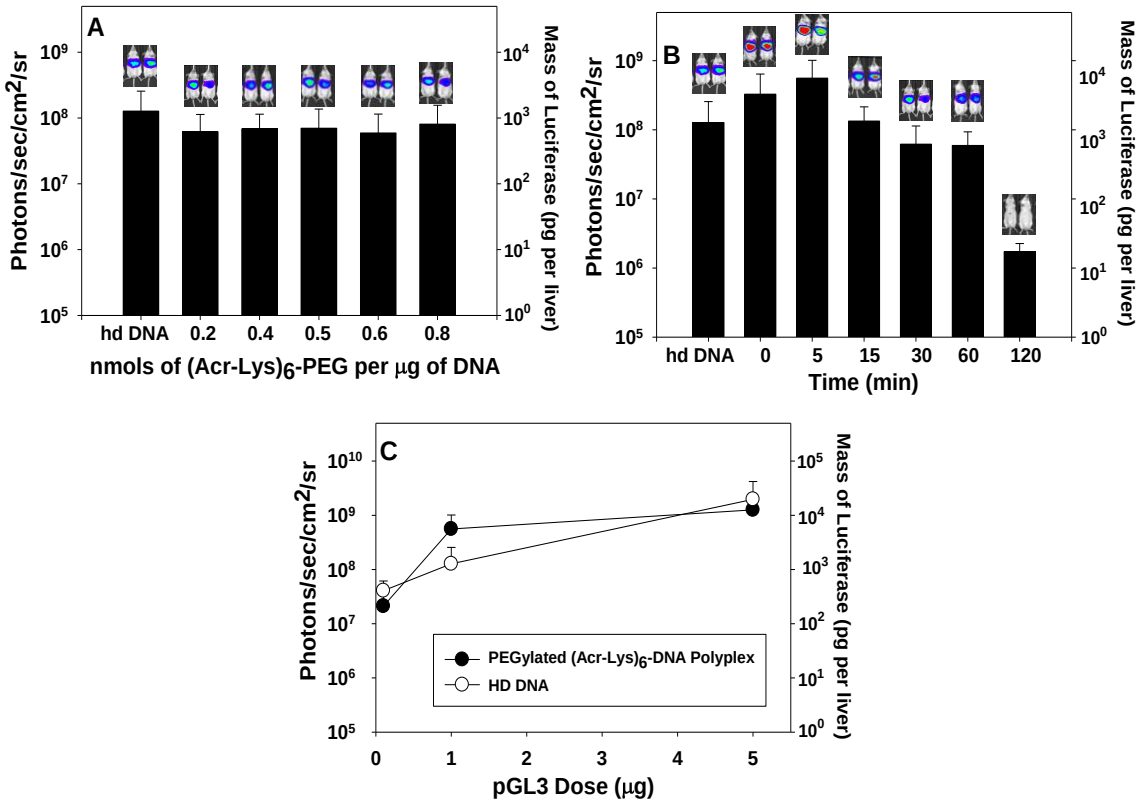

Figure 5-9. *Stimulated Gene Expression of PEGylated (Acr-Lys)$_6$ DNA Polyplexes.* In panel A, the level of expression measured at 24 hrs, following HD stimulation 30 min after DNA dosing, remains nearly constant when delivering PEGylated (Acr-Lys)$_6$ DNA polyplexes prepared at stoichiometries ranging from 0.2-0.8 nmols of peptide per μg of DNA. The results in panel B illustrate that varying the HD stimulation delay-time following delivery of PEGylated (Acr-Lys)$_6$ DNA polyplexes results in expression of approximately 10^8 photons/sec/cm^2/sr up to 60 min, whereas the expression decreased nearly 100-fold when delaying HD stimulation to 120 min. The dose-response curve in panel C for in vivo stimulated gene expression of PEGylated (Acr-Lys)$_6$ DNA polyplexes with 5 min delay in stimulation (●) is compared with direct HD of pGL3 DNA (○). The luciferase expression after 24 hrs determined by BLI suggests that HD delivery of 1 μg of PEGylated (Acr-Lys)$_6$ DNA polyplexes results in is approximately 5-fold higher gene expression (not statistically significant) relative to direct delivery of pGL3 (panel C). See Figure 5-10 for larger scale images of the representative mice above each bar. Formulation administration was performed in collaboration with Jason Duskey, Medicinal and Natural Product Chemistry, University of Iowa.

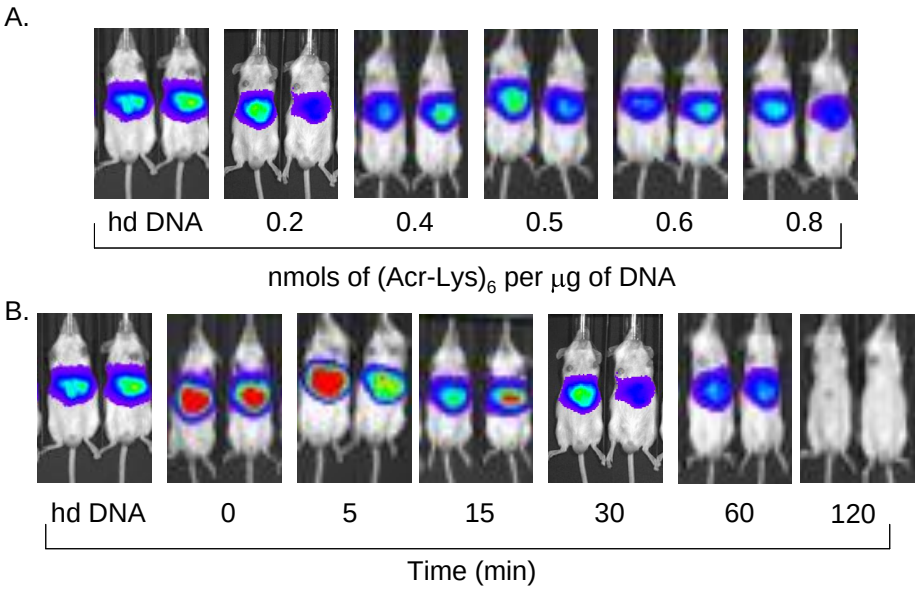

Figure 5-10. *Bioluminescence Images of the Stimulated Gene Expression Mediated by PEGylated (Acr-Lys)$_6$ DNA Polyplexes.* The luciferase expression of representative mice is shown for PEGylated (Acr-Lys)$_6$ DNA polyplexes imaged 24 hours after administration by bioluminescence imaging (BLI). Panel A demonstrates the effect of stoichiometry on gene expression following HD stimulation 30 min after dosing. Panel B represents the stimulated gene expression of PEGylated (Acr-Lys)$_6$ DNA polyplexes prepared at 0.2 nmol per μg of DNA when varying the HD stimulation lag time from 0 to 120 min. The average expression mediated by each formulation was calculated and reported as photons/sec/cm^2/seradian and pmols of luciferase in the liver on Figure 5-9.

To establish the dose-equivalency of direct HD administration of DNA, relative to the stimulated expression of PEGylated polyacridine polyplexes, a dose-response experiment was performed (Figure 5-9C). The BLI detected expression at 24 hrs post-DNA delivery was determined for direct HD delivered pGL3, dosed at 0.1, 1 and 5 μg of DNA (Figure 5-9C). This was compared with the 24 hr luciferase expression from identical DNA doses of PEGylated (Acr-Lys)$_6$ polyplexes prepared with 0.2 nmol of peptide and administered with a 5 min delay in stimulation. A nearly linear dose-response curve was identified for direct HD dosing of pGL3, whereas PEGylated (Acr-Lys)$_6$ polyplexes showed an increase from 0.1-1 μg, followed by a plateau at 5 μg dose (Figure

5-9C). At 1 μg dose, PEGylated $(Acr\text{-}Lys)_6$ DNA polyplexes demonstrated a 5-fold higher trend in gene expression compared to HD dosed plasmid DNA (Figure 5-9C).

Pharmacokinetic and biodistribution studies were performed in order to gain further insights into the mechanism behind the stimulated gene expression mediated by PEGylated polyacridine polyplexes. Administration of ^{125}I-DNA or PEGylated $(Acr\text{-}Lys)_2$ polyplexes resulted in a rapid 10-fold loss of radioactivity from the blood within 20-30 min (Figure 5-11A) which represents the initial distribution associated with the α disposition phase. The radioactivity measured beyond 30 minutes suggests an apparent long drug elimination half-life associated with the β disposition phase (Figure 5-11A). Isolation of ^{125}I-DNA from blood, followed by gel electrophoresis and autoradiography demonstrated that plasmid DNA was rapidly degraded to fragments within 1 min (Figure 5-12A). Likewise, electrophoretic analysis of blood samples following dosing of PEGylated $(Acr\text{-}Lys)_2$ ^{125}I-DNA polyplexes demonstrated complete loss of plasmid DNA within 20 min (Figure 5-12B), suggesting that the modest binding from PEGylated $(Acr\text{-}Lys)_2$ leads to slightly delayed metabolism.

The pharmacokinetic profile for PEGylated $(Acr\text{-}Lys)_{4 \text{ and } 6}$ ^{125}I-DNA polyplexes were both very similar and distinct from those of ^{125}I-DNA and PEGylated $(Acr\text{-}Lys)_2$ ^{125}I-DNA polyplexes (Figure 5-11A). The radioactivity in blood only decreased 3-4 fold in the first 20 min (α disposition phase) and proceeded with an apparent long half-life (β disposition phase) (Figure 5-11A). Recovery of ^{125}I-DNA from PEGylated $(Acr\text{-}Lys)_{4 \text{ and } 6}$ polyplexes resulted in an agarose gel autoradiographic analysis that established the blood stability of plasmid DNA up to 30 min for PEGylated $(Acr\text{-}Lys)_4$ (Figure 5-12C), and up to 120 min for PEGylated $(Acr\text{-}Lys)_6$ (Figure 5-12C). Non-linear least squares analysis of the radioactivity in blood over time was used to calculate an apparent α-half-life from the α disposition phase of 2-3 min and a β-half-life from the β disposition phase of 65 min for PEGylated $(Acr\text{-}Lys)_4$ and 182 min for PEGylated $(Acr\text{-}Lys)_6$ (Table 5-2). For the purpose of comparison, complete metabolic stability of plasmid DNA was

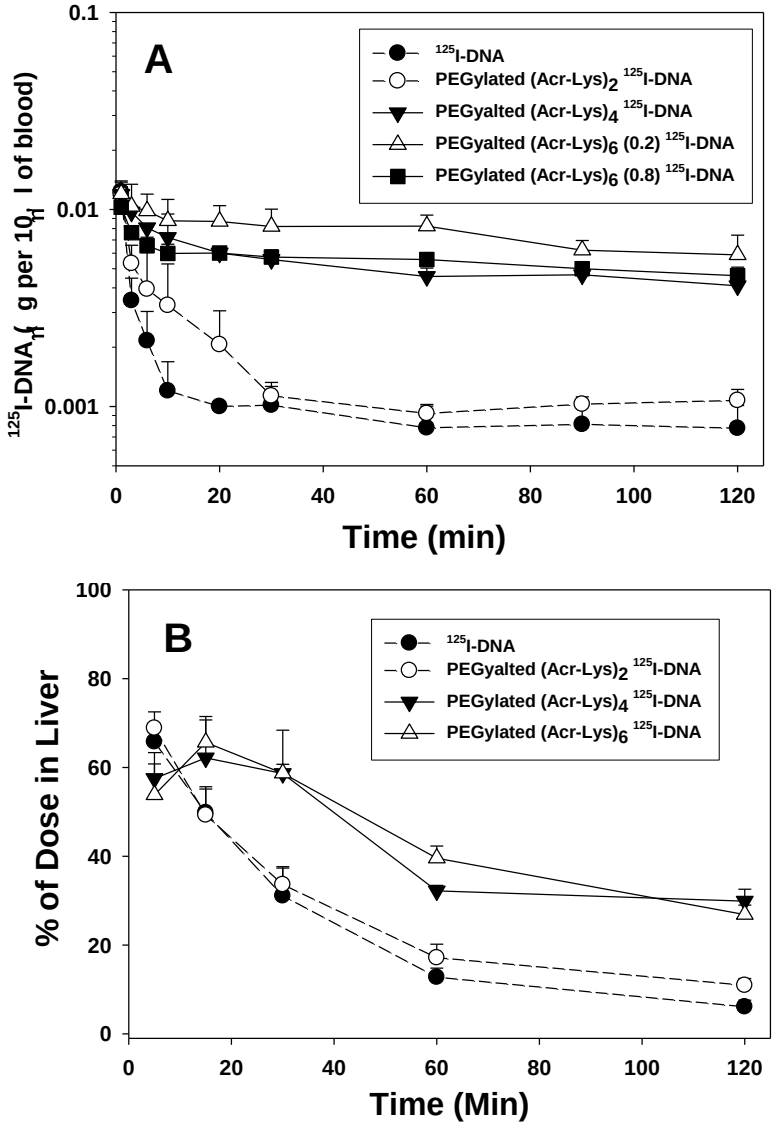

Figure 5-11. *Pharmacokinetic and Liver Targeting of PEGylated Polyacridine Polyplexes*. The pharmacokinetic profile for PEGylated $(Acr\text{-}Lys)_2$, PEGylated $(Acr\text{-}Lys)_4$, and PEGylated $(Acr\text{-}Lys)_6$ ^{125}I-DNA polyplexes is compared with ^{125}I-DNA (panel A). The results establish that PEGylated $(Acr\text{-}Lys)_6$ stabilizes DNA in the blood for up to two hours. Biodistribution analysis of ^{125}I-DNA and PEGylated polyacridine ^{125}I-DNA polyplexes was determined by harvesting the major organs and directly γ-counting each organ for radioactivity (panel B). The data are expressed as percent of dose in liver, and the result suggest improved DNA stability for PEGylated $(Acr\text{-}Lys)_4$ and PEGylated $(Acr\text{-}Lys)_6$ ^{125}I-DNA polyplexes. Pharmacokinetics and biodistribution analysis was performed in collaboration with Sanjib Khargharia, Medicinal Chemistry and Natural Products, University of Iowa.

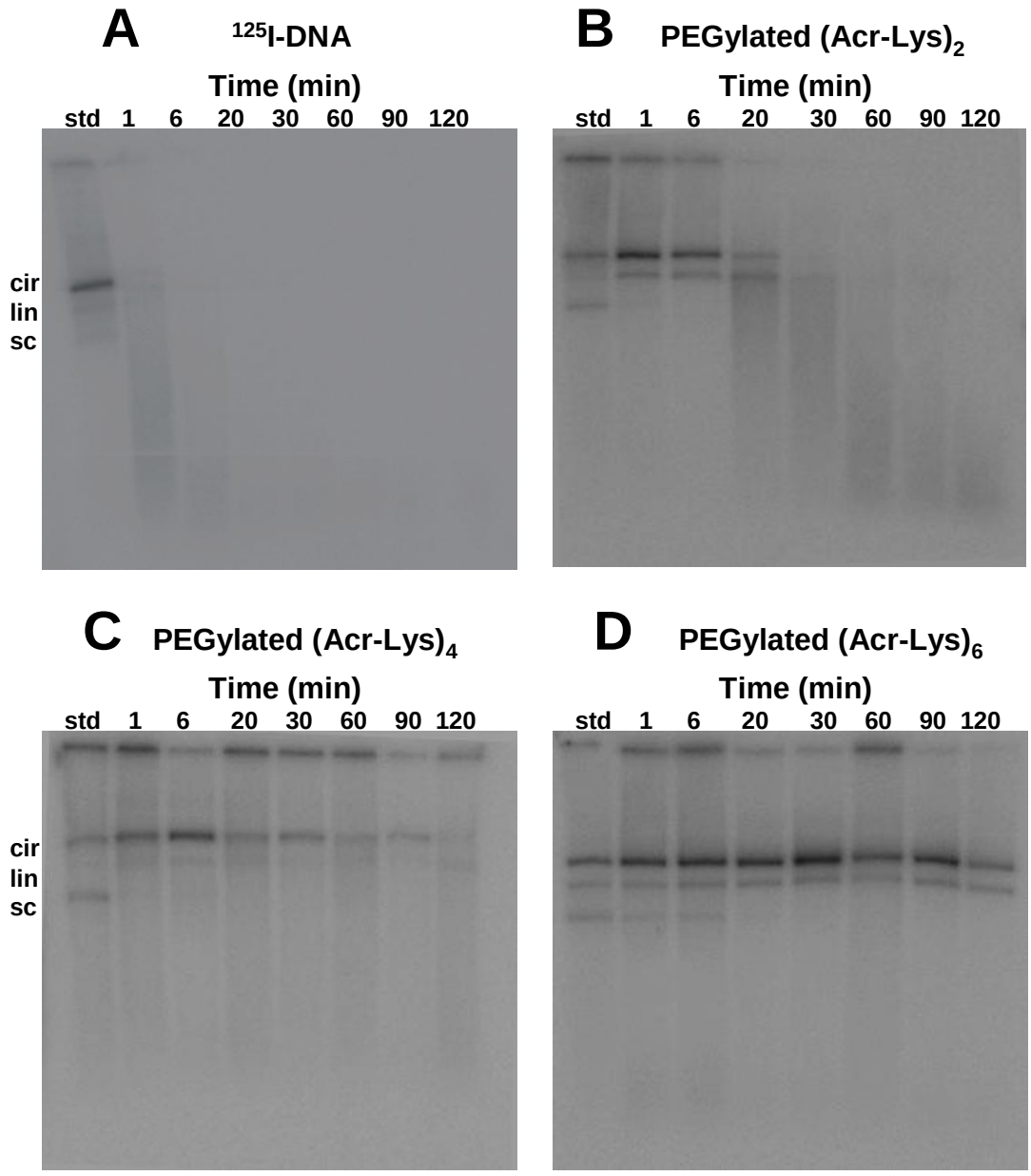

Figure 5-12. *Electrophoretic Analysis of PEGylated Polyacridine Polyplexes Blood Samples.* Extraction of the ^{125}I-DNA from the blood time points presented on Figure 5-11 were followed by agarose electrophoresis and autoradiography produced the images in A-D. The results demonstrate that only PEGylated $(Acr\text{-}Lys)_6$ ^{125}I-DNA polyplexes are stable through out the two hour analysis. Pharmacokinetics analysis was performed in collaboration with Sanjib Khargharia, Medicinal Chemistry and Natural Products, University of Iowa.

assumed in the pharmacokinetic calculation unless the gel electrophoretic and autoradiographic analysis for the DNA polyplexes revealed complete degradation of DNA upon extraction. The improved pharmacokinetic properties observed (Figure 5-11) correlate with the relative binding affinity measured for each PEGylated polyacridine peptides (Figure 5-3). As the binding affinities of PEGylated polyacridine peptides increases, the apparent clearance rates of the DNA polyplexes decrease (Table 5-2). This relationship suggests that the improved metabolic stability in the blood is afforded by the high affinity binding of the peptides and leads to an increase in the β-half-life (Table 5-2).

The unique long pharmacokinetic β-half-life for PEGylated $(Acr\text{-}Lys)_{4 \text{ and } 6}$ polyplexes and the nearly coincident volume of distribution suggested there would be similar biodistribution to the organs. The experimental results established that the liver was the major site of biodistribution for PEGylated $(Acr\text{-}Lys)_{2,\ 4 \text{ and } 6}$ ^{125}I-DNA polyplexes (Table 5-3 and Figure 5-11B). In each of these experiments, it was not possible to extract ^{125}I-DNA from liver or other tissues to determine its metabolic status, as was performed for DNA in blood.

Table 5-2. Parameters for PEGylated Polyacridine DNA Polyplex

Polyacridine Peptide Polyplex	**$t_{1/2}\alpha$ [a] (min)**	**$t_{1/2}\beta$ [b] (min)**	**Vol Dis [c] (mL)**	**Cl [d] (mL/min)**	**MRT [e] (min)**	**K10 [f] (min)**
PEGylated $(Acr\text{-}Lys)_2$ [g]	0.7 +/- 0.0	15.2 +/- 0.8	42.8 +/- 0.1	2.3 +/- 0.0	18.9 +/- 0.1	0.192+/ 0.001
PEGylated $(Acr\text{-}Lys)_4$ [h]	2.3 +/- 0.3	65.6 +/- 13.5	37.4 +/- 1.9	0.4 +/- 0.1	92.2 +/- 18.9	0.018 +/ 0.003
PEGylated $(Acr\text{-}Lys)_6$ [i]	1.8 +/- 0.9	181.5 +/- 33.4	31.6 +/- 1.3	0.1 +/- 0.0	260.8 +/- 47.8	0.005 +/ 0.001

a. α half-life b. β half-life c. Volume of distribution d. Total clearance rate

e. Mean residence time f. Elimination rate g. Calculated using cpm values over 30 min

h. Calculated using cpm values over 60 min i. Calculated using cpm values over 120 min

Table 5-3. Biodistribution of PEGylated Polyacridine DNA Polyplexes in Blood and Major Organs

Polyacridine Peptide Polyplex	Time (min)	Blood[a]	Liver[b]	Lung[b]	Spleen[b]	Stomach[b]	Kidney[b]	Heart[b]	LI[b]	SI[b]	Total[c]
^{125}I-DNA	5	14.4+/-5.8	65.7+/-2.5	6.1+/-2.2	2.8+/-0.3	0.2+/-0.0	0.9+/-0.2	0.1+/-0.0	0.2+/-0.1	0.4+/-0.1	84.7+/-11.2
	30	6.8+/-1.7	31.1+/-6.2	1.4+/-0.1	2.1+/-0.6	1.6+/-1.3	3.5+/-1.0	0.2+/-0.0	1.6+/-0.7	2.8+/-0.3	51.1+/-11.9
	60	5.2+/-1.6	12.7+/-2.0	0.9+/-0.2	1.3+/-0.2	4.5+/-1.0	3.5+/-0.6	0.2+/-0.0	1.1+/-0.2	2.1+/-0.3	31.5+/-6.2
	120	5.2+/-1.5	6.1+/-1.5	0.5+/-0.2	0.8+/-0.2	9.4+/-3.2	1.6+/-0.9	0.1+/-0.1	1.9+/-0.8	2.6+/-0.5	28.2+/-8.9
PEGylated (Acr-Lys)$_2$ ^{125}I-DNA	5	26.4+/-14.0	68.9+/-3.6	1.9+/-0.1	5.3+/-1.8	0.2+/-0.0	0.8+/-0.5	0.1+/-0.1	0.3+/-0.2	0.4+/-0.1	104.2+/-20.5
	30	7.6+/-1.3	33.6+/-4.0	1.0+/-0.3	1.7+/-0.4	1.5+/-0.3	2.8+/-0.6	0.2+/-0.1	1.9+/-0.5	2.5+/-0.5	52.8+/-8.1
	60	6.2+/-0.6	17.1+/-3.1	0.7+/-0.2	0.7+/-0.5	6.1+/-2.0	2.6+/-1.1	0.2+/-0.1	2.3+/-0.5	3.1+/-1.1	39.1+/-9.3
	120	7.2+/-1.0	10.9+/-1.5	0.8+/-0.2	1.0+/-0.4	8.3+/-1.7	2.3+/-0.4	0.2+/-0.0	1.9+/-0.4	3.6+/-0.7	36.2+/-6.4
PEGylated (Acr-Lys)$_4$ ^{125}I-DNA	5	54.1+/-2.7	57.5+/-5.8	2.2+/-0.9	2.1+/-0.5	0.3+/-0.2	0.9+/-0.5	0.2+/-0.1	0.3+/-0.2	0.5+/-0.2	118.0+/-11.1
	30	37.3+/-4.4	58.6+/-9.7	1.0+/-0.1	4.5+/-2.3	0.5+/-0.1	1.4+/-0.9	0.1+/-0.1	0.5+/-0.1	0.9+/-0.5	104.8+/-18.3
	60	31.2+/-2.2	32.2+/-1.2	0.8+/-0.3	4.7+/-0.3	2.6+/-0.4	2.1+/-0.8	0.2+/-0.0	1.1+/-0.2	2.7+/-0.7	77.6+/-6.1
	120	27.4+/-3.2	29.9+/-2.7	1.0+/-0.2	4.1+/-2.4	5.3+/-2.4	2.7+/-1.5	0.2+/-0.1	1.5+/-0.6	1.7+/-0.1	73.9+/-13.3
PEGylated (Acr-Lys)$_6$ ^{125}I-DNA	5	65.8+/-14.3	53.8+/-7.0	1.3+/-0.5	6.8+/-3.1	0.4+/-0.2	0.7+/-0.1	0.2+/-0.0	0.2+/-0.1	0.5+/-0.0	129.6+/-25.3
	30	54.9+/-12.3	58.7+/-2.0	0.9+/-0.2	11.7+/-1.1	0.7+/-0.2	1.1+/-0.1	0.2+/-0.1	0.5+/-0.3	0.9+/-0.2	129.6+/-16.5
	60	55.2+/-7.6	39.6+/-2.8	0.6+/-0.1	15.4+/-0.1	1.3+/-0.3	1.3+/-0.4	0.1+/-0.1	0.8+/-0.3	1.5+/-0.2	115.9+/-11.8
	120	39.4+/-10.2	26.8+/-2.1	0.8+/-0.2	18.0+/-1.4	3.2+/-2.8	1.5+/-0.2	0.1+/-0.0	1.1+/-0.7	2.2+/-0.3	93.2+/-17.9

a. Percent of dose based on pharmacokinetic analysis

b. Percent of dose based on gamma counting of tissue

c. Total percent of dose recovered

The biodistribution of ^{125}I-DNA and PEGylated (Acr-Lys)$_2$ ^{125}I-DNA polyplexes both reached a maximum of approximately 65% in the liver at 5 min, followed by a decrease to less than 10% by 120 min (Figure 5-11B, Table 5-3). In contrast, when dosing PEGylated (Acr-Lys)$_{4 \text{ and } 6}$ ^{125}I-DNA polyplexes, the percent of radioactive dose in liver was approximately 55% at 5 min, which accumulated to over 60% at 15 min, followed by a decline to 30-40% at 120 min (Figure 5-11B, Table 5-3). By comparison, a maximum of 5-9% of the total radioactive dose distributed to lungs, heart, kidneys or intestine at all time points (Figure 5-13A-D, Table 5-3). The only exception being spleen accumulation when dosing PEGylated (Acr-Lys)$_6$ polyplexes, which showed a steady accumulation over time reaching 18% at 2 hrs (Figure 5-13D, Table 5-3). In addition to the liver and spleen, the blood accounted for the majority of the radioactive dose, which ranged from 65-40% in the circulation during the two hours following dosing of PEGylated (Acr-Lys)$_6$ polyplexes (Table 5-3).

The elimination of DNA polyplexes, determined by monitoring the radioactivity of various ^{125}I-DNA formulations (Table 5-3), indicates that more than 40% of the dose is eliminated for PEGylated (Acr-Lys)$_2$ and (Acr-Lys)$_4$ DNA polyplexes by 30 and 60 min respectively (Figure 5-14). In contrast, PEGylated (Acr-Lys)$_6$ reaches a similar magnitude of elimination only after 120 minutes post-administration (Figure 5-14). Furthermore, the pharmacokinetic analysis for PEGylated (Acr-Lys)$_6$ DNA polyplexes (Table 5-2) determines a 3.6 fold reduction in the elimination rate (K10) calculated in comparison to PEGylated (Acr-Lys)$_4$ polyplexes, which may explain the improved persistence of expression for PEGylated (Acr-Lys)$_6$ DNA polyplexes (Figure 5-9B).

Discussion

PEGylated polyacridine peptides were designed to bind to plasmid DNA for the purpose of making it more blood compatible as a first step toward ultimately adding a targeting ligand and sub-cellular targeting peptides needed to complete the delivery

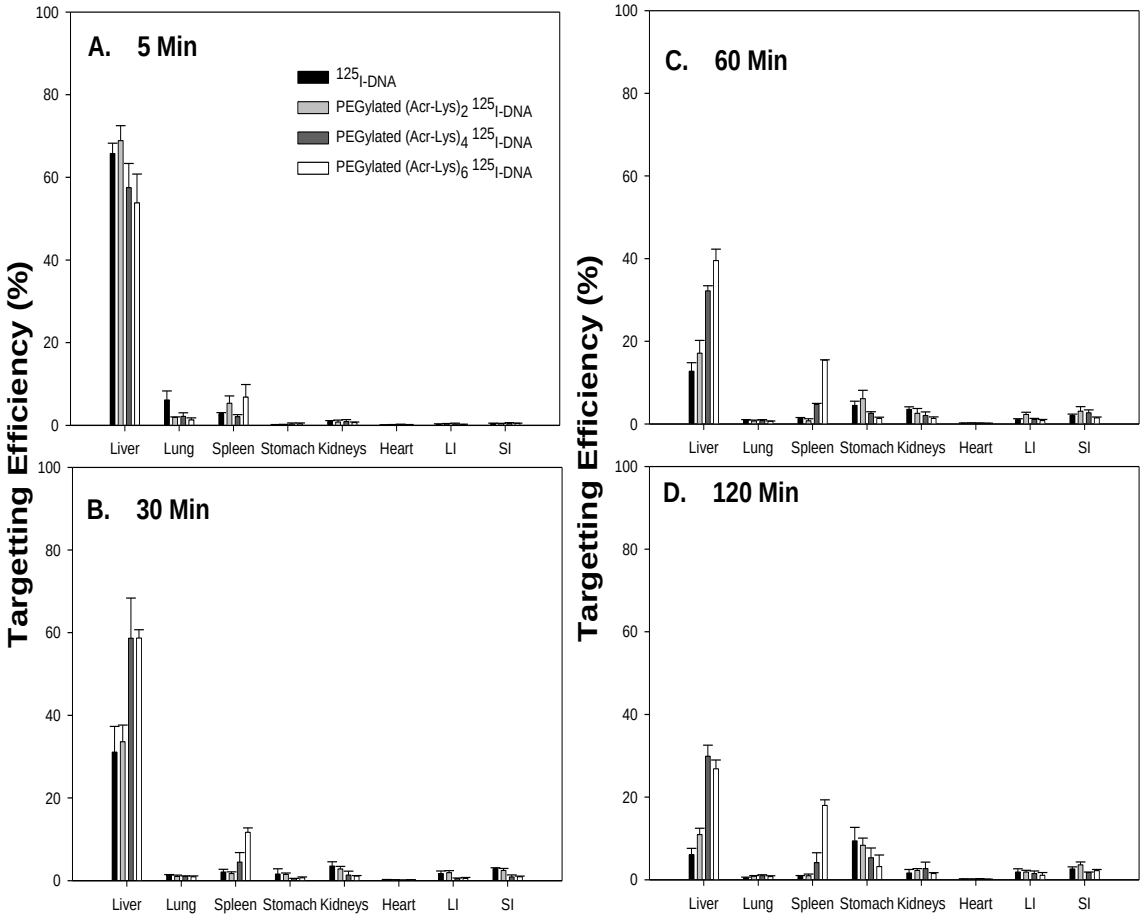

Figure 5-13 *Biodistribution of PEGylated Polyacridine DNA Polyplexes*. The biodistribution of PEGylated $(Acr\text{-}Lys)_2$, $(Acr\text{-}Lys)_4$, and $(Acr\text{-}Lys)_6$ ^{125}I-DNA polyplexes was determined and compared to the biodistribution of ^{125}I-DNA. The result identify the liver as the major organ of distribution for all formulations prepared, and furthermore demonstrate improved metabolic stability for both PEGylated $(Acr\text{-}Lys)_4$ and $(Acr\text{-}Lys)_6$ ^{125}I-DNA polyplexes in the liver. Biodistribution analysis was performed in collaboration with Sanjib Khargharia, Medicinal Chemistry and Natural Products, University of Iowa.

system and achieve significant in vivo gene expression following iv dosing, without the requirement of an additional stimulation. To accomplish this goal, an optimal polyacridine peptide would need to bind to DNA with sufficient affinity to protect from

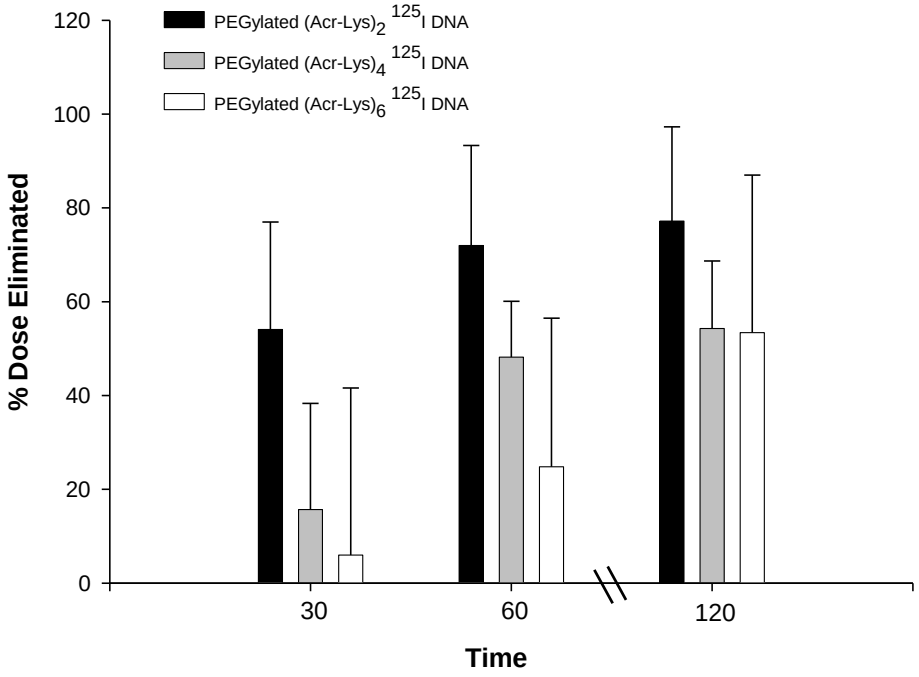

Figure 5-14. *Elimination of PEGylated Polyacridine DNA Polyplexes*. The elimination of PEGylated $(Acr\text{-}Lys)_2$, $(Acr\text{-}Lys)_4$, and $(Acr\text{-}Lys)_6$ ^{125}I-DNA polyplexes was determined using the data on Table 5-3. The result indicate that both PEGylated $(Acr\text{-}Lys)_4$ and $(Acr\text{-}Lys)_6$ stabilize the DNA from elimination for up to 30 minutes in systemic circulation. At 1 hour after administration, only the PEGylated $(Acr\text{-}Lys)_6$ DNA polyplexes remained below an elimination of 40%. These results along with the stimulated gene expression data for PEGylated $(Acr\text{-}Lys)_2$ (Figure 5-9) and $(Acr\text{-}Lys)_6$ (Figure 5-7B) DNA polyplexes suggest that the DNA in the blood and liver are responsible for the stimulated gene expression observed.

DNase metabolism in the circulation, while being able to release the DNA inside the cell to gain access to the nucleus.

It is likely there are many unique sequences of polyacridine peptides that accomplish this goal. The aim of the structure-activity study described was to determine a relationship between the number of Acr, the binding affinity for DNA, the polyplex pharmacokinetic half-life, and the magnitude of stimulated expression in mice. Initially, a

nine amino acid peptide allowed the incorporation of four Acr spaced by a hydrophobic (Leu), anionic (Glu), or cationic (Lys and Arg) residue, along with a C-terminal Cys for modification (Figure 4-1). Prior studies from our group established that spacing amino acids that lacked a bulky side-chain or protecting group (Gly or Ala) resulted in low peptide yields.[210] During the course of this study it was necessary to further optimize peptide yield to prepare $(Acr\text{-}Lys)_6$-Cys. While it is possible to prepare even longer polyacridine peptides of this design, we found the yields began to diminish. Each of the polyacridine peptides was coupled to PEG_{5000Da}, resulting in PEGylated polyacridine peptide that produced a single symmetrical peak on RP-HPLC and a MALDI-TOF MS that verified the structure (Figure 5-2).

The primary structural features that influence the level of gene expression mediated by PEGylated polyacridine peptides was the presence of at least four Acr residues combined with cationic (Lys or Arg) spacing amino acid (Figure 4-8A). PEGylated $(Acr\text{-}X)_n$ peptides possessing weak binding to DNA (Figure 4-3A and Figure 5-3A), result in no stimulated gene expression (Figure 4-8A and Figure 5-7), presumably due to the inability to protect DNA from metabolism in vivo. Conversely, PEGylated $(Acr\text{-}Arg)_4$, $(Acr\text{-}Lys)_4$, or $(Acr\text{-}Lys)_6$ possessed higher affinity for binding with DNA (Figure 4-3A and Figure 5-3A), which correlated with their high stimulated gene expression (Figure 4-8A and Figure 5-7) due to their ability to stabilize DNA from premature metabolism in vivo (Figure 5-11 & Figure 5-12C and D).

PEGylated $(Acr\text{-}Lys)_6$ binds to DNA with higher affinity compared to all other peptides studied (Figure 5-3A). It also possessed an unusual zeta potential titration curve that produced anionic open-polyplexes at 0.2 nmols of peptide, which converted to cationic closed-polyplexes at 0.8 nmols and higher (Figure 5-4A and Figure 5-5B & D). The DNase stability afforded to PEGylated $(Acr\text{-}Lys)_6$ polyplexes at both 0.2 and 0.8 nmols of peptide (Figure 5-6C) resulted in equivalent, high-level stimulated gene expression at each stoichiometry from 0.2-0.8 nmols (Figure 5-9A). The greater affinity

also led to greater stimulated expression for longer delay times compared to PEGylated $(Acr\text{-}Arg)_4$ polyplexes (Figure 4-7B), such that following the administration of 1 μg of DNA, a 1 hour delayed stimulation produced high-level gene expression, and at 2 hour delay, measurable expression was still detected (Figure 5-9B). These results established that PEGylated $(Acr\text{-}Lys)_6$ polyplexes mediated equal gene expression as either closed or open-polyplex structures, and suggest that enhanced binding affinity translates to higher expression at longer delay times due to postponing metabolism.

Pharmacokinetic and biodistribution studies were used to gain insight into the underlying mechanism of how delayed hydrodynamic stimulation caused PEGylated $(Acr\text{-}Lys)_6$ polyplexes to mediate gene expression in the liver. The most striking result was the apparent long pharmacokinetic half-life of PEGylated $(Acr\text{-}Lys)_4$ and PEGylated $(Acr\text{-}Lys)_6$ polyplexes, compared to the rapid loss of ^{125}I-DNA and PEGylated $(Acr\text{-}Lys)_2$ polyplexes (Figure 5-11A). Electrophoretic analysis of the ^{125}I-DNA recovered from blood clearly established that PEGylated $(Acr\text{-}Lys)_6$ stabilized DNA in the circulation for 2 hrs (Figure 5-12D), whereas PEGylated $(Acr\text{-}Lys)_4$ stabilized open circular DNA bands for at least 30 min (Figure 5-12C), and PEGylated $(Acr\text{-}Lys)_2$ for no more than 20 min (Figure 5-12B). Most importantly, approximately 40% of the radioactive dose remained in the blood after 2 hrs when dosing PEGylated $(Acr\text{-}Lys)_6$ ^{125}I-DNA polyplexes (Table 5-3), and the pharmacokinetic profile appears to be the same whether dosing anionic-open or cationic-closed polyplexes (Figure 5-11A).

These results cannot be directly compared with several prior studies that reported long circulating DNA or siRNA formulations by analyzing the pharmacokinetics of polyplexes by incorporating a fluorophore radiolabel into the carrier component.[222-225] Three prior studies are more closely related in their direct analysis of pharmacokinetics using radiolabeled DNA [226, 227] or by quantifying DNA in blood and tissues by PCR.[228] These reports establish the ability to extend the half-life of DNA in the circulation, but stop short of establishing the metabolic status of recovered DNA. This is the first study to

demonstrate stabilized plasmid DNA circulating in mice by gel electrophoresis and autoradiography. The metabolic stability of DNA is directly related to the mode and affinity of binding achieved by PEGylated $(Acr\text{-}Lys)_6$. A similar PEGylated polylysine peptide (PEG-Cys-Trp-Lys_{18}) also binds with high affinity to DNA through ionic interaction and forms cationic-closed polyplexes.[169] However, despite being a longer peptide than PEGylated $(Acr\text{-}Lys)_6$, PEG-Cys-Trp-Lys_{18} polyplexes rapidly dissociate following iv dosing leading to the complete metabolism of plasmid DNA in the circulation within 3 min.[82] Thereby, it is the combination of polyintercalation and cationic binding that appears to be essential to achieve DNA stability during circulation, whereas PEGylated peptides that bind DNA by either mode individually are insufficient. This unique feature suggests that PEGylated $(Acr\text{-}Lys)_6$ polyplexes may find application in targeting DNA to tissues outside the liver.

Analysis of the tissue distribution of ^{125}I-DNA polyplexes over time established the liver as the major site of distribution accounting for approximately 54-69% of the dose within the first 5 min, with only minor distribution to other organs (Figure 5-13). PEGylated $(Acr\text{-}Lys)_{4 \text{ and } 6}$ polyplexes produced a distinct liver distribution and metabolism profile, with maximal accumulation of 60% at 20 min followed by a decrease to 30% over two hrs (Figure 5-11A). The liver biodistribution profile of ^{125}I-DNA and PEGylated $(Acr\text{-}Lys)_2$ ^{125}I-DNA polyplexes were coincident with maximal accumulation of 65% at 5 min, followed by a decrease to 10% over 2 hrs (Table 5-3). The stability of plasmid DNA in the blood afforded by PEGylated $(Acr\text{-}Lys)_6$ appears to extrapolate to similar stability in the liver (Figure 5-11A &B).

The pharmacokinetic and biodistribution data support a hypothesis in which both the DNA that distributes to the liver and the DNA that remains in the blood are responsible for the stimulated expression. Nevertheless, the polyplexed DNA in both of these compartments must also be metabolically stabilized in order to mediate significant stimulated expression with delay times up to an hour. The hypothesis that both liver-

associated and DNA in the blood are responsible for stimulated expression is deduced by comparing the levels of stimulated expression from PEGylated $(Acr\text{-}Lys)_6$ polyplexes (Figure 5-9B) to the pharmacokinetic results (Figure 5-11A). Stimulated gene expression decreases by nearly 100-fold between 60 and 120 min, and yet the levels of DNA in the blood and liver drop by nearly identical quantities (16% and 13% respectively) during the same time frame (Table 5-3). Incorporating the elimination analysis (Figure 5-14) with the stimulated expression data suggests PEGylated $(Acr\text{-}Lys)_{2 \text{ and } 6}$ DNA polyplexes are no longer capable of transfecting the hepatocytes in the liver when 40% or greater of the ^{125}I-DNA dose has been eliminated. PEGylated $(Acr\text{-}Lys)_2$ fails to stimulate gene expression at a HD stimulation lag time of 30 minutes (Figure 5-7), which correlates with approximately 40% of the radiolabeled DNA dose remaining (60% elimination) in mice 30 min after administration (Figure 5-14). In contrast, PEGylated $(Acr\text{-}Lys)_6$ is capable of stimulating high levels of gene expression at 30 and 60 minutes (Figure 5-9B) which correlates with 90% and 80% of the dose remaining in the mice (Figure 5-14), respectively. It is only when the radiolabeled PEGylated $(Acr\text{-}Lys)_6$ DNA polyplex reaches over 40% elimination at 120 min after dosing (Figure 5-14) that the stimulated gene expression fails to achieve high levels of gene expression (Figure 5-9B). Assuming similar pharmacokinetic properties for PEGylated $(Acr\text{-}Arg)_4$ and $(Acr\text{-}Lys)_4$ DNA polyplexes would further correlate the observed inactivation of PEGylated $(Acr\text{-}Lys)_4$ DNA polyplexes at 60 min stimulation (Figure 4-7A) to a dose elimination slightly above 40% (Figure 5-14). Taken together, the data suggest that both the DNA in the liver and the blood are transported selectively into hepatocytes during hydrodynamic stimulation, and that all other mechanistic events thereafter remain similar to those seen using a direct hydrodynamic injection.[132]

In conclusion, this is the first report of high-level stimulated gene expression from a non-viral delivery system that mirrors the level of expression produced by the same dose administered by direct hydrodynamic dosing. The unique attributes of PEGylated

polyacridine peptides establish their ability to form open or closed polyplex structures that stabilize DNA from metabolism in mice and allow a stimulation of a high volume rapid dose of saline to complete the gene transfer, even after a 1 hour delay following the primary dose. This is still only a starting point toward the development of a non-viral delivery system that produces high level expression in animals without stimulation. However, given the modularity of polyacridine peptides, it should be possible to build multi-component gene delivery systems that drive the DNA further toward the nucleus, to ultimately achieve this aim.

CHAPTER 6: TARGETED POLYACRIDINE PEPTIDE DNA POLYPLEXES FOR HYDRODYNAMICALLY STIMULATED GENE EXPRESSION IN THE LIVER

Abstract

Multi-component DNA polyplexes are required for optimal pharmacokinetic properties and to achieve selective drug delivery to targeted cells. The minimum components required for efficient drug delivery are a masking agent for blood compatibility and a targeting moiety to achieve receptor-mediated endocytosis. Chapter 4 and 5 described the preparation of several polyacridine PEG-peptides with the general structure PEG-(Acr-X)$_n$, where X and n were optimized in order to achieve high affinity binding to DNA while maintaining reasonable sizes and surface charges for improved in vivo compatibility. The results determined that PEG-(Acr-Lys)$_6$ possessed the best overall in vivo properties for the preparation of targeted gene delivery.

The current chapter investigates multi-component systems for their ability to improve stimulated gene expression compared to non-targeted formulations. A triantennary glycopeptide was designed to incorporate the (Acr-Lys)$_6$-Cys peptide for high affinity binding to DNA and a triantennary N-glycan oligosaccharide for selective targeting to the asialoglycoprotein receptor (ASGP-R). The multi-component DNA polyplexes possessed particles sizes below 200 nm in diameter and neutral surface charges when prepared with 30% Tri-(Acr-Lys)$_6$. The stimulated in vivo gene expression was determined using bioluminescence imaging (BLI) and the results demonstrate a slight influence of Tri-(Acr-Lys)$_6$ on gene expression when iv dosed DNA was stimulated at 2 or 5 min after dosing. Nevertheless, no significant improvement is determined for multi-component polyplexes prepared with Tri-(Acr-Lys)$_6$ regardless of the percent of targeting peptide included, or the lag time between iv administration and HD stimulation.

Introduction

The development of targeted DNA formulations for in vivo applications have been limited due to the complications associated with engineering DNA polyplexes or lipoplexes that are compatible with iv administration routes. Previous peptide-based targeted formulations have failed to mediate gene expression due to their inability to protect DNA in circulation or due to the inability to release the DNA once internalized.[168, 229] Improving gene transfer and cell specificity requires multi-component systems that can incorporate a PEG layer to limit detection by the reticuloendothelial system (RES) and simultaneously possess a targeting ligand that can protrude across the PEG coating for efficient recognition by the cell surface receptor.

The asialoglycoprotein receptor (ASGP-R) is a cell surface receptor expressed on hepatocytes that can improve cell entry by receptor-mediated endocytosis. The ASGP-R is composed of three subunits that recognize non-reducing end galactose or N-acetyl galactosamine (GalNac).[230, 231] The affinity and selectivity of targeting ligands for cell receptors is dependent on monosaccharide specificity as well in differences in the topology of the receptors that require specific spatial arrangements between monosaccharides for efficient binding to the receptor.[168] The galactose-terminated triantennary N-glycan oligosaccharide is a highly specific ligand for the ASGP-R that binds with high affinity and can be prepared from bovine feutin in high yields.[232] Several gene delivery systems targeting hepatocytes have been developed using triantennary N-glycan, and high selectivity for DNA nanoparticles to the ASGP-R has been demonstrated using DNA condensing peptides.[229]

The present chapter introduces multi-component DNA polyplexes based on the $(Acr\text{-}Lys)_6$-Cys backbone peptide that is conjugated with either a PEG maleimide of 5000 Da, as demonstrated in chapter 5, or to an N-linked triantennary oligosaccharide via the cysteine residue of the polyacridine peptide. The PEGylated polyacridine peptide was designed to prepare DNA polyplexes with a long pharmacokinetic half-life and

preferential biodistribution to the liver, while the triantennary glycopeptide, Tri-(Acr-Lys)$_6$, was designed for selective targeting of the DNA polyplex to the ASGP-R. The objective in this chapter was to prepare multi-component DNA polyplexes that include a PEG for stealthing the polyplex, and a triantennary N-glycan for mediating efficient cell entry. The results in this section demonstrate the ability to form targeted DNA polyplexes for gene delivery to the liver that are blood compatible, but that require optimization for efficient gene delivery.

Materials and Methods

Unsubstituted Wang resin, 9-hydroxybenzotriazole, Fmoc-protected amino acids, O-(7-Azabenzo-triazol-1-yl)-N,N,N',N'-tetramethylurionium hexafluorophosphate (HATU), Fmoc-Lysine-OH, and N-Methyl-2-pyrrolidinone (NMP) were obtained from Advanced Chemtech (Lexington, KY). N,N-Dimethylformamide (DMF), trifluoroacetic acid (TFA), and acetonitrile were purchased from Fisher Scientific (Pittsburgh, PA). Diisopropylethylamine, piperidine, acetic anhydride, Tris(2-carboxyethyl)-phosphine hydrochloride (TCEP), 9-chloroacridine and thiazole orange were obtained from Sigma Chemical Co. (St. Louis, MO). Agarose was obtained from Gibco-BRL. mPEG-maleimide was purchased from Laysen Bio (Arab, AL). D-Luciferin and luciferase from *Photinus pyralis* were obtained from Roche Applied Science (Indianapolis, IN). pGL3 control vector, a 5.3 kb luciferase plasmid containing a SV40 promoter and enhancer, was obtained from Promega (Madison, WI). pGL3 was amplified in a DH5α strain of *Escherichia coli* and purified according to manufacturer's instructions.

Synthesis and Characterization of (Acr-Lys)$_6$-Cys-Peptide

9-Phenoxyacridine and Fmoc-Lysine(Acridine)-OH were prepared as recently reported. [210, 211] The (Acr-Lys)$_6$-Cys peptide was prepared by solid phase peptide synthesis on a 30 µmol scale on an APEX 396 Synthesizer using standard Fmoc procedures including 9-hydroxybenzotriazole and HATU activation while employing

double coupling of Fmoc-Lys(Acr)-OH and triple coupling for the spacing amino acid while using a 5-fold excess of amino acid over resin and omitting N-capping of truncated peptide species. The peptide was removed from resin and side chain deprotected using a cleavage cocktail of TFA/ethanedithiol/water (93:4:3 v/v/v) for 3 hrs followed by precipitation in cold ether. Precipitates were centrifuged for 10 min at 5000 x g at 4ºC and the supernatant decanted. $(Acr\text{-}Lys)_6$-Cys was then reconstituted with 0.1 v/v % TFA and purified to homogeneity on RP-HPLC by injecting 0.5-2 µmol onto a Vydac C18 semi-preparative column (2 x 25 cm) eluted at 5 mL per min with 0.1 v/v % TFA with an acetonitrile gradient of 20-30 v/v % over 30 min while monitoring acridine at 409 nm. The major peak was collected and pooled from multiple runs, concentrated by rotary evaporation, lyophilized, and stored at -20ºC. The purified peptide was reconstituted in 0.1 v/v % TFA and quantified by absorbance (acridine $\varepsilon_{409\ nm} = 9266\ M^{-1}\ cm^{-1}$ assuming additivity of ε for multiple acridines) to determine an isolated yield of 20%. Purified $(Acr\text{-}Lys)_6$-Cys peptides was characterized by LC-MS by injecting 2 nmol onto a Vydac C18 analytical column (0.47 x 25 cm) eluted at 0.7 ml per min with 0.1 v/v % TFA and an acetonitrile gradient of 10-55 v/v % over 30 min while acquiring ESI-MS in the positive mode. Synthesis of peptide was done in collaboration with Nicholas J. Baumhover, Medicinal and Natural Products Chemistry, University of Iowa.

Synthesis and Characterization of PEGylated $(Acr\text{-}Lys)_6$ Peptide

PEGylation of the Cys residue on $(Acr\text{-}Lys)_6$-Cys was achieved by reacting 1 µmol of peptide with 1.2 µmol of $PEG_{5000\ Da}$–maleimide in 4 mL of 10 mM ammonium acetate buffer pH 7 for 12 hrs at RT. The PEGylated peptide was purified by semipreparative HPLC as previously described and eluted with 0.1 v/v % TFA with an acetonitrile gradient of 25-65 v/v % acetonitrile while monitoring acridine at 409 nm. The major peak was collected and pooled from multiple runs, concentrated by rotary

evaporation, lyophilized, and stored at -20ºC. Counter-ion exchange was accomplished by chromatography on a G-25 column (2.5 x 50 cm) equilibrated with 0.1 v/v % acetic acid to obtain the peptide in an acetate salt form. The major peak corresponding to the PEG-peptide eluted in the void volume (100 mL) was pooled, concentrated by rotary evaporation, and freeze-dried. The PEG-peptide was reconstituted in water and quantified by Abs_{409nm} to determine an isolated yield of 66%. PEGylated $(Acr\text{-}Lys)_6$ was characterized by MALDI-TOF MS by combining 1 nmol with 10 μL of 2 mg per mL α-cyano-4-hydroxycinnamic acid (CHCA) in 50 v/v % acetonitrile and 0.1 v/v % TFA. Samples were spotted onto the target and ionized on a Bruker Biflex III Mass Spectrometer operated in the positive ion mode. Synthesis performed in collaboration with Nicholas J. Baumhover, Medicinal and Natural Products Chemistry, University of Iowa.

Synthesis and Characterization of $(Acr\text{-}Lys)_6$ Cys-Triantennary Glycopeptide

Glycosylation of the Cys residue on $(Acr\text{-}Lys)_6$-Cys was achieved by reaction of 1 mole of iodoacetamide-triantennary N-glycan (I-TRI) with 1.125 mol of $(Acr\text{-}Lys)_6$-Cys in 5 mL of 100 mM Tris buffer pH 8 for 12 hrs at RT. The polyacridine glycopeptide was purified by semipreparative HPLC and eluted with 0.1 v/v % TFA with an acetonitrile gradient of 15-30 v/v % acetonitrile at 8 mL/min while monitoring acridine at 409 nm. The major peak was collected and pooled from multiple runs, concentrated by rotary evaporation, lyophilized, and stored at -20ºC. Counterion exchange was accomplished and reconstituted in water and quantified by Abs_{409nm} to determine isolated yield. The glycopeptide was characterized by LC-MS by injecting 1 nmol and eluted 0.7 ml per min with 0.1 v/v % TFA and an acetonitrile gradient of 10-40 v/v % over 30 min while acquiring ESI-MS in the positive mode. Synthesis performed in collaboration with Nicholas J. Baumhover, Medicinal and Natural Products Chemistry, University of Iowa.

Characterization of Multi-Component Polyacridine Peptide DNA Polyplexes

The relative binding affinity of PEGylated $(Acr\text{-}Lys)_6$ and Tri-$(Acr\text{-}Lys)_6$ for DNA was determined by a fluorophore exclusion assay [16]. pGL3 (200 μl of 5 μg/ml in 5 mM HEPES pH 7.5 containing 0.1 μM thiazole orange) was combined with 0, 0.2, 0.3, 0.4, 0.5, or 1 nmol PEGylated $(Acr\text{-}Lys)_6$ or Tri-$(Acr\text{-}Lys)_6$ peptide in 300 μl of HEPES and allowed to bind at RT for 30 min. Thiazole orange fluorescence was measured using an LS50B fluorometer (Perkin-Elmer, U.K.) by exciting at 498 nm while monitoring emission at 546 nm with the slit widths set at 10 nm. A fluorescence blank of thiazole orange in the absence of DNA was subtracted from all values before data analysis. The data is presented as nmol of PEGylated polyacridine peptide per μg of DNA versus the percent fluorescence intensity ± the standard deviation determined by three independent measurements.

The particle size and zeta potential were determined by preparing 2 mL of polyplex in 5 mM HEPES pH 7.5 at a DNA concentration of 30 μg per mL. Multi-component DNA polyplex were prepared by admixing Tri-$(Acr\text{-}Lys)_6$ at 0, 10, 20, 30, 40, and 50 % with PEG-Mal-$(Acr\text{-}Lys)_6$ peptide at stoichiometry of 0.2 nmol per ug of DNA. The particle size was measured by quasi-elastic light scattering (QELS) at a scatter angle of 90º on a Brookhaven ZetaPlus particle sizer (Brookhaven Instruments Corporation, NY). The zeta potential was determined as the mean of ten measurements immediately following acquisition of the particle size.

Hydrodynamic Stimulation and Bioluminescence Imaging of Multi-Component DNA Polyplexes

Mice were dosed via tail vein with 1 μg of PEGylated polyacridine polyplex or of multi-component polyacridine polyplexes in 50 μL of HBM (5 mM HEPES, 0.27 M mannitol, pH 7.4). At times ranging from 2-10 minutes after iv dosing, a stimulatory

hydrodynamic dose of normal saline (9% wt/vol of the body weight) was administered over 5 seconds. At 24 hrs post-DNA dose, mice were anesthetized by 3% isofluorane, then administered an ip dose of 80 μL (2.4 mg) of D-luciferin (30 μg/μL in phosphate-buffered saline). At 5 min following the D-luciferin dose, mice were imaged for bioluminescence (BLI) on an IVIS Imaging 200 Series (Xenogen). Images were acquired at a 'medium' binning level and a 20 cm field of view. Acquisition times were varied (1 sec - 1 min) depending on the intensity of the luminescence. The Xenogen system reported bioluminescence as photons/sec/cm^2/seradian in a 2.86 cm diameter region of interest covering the liver. The integration area was transformed to pmols of luciferase in the liver using a previously reported standard curve. [213] In collaboration with Jason Duskey, Medicinal and Natural Products Chemistry, University of Iowa.

Results

The preparation of targeted DNA polyplexes that can enter a specific cell type requires a long pharmacokinetic half-life and a targeting moiety with high selectivity for that respective receptor in order to avoid non-specific cellular uptake. Previous chapters focused on the preparation of PEGylated DNA polyplex that can improve the pharmacokinetic properties of DNA. The optimal peptide backbone developed for DNA delivery was identified in chapter 5 to be the (Acr-Lys)$_6$-Cys peptide. A PEG of 5000 Da was incorporated onto the polyacridine peptide, and the resulting PEGylated (Acr-Lys)$_6$ peptide (Figure 6-1) showed optimal DNA binding, nuclease stability, improved pharmacokinetic properties, and the ability to mediate high levels of stimulated gene expression.

The next priority toward the development of efficient gene delivery systems is to incorporate a targeting component onto the polyplex in order to provide receptor-mediated endocytosis into to the cells of interest. The asialoglycoprotein receptor (ASGP-R) is a type II C-type lectin on the surface of hepatocytes that mediates efficient

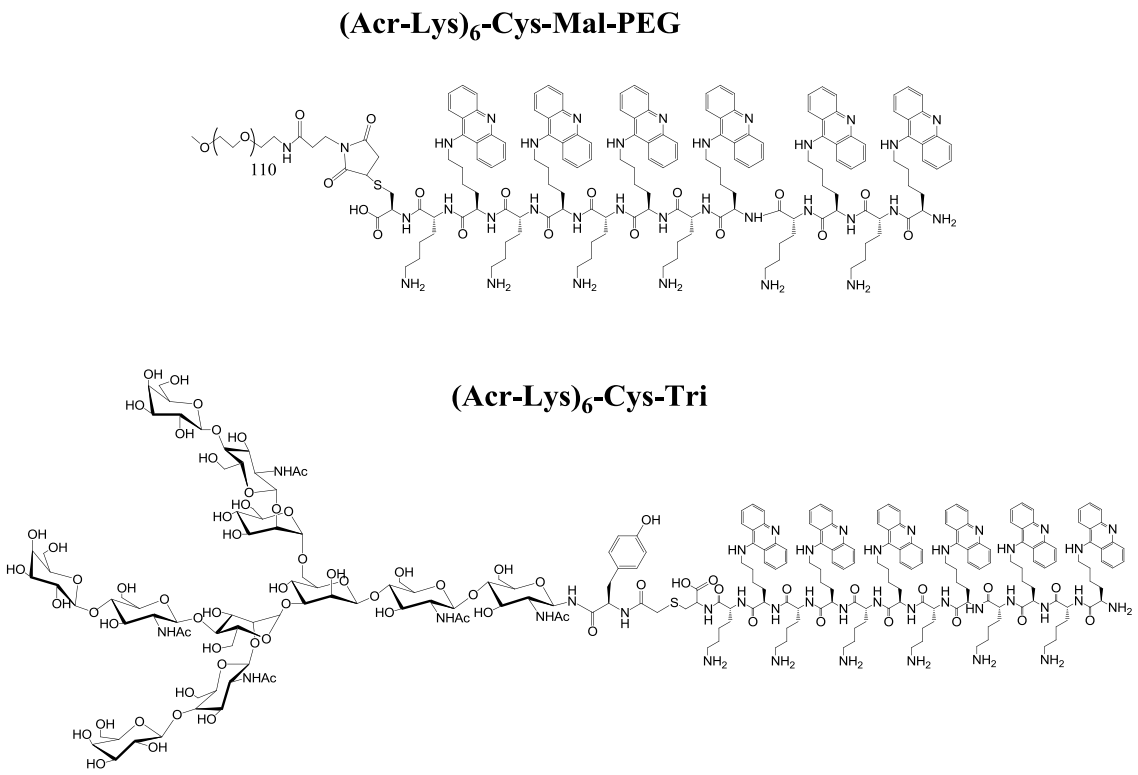

Figure 6-1. *Structure of Tri and PEG-Mal-(Acr-Lys)$_6$ Peptides for Targeted Gene Delivery*. The structure of PEG-Mal-(Acr-Lys)$_6$ and Tri-(Acr-Lys)$_6$ is illustrated. A PEG maleimide of 5000 Da was used to protect against nuclease degradation and a triantennary N-glycan was used to target the asialoglycoprotein receptor in the hepatocytes of the liver. In collaboration with Nicholas J. Baumhover, Medicinal and Natural Products Chemistry, University of Iowa.

endocytosis and naturally binds N-glycans.[233-235] Additionally, galactose terminated triantennary oligosaccharides has been previously shown to bind with selectively and high affinity to the ASGP-R in vivo.[235] Therefore, a triantennary glycopeptide (Figure 6-1) was prepared that binds to DNA by the (Acr-Lys)$_6$ peptide backbone, yet possesses a large targeting ligand that can protrude from the PEG layer and bind to the ASGP-R receptor on hepatocytes.

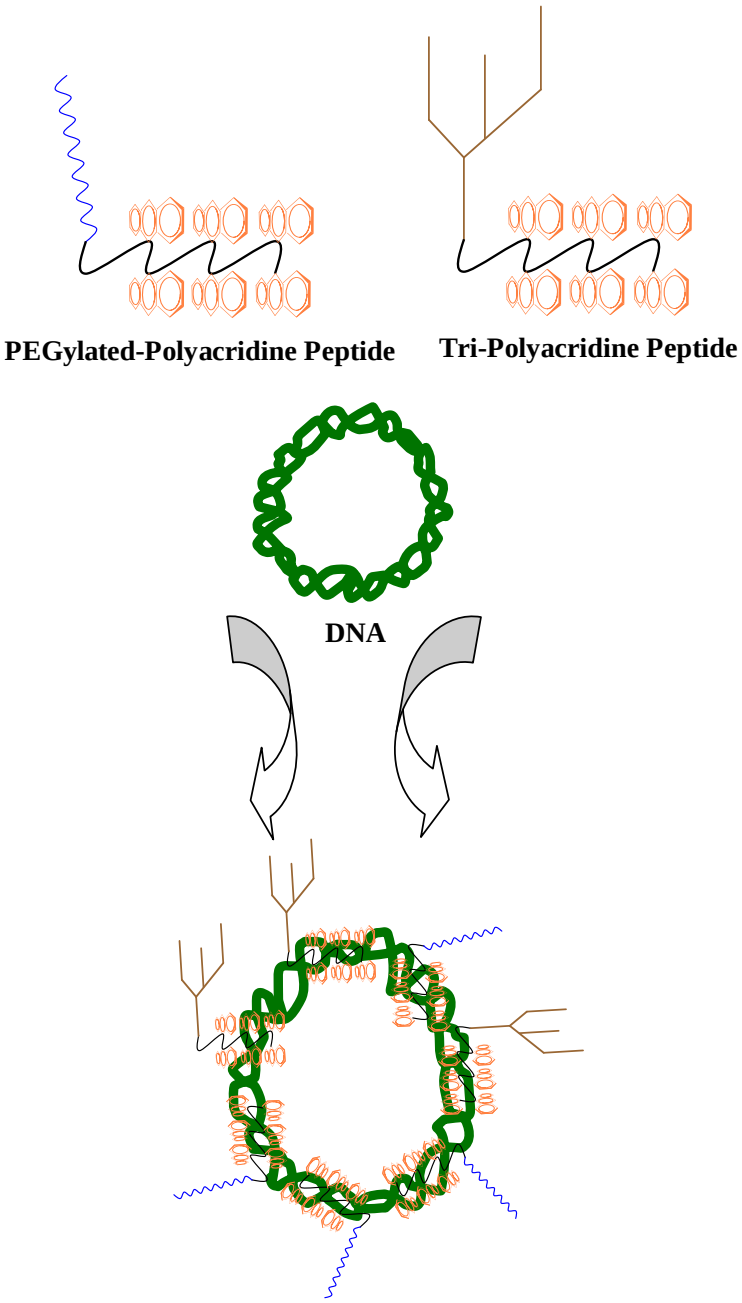

Figure 6-2. *Preparation of Multi-Component DNA Polyplex for In Vivo Gene Delivery.* Multi-component DNA polyplexes are prepared by admixing PEGylated (Acr-Lys)$_6$ and Tri-(Acr-Lys)$_6$ peptides at different ratios to yield PEGylated DNA polyplexes that are resistant to nuclease metabolism and that target the asialoglycoprotein receptor on the surface of hepatocytes.

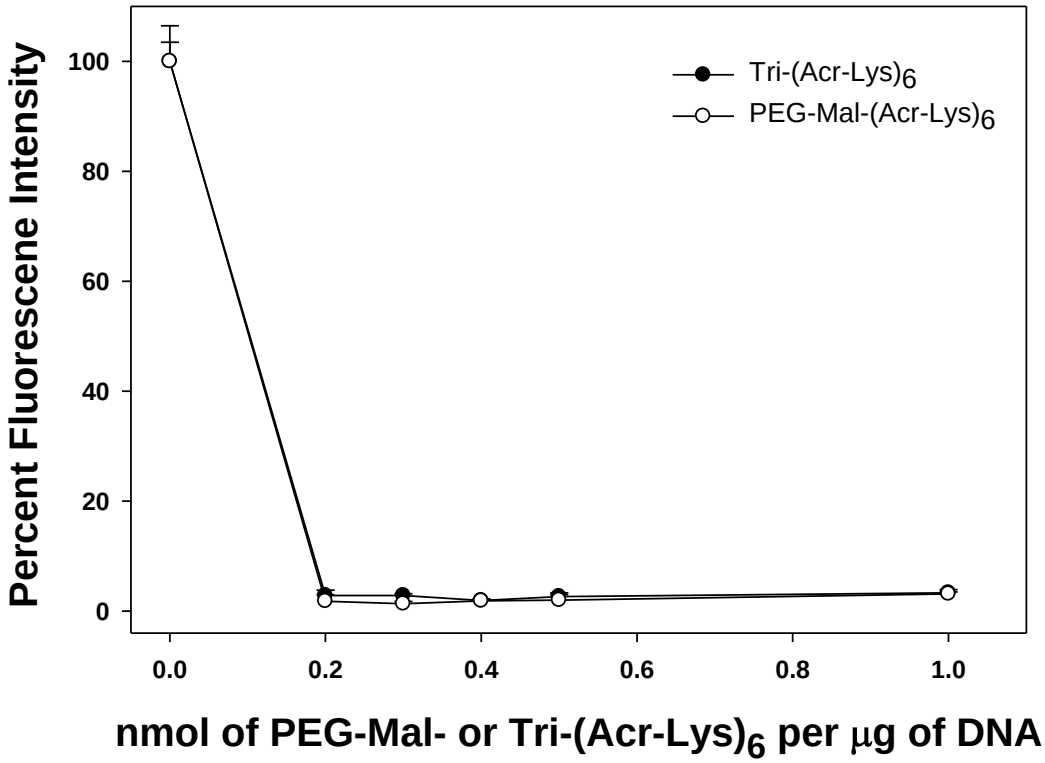

Figure 6-3. *Relative Binding Affinity of PEG-Mal-(Acr-Lys)$_6$ and Tri-(Acr-Lys)$_6$.* The thiazole orange displacement assay was used to compare the relative binding affinities of PEG-Mal-(Acr-Lys)$_6$ (-○-) and Tri-(Acr-Lys)$_6$ (-●-). Polyacridine peptides were titrated from 0 to 1 nmol into a solution containing1 μg of DNA and 0.1 μM thiazole orange. The results determine that both PEG-Mal-(Acr-Lys)$_6$ and Tri-(Acr-Lys)$_6$ possess similar binding affinities for DNA, which suggest that multifunctional polyplexes can be prepared a various ratios of each peptide.

Multi-component gene delivery systems are needed to maintain a long pharmacokinetic half-life while simultaneously targeting a specific cellular receptor. Multi-component polyacridine gene delivery systems were prepared by admixing different ratios of PEGylated and Tri (Acr-Lys)$_6$ (Figure 6-2). Incorporating the

polyacridine peptides onto the DNA requires both to possess similar binding affinities for DNA. Therefore, the thiazole orange displacement assay was used, as previously, to

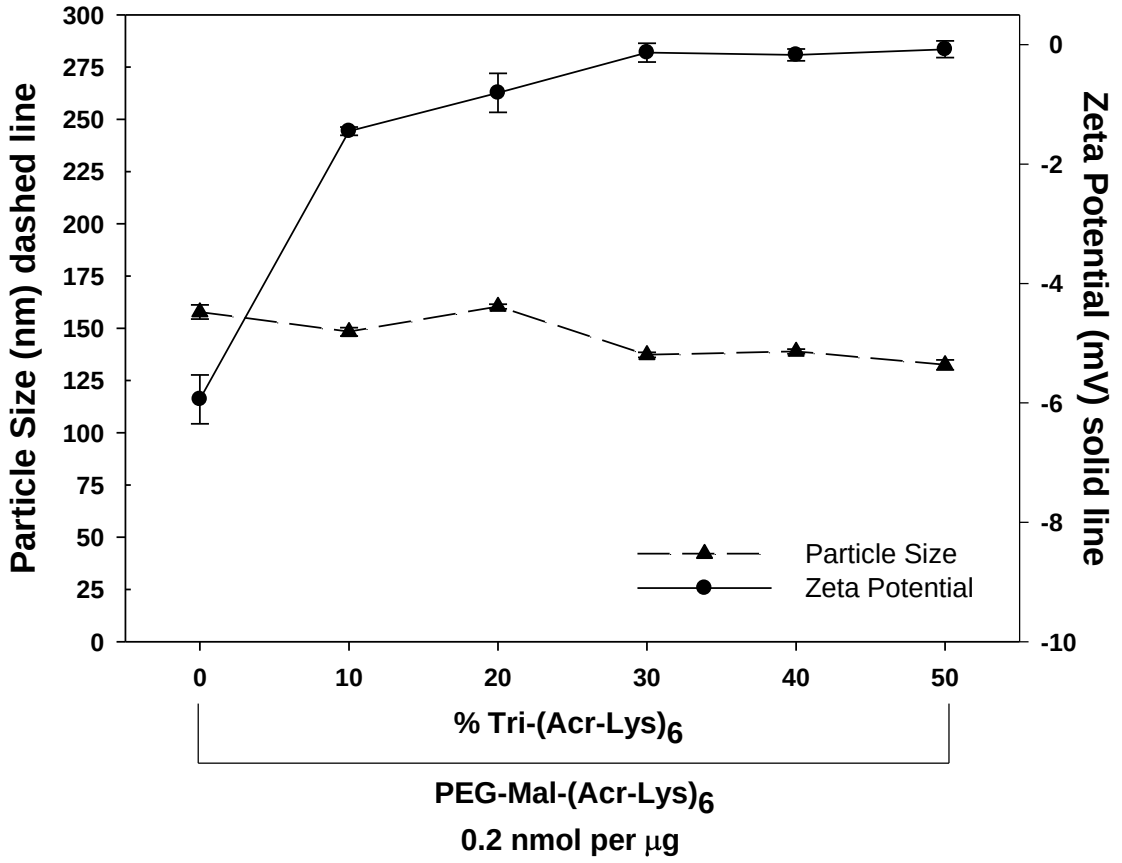

Figure 6-4. *Particle Size and Zeta Potential of Multi-Component Polyacridine PEG-Peptides.* The particle size (-▲-) and zeta potential (-●-) of multi-component DNA polyplexes was determined with 0.2 nmol of PEGylated $(Acr\text{-}Lys)_6$ at various percentages of Tri-$(Acr\text{-}Lys)_6$. The results suggest that Tri-$(Acr\text{-}Lys)_6$ binds with PEG-Mal-$(Acr\text{-}Lys)_6$ up to 30% and forms multi-component polyplexes with a surface charge approaching zero and particle sizes below 200 nm.

confirm high affinity binding to DNA by Tri-$(Acr\text{-}Lys)_6$ (Figure 6-3). The results verify that both polyacridine peptides bind to DNA with equal affinity and therefore, both should be capable of forming multi-component delivery systems.

In order to characterize the binding of the peptides and the physical properties of the multi-component DNA polyplexes, the particle size and zeta potential was measured at various percentages of Tri-$(Acr\text{-}Lys)_6$ and PEGylated $(Acr\text{-}Lys)_6$ (Figure 6-4). The results indicate that there is no significant change in the size of polyplex even when 50% of the multi-component system consists of Tri-$(Acr\text{-}Lys)_6$ peptide. In contrast, an increase in the zeta potential is observed from approximately -6 mV at 0% Tri-$(Acr\text{-}Lys)_6$ to an asymptotic value of 0 mV at or above 30%. The change in the surface charge of the polyplex upon binding confirms the formation of multi-component DNA polyplexes, and suggest that maximum binding of the targeting peptide occurs at 30% Tri-$(Acr\text{-}Lys)_6$. Furthermore, the neutral surface charges observed and the stability in particle size upon binding indicates that the polyplexes should possess similar in vivo properties to that of polyplexes prepared with only PEGylated $(Acr\text{-}Lys)_6$.

The stimulated in vivo gene expression of multi-component DNA polyplexes was determined by administering 1 μg of DNA polyplexed with 0.2 nmol of PEGylated $(Acr\text{-}Lys)_6$ at either 0, 10, or 20% Tri-$(Acr\text{-}Lys)_6$ in 50 μL of HBM (5 mM HEPES, 0.27 M mannitol, pH 7.4). Luciferase expression was stimulated at 2, 5, or 10 minutes following the initial iv dose with a hydrodynamic injection of normal saline (Figure 6-5). The data indicates that an increase in gene expression is only observed at HD stimulations of five minutes. The gene expression levels for polyplexes prepared with 10% Tri-$(Acr\text{-}Lys)_6$ demonstrated a 1.6-fold increase compared to formulations with no Tri, whereas polyplexes prepared with 20% Tri showed a 2.3 fold increase in luciferase expression. However, a slight drop in gene expression is seen when HD stimulation is extended out to 10 minutes, and this observation is exacerbated at HD stimulations of 30 minutes (data

not shown). These results indicate that there is no clear advantage of incorporating Tri-$(Acr\text{-}Lys)_6$ onto the DNA polyplex for stimulated gene expression.

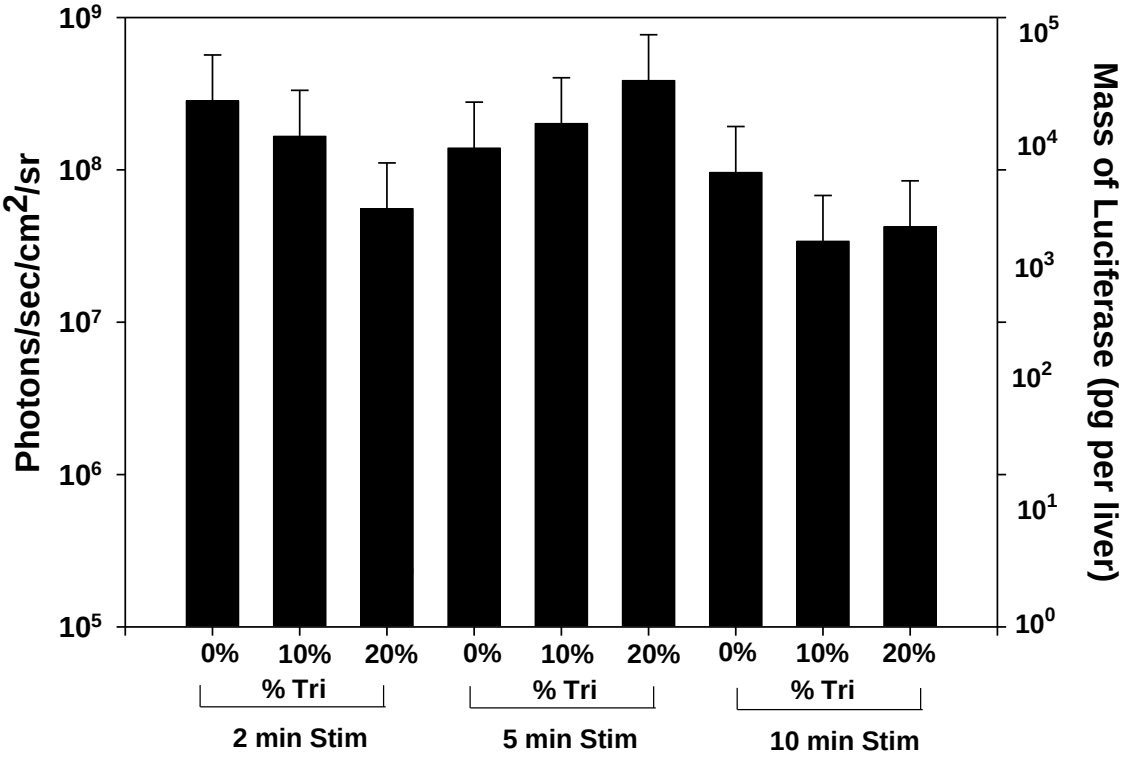

Figure 6-5. *Stimulated In Vivo Gene Transfer Efficiencies of Multi-Component DNA Polyplexes.* The luciferase expression was determined for iv dosed multi-functional DNA polyplexes (1 μg) prepared with 0.2 nmol of PEGylated $(Acr\text{-}Lys)_6$ at various percentages of Tri-$(Acr\text{-}Lys)_6$ followed by an HD stimulation at either 2, 5, or 10 min after administration. The results indicate that there was no influence of triantennary N-glycan on stimulated gene expression. Formulation administration was performed in collaboration with Jason Duskey, Medicinal and Natural Product Chemistry, University of Iowa.

Discussion

PEGylated $(Acr\text{-}Lys)_6$ DNA polyplexes were shown to protect DNA from nuclease metabolism in the blood (Figure 5-10) and maintain DNA transfection competent for up to two hours after iv administration (Figure 5-8). Pharmacokinetic and

biodistribution analysis revealed that over 50% of iv dosed DNA remains compartmentalized either in the blood or liver two hours post administration (Table 5-3). Nevertheless the absence of a stimulatory HD injection of normal saline results in no gene expression. Prior published dose response curves coupling bioluminescence imaging (BLI) and HD DNA delivery determines that the lower limit of detection for BLI corresponds to 100 pg of luciferin at dose of 0.1 ng of DNA.[213] Therefore, considering that a 1 μg iv dose of DNA fails to produce even this minimum of expression, the dose response curve suggests that the delivery system fails to introduce even 0.01% of the administered DNA into hepatocytes.

In order to improve on the inefficiency of gene delivery, targeting ligands have been incorporated onto the polyacridine-based gene delivery system in this chapter to improve receptor-mediated endocytosis. Selection of the targeting ligand for improved gene delivery to the liver is based on the ASGP-R expressed on the surface of hepatocytes. This receptor is composed of a cluster of three carbohydrate recognition domains (CRD) that bind simultaneously to three galactose residues on a single triantennary N-glycan.[236] While a single galactose residue binds to the receptor with modest affinity, including three galactose residues creates a cluster effect that boost the affinity of the ligand to nM dissociation constants.[237] Furthermore, this targeting ligand has been used in the development of several gene delivery systems,[82, 119, 168, 238] and it has demonstrated 80% targeting selectivity of DNA nanoparticles to hepatocytes via the ASGP-R while requiring low copies of the ligand (2 mol%).[82]

The Tri-$(Acr\text{-}Lys)_6$ prepared possessed a similar binding affinity for DNA compared to PEGylated $(Acr\text{-}Lys)_6$ (Figure 6-3), and therefore it is possible to create multi-component DNA polyplexes that possessed both a PEG component to protect DNA form nuclease attack in circulation, and a target ligand to mediate efficient cell entry upon biodistribution to the liver (Figure 6-2). Characterization of multi-component polyplexes was achieved by monitoring the particle size and zeta potential of the

polyplexes at various percentages of PEG and Tri-(Acr-Lys)$_6$. The data indicate that efficient binding of Tri-(Acr-Lys)$_6$ to DNA is detected up to a targeting composition of 30% of the total peptide.

In vivo formulations were, therefore, prepared at either 0, 10, or 20% Tri-(Acr-Lys)$_6$. While the triantennary oligosaccharide has previously shown to have strong affinity and selectivity for the ASGP-R, the stimulated in vivo data did not show any improvement of luciferase expression when incorporating the targeting ligand. At 2 minute stimulations, a negative effect on gene expression was observed that was dependent on the percent of Tri-(Acr-Lys)$_6$ on the polyplex (Figure 6-5, 2 min Stim). These results could indicate that the polyplex was bound to the surface of hepatocytes, but failed to internalize properly upon hydrodynamic injection. In contrast, at 5 minute stimulations the opposite trend is observed in the data and this indicates that the DNA has been internalized and compartmentalized to lysosome, but remains stable and available for transfection (Figure 6-5, 5 min Stim). Upon stimulation at 10 minutes, no apparent trend is observed in the results, as both 10% and 20% Tri-(Acr-Lys)$_6$ formulations possess similar expression levels, and both are lower than the formulation with no Tri-(Acr-Lys)$_6$. This may indicate that both formulations have endured similar extents of lysosomal degradation, and the gene expression observed may be more representative of gene transfer mediated by the DNA in the blood, rather than by liver associated DNA.

Initial expectations of multi-component polyacridine delivery systems were based on the hypothesis that improving the amount of DNA associated on the surface or within the hepatocytes of the liver would lead to improved luciferase expression. Determining the factors that led to the discoveries presented in this chapter is rather challenging. Delivery may be impeded by the size limitations of the liver endothelium (100 nm).[61], or perhaps the high affinity of the Tri-(Acr-Lys)$_6$ targeting glycopeptide for the ASGP-R leads to rapid lysosomal degradation. In order to clarify the targeting capabilities of PEG and Tri-(Acr-Lys)$_6$ multi-functional polyplexes, a separation of parenchymal and non-

parenchymal cells following iv dosing of radiolabeled DNA polyplexes is required. Alternatively, siRNA delivery using polyacridine gene delivery systems may produce smaller polyplexes that are more suitable for crossing the liver fenestration, and furthermore, siRNA polyplexes will no longer require delivery to the nucleus of the target cells.

CHAPTER 7: POLYACRIDINE PEG-PEPTIDE GENE DELIVERY SYSTEMS FOR THE IN VIVO DELIVERY OF PLASMID DNA: A REVIEW OF THE RESULTS

Molecular Conjugates for IM-EP

Reviewing past literature on IM-EP gene delivery systems reveals that no DNA binding carrier has been developed that can improve the in vivo gene expression efficiencies observed when dosing naked, unpackaged DNA. Many polymers, lipids, and peptides fail to efficiently deliver DNA inside cells during electroporation due to aggregation at the cell surface or to poor transport under the applied electric field. Developing DNA formulations for IM-EP administration would be beneficial in order to protect the DNA from nuclease degradation within the cell or tissue, and to perhaps provide controlled-release properties that could be advantageous therapeutically.

It was hypothesized that anionic formulations would be more compatible with IM-EP administration considering that naked DNA is anionic and achieves high gene transfer with IM-EP. Generally, there are two ways of improving gene expression using a delivery system for IM-EP. The first would be to improve the transport of DNA during electroporation in order to deliver more DNA into the cell. The second would be to protect the DNA that is transported during electroporation from nuclease degradation since DNA is susceptible to metabolism by DNases while in the tissue prior to electroporation and after electroporation within the cell. Both strategies would lead to higher expression levels at lower doses.

Two general strategies were sought to improve gene expression. The first approach was to condense DNA using a PEGylated Cys-Trp-Lys_{18} peptide that had demonstrated the ability to prevent aggregation of DNA nanoparticles and reduced surface charges (~ 25 mV to 10 mV) compared to Cys-Trp-Lys_{18} peptide (no PEG).[19] While improving gene transfer using PEGylated Cys-Trp-Lys_{18} was anticipated, the DNA

nanoparticles possessed expression levels 10-fold lower than that of naked DNA. However, the DNA nanoparticles showed better persistence of initial gene expression by over 25% compared to naked DNA. The result led us to investigate two additional modifications of PEGylated DNA nanoparticles that were presented in chapter 3. The first was to improve the release properties of DNA from the polyplex within the cell by incorporating a reducible disulfide bond between the polymer and the peptide, and the second was to cross-link the PEGylated DNA nanoparticle to form anionic DNA polyplexes that simultaneously improve the metabolic stability of the polyplex. The reducible linkage had been determined to be a beneficial component of a PEGylated DNA polyplex prior in vitro,[169] but it failed to improve gene expression following IM-EP. Upon reduction with TCEP, it was discovered that these DNA nanoparticles considerably increased in size, suggesting that perhaps reduction was occurring prematurely thus impeding gene delivery and expression.

Cross-linked nanoparticles, likewise, failed to improve gene expression. Previous studies within our group had suggested that DNA release could be jeopardized after cross-linking,[82] but it was believed that incorporating cross-linking with IM-EP would improve cell entry and lead to sustained gene expression. Nevertheless, cross-linking resulted in a sharp drop in gene expression in comparison to non-cross-linked formulations, thus confirming the suspicion that DNA release was compromised upon cross-linking. These experiments did, however, disprove the theory that gene delivery using nanoparticles was inhibited during electroporation due to the small sizes of the pores that form under an electric field. Rather, the evidence suggests that improving electrophoresis and avoiding aggregation are the most important parameters to consider for improving gene delivery systems for IM-EP.

The second general strategy used to improve IM-EP involved polyacridine PEG-peptides that bound to DNA by intercalation and formed anionic open DNA polyplexes. The affinity of the peptides was found to be dependent on the units of acridine

incorporated onto the peptide, and the results determined that at least five (Lys-Acr) units were required for high affinity binding (Figure 2-10A) which also correlated with improved nuclease stability. The PEG-Mal-Cys-Trp-$(Lys(Acr))_5$ peptide was capable of mediating high levels of gene expression that were nearly identical to that of naked DNA, and expression was shown to be dependent on the stoichiometry of peptide used for preparation (Figure 2-14). The data suggested that the peptide prepared at 2 nmol per μg of DNA was able to provide improved nuclease stability, while higher ratios led to unstable formulations that resulted in lower gene expression. A similar analogue of this peptide, PEG-SS-Cys-Trp-$(Lys(Acr))_5$, was also investigated and it resulted in lower gene expression than the non-reducible counterpart, thus indicating that a disulfide linkage is generally incompatible with delivery via this administration route (Figure 3-11).

The combination of the results from both electroporation chapters defines key fundamental aspects that are necessary for future molecular conjugate design. Nuclease stability is necessary for improved gene expression, but the slight anionic charges observed at higher ratios of peptide are not optimal for electrophoretic transport during electroporation since the electrophoretic mobility of a polyplex is directly proportional to its charge and inversely proportional to size. Therefore, future conjugates should contain an anionic component that does not interfere with binding of the peptide to DNA, solely to improve electrophoresis during electroporation. Such strategies can be achieved by using heterobifunctional PEGs that can separate the DNA binding sequence of the peptide from the anionic head group.

In Vivo DNA Delivery to the Liver Using Polyacridine PEG-Peptides

The conceptual design for the initial panel of polyacridine PEG-peptides that were developed were based on the results from the IM-EP experiments. The belief at the time

of design was that peptides were required to bind with high affinity to DNA, while forming anionic open-DNA polyplexes that were resistant against nuclease degradation. The initial parameters investigated by designing the PEG-Mal-$(Acr\text{-}X)_4$ peptides was the influence of a hydrophobic, cationic, or anionic spacing amino acid. Considering that our goal at the time was to create blood compatible DNA polyplexes, we believed that leucine spaced peptides would provide the best physical properties if polyintercalation provided a high enough affinity to prevent premature dissociation during transit. Surprisingly, not only did the leucine spaced peptide fail to mediate gene transfer, but the polyplexes formed at 1 nmol per μg of DNA possessed nearly neutral surface charges without the incorporation of cationic residues to neutralize the anionic phosphates of DNA. The results from chapter 4 further identified key components of successful delivery peptides. Surface charge seemed important to the fate of the polyplex, but binding affinity seemed to be the most important feature, as only PEG-Mal-$(Acr\text{-}X)_4$ peptides spaced with a lysine or arginine amino acid were capable of mediating high levels of stimulated gene expression (Figure 4-3A). Additionally, up to this point, all successful formulations consisted of open-DNA polyplex, thus we believed that the formation of cationic DNA nanoparticles were detrimental to delivery. The ability to maintain high levels of gene expression out to a stimulation time of 30 minutes was encouraging, but more information was needed to explain the failure of formulations without stimulation.

The third panel of polyacridine PEG-peptides was introduced to optimize the intercalation of the peptide to DNA. Given the results from chapter 4, we prepared PEG-Mal-$(Acr\text{-}Lys)_n$ peptides where n was varied to be either 2, 4, or 6. The initial surface charge for DNA polyplex prepared at 0.2 nmol per μg of DNA was dependent on n, thus, as expected, increasing the (Acr-Lys) chains lead to a higher binding affinity by increasing both intercalation and electrostatic interactions (Figure 5-4A). The relative binding affinities for the peptides was therefore $(Acr\text{-}Lys)_6 > (Acr\text{-}Lys)_4 > (Acr\text{-}Lys)_2$,

and surprisingly the $(Acr\text{-}Lys)_6$ peptide resulted in cationic surface charges at and above a stoichiometry of 0.4 nmol per μg of DNA (Figure 5-4A). This led us to believe that only polyplex prepared at 0.2 nmol per μg would be capable of mediating stimulated gene expression, especially considering that the gene transfer efficiencies at the highest stoichiometries evaluated for PEG-Mal-$(Acr\text{-}Arg/Lys)_4$ lead to a decrease in luciferase expression (Figure 4-8B). Nevertheless, nuclease stability was determined for polyplexes prepared with PEG-Mal-$(Acr\text{-}Lys)_6$ at both 0.2 and 0.8 nmol per μg, while PEG-Mal-$(Acr\text{-}Lys)_4$ only displayed clear stability at the higher ratio of 0.8 nmol per μg. Both PEG-Mal-$(Acr\text{-}Lys)_4$ DNA polyplexes prepared at 0.8 nmol per μg and PEG-Mal-$(Acr\text{-}Lys)_6$ DNA polyplexes at 0.2 nmol per μg possessed similar properties. Both had similar surface charges, particle sizes, morphology, and resistance to DNase degradation. Upon pharmacokinetic and biodistribution analysis using radiolabeled DNA, both formulations displayed similar blood concentration and liver accumulation profiles, thus suggesting that they would possess similar biological activities (Figure 5-11). Nevertheless, gel electrophoresis of the blood time collected from the pharmacokinetic analysis revealed that only the PEG-Mal-$(Acr\text{-}Lys)_6$ DNA polyplexes were stabilized throughout the analysis, thus providing evidence of superior DNA delivery potentials using this peptide (Figure 5-12).

The stimulated gene expression data was a quite surprising discovery. There was apparently no difference on stimulated gene expression between an anionic DNA open-polyplex and a cationic DNA nanoparticle that was prepared with PEG-Mal-$(Acr\text{-}Lys)_6$ (Figure 5-9A). Furthermore, PEG-Mal-$(Acr\text{-}Lys)_4$ DNA polyplexes required four times the amount of peptide to yield similar expression levels with HD stimulations at 30 minutes after iv administration (Figure 5-7). In contrast, only polyplexes prepared with PEG-Mal-$(Acr\text{-}Lys)_6$ were capable of mediating gene transfer at HD stimulations administered 1 hour after iv dosing, thus consistent with the stability suggested by the pk data.

It is difficult to explain the reason why gene expression failed without HD stimulation, but could be due to the rather large size of the polyplex relative to the fenestration size on liver endothelial. That would explain why there was no effect on stimulated gene expression when triantennary N-glycan was incorporated onto the polyplex at various ratios, but nevertheless, a thorough understanding can only be determined by separating the parenchymal and non-parenchymal cells after iv administration of radiolabeled formulations to determine if hepatocytes targeting was achieved.

Possible Toxicity of PEGylated Polyacridine Peptides

DNA intercalators have been of interest in the past due to their potential as chemotherapeutics. FDA approved intercalating drugs include doxorubicin, daunorubicin, and dactinomycin all of which also inhibit the DNA unwinding enzyme, topoisomerase.[239] The inhibition of topoisomerase has been linked to mutagenic properties and 9-aminoacridine, and several of its derivatives, are know frameshift mutagens.[240] However, Ferguson et al. demonstrated that simple mono-acridines lead to frameshifts in repetitive DNA sequences, whereas bis-acridines with higher binding affinities for DNA were not effective frameshift mutagens. Therefore, the properties of an intercalator that lead to mutagenesis are not completely understood, as no strong correlation has been established that links binding affinity, drug hydrophobicity, or DNA synthesis inhibition with toxicity.[241] Nonetheless, the mutagenic properties of several acridine-based intercalators has been reviewed in various manuscripts and the results suggest that genotoxicity is dependent on the chemical structure and dose of the intercalator administered as not all intercalators are mutagens, thus making it difficult to predict the possible toxicity potentials of an intercalator without direct evaluation.[240, 242-244] Furthermore, while intercalators may lead to a propensity for frameshift mutagenesis

in bacteria and bacteriophages, these results do not accurately reflects drug genotoxicity properties in mammalian cells.[240, 245]

In addition to genotoxicity concerns, peptide-based drug delivery carriers must also avoid potential dangerous immune responses that have been previously reported using synthetic peptides.[246] Nevertheless, immunogenicity against the peptide carrier can be minimized by covalently attaching poly(ethylene glycol) to the peptide in order to limit interactions between the polyplex and antigen-processing cells.[247] While few published studies measure cytokine levels for assessing the innate immune responses of DNA polyplexes,[8] future studies involving PEGylated polyacridine peptides should also include this experiment to ensure the safety of this gene delivery system.

The toxicity of PEGylated polyacridine peptides was not directly determined in this thesis. However, the cytotoxicity of polyacridine-melittin peptides with the same peptide sequences, but containing a fusogenic melittin peptide rather than PEG, was determined by the MTT assay.[210] The results revealed an average cell viability of 83% in three different cell lines (CHO, HepG2, and 3T3 cells) when DNA polyplexes were prepared at 0.5 nmol per μg of DNA,[210] which is similar to the toxicity levels observed by PEI DNA polyplexes prepared with 25 kDa branched PEI at an n to p of 4 in COS-7 cells using the same assay.[248] These results would suggest that PEGylated polyacridine peptides without the possibly toxic fusogenic peptide should possess better toxicity profiles than both PEI and polyacridine-melittin peptides. Nonetheless, cytotoxicity and genotoxicity are a concern for PEGylated polyacridine peptides and both should be properly evaluated in future experiments.

Final Remarks

Polyacridine PEG-peptides demonstrated improved biocompatibility for both iv and IM-EP administration. The data presented in this thesis provides a comprehensive investigation on the features required for optimal non-viral gene delivery system. PEG is

obviously required for nuclease protection and to prevent polyplex aggregation. Additionally, the high affinity binding of PEGylated polyacridine peptides was required to avoid premature polyplex dissociation during transit in circulation. This was achieved by incorporating six (Acr-Lys) repeats into the peptide that binds to DNA by both ionic interactions and intercalation. These results are not the first to report improved pharmacokinetics properties of DNA polyplexes,[222, 223, 225-228] but rather these results are the first to comprehensively demonstrate that the systemically dosed DNA is protected from metabolism in the blood by gel electrophoresis (Figure 5-10), and that the DNA in the blood remains transfection competent through the hydrodynamic stimulation procedure incorporated (Figure 5-9A). Nevertheless, the other key features required for successful polyacridine-based DNA delivery systems remains to be identified, but their need is evident due to the lack of expression observed without HD stimulation.

The barriers that can impede the delivery of stable PEGylated polyacridine DNA polyplexes from systemic circulation to inside the hepatocytes of the liver can be cellular uptake, endosomal escape, or nuclear localization once within the cell. Determining which of these delivery stages impedes efficient gene transfer requires a stepwise analysis to identify and improve the DNA polyplex without influencing the enhanced pharmacokinetic properties. Although over 50% of the dose is distributed to the liver within the first 50 minutes of circulation (Table 5-3), these results do not necessarily indicate that the DNA is located within hepatocytes, nor does it mean that the DNA in the liver is intact (non-metabolized). Therefore additional studies are required to elucidate which cells are predominantly accumulating the radiolabeled DNA and if the DNA within the liver is stabilized. Separation of Kupffer cells and hepatocytes can be performed as described previously,[168] and the influence of triantennary N-glycan (Figure 6-1) on the accumulation of the DNA polyplex into hepatocytes can also be determined using this method at increasing percentages of targeting peptide to optimize the cellular uptake of PEGylated polyacridine DNA polyplexes. An important expansion of the work

presented in the thesis would be to develop an extraction method to verify DNA stability within the liver using radiolabeled DNA.[249] This in-depth analysis will demonstrate the ability to target PEGylated polyacridine DNA polyplexes to hepatocytes, determine the optimal amount of Tri-(Acr-Lys)$_6$ needed for efficient uptake into hepatocytes, and verify the stability of DNA polyplexes in the liver using this DNA delivery system.

In vitro analysis using confocal microscopy can provide further information on the cellular trafficking of the DNA polyplex after internalization. To determine the extent of endosomal escape by PEGylated polyacridine DNA polyplexes, cells transfected with fluorescently labeled DNA polyplexes can be imaged using a confocal microscope to determine the ability of the polyplex or DNA to escape the endosome prior to fusion with the lysosome.[250-252] The fluorescence intensity of the DNA polyplex will either suggest endosomal compartmentalization, or show homogeneously dispersed DNA polyplexes inside the cell that would indicate disruption of the endosome and free DNA polyplex in the cytoplasm.[253] The ability of polyplexed DNA to reach the nucleus of the cell can be determined by comparing the transfection efficiencies of PEGylated polyacridine DNA polyplexes that are directly injected either into the cytoplasm of the cell or into the nucleus using fluorescently labeled DNA polyplexes.[254] The confocal microscope can also provide information indicating whether DNA polyplexes traffic from the cytoplasm to the nucleus.[255]

By optimizing cellular uptake and studying the cellular trafficking of the DNA polyplex, a significant amount of information will be acquired to elucidate the delivery barriers responsible for the poor in vivo transfection efficiencies without hydrodynamic stimulation. Once these parameters are identified, then additional peptide components such as fusogenic peptides and nuclear localizing sequences (NLS) can be developed that bind to DNA with high affinity, form multiple component DNA polyplexes, and overcome the barriers that limit the delivery of PEGylated polyacridine DNA polyplexes.

The biodistribution and pharmacokinetic analysis presented in Chapter 5 suggest that polyacridine-PEG peptide DNA polyplexes can be easily adapted for DNA delivery to tumor models. These models may provide several advantages over hepatocyte targeting to the liver, where rapid cellular division may provide more efficient nuclear targeting of DNA, and the EPR effect may provide an easy method of biodistributing DNA polyplexes to the tumor. Furthermore, targeting ligands can be customized to the tumor, based on the over expression of receptors on the surface of those cells. It has been suggested that nuclear localization of DNA is a significant limiting delivery barrier for efficient transfection efficiencies.[256] Therefore it is possible that polyacridine-based delivery systems are more suitable for siRNA constructs that only require gene delivery to the cytoplasm of cells rather than to the nucleus. Regardless of the model or genes chosen for future experiments, the polyacridine PEG-peptides presented in this thesis fulfill the first requirement for targeted gene delivery, and future DNA polyplexes will be designed to elucidate the cellular machinery that currently limits their in vivo gene expression.

REFERENCES

1 Glover, D. J., Lipps, H. J., and Jans, D. A. (2005) Towards safe, non-viral therapeutic gene expression in humans. *Nat Rev Genet 6*, 299-310.

2 Schwartz, J. J., and Zhang, S. (2000) Peptide-mediated cellular delivery. *Curr Opin Mol Ther 2*, 162-167.

3 Jackson, D. A., Juranek, S., and Lipps, H. J. (2006) Designing nonviral vectors for efficient gene transfer and long-term gene expression. *Mol Ther 14*, 613-626.

4 Karmali, P. P., and Chaudhuri, A. (2007) Cationic liposomes as non-viral carriers of gene medicine: resolved issues, open questions, and future promises. *Med Res Rev 27*, 696-722.

5 Schwendener, R. A. (2007) Liposomes in biology and medicine. *Adv Exp Med Biol 620*, 117-128.

6 Dykxhoorn, D. M., Palliser, D., and Lieberman, J. (2006) The silent treatment: siRNAs as small molecule drugs. *Gene Ther 13*, 541-552.

7 Elbashir, S. M., Harborth, J., Weber, K., and Tuschl, T. (2002) Analysis of gene function in somatic mammalian cells using small interfering RNAs. *Methods 26*, 199-213.

8 Behlke, M. A. (2006) Progress towards in vivo use of siRNAs. *Mol Ther 13*, 644-670.

9 Kim, W. J., and Kim, S. W. (2009) Efficient siRNA delivery with non-viral polymeric vehicles. *Pharm Res 26*, 657-666.

10 Behlke, M. A. (2008) Chemical modification of siRNAs for in vivo use. *Oligonucleotides 18*, 305-319.

11 Roberts, M. J., Bentley, M. D., and Harris, J. M. (2002) Chemistry for peptide and protein PEGylation. *Adv Drug Deliv Rev 54*, 459-476.

12 Liang, K. W., Nishikawa, M., Liu, F., Sun, B., Ye, Q., and Huang, L. (2004) Restoration of dystrophin expression in mdx mice by intravascular injection of naked DNA containing full-length dystrophin cDNA. *Gene Ther 11*, 901-908.

13 Sato, Y., Ajiki, T., Inoue, S., Hakamata, Y., Murakami, T., Kaneko, T., Takahashi, M., and Kobayashi, E. (2003) A novel gene therapy to the graft organ by a rapid injection of naked DNA I: long-lasting gene expression in a rat model of limb transplantation. *Transplantation 76*, 1294-1298.

14 Liu, F., Song, Y., and Liu, D. (1999) Hydrodynamics-based transfection in animals by systemic administration of plasmid DNA. *Gene Ther 6*, 1258-1266.

15 Klenchin, V. A., Sukharev, S. I., Serov, S. M., Chernomordik, L. V., and Chizmadzhev Yu, A. (1991) Electrically induced DNA uptake by cells is a fast process involving DNA electrophoresis. *Biophys J 60*, 804-811.

16 Wadhwa, M. S., Collard, W. T., Adami, R. C., McKenzie, D. L., and Rice, K. G. (1997) Peptide-mediated gene delivery: influence of peptide structure on gene expression. *Bioconj Chem 8*, 81-88.

17 Farjo, R., Skaggs, J., Quiambao, A. B., Cooper, M. J., and Naash, M. I. (2006) Efficient non-viral ocular gene transfer with compacted DNA nanoparticles. *PLoS ONE 1*, e38.

18 C. Conwell, I. V., and V. Hud. (2003) Controlling the size of nanoscale torodial DNA condensates with static curvature and ionic strength. *PNAS 100*, 9296-9301.

19 Kwok, K. Y., Adami, R. C., Hester, K. C., Park, Y., Thomas, S., and Rice, K. G. (2000) Strategies for maintaining the particle size of peptide DNA condensates following freeze-drying. *Int J Pharm 203*, 81-88.

20 McKenzie, D. L., Collard, W. T., and Rice, K. G. (1999) Comparative gene transfer efficiency of low molecular weight polylysine DNA-condensing peptides. *J Pept Res 54*, 311-318.

21 Templeton, N. S., Lasic, D. D., Frederik, P. M., Strey, H. H., Roberts, D. D., and Pavlakis, G. N. (1997) Improved DNA: liposome complexes for increased systemic delivery and gene expression. *Nat Biotechnol 15*, 647-652.

22 Wadhwa, M., Knoell, D.L., Young, A.P., and Rice, K.G. (1995) Targeted gene delivery with A low molecular weight glycopeptide. *Bioconj Chem 6*, 283-291.

23 Morgan, A. R., Evans, D. H., Lee, J. S., and Pulleyblank, D. E. (1979) Review: ethidium fluorescence assay. Part II. Enzymatic studies and DNA-protein interactions. *Nucleic Acids Res 7*, 571-594.

24 Yu, H., Chen, X., Lu, T., Sun, J., Tian, H., Hu, J., Wang, Y., Zhang, P., and Jing, X. (2007) Poly(L-lysine)-graft-chitosan copolymers: synthesis, characterization, and gene transfection effect. *Biomacromolecules 8*, 1425-1435.

25 Adami, R. C., Collard, W. T., Gupta, S. A., Kwok, K. Y., Bonadio, J., and Rice, K. G. (1998) Stability of peptide-condensed plasmid DNA formulations. *J Pharm Sci 87*, 678-683.

26 YP Zhang, L. S., EG Saravolac, JJ Wheeler, P Tardi, K Clow, E Leng, R Sun, PR Cullis and P Scherreer. (1999) Stabalized plasmid-lipid particles for regional gene therapy: formulation and transfection properties. *Gene Ther 6*, 1438-1447.

27 Liu, G., Li, D., Pasumarthy, M. K., Kowalczyk, T. H., Gedeon, C. R., Hyatt, S. L., Payne, J. M., Miller, T. J., Brunovskis, P., Fink, T. L., Muhammad, O., Moen, R. C., Hanson, R. W., and Cooper, M. J. (2003) Nanoparticles of compacted DNA transfect postmitotic cells. *J Biol Chem 278*, 32578-32586.

28 Zhou, X., Liu, B., Yu, X., Zha, X., Zhang, X., Chen, Y., Wang, X., Jin, Y., Wu, Y., Chen, Y., Shan, Y., Chen, Y., Liu, J., Kong, W., and Shen, J. (2007) Controlled release of PEI/DNA complexes from mannose-bearing chitosan microspheres as a potent delivery system to enhance immune response to HBV DNA vaccine. *J Control Release 121*, 200-207.

29 Tickler, A. K., and Wade, J. D. (2007) Overview of solid phase synthesis of "difficult peptide" sequences. *Curr Protoc Protein Sci Chapter 18*, Unit 18 18.

30 Martin, M. E., and Rice, K. G. (2007) Peptide-guided gene delivery. *AAPS J 9*, E18-E29.

31 Wheate, N. J., Brodie, C. R., Collins, J. G., Kemp, S., and Aldrich-Wright, J. R. (2007) DNA intercalators in cancer therapy: organic and inorganic drugs and their spectroscopic tools of analysis. *Mini Rev Med Chem. 7*, 627-648.

32 Boulanger, C., Di Giorgio, C., and Vierling, P. (2005) Synthesis of acridine-nuclear localization signal (NLS) conjugates and evaluation of their impact on lipoplex and polyplex-based transfection. *Eur J Med Chem 40*, 1295-1306.

33 Nielsen, P. E., Zhen, W., Henriksen, U., and Buchardt, O. (2002) Sequence-influenced interactions of oligoacridines with DNA detected by retarded gel electrophoretic migrations. *Biochemistry 27*, 67-73.

34 Wirth, M., Buchardt, O., Koch, T., Nielsen, P. E., and Norden, B. (2002) Interactions between DNA and mono-, bis-, tris-, tetrakis-, and hexakis(aminoacridines). A linear and circular dichroism, electric orientation relaxation, viscometry, and equilibrium study. *J Am Chem Soc 110*, 932-939.

35 Shiraishi, T., and Nielsen, P. E. (2004) Down-regulation of MDM2 and activation of p53 in human cancer cells by antisense 9-aminoacridine-PNA (peptide nucleic acid) conjugates. *Nucleic Acids Res 32*, 4893-4902.

36 Haensler, J., and Szoka, J. F. C. (1993) Synthesis and characterization of a trigalactosylated bisacridine compound to target DNA to hepatocytes. *Bioconj Chem 4*, 85-93.

37 Shiraishi, T., Bendifallah, N., and Nielsen, P. E. (2006) Cellular delivery of polyheteroaromate-peptide nucleic acid conjugates mediated by cationic lipids. *Bioconj Chem 17*, 189-194.

38 Shiraishi, T., Hamzavi, R., and Nielsen, P. E. (2005) Targeted delivery of plasmid DNA into the nucleus of cells via nuclear localization signal peptide conjugated to DNA intercalating Bis- and Trisacridines *Bioconj Chem 16*, 1112-1116.

39 Vinogradov, S. V., Zhang, H., Mitin, A., and Warren, G. (2008) Intercalating conjugates of PEG with nuclear localization signal (NLS) peptide. *Polymer Prepr 49*, 434-435.

40 Zhang, H., and Vinogradov, S. V. (2010) Short biodegradable polyamines for gene delivery and transfection of brain capillary endothelial cells. *J Control Release 143*, 359-366.

41 Woodle, M. C. (1998) Controlling liposome blood clearance by surface-grafted polymers. *Adv Drug Deliv Rev 32*, 139-152.

42 Molineux, G. (2003) Pegylation: engineering improved biopharmaceuticals for oncology. *Pharmacotherapy 23*, 3S-8S.

43 Veronese, F. M., and Pasut, G. (2005) PEGylation, successful approach to drug delivery. *Drug Discov Today 10*, 1451-1458.

44 Chapman, R., Ostuni E, Takayama S, Holmlin E, Yan L, and Whitesides GM. (2000) Surveying for surfaces that resist the adsorption of proteins. *J Am Chem Soc 122*.

45 Wang, S., Lee, R. J., Cauchon, G., Gorenstein, D. G., and Low, P. S. (1995) Delivery of antisense oligodeoxyribonucleotides against the human epidermal growth factor receptor into cultured KB cells with liposomes conjugated to folate via polyethylene glycol. *PNAS 92*, 3318-3322.

46 Weecharangsan, W., Opanasopit, P., and Lee, R. J. (2007) In vitro gene transfer using cationic vectors, electroporation and their combination. *Anticancer Res 27*, 309-313.

47 Veronese, F. M. (2001) Peptide and protein PEGylation: a review of problems and solutions. *Biomaterials 22*, 405-417.

48 Ward, C. M., Read, M. L., and Seymour, L. W. (2001) Systemic circulation of poly(L-lysine)/DNA vectors is influenced by polycation molecular weight and type of DNA: differential circulation in mice and rats and the implications for human gene therapy. *Blood 97*, 2221-2229.

49 Dash, P. R., Read, M. L., Barrett, L. B., Wolfert, M. A., and Seymour, L. W. (1999) Factors affecting blood clearance and in vivo distribution of polyelectrolyte complexes for gene delivery. *Gene Ther 6*, 643-650.

50 Plank, C., Mechtler, K., Szoka, F. C., Jr., and Wagner, E. (1996) Activation of the complement system by synthetic DNA complexes: a potential barrier for intravenous gene delivery. *Hum Gene Ther 7*, 1437-1446.

51 Ogris, M., Brunner, S., Schuller, S., Kircheis, R., and Wagner, E. (1999) PEGylated DNA/transferrin-PEI complexes: reduced interaction with blood components, extended circulation in blood and potential for systemic gene delivery. *Gene Ther 6*, 595-605.

52 Ogris, M., Walker, G., Blessing, T., Kircheis, R., Wolschek, M., and Wagner, E. (2003) Tumor-targeted gene therapy: strategies for the preparation of ligand-polyethylene glycol-polyethylenimine/DNA complexes. *J Control Release 91*, 173-181.

53 Erbacher, P., Bettinger, T., Belguise-Valladier, P., Zou, S., Coll, J. L., Behr, J. P., and Remy, J. S. (1999) Transfection and physical properties of various saccharide, poly(ethylene glycol), and antibody-derivatized polyethylenimines (PEI). *J Gene Med. 1*, 210-222.

54 Oupicky, D., Ogris, M., Howard, K. A., Dash, P. R., Ulbrich, K., and Seymour, L. W. (2002) Importance of lateral and steric stabilization of polyelectrolyte gene delivery vectors for extended systemic circulation. *Mol Ther 5*, 463-472.

55 Walker, G. F., Fella, C., Pelisek, J., Fahrmeir, J., Boeckle, S., Ogris, M., and Wagner, E. (2005) Toward synthetic viruses: endosomal pH-triggered deshielding of targeted polyplexes greatly enhances gene transfer in vitro and in vivo. *Mol Ther 11*, 418-425.

56 Lin, S., Du, F., Wang, Y., Ji, S., Liang, D., Yu, L., and Li, Z. (2008) An acid-labile block copolymer of PDMAEMA and PEG as potential carrier for intelligent gene delivery systems. *Biomacromolecules 9*, 109-115.

57 Tomlinson, R., Heller, J., Brocchini, S., and Duncan, R. (2003) Polyacetal-doxorubicin conjugates designed for pH-dependent degradation. *Bioconj Chem 14*, 1096-1106.

58 Murthy, N., Campbell, J., Fausto, N., Hoffman, A. S., and Stayton, P. S. (2003) Design and synthesis of pH-responsive polymeric carriers that target uptake and enhance the intracellular delivery of oligonucleotides. *J Control Release 89*, 365-374.

59 Shin, J., Shum, P., and Thompson, D. H. (2003) Acid-triggered release via dePEGylation of DOPE liposomes containing acid-labile vinyl ether PEG-lipids. *J Control Release 91*, 187-200.

60 Choi, J. S., MacKay, J. A., and Szoka, F. C., Jr. (2003) Low-pH-sensitive PEG-stabilized plasmid-lipid nanoparticles: preparation and characterization. *Bioconj Chem 14*, 420-429.

61 Dvorak, H. F., Nagy, J. A., Dvorak, J. T., and Dvorak, A. M. (1988) Identification and characterization of the blood vessels of solid tumors that are leaky to circulating macromolecules. *Am J Pathol 133*, 95-109.

62 Arlt, M., Haase, D., Hampel, S., Oswald, S., Bachmatiuk, A., Klingeler, R., Schulze, R., Ritschel, M., Leonhardt, A., Fuessel, S., Buchner, B., Kraemer, K., and Wirth, M. P. (2010) Delivery of carboplatin by carbon-based nanocontainers mediates increased cancer cell death. *Nanotechnology 21*, 335101.

63 Matsumura, Y., and Maeda, H. (1986) A new concept for macromolecular therapeutics in cancer chemotherapy: mechanism of tumoritropic accumulation of proteins and the antitumor agent smancs. *Cancer Res 46*, 6387-6392.

64 Nichols, B. J., and Lippincott-Schwartz, J. (2001) Endocytosis without clathrin coats. *Trends Cell Biol 11*, 406-412.

65 Goncalves, C., Mennesson, E., Fuchs, R., Gorvel, J. P., Midoux, P., and Pichon, C. (2004) Macropinocytosis of polyplexes and recycling of plasmid via the clathrin-dependent pathway impair the transfection efficiency of human hepatocarcinoma cells. *Mol Ther 10*, 373-385.

66 Rejman, J., Bragonzi, A., and Conese, M. (2005) Role of clathrin- and caveolae-mediated endocytosis in gene transfer mediated by lipo- and polyplexes. *Mol Ther 12*, 468-474.

67 Mislick, K. A., and Baldeschwieler, J. D. (1996) Evidence for the role of proteoglycans in cation-mediated gene transfer. *PNAS 93*, 12349-12354.

68 Gratton, S. E., Ropp, P. A., Pohlhaus, P. D., Luft, J. C., Madden, V. J., Napier, M. E., and DeSimone, J. M. (2008) The effect of particle design on cellular internalization pathways. *PNAS 105*, 11613-11618.

69 Doherty, G. J., and McMahon, H. T. (2009) Mechanisms of endocytosis. *Annu Rev Biochem 78*, 857-902.

70 Kirchhausen, T. (2000) Three ways to make a vesicle. *Nat Rev Mol Cell Biol 1*, 187-198.

71 Mukherjee, S., Ghosh, R. N., and Maxfield, F. R. (1997) Endocytosis. *Physiol Rev 77*, 759-803.

72 Modi, S., Prakash Jain, J., Domb, A. J., and Kumar, N. (2006) Exploiting EPR in polymer drug conjugate delivery for tumor targeting. *Curr Pharm Des 12*, 4785-4796.

73 Pirollo, K. F., and Chang, E. H. (2008) Does a targeting ligand influence nanoparticle tumor localization or uptake? *Trends Biotechnol 26*, 552-558.

74 Li SD, C. S., Huang L. (2008) Efficient gene silencing in metastatic tumor by siRNA formulated in surface-modified nanoparticles. *J Control Release 126*, 77-84.

75 Collins, L., Gustafsson, K., and Fabre, J. W. (2000) Tissue-binding properties of a synthetic peptide DNA vector targeted to cell membrane integrins: a possible universal nonviral vector for organ and tissue transplantation. *Transplantation. 69*, 1041-1050.

76 Collins, L., and Fabre, J. W. (2004) A synthetic peptide vector system for optimal gene delivery to corneal endothelium. *J Gene Med 6*, 185-194.

77 McKay, T., Reynolds, P., Jezzard, S., Curiel, D., and Coutelle, C. (2002) Secretin-mediated gene delivery, a specific targeting mechanism with potential for treatment of biliary and pancreatic disease in cystic fibrosis. *Mol Ther 5*, 447-454.

78 Schaffer, D. V., Fidelman, N. A., Dan, N., and Lauffenburger, D. A. (2000) Vector unpacking as a potential barrier for receptor-mediated polyplex gene delivery. *Biotechnol Bioeng 67*, 598-606.

79 Schaffer, D. V., and Lauffenburger, D. A. (1998) Optimization of cell surface binding enhances efficiency and specificity of molecular conjugate gene delivery. *J Biol Chem 273*, 28004-28009.

80 Martinez-Fong, D., Navarro-Quiroga, I., Ochoa, I., Alvarez-Maya, I., Meraz, M. A., Luna, J., and Arias-Montano, J. A. (1999) Neurotensin-SPDP-poly-L-lysine conjugate: a nonviral vector for targeted gene delivery to neural cells. *Brain Res Mol Brain Res 69*, 249-262.

81 Sudimack, J., and Lee, R. J. (2000) Targeted drug delivery via the folate receptor. *Adv Drug Deliv Rev 41*, 147-162.

82 Collard, W. T., Yang, Y., Kwok, K. Y., Park, Y., and Rice, K. G. (2000) Biodistribution, metabolism, and *in vivo* gene expression of low molecular weight glycopeptide polyethylene glycol peptide DNA co-condensates. *J Pharm Sci 89*, 499-512.

83 Wu, G. Y., and Wu, C. H. (1987) Receptor-mediated in vitro gene transformation by a soluble DNA carrier system [published erratum appears in J Biol Chem 1988 Jan 5;263(1):588. *J Biol Chem 262*, 4429-4432.

84 Wu, G. Y., and Wu, C. H. (1988) Receptor-mediated gene delivery and expression in vivo. *J Biol Chem 263*, 14621-14624.

85 Wu, G. Y., and Wu, C. H. (1998) Receptor-mediate delivery of foreign genes to hepatocytes. *Adv Drug Deliver Rev 29*, 243-248.

86 McGreal, E. P., Rosas, M., Brown, G. D., Zamze, S., Wong, S. Y., Gordon, S., Martinez-Pomares, L., and Taylor, P. R. (2006) The carbohydrate-recognition domain of Dectin-2 is a C-type lectin with specificity for high mannose. *Glycobiology 16*, 422-430.

87 Wagner, E., Zenke, M., Cotten, M., Beug, H., and Birnstiel, M. L. (1990) Transferrin-polycation conjugates as carriers for DNA uptake into cells. *PNAS 87*, 3410-3414.

88 Kircheis, R., Blessing, T., Brunner, S., Wightman, L., and Wagner, E. (2001) Tumor targeting with surface-shielded ligand--polycation DNA complexes. *J Control Release 72*, 165-170.

89 Hoganson, D. K., Chandler, L. A., Fleurbaaij, G. A., Ying, W., Black, M. E., Doukas, J., Pierce, G. F., Baird, A., and Sosnowski, B. A. (1998) Targeted delivery of DNA encoding cytotoxic proteins through high-affinity fibroblast growth factor receptors. *Hum Gene Ther 9*, 2565-2575.

90 Sosnowski, B. A., Gonzalez, A. M., Chandler, L. A., Buechler, Y. J., Pierce, G. F., and Baird, A. (1996) Targeting DNA to cells with basic fibroblast growth factor (FGF2). *J Biol Chem 271*, 33647-33653.

91 Li, S., Tan, Y., Viroonchatapan, E., Pitt, B. R., and Huang, L. (2000) Targeted gene delivery to pulmonary endothelium by anti-PECAM antibody. *Am J Physiol Lung Cell Mol Physiol 278*, L504-511.

92 Wang, C. Y., and Huang, L. (1987) pH-sensitive immunoliposomes mediate target-cell-specific delivery and controlled expression of a foreign gene in mouse. *PNAS 84*, 7851-7855.

93 Mohr, L., Schauer, J. I., Boutin, R. H., Moradpour, D., and Wands, J. R. (1999) Targeted gene transfer to hepatocellular carcinoma cells in vitro using a novel monoclonal antibody-based gene delivery system. *Hepatology 29*, 82-89.

94 Li, S. D., Chono, S., and Huang, L. (2008) Efficient oncogene silencing and metastasis inhibition via systemic delivery of siRNA. *Mol Ther 16*, 942-946.

95 Wang, X., Yin, L., Rao, P., Stein, R., Harsch, K. M., Lee, Z., and Heston, W. D. (2007) Targeted treatment of prostate cancer. *J Cell Biochem 102*, 571-579.

96 Farokhzad, O. C., Jon, S., Khademhosseini, A., Tran, T. N., Lavan, D. A., and Langer, R. (2004) Nanoparticle-aptamer bioconjugates: a new approach for targeting prostate cancer cells. *Cancer Res 64*, 7668-7672.

97 Schmid, S., Fuchs, R., Kielian, M., Helenius, A., and Mellman, I. (1989) Acidification of endosome subpopulations in wild-type Chinese hamster ovary cells and temperature-sensitive acidification-defective mutants. *J Cell Biol 108*, 1291-1300.

98 Ciftci, K., and Levy, R. J. (2001) Enhanced plasmid DNA transfection with lysosomotropic agents in cultured fibroblasts. *Int J Pharm 218*, 81-92.

99 Behr, J. P. (1996) Gene transfer with amino lipids and amino polymers. *Comptes Rendus des Seances de la Societe de Biologie et de Ses Filiales 190*, 33-38.

100 Boussif, O., Lezoualc'h, F., Zanta, M. A., Mergny, M. D., Scherman, D., Demeneix, B., and Behr, J. P. (1995) A versatile vector for gene and oligonucleotide transfer into cells in culture and in vivo: polyethylenimine. *PNAS 92*, 7297-7301.

101 Gupta, B., Levchenko, T. S., and Torchilin, V. P. (2005) Intracellular delivery of large molecules and small particles by cell-penetrating proteins and peptides. *Adv Drug Deliv Rev 57*, 637-651.

102 Mahat, R. I., Monera, O. D., Smith, L. C., and Rolland, A. (1999) Peptide-based gene delivery. *Curr Opin Mol Ther 1*, 226-243.

103 Rettig, G. R., and Rice, K. G. (2007) Non-viral gene delivery: from the needle to the nucleus. *Expert Opin Biol Ther 7*, 799-808.

104 Deshayes, S., Morris, M. C., Divita, G., and Heitz, F. (2005) Cell-penetrating peptides: tools for intracellular delivery of therapeutics. *Cell Mol Life Sci 62*, 1839-1849.

105 Gottschalk, S., Sparrow, J. T., Hauer, J., Mims, M. P., Leland, F. E., Woo, S. L. C., and Smith, L. C. (1996) A novel DNA-peptide complex for efficient gene transfer and expression in mammalian cells. *Gene Ther 3*, 448-457.

106 A. Kichler, A. M., B. Bechinger. (2006) Cationic amphipathic histidine-rich peptides for gene delivery. *Biochim Biophys Acta (BBA)- Biomembranes 1758*, 301-307.

107 Goto, Y., and Hagihara, Y. (1992) Mechanism of the conformational transition of melittin. *Biochemistry 31*, 732-738.

108 Chen, C. P., Kim, J. S., Steenblock, E., Liu, D., and Rice, K. G. (2006) Gene transfer with poly-melittin peptides. *Bioconj Chem 17*, 1057-1062.

109 Li, F. Q., Su, H., Wang, J., Liu, J. Y., Zhu, Q. G., Fei, Y. B., Pan, Y. H., and Hu, J. H. (2007) Preparation and characterization of sodium ferulate entrapped bovine serum albumin nanoparticles for liver targeting. *Int J Pharm 1-2, 274-282*.

110 Jones, C., Burton, M. A., and Gray, B. N. (1989) Albumin Microspheres as vehicles for the sustained and controlled release of doxorubicin. *J Pharm Pharmacol 41*, 813-816.

111 Gupta, P. K., and Hung, C. T. (1989) Albumin microspheres I: physico-chemical characteristics. *J Microencapsulation 6*, 427-462.

112 Kwok, K. Y., Yang, Y., and Rice, K. G. (2001) Evolution of cross-linked non-viral gene delivery systems. *Curr Opin Mol Ther 3*, 142-146.

113 Adami, R. C., and Rice, K. G. (1999) Metabolic stability of glutaraldehyde cross-linked peptide DNA condensates. *J Pharm Sci 88*, 739-746.

114 Yang, Y., Park, Y., Man, S., Liu, Y., and Rice, K. G. (2001) Cross-linked low molecular weight glycopeptide mediated gene delivery: Relationship between DNA metabolic stability and the level of transient gene expression in vivo. *J Pharm Sci 90*, 2010-2022.

115 Dauty, E., Remy, J. S., Blessing, T., and Behr, J. P. (2001) Dimerizable cationic detergents with a low cmc condense plasmid DNA into nanometric particles and transfect cells in culture. *J Am Chem Soc 123*, 9227-9234.

116 Ouyang, M., Remy, J. S., and Szoka Jr, F. C. (2000) Controlled template-assisted assembly of plasmid DNA into nanometric particles with high DNA concentration. *Bioconj Chem 11*, 104-112.

117 McKenzie, D. L., Kwok, K. Y., and Rice, K. G. (2000) A potent new class of reductively activated peptide gene delivery agents. *J Biol Chem 275*, 9970-9977.

118 Park, Y., Kwok, K. Y., Boukarim, C., and Rice, K. G. (2002) Synthesis of sulfhydryl crosslinking poly (ethylene glycol) peptides and glycopeptides as carriers for gene delivery. *Bioconj Chem 13*, 232-239.

119 Kwok, K. Y., Park, Y., Yongsheng, Y., McKenzie, D.L., Rice, K.G. (2003) In vivo gene transfer using sulfhydryl crosslinked PEG-peptide/glycopeptide DNA co-condensates. *J Pharm Sci 92*, 1174-1185.

120 Pouton, C. W., Wagstaff, K. M., Roth, D. M., Moseley, G. W., and Jans, D. A. (2007) Targeted delivery to the nucleus. *Adv Drug Deliv Rev 59*, 698-717.

121 Young, J. L., Benoit, J. N., and Dean, D. A. (2003) Effect of a DNA nuclear targeting sequence on gene transfer and expression of plasmids in the intact vasculature. *Gene Ther 10*, 1465-1470.

122 Dean, D. A., Dean, B. S., Muller, S., and Smith, L. C. (1999) Sequence requirements for plasmid nuclear import. *Exp Cell Res 253*, 713-722.

123 Zanta, M. A., Belguise-Valladier, P., and Behr, J. P. (1999) Gene delivery: a single nuclear localization signal peptide is sufficient to carry DNA to the cell nucleus. *PNAS 96*, 91-96.

124 Tanimoto, M., Kamiya, H., Minakawa, N., Matsuda, A., and Harashima, H. (2003) No enhancement of nuclear entry by direct conjugation of a nuclear localization signal peptide to linearized DNA. *Bioconj Chem 14*, 1197-1202.

125 van der Aa, M., Koning, G., van der Gugten, J., d'Oliveira, C., Oosting, R., Hennink, W. E., and Crommelin, D. J. (2005) Covalent attachment of an NLS-peptide to linear DNA does not enhance transfection efficiency of cationic polymer based gene delivery systems. *J Control Release 101*, 395-397.

126 Van der Aa, M. A., Koning, G. A., d'Oliveira, C., Oosting, R. S., Wilschut, K. J., Hennink, W. E., and Crommelin, D. J. (2005) An NLS peptide covalently linked to linear DNA does not enhance transfection efficiency of cationic polymer based gene delivery systems. *J Gene Med 7*, 208-217.

127 Felgner, P. L., and Rhodes, G. (1991) Gene therapeutics. *Nature 349*, 351-352.

128 Yang, J. P., and Huang, L. (1996) Direct gene transfer to mouse melanoma by intratumor injection of free DNA. *Gene Ther 3*, 542-548.

129 Niidome, T., and Huang, L. (2002) Gene therapy progress and prospects: nonviral vectors. *Gene Ther 9*, 1647-1652.

130 Felgner, P. L., Tsai, Y. J., Sukhu, L., Wheeler, C. J., Manthorpe, M., Marshall, J., and Cheng, S. H. (1995) Improved cationic lipid formulations for in vivo gene therapy. *Ann Ny Acad Sci 772*, 126-139.

131 Liu, F., and Huang, L. (2002) A syringe electrode device for simultaneous injection of DNA and electrotransfer. *Mol Ther 5*, 323-328.

132 Zhang, G., Gao, X., Song, Y. K., Vollmer, R., D.B., S., Gaskowski, J. Z., Dean, D. A., and Liu, D. (2004) Hydroporation as the mechanism of hydrodynamic delivery. *Gene Ther. 11*, 675-682.

133 Wisse, E., De Zanger, R. B., Charels, K., Van Der Smissen, P., and McCuskey, R. S. (1985) The liver sieve: considerations concerning the structure and function of endothelial fenestrae, the sinusoidal wall and the space of Disse. *Hepatology 5*, 683-692.

134 Bloquel, C., Trollet, C., Pradines, E., Seguin, J., Scherman, D., and Bureau, M. F. (2006) Optical imaging of luminescence for in vivo quantification of gene electrotransfer in mouse muscle and knee. *BMC Biotechnol 6*, 16.

135 Blair-Parks, K., Weston, B. C., and Dean, D. A. (2002) High-level gene transfer to the cornea using electroporation. *J Gene Med 4*, 92-100.

136 Jayankura, M., Boggione, C., Frisen, C., Boyer, O., Fouret, P., Saillant, G., and Klatzmann, D. (2003) In situ gene transfer into animal tendons by injection of naked DNA and electrotransfer. *J Gene Med 5*, 618-624.

137 Heller, L., Jaroszeski, M. J., Coppola, D., Pottinger, C., Gilbert, R., and Heller, R. (2000) Electrically mediated plasmid DNA delivery to hepatocellular carcinomas in vivo. *Gene Ther 7*, 826-829.

138 Harimoto, K., Sugimura, K., Lee, C. R., Kuratsukuri, K., and Kishimoto, T. (1998) In vivo gene transfer methods in the bladder without viral vectors. *Br J Urol 81*, 870-874.

139 Inoue, T., and Krumlauf, R. (2001) An impulse to the brain--using in vivo electroporation. *Nat Neurosci 4 Suppl*, 1156-1158.

140 Hamar, P., Song, E., Kokeny, G., Chen, A., Ouyang, N., and Lieberman, J. (2004) Small interfering RNA targeting Fas protects mice against renal ischemia-reperfusion injury. *PNAS 101*, 14883-14888.

141 Mann, M. J., Gibbons, G. H., Hutchinson, H., Poston, R. S., Hoyt, E. G., Robbins, R. C., and Dzau, V. J. (1999) Pressure-mediated oligonucleotide transfection of rat and human cardiovascular tissues. *PNAS 96*, 6411-6416.

142 Barnett, F. H., Scharer-Schuksz, M., Wood, M., Yu, X., Wagner, T. E., and Friedlander, M. (2004) Intra-arterial delivery of endostatin gene to brain tumors prolongs survival and alters tumor vessel ultrastructure. *Gene Ther 11*, 1283-1289.

143 Tada, M., Hatano, E., Taura, K., Nitta, T., Koizumi, N., Ikai, I., and Shimahara, Y. (2006) High volume hydrodynamic injection of plasmid DNA via the hepatic artery results in a high level of gene expression in rat hepatocellular carcinoma induced by diethylnitrosamine. *J Gene Med 8*, 1018-1026.

144 Lin, M. T., Pulkkinen, L., Uitto, J., and Yoon, K. (2000) The gene gun: current applications in cutaneous gene therapy. *Int J Dermatol 39*, 161-170.

145 Davidson, J. M., Krieg, T., and Eming, S. A. (2000) Particle-mediated gene therapy of wounds. *Wound Repair Regen 8*, 452-459.

146 Muangmoonchai, R., Wong, S. C., Smirlis, D., Phillips, I. R., and Shephardl, E. A. (2002) Transfection of liver in vivo by biolistic particle delivery: its use in the investigation of cytochrome P450 gene regulation. *Mol Biotechnol 20*, 145-151.

147 Kuriyama, S., Mitoro, A., Tsujinoue, H., Nakatani, T., Yoshiji, H., Tsujimoto, T., Yamazaki, M., and Fukui, H. (2000) Particle-mediated gene transfer into murine livers using a newly developed gene gun. *Gene Ther 7*, 1132-1136.

148 Taniyama, Y., Tachibana, K., Hiraoka, K., Namba, T., Yamasaki, K., Hashiya, N., Aoki, M., Ogihara, T., Yasufumi, K., and Morishita, R. (2002) Local delivery of plasmid DNA into rat carotid artery using ultrasound. *Circulation 105*, 1233-1239.

149 Teupe, C., Richter, S., Fisslthaler, B., Randriamboavonjy, V., Ihling, C., Fleming, I., Busse, R., Zeiher, A. M., and Dimmeler, S. (2002) Vascular gene transfer of phosphomimetic endothelial nitric oxide synthase (S1177D) using ultrasound-enhanced destruction of plasmid-loaded microbubbles improves vasoreactivity. *Circulation 105*, 1104-1109.

150 Unger, E. C., Hersh, E., Vannan, M., and McCreery, T. (2001) Gene delivery using ultrasound contrast agents. *Echocardiography 18*, 355-361.

151 Lawrie, A., Brisken, A. F., Francis, S. E., Cumberland, D. C., Crossman, D. C., and Newman, C. M. (2000) Microbubble-enhanced ultrasound for vascular gene delivery. *Gene Ther 7*, 2023-2027.

152 Shohet, R. V., Chen, S., Zhou, Y. T., Wang, Z., Meidell, R. S., Unger, R. H., and Grayburn, P. A. (2000) Echocardiographic destruction of albumin microbubbles directs gene delivery to the myocardium. *Circulation 101*, 2554-2556.

153 Song, J., Chappell, J. C., Qi, M., VanGieson, E. J., Kaul, S., and Price, R. J. (2002) Influence of injection site, microvascular pressure and ultrasound variables on microbubble-mediated delivery of microspheres to muscle. *J Am Coll Cardiol 39*, 726-731.

154 Dimitrov, D. S., and Sowers, A. E. (1990) Membrane electroporation--fast molecular exchange by electroosmosis. *Biochim Biophys Acta 1022*, 381-392.

155 Klenchin, V. A., Sukharev, S. I., Serov, S. M., Chernomordik, L. V., and Chizmadzhev Yu, A. (1991) Electrically induced DNA uptake by cells is a fast process involving DNA electrophoresis. *Biophys J 60*, 804-811.

156 Chang, D. C., and Reese, T. S. (1990) Changes in membrane structure induced by electroporation as revealed by rapid-freezing electron microscopy. *Biophys J 58*, 1-12.

157 Liu, F., and L, H. (2002) A syringe electrode device for simultaneous injection of DNA and electrotransfer. *Mol Ther 5*, 323-328.

158 Suzuki, T., Shin, B. C., Fujikura, K., Matsuzaki, T., and Takata, K. (1998) Direct gene transfer into rat liver cells by in vivo electroporation. *FEBS Lett 425*, 436-440.

159 Muramatsu, T., Shibata, O., Ryoki, S., Ohmori, Y., and Okumura, J. (1997) Foreign gene expression in the mouse testis by localized in vivo gene transfer. *Biochem Biophys Res Commun 233*, 45-49.

160 Chen, C., Smye, S. W., Robinson, M. P., and Evans, J. A. (2006) Membrane electroporation theories: a review. *Med Biol Eng Comput 44*, 5-14.

161 Alino, S. F., Crespo, A., and Dasi, F. (2003) Long-term therapeutic levels of human alpha-1 antitrypsin in plasma after hydrodynamic injection of nonviral DNA. *Gene Ther 10*, 1672-1679.

162 Miao, C. H., Thompson, A. R., Loeb, K., and Ye, X. (2001) Long-term and therapeutic-level hepatic gene expression of human factor IX after naked plasmid transfer in vivo. *Mol Ther 3*, 947-957.

163 Gao, X., Kim, K. S., and Liu, D. (2007) Nonviral gene delivery: what we know and what is next. *AAPS J 9*, E92-104.

164 Vaughan, E. E., DeGiulio, J. V., and Dean, D. A. (2006) Intracellular trafficking of plasmids for gene therapy: mechanisms of cytoplasmic movement and nuclear import. *Curr Gene Ther 6*, 671-681.

165 Hegge, J. O., Wooddell, C. I., Zhang, G., Hagstrom, J. E., Braun, S., Huss, T., Sebestyen, M. G., Emborg, M. E., and Wolff, J. A. Evaluation of hydrodynamic limb vein injections in nonhuman primates. *Hum Gene Ther 21*, 829-842.

166 Kamimura, K., Zhang, G., and Liu, D. Image-guided, intravascular hydrodynamic gene delivery to skeletal muscle in pigs. *Mol Ther 18*, 93-100.

167 Heller, L. C., and Heller, R. Electroporation gene therapy preclinical and clinical trials for melanoma. *Curr Gene Ther*.

168 Yang, Y., Park, Y., Man, S., Liu, Y., and Rice, K. G. (2001) Cross-linked low molecular weight glycopeptide-mediated gene delivery: relationship between DNA metabolic stability and the level of transient gene expression in vivo. *J Pharm Sci 90*, 2010-2022.

169 Kwok, K. Y., McKenzie, D. L., Evers, D. L., and Rice, K. G. (1999) Formulation of highly soluble poly(ethylene glycol)-peptide DNA condensates. *J Pharm Sci 88*, 996-1003.

170 Wu, G. Y., and Wu, C. H. (1988) Evidence for targeted gene delivery to Hep G2 hepatoma cells in vitro. *Biochemistry 27*, 887-892.

171 Gao, X., and Huang, L. (1991) A novel cationic liposome reagent for efficient transfection of mammalian cells. *Biochem Bioph Res Co 179*, 280-285.

172 Yang, J. P., and Huang, L. (1997) Overcoming the inhibitory effect of serum on lipofection by increasing the charge ratio of cationic liposome to DNA. *Gene Ther 4*, 950-960.

173 Wolfert, M. A., Dash, P. R., Nazarova, O., Oupicky, D., Seymour, L. W., Smart, S., Strohalm, J., and Ulbrich, K. (1999) Polyelectrolyte vectors for gene delivery: influence of cationic polymer on biophysical properties of complexes formed with DNA. *Bioconj Chem 10*, 993-1004.

174 Choi, Y. H., Liu, F., Park, J. S., and Kim, S. W. (1998) Lactose-poly(ethylene glycol)-grafted poly-L-lysine as hepatoma cell-tapgeted gene carrier. *Bioconjug Chem 9*, 708-718.

175 Choi, Y. H., Liu, F., Choi, J. S., Kim, S. W., and Park, J. S. (1999) Characterization of a targeted gene carrier, lactose-polyethylene glycol-grafted poly-L-lysine and its complex with plasmid DNA. *Hum Gene Ther 10*, 2657-2665.

176 Peracchia, M. T., Fattal, E., Desmaele, D., Besnard, M., Noel, J. P., Gomis, J. M., Appel, M., d'Angelo, J., and Couvreur, P. (1999) Stealth PEGylated polycyanoacrylate nanoparticles for intravenous administration and splenic targeting. *J Control Release 60*, 121-128.

177 Lee, H., Jeong, J. H., and Park, T. G. (2002) PEG grafted polylysine with fusogenic peptide for gene delivery: high transfection efficiency with low cytotoxicity. *J Control Release 79*, 283-291.

178 Hosseinkhani, H., and Tabata, Y. (2004) PEGylation enhances tumor targeting of plasmid DNA by an artificial cationized protein with repeated RGD sequences, Pronectin*R*. *J Control Release 97*, 157-171.

179 Trubetskoy VS, L. A., Hagstrom JE, Budker VG, Wolff JA. (1999) Layer-by-layer deposition of oppositely charged polyelectrolytes on the surface of condensed DNA particles. *Nucleic Acids Res 27*, 3090-3095.

180 Taori VP, Liu Y, and TM, R. (2009) DNA delivery in vitro via surface release from multilayer assemblies with poly(glycoamidoamine)s. *Acta Biomater 5*, 925-933.

181 Blacklock J, You YZ, Zhou QH, Mao G, and D., O. (2009) Gene delivery in vitro and in vivo from bioreducible multilayered polyelectrolyte films of plasmid DNA. *Biomaterials 30*, 939-950.

182 Ueyama, H., Waki, M., Takagi, M., and Takenaka, S. (2000) Novel synthesis of a tetra-acridinyl peptide as a new DNA polyintercalator. *Nucleic Acids Symp Ser*, 133-134.

183 Satkauskas, S., Bureau, M. F., Puc, M., Mahfoudi, A., Scherman, D., Miklavcic, D., and Mir, L. M. (2002) Mechanisms of in vivo DNA electrotransfer: respective contributions of cell electropermeabilization and DNA electrophoresis. *Mol Ther 5*, 133-140.

184 Molnar, M. J., Gilbert, R., Lu, Y., Liu, A. B., Guo, A., Larochelle, N., Orlopp, K., Lochmuller, H., Petrof, B. J., Nalbantoglu, J., and Karpati, G. (2004) Factors influencing the efficacy, longevity, and safety of electroporation-assisted plasmid-based gene transfer into mouse muscles. *Mol Ther 10*, 447-455.

185 van der Aa, M. A., Koning, G. A., d'Oliveira, C., Oosting, R. S., Wilschut, K. J., Hennink, W. E., and Crommelin, D. J. A. (2005) An NLS peptide covalently linked to linear DNA does not enhance transfection efficiency of cationic polymer based gene delivery systems. *J Gene Med 7*, 208-217.

186 Baumhover, N. J., Anderson, K., Fernandez, C. A., and Rice, K. G. (2009) Synthesis and in vitro testing of new potent polyacridine-melittin gene delivery peptides *Bioconj Chem*, In Press.

187 Chen, C. P., Park, Y., and Rice, K. G. (2004) An improved large-scale synthesis of PEG-peptides for gene delivery. *J Pep Res 64*, 237-243.

188 Thumser, A. E., and Wilton, D. C. (1994) Characterization of binding and structural properties of rat liver fatty-acid-binding protein using tryptophan mutants. *Biochem J 300 (Pt 3)*, 827-833.

189 Karup, G., Meldal, M., Nielsen, P. E., and Buchardt, O. (1988) 9-Acridinylpeptides and 9-acridinyl-4-nitrophenylsulfonylpeptides. Synthesis, binding to DNA, and photoinduced DNA cleavage. *Int J Pept Protein Res. 32*, 331-343.

190 Crenshaw, J. M., Graves, D. E., and Denny, W. A. (1995) Interactions of acridine antitumor agents with DNA: binding energies and groove preferences. *Biochemistry 34*, 13682-13687.

191 Bezanilla, M., Drake, B., Nudler, E., Kashlev, M., Hansma, P. K., and Hansma, H. G. (1994) Motion and enzymatic degreadation of DNA in the atomic force microscope. *Biophysical J 67*, 2454-2459.

192 Wu, J. C., Sundaresan, G., Iyer, M., and Gambhir, S. S. (2001) Noninvasive optical imaging of firefly luciferase reporter gene expression in skeletal muscles of living mice. *Mol Ther 4*, 297-306.

193 Camesano, T. A., Natan, M. J., and Logan, B. E. (2000) Observation of changes in bacterial cell morphology using tapping mode atomic force microscopy. *Langmuir 16*, 4563-4572.

194 Sakai, M., Nishikawa, M., Thankaketpaisarn, O., Yamashita, F., and Hahida, M. (2005) Hepatocyte-targeted gene transfer by combination of vascularly delivered plasmid DNA and in vivo electroporation. *Gene Ther 12*, 607-616.

195 Kawano, T., Yamagata, M., Takahashi, H., Niidome, Y., Yamada, S., Katayama, Y., and Niidome, T. (2006) Stabilizing of plasmid DNA in vivo by PEG-modified cationic gold nanoparticles and the gene expression assisted with electrical pulses. *J Control Release 111*, 382-389.

196 Karup, G., Meldal, M., Nielsen, P. E., and Buchardt, O. (1988) 9-Acridinylpeptides and 9-acridinyl-4-nitrophenylsulfonylpeptides. Synthesis, binding to DNA, and photoinduced DNA cleavage. *Int J Pept Protein Res 32*, 331-343.

197 Coulberson, A. L., Hud, N. V., LeDoux, J. M., Vilfan, I. D., and Prausnitz, M. R. (2003) Gene packaging with lipids, peptides and viruses inhibits transfection by electroporation in vitro. *J Control Release 86*, 361-370.

198 Golzio, M., Teissie, J., and Rols, M. P. (2002) Direct visualization at the single-cell level of electrically mediated gene delivery. *PNAS 99*, 1292-1297.

199 Nabel, G. J., and Felgner, P. L. (1993) Direct gene transfer for immunotherapy and immunization. *Trends In Biotechnology 11*, 211-215.

200 Wolff, J. A., Malone, R. W., Williams, P., Chong, W., Acsadi, G., Jani, A., and Felgner, P. L. (1990) Direct gene transfer into mouse muscle in vivo. *Science 247*, 1465-1468.

201 Burke, R. S., and Pun, S. H. (2008) Extracellular barriers to in Vivo PEI and PEGylated PEI polyplex-mediated gene delivery to the liver. *Bioconj Chem 19*, 693-704.

202 Boeckle, S., von Gersdorff, K., van der Piepen, S., Culmsee, C., Wagner, E., and Ogris, M. (2004) Purification of polyethylenimine polyplexes highlights the role of free polycations in gene transfer. *J Gene Med 6*, 1102-1111.

203 Rudolph, C., Schillinger, U., Plank, C., Gessner, A., Nicklaus, P., Muller, R., and Rosenecker, J. (2002) Nonviral gene delivery to the lung with copolymer-protected and transferrin-modified polyethylenimine. *Biochim Biophys Acta. 1573*, 75-83.

204 Guillaume, C., Delepine, P., Droal, C., Montier, T., Tymen, G., and Claude, F. (2001) Aerosolization of cationic lipid-DNA complexes: lipoplex characterization and optimization of aerosol delivery conditions. *Biochem Bioph Res Co 286*, 464-471.

205 Mahato, R. I., Anwer, K., Tagliaferri, F., Meaney, C., Leonard, P., Wadhwa, M. S., Logan, M., French, M., and Rolland, A. (1998) Biodistribution and gene expression of lipid/plasmid complexes after systemic administration. *Hum Gene Ther 9*, 2083-2099.

206 Li, S., Rizzo, M. A., Bhattacharya, S., and Huang, L. (1998) Characterization of cationic lipid-protamine-DNA (LPD) complexes for intravenous gene delivery. *Gene Ther 5*, 930-937.

207 Liu, F., Qi, H., Huang, L., and Liu, D. (1997) Factors controlling the efficiency of cationic lipid-mediated transfection in vivo via intravenous administration. *Gene Ther 4*, 517-523.

208 Dash, P. R., Read, M. L., Barrett, L. B., Wolfert, M. A., and Seymour, L. W. (1999) Factors affecting blood clearance and in vivo distribution of polyelectrolyte complexes for gene delivery. *Gene Ther 6*, 643-650.

209 Fernandez, C., A., Baumhover, N., J., Anderson, K., and Rice, K., G. (2010) Discovery of metabolically stabilized electronegative polyacridine-PEG peptide DNA open polyplexes. *Bioconj Chem*, in press.

210 Baumhover, N. J., Anderson, K., Fernandez, C. A., and Rice, K. G. (2010) Synthesis and in vitro testing of new potent polyacridine-melittin gene delivery peptides *Bioconj Chem 21*, 74-86.

211 Anderson, K., Fernandez, C. A., and Rice, K. G. (2010) N-Glycan targeted gene delivery to the dendritic cell SIGN receptor. *Bioconj Chem*, in press.

212 Zhang, G., Budker, V., and Wolff, J. A. (1999) High levels of foreign gene expression in hepatocytes after tail vein injections of naked plasmid DNA. *Hum Gene Ther 10*, 1735-1737.

213 Rettig, G., McAnuff, M., Kim, J., Liu, D., and Rice, K. G. (2006) Quantitative bioluminescence imaging of transgene expression in vivo. *Anal Biochem 335*, 90-94.

214 Abdallah, B., Hassan, A., Benoist, C., Goula, D., Behr, J. P., and Demeneix, B. A. (1996) A powerful nonviral vector for in vivo gene transfer into the adult mammalian brain: polyethylenimine. *Hum Gene Ther 7*, 1947-1954.

215 Blessing, T., Remy, J. S., and Behr, J. P. (1998) Monomolecular collapse of plasmid DNA into stable virus-like particles. *PNAS 95*, 1427-1431.

216 Chen, C. p., Kim, J. s., Liu, D., Rettig, G. R., McAnuff, M. A., Martin, M. E., and Rice, K. G. (2007) Synthetic PEGylated glycoproteins and their utility in gene delivery. *Bioconj Chem 18*, 371-378.

217 Al-Dosari, M. S., Knapp, J. E., and Liu, D. (2005) Hydrodynamic delivery. *Adv Genet 54*, 65-81.

218 Dean, D. A., Machado-Aranda, D., Blair-Parks, K., Yeldandi, A. V., and Young, J. L. (2003) Electroporation as a method for high-level nonviral gene transfer to the lung. *Gene Ther 10*, 1608-1615.

219 Fattori, E., La Monica, N., Ciliberto, G., and Toniatti, C. (2002) Electro-gene-transfer: a new approach for muscle gene delivery. *Somat Cell Mol Genet 27*, 75-83.

220 Li, S., MacLaughlin, F. C., Fewell, J. G., Gondo, M., Wang, J., Nicol, F., Dean, D. A., and Smith, L. C. (2001) Muscle-specific enhancement of gene expression by incorporation of SV40 enhancer in the expression plasmid. *Gene Ther 8*, 494-497.

221 Terebesi, J., Kwok, K. Y., and Rice, K. G. (1998) Iodinated plasmid DNA as a tool for studying gene delivery. *Anal Biochem 263*, 120-123.

222 Heyes, J., Palmer, L., Chan, K., Giesbrecht, C., Jeffs, L., and MacLachlan, I. (2007) Lipid encapsulation enables the effective systemic delivery of polyplex plasmid DNA. *Mol Ther 15*, 713-720.

223 Kunath, K., von Harpe, A., Petersen, H., Fischer, D., Voigt, K., Kissel, T., and Bickel, U. (2002) The structure of PEG-modified poly(ethylene imines) influences biodistribution and pharmacokinetics of their complexes with NF-κB decoy in mice. *Pharm Res 19*, 810-817.

224 Li, S.-D., Chen, Y.-C., Hackett, M. J., and Huang, L. (2007) Tumor-targeted delivery of siRNA by self-assembled nanoparticles. *Mol Ther 16*, 163-169.

225 Morille, M., Montier, T., Legras, P., Carmoy, N., Brodin, P., Pitard, B., Benoît, J.-P., and Passirani, C. (2010) Long-circulating DNA lipid nanocapsules as new vector for passive tumor targeting. *Biomaterials 31*, 321-329.

226 Oupicky, D., Ogris, M., Howard, K. A., Dash, P. R., Ulbrich, L., and Seymour, L. W. (2002) Importance of lateral an steric stabilization of polyelectrolyte gene delivery vectors for extended systemic circulation. *Mol Ther 5*, 463-472.

227 Ko, Y. T., K, A., Hartner, W. C., Papahadjopoulos-Sternberg, B., and Torchilin, V. P. (2009) Self-assembling micelle-like nanoparticles based on phospholipid-polyethyleneimine conjugates for systemic gene delivery. *J Control Release*, 132-138.

228 Zhou, Q.-H., Wu, C., Manickam, D., and Oupický, D. (2009) Evaluation of pharmacokinetics of bioreducible gene delivery vectors by real-time PCR. *Pharm Res 26*, 1581-1589.

229 Collard, W. T., Evers, D. L., and McKenzie, D. L. (2000) Synthesis of homogenous glycopeptides and their utility as DNA condensing agents. *Carbohyd Res 323*, 176-184.

230 Ashwell, G., and Morell, A. G. (1974) The role of surface carbohydrates in the hepatic recognition and transport of circulating glycoproteins. *Adv Enzymol Ramb 41*, 99-128.

231 Ng, K. K. S., Iobst, S. T., Weis, W. I., and Drickamer, K. (1996) Structural analysis of monosaccharide recognition by rat liver mannose-binding protein. *J Biol Chem 271*, 663-674.

232 Tamura, T., Wadhwa, M. S., Chiu, M. H., Corradi Da Silva, M. L., McBroom, T., and Rice, K. G. (1994) Preparation of tyrosinamide oligosaccharides as iodinatable glycoconjugates. *Meth Enzymol 247*, 43-55.

233 Baenziger, J. U., and Fiete, D. (1980) Galactose and N-acetylgalactosamine-specific endocytosis of glycopeptides by isolated rat hepatocytes. *Cell 22*, 611-620.

234 Lee, Y. C., Townsend, R. R., Hardy, M. R., Lonngren, J., Arnarp, J., Haraldsson, M., and Lonn, H. (1983) Binding of synthetic oligosaccharides to the hepatic Gal/GalNAc lectin. Dependence on fine structural features. *J Biol Chem 258*, 199-202.

235 Chiu, M. H., Tamura, T., Wadhwa, M. S., and Rice, K. G. (1994) In vivo targeting function of N-linked oligosaccharides with terminating galactose and N-acetylgalactosamine residues. *J Biol Chem 269*, 16195-16202.

236 Rice, K. G., Weisz, O. A., Barthel, T., Lee, R. T., and Lee, Y. C. (1990) Defined geometry of binding between triantennary glycopeptide and the asialoglycoprotein receptor of rat hepatocytes. *J Biol Chem 265*, 18429-18434.

237 Lee, Y. C. (1989) Binding modes of mammalian hepatic Gal/GalNAc receptors. *Ciba Foundation Symposium 145*, 80-95.

238 Wadhwa, M. S., Knoell, D. L., Young, A. P., and Rice, K. G. (1995) Targeted gene delivery with a low molecular weight glycopeptide carrier. *Bioconj Chem 6*, 283-291.

239 Ferguson, L. R., and Baguley, B. C. (1996) Mutagenicity of anticancer drugs that inhibit topoisomerase enzymes. *Mutat Res 355*, 91-101.

240 Ferguson, L. R., and Denny, W. A. (2007) Genotoxicity of non-covalent interactions: DNA intercalators. *Mutat Res 623*, 14-23.

241 Liu, L. F. (1989) DNA topoisomerase poisons as antitumor drugs. *Annu Rev Biochem 58*, 351-375.

242 Denny, W. A., Turner, P. M., Atwell, G. J., Rewcastle, G. W., and Ferguson, L. R. (1990) Structure-activity relationships for the mutagenic activity of tricyclic intercalating agents in Salmonella typhimurium. *Mutat Res 232*, 233-241.

243 Ferguson, L. R., and Denny, W. A. (1990) Frameshift mutagenesis by acridines and other reversibly-binding DNA ligands. *Mutagenesis 5*, 529-540.

244 Ferguson, L. R., and Denny, W. A. (1991) The genetic toxicology of acridines. *Mutat Res 258*, 123-160.

245 Wilson, W. R., Harris, N. M., and Ferguson, L. R. (1984) Comparison of the mutagenic and clastogenic activity of amsacrine and other DNA-intercalating drugs in cultured V79 Chinese hamster cells. *Cancer Res 44*, 4420-4431.

246 Kent, S. B. H. (1988) Chemical synthesis of peptides and proteins. *Annu Rev Biochem 57*, 957-989.

247 Torchilin, V. P., and Lukyanov, A. N. (2003) Peptide and protein drug delivery to and into tumors: challenges and solutions. *Drug Discov Today 8*, 259-266.

248 Nguyen, H. K., Lemieux, P., Vinogradov, S. V., Gebhart, C. L., Guerin, N., Paradis, G., Bronich, T. K., Alakhov, V. Y., and Kabanov, A. V. (2000) Evaluation of polyether-polyethyleneimine graft copolymers as gene transfer agents. *Gene Ther 7*, 126-138.

249 Mason, W. S., Aldrich, C., Summers, J., and Taylor, J. M. (1982) Asymmetric replication of duck hepatitis B virus DNA in liver cells: Free minus-strand DNA. *PNAS 79*, 3997-4001.

250 Sonawane, N. D., Szoka, F. C., Jr., and Verkman, A. S. (2003) Chloride accumulation and swelling in endosomes enhances DNA transfer by polyamine-DNA polyplexes. *J Biol Chem 278*, 44826-44831.

251 Elouahabi, A., and Ruysschaert, J. M. (2005) Formation and intracellular trafficking of lipoplexes and polyplexes. *Mol Ther 11*, 336-347.

252 Bieber, T., Meissner, W., Kostin, S., Niemann, A., and Elsasser, H. P. (2002) Intracellular route and transcriptional competence of polyethylenimine-DNA complexes. *J Control Release 82*, 441-454.

253 Godbey, W. T., Wu, K. K., and Mikos, A. G. (1999) Tracking the intracellular path of poly(ethylenimine)/DNA complexes for gene delivery. *PNAS 96*, 5177-5181.

254 Pollard, H., Remy, J. S., Loussouarn, G., Demolombe, S., Behr, J. P., and Escande, D. (1998) Polyethylenimine but not cationic lipids promotes transgene delivery to the nucleus in mammalian cells. *J Biol Chem 273*, 7507-7511.

255 Neves, C., Escriou, V., Byk, G., Scherman, D., and Wils, P. (1999) Intracellular fate and nuclear targeting of plasmid DNA. *Cell Biol Toxicol 15*, 193-202.

256 Shen, Y. M., Hirschhorn, R. R., Mercer, W. E., Surmacz, E., Tsutsui, Y., Soprano, K. J., and Baserga, R. (1982) Gene transfer: DNA microinjection compared with DNA transfection with a very high efficiency. *Mol Cell Biol 2*, 1145-1154.